Characterisation of novel ubiquitin-dependent mechanisms in the regulation of the cell cycle

Vaughan, Natalie

Award date:
2018

Awarding institution:
University of Bath

Characterisation of novel ubiquitin-dependent mechanisms in the regulation of the cell cycle

Natalie Vaughan

A thesis submitted for the degree of Doctor of Philosophy

University of Bath

Department of Biology and Biochemistry

March 2018

Acknowledgements

I would like to thank my supervisor Dr Julien Licchesi for his continual patience and support throughout my PhD. In addition, I would like to thank Dr Andrew Chalmers for his support as a second supervisor.

I would like to thank the University of Bath Research Studentship, University of Bath Alumni & Friends, the Royal Society, the Biochemical Society and COST ACTION BM1307 PROTEOSTASIS for funding. I would also like to thank the University of Bath Microscopy and Analysis Suite for their expertise in microscopy and technical assistance regarding image acquisition and data analysis. With special thanks to Dr Catherine Lindon, Dr Kathreena Kurian and Dr Mariann Bienz for their help and collaboration on this project.

I would like to thank all present and past members of the Licchesi, Caunt, Chalmers, Whitley, Williams and van den Elsen laboratories who have made my PhD a memorable and enjoyable experience. Special thanks go to Sarah Jasem, who has been the most supportive lab mate I could have asked for. In addition, I would also like to thank Cassidy Bayley who supported me both academically and personally, I honestly do not know what I would have done without her. Furthermore, I would like to thank Dr Tülay Gülşen, Naomi Lyons, Dr William Bradshaw, Elena Corujo, Steve Weston, Dr Emanuele Kendrick and members of the “Never gonna quiz you up” quiz team for being such great friends during my time at Bath.

I would also like to thank my family who have supported me throughout my PhD. I could not have asked for a more encouraging family who have supported me wholeheartedly, thank you for always believing in me. Finally, thank you to all of my amazing friends from home, Durham University and Bristol who despite having no idea what I was doing, completely supported me.

In memory of Dr Jim Caunt, who was a brilliant scientist, mentor, and friend. He is very much missed.

Abstract

Ubiquitination is a type of post translational modification that principally functions in protein turnover via the ubiquitin-proteasome system (UPS), however it also has roles in endocytosis, cell signalling, and DNA repair. Ubiquitination is a diverse modification with each ubiquitin molecule able to form differently linked polyubiquitin chains by any one of the seven lysine residues or the N-terminal methionine residue. Ubiquitin is conjugated to target proteins by enzymes called ubiquitin E3 ligases. HECTD1 is a HECT (Homologous to the E6-AP Carboxyl Terminus) E3 ubiquitin ligase. The HECT domain is responsible for HECTD1 E3 ligase activity and is conserved from yeast to humans. Interestingly, our lab showed that, at least *in vitro*, HECTD1 synthesises K29/K48-linked ubiquitin chains. The cellular function of these atypical ubiquitin chains remains poorly understood. Therefore, in order to elucidate the function of this chain type, gain and loss-of-function studies of HECTD1 in mammalian cells were carried out. This revealed that HECTD1-depleted or CRISPR/Cas9 knockout cells, exhibited reduced cell proliferation, were enriched in metaphase, and were slower to progress through mitosis. Furthermore, expression of HA-FL-mHectd1 revealed a mitotic spindle specific localisation during metaphase further suggesting a mitotic function. Strikingly, only the catalytically active wild-type HECTD1 was able to rescue the observed cellular phenotypes, strongly suggesting that K29/K48 chains might be involved in cell cycle function. Taken together, this suggests that cells are being delayed at the spindle assembly checkpoint (SAC), and that HECTD1 may regulate mitotic spindle formation, however further work would be required to establish this. In order to define the mechanism involved and identify cell cycle components, which might carry K29 chains assembled by HECTD1, we have optimised the enrichment of K29 chains from synchronised cells using the $TRABID_{1-200}$ ubiquitin binding domain. Finally, given that HECTD1 has been implicated in Wnt signalling, cell migration, and the cell cycle, and now in cell proliferation, its role in cancer was studied. It was identified that overexpression of mHectd1 wild-type only resulted in increased proliferation in glioblastoma cells, and that depletion of HECTD1 resulted in decreased cell proliferation, suggesting that inhibition of HECTD1 may lead to a reduction in cell proliferation. Thus, demonstrating the potential of targeting the catalytic activity of HECTD1 to provide a novel therapeutic for glioblastoma.

Abbreviations

5-AZA	5-aza-2'-deoxycytidine
53BP1	p53-binding protein 1
ABP	Activity-based probe(s)
AHR	Aryl hydrocarbon receptor
AMP	3',5'-cyclic adenosine monophosphate
AMPK	AMP-activated protein kinases
A-MT	Astral microtubules
ANK	Ankyrin repeats
ANOVA	Analysis of variance
ANXA7	Annexin A7
APC	Adenomatous polyposis coli
APC/C	Anaphase promoting complex/Cyclosome
AQUA	Absolute quantification
ARNT	Aryl hydrocarbon receptor nuclear translocator
ATM	Ataxia telangiectasia mutated kinase
ATP	Adenosine-5'-triphosphate
ATR	Ataxia telangiectasia and Rad3-related protein
ATX3	Ataxin 3
AREL1	Apoptosis-resistant E3 Ub protein ligase 1
BAC	Bacterial artificial chromosomes
BAP1	BRCA1 associated protein 1
BAX	Bcl-2-associated X
BCA	Bicinchoninic acid
BSA	Bovine serum albumin
BRCA1	Breast cancer 1
BrdU	Bromodeoxyuridine
BRISC	BRCC36 isopeptidase complex
BUB3	Budding uninhibited by benzimidazoles 3 homolog
CAN	Cancer candidate
CDC	Cell division cycle protein
CDH	Cadherin 1
CDK	Cyclin-dependent kinase
CM	Catalytic mutant
CNKSR2	Connector enhancer of kinase suppressor of ras 2
ChIP	Chromatin immunoprecipitation pulldown
CHK	Checkpoint kinase
Ch-TOG	Colonic and hepatic tumor overexpressed gene protein
CHX	Cycloheximide
CP110	Centriolar coiled-coil protein of 110 kDa
CPC	Chromosome passenger complex
CRISPR	Clustered regularly interspaced short palindromic repeats
CUL1	Cullin1
CYLD	Cylindromatosis
DAPI	4', 6'-diamino-2-phenylindole
DAPK1	Death associated protein kinase 1
DDB1	Damage specific DNA binding protein 1
ddH2O	Double distilled water
DECODE	Decipherment of DNA elements
DIC	Differential interference contrast
DMEM	Dulbecco's modified Eagle's medium
DMSO	Dimethyl sulphoxide
DNA	Deoxyribonucleic acid
DNMTs	DNA methyltransferases
DTT	Diothiothreitol
DUB	Deubiquitinase
Dvl2	Dishevelled
EB1	End-binding protein 1
EBNA	Epstein–Barr nuclear antigen 1
ECL	Enhanced chemiluminescence substrate
EDD	E3 identified by differential display
EDTA	Ethylenediaminetetraacetic acid
EGTA	Ethylene glycol-bis(β-aminoethyl ether)-N,N,N',N'-tetraacetic acid
EGF	Epidermal growth factor
EGFR	Epidermal growth factor receptor
ENaC	Epithelial sodium channel
EMEM	Eagle's minimum essential media

EMT	Epithelial to mesenchymal transition
FA	Focal adhesion
FACS	Fluorescence activated cell sorting
FBS	Fetal bovine serum
FBW7	F-box/WD repeat-containing protein 7
FGFR1	Fibroblast growth factor receptor 1
FL	Full length
FUCCI	Fluorescent ubiquitination-based cell cycle indicator
G1	Gap 1 phase
G2	Gap 2 phase
Gadd45	Growth arrest and DNA damage 45
GAPDH	Glyceraldehyde 3-phosphate dehydrogenase
GBM	Glioblastoma
GEF	Guanine exchange factor
GFP	Green fluorescent protein
GRAIL	Gene related to anergy in lymphocytes
GRB10	Growth Factor Receptor Bound Protein 10
GST	Glutathione S-transferase
GTP	Guanosine triphosphate
GTEx	Genotype-Tissue Expression
HA	Human influenza hemagglutinin
HACE1	HECT domain and ankyrin repeat containing E3
HATs	Histone acetyltransferases
HCC	Hepatocellular carcinoma
HDACs	Histone deacetylases
HDMs	Histone demethylases
HECT	Homologous to the E6AP carboxyl terminus
HECTD1	Homologous to the E6AP carboxyl terminus- domain 1
HeLa	Henrietta Lacks (cell line)
HEK293	Human embryonic kidney (cell line)
HEPES	4-(2-hydroxyethyl)-1-piperazineethanesulphonic acid
HERC	HECT and RLD domain containing
hESCs	Human embryonic stem cells
HNPCC	Hereditary nonpolyposis colon cancer
HOIL1	Heme-oxidized IRP2 ubiquitin ligase 1
HOIP	HOIL-1-interacting protein
HPRT1	Hypoxanthine Phosphoribosyltransferase 1
HPV	Human papillomavirus
hr	Hour
HRP	Horseradish peroxidase
HSP	Heat shock protein
HUWE1	HECT, UBA and WWE domain containing 1
IDH1	Isocitrate dehydrogenase 1
IF	Immunofluorescence
IGF1R	Insulin-like growth factor 1 receptor
IgG	Immunoglobulin G
IκB	Inhibitor of nuclear factor Kappa B kinase subunit Beta
INCENP	Inner centromere protein
IP_3	1,4,5-trisphosphate
IQGAP1	IQ motif containing GTPase activating protein 1
JAMMs	Josephins, and JAB1/ MPN/ MOV34 metalloenzymes
JMJD5	Jumonji domain protein 5
kb	Kilobases
KD	Knock Down (i..e transient)
kDa	Kilodaltons
K-fibre	Kinetochore fibres
K-MT	Kinetochore microtubules
KO	Knock out (i.e. genetic)
K6	K-linked ubiquitin chains (same abbreviation style for other Ks)
LATS1	Large tumor suppressor kinase 1
LB	Lysogeny broth
LSM	Laser scanning microscopy
LUBAC	Linear ubiquitin chain assembly complex
M phase	Mitosis
MAD2	Mitotic arrest deficient 2
MAPK	Mitogen-activated protein kinase
MCAK	Mitotic centromere-associated kinesin
MCC	Mitotic checkpoint complex
MCM	Minichromosome maintenance complex component

MDM2	Mouse double minute 2
MEI1	Meiotic double strand break formation protein
MEM	Minimum essential media
MGMT	O-6-methylguanine-DNA methyltransferase
MHC	Major histocompatibility complex
MINDY	Motif interacting with Ub-containing novel DUB family
MIZ1	Myc-interacting Zn finger protein-1
MPS1	Mucopolysaccharidosis type I
mRNA	Messenger ribonucleic acid
miRNA	Micro-ribonucleic acid
MISU	Myc-induced SUN domain-containing protein
MSP58	Microspherule protein 58
MSPS	Mini-spindles
MT	Microtubules
MTT	3-(4,5-dimethylthiazol-2-yl)-2,5-diphenyltetrazolium bromide
N4BP1	NEDD4 binding protein 1
NDFIP	Nedd4 family interacting protein
NEBD	Nuclear envelope breakdown
NEDD4	Neural precursor cell expressed developmentally down-regulated protein 4
NEDD4-L	Neural precursor cell expressed, developmentally down-regulated 4-like
NEDL2	Nedd4-like ubiquitin ligase 2
NEK2A	NIMA (never in mitosis gene A)-related kinase 2A
NEMO	NF-Kappa-B essential modifier
NES	Nuclear export sequence
NEURL4	Neuralized E3 ubiquitin protein ligase 4
NFκB	Nuclear factor Kappa B subunit 1
nK-MT	Non-kinetochore microtubules
NLS	Nuclear localisation sequence
NSCLC	Non-small cell lung cancer
NSF	*N*-ethylmaleimide-sensitive factor
NT	Non-targeting
NuMA	Nuclear mitotic apparatus protein
NZF1	NPL4 zinc finger 1
OTU	Ovarian tumour proteases
OTULIN	OTU deubiquitinase with linear linkage specificity
PA	Propargylamide
PAX5	Paired box family protein 5
PBS	Phosphate-buffered saline
PBST	Phosphate-buffered saline Tween 20
PCR	Polymerase chain reaction
PDX1	Pancreas/duodenum homeobox protein 1
PEI	Polyethylenimine
PFA	Paraformaldehyde
PHD	Plant homeodomain
PI	Propidium Iodide
PI3K	Phosphatidylinositol-4,5-bisphosphate 3-kinase
PIPK1	Phosphatidylinositol 4-phosphate 5-kinase type-1 gamma
PLK1	Polo-like kinase 1
PP6	Protein phosphatase 6
PPARγ	Peroxisome proliferator-activated receptor
PTEN	Phosphatase and tensin homolog
Pub-1/-2	PolyUridylate binding
PVDF	Polyvinylidene fluoride
RAP80	Receptor associated protein 80
RASSF	Ras association domain family member
Rb	Retinoblastoma protein
RBR	Ring-between-ring
REST	REI silencing transcription factor
RhoA	Ras homolog gene family, member A
RING	Really new interesting gene
RIPA	Radioimmunoprecipitation assay buffer
RISC	RNA-induced silencing complex
RNA	Ribonucleic acid
RNAi	RNA interference
RNA Pol II	RNA polymerase 2
RNF8	Ring finger protein 8
ROS	Reactive oxygen species
RPN1	Ribophorin I
RPS18	Ribosomal protein S18

Rsp5	Reverses Spt- phenotype 5
RTKs	Receptor tyrosine kinases
RT-qPCR	Reverse transcription quantitative polymerase chain reaction
S phase	Synthesis phase
SAC	Spindle assembly checkpoint
SCF	Skp1-Cullin-F-box protein
SDS	Sodium dodecylsulphate
SDS-PAGE	Sodium dodecylsulphate polyacrylamide gel electrophoresis
S.E.M	Standard error of the mean
SGK1	Serum and glucocorticoid regulated kinase 1
SH2	Src homology 2
SILAC	Stable isotopic labelling by amino acids in cell culture
siRNA	Short interfering RNA
Skp	S-phase kinase associated
SMURF	Smad ubiquitination regulatory factor
SP	SMARTpool
STED	Stimulated emission depletion
STM1	Stathmin
SUMO	Small ubiquitin-like modifier
TAE	Tris/Acetate/EDTA buffer
TARA	Trio-associated repeat on actin
TBP	TATA-binding protein
TERT	Telomerase reverse transcriptase
TEV	Tobacco etch virus
TGF	Tumour growth factor
TIAM1	T-lymphoma invasion and metastasis-inducing protein 1
TMT	Tandem mass tag
TMZ	Temozolomide
TNFα	Tumour necrosis factor alpha
TOM1	Temperature dependent organisation in mitotic nucleus 1
TOPBP1	DNA Topoisomerase II binding protein 1
TRABID	TRAF-binding domain-containing protein
TRAF6	TNF receptor associated factor 6
TRAIP	TRAF interacting protein
TRIP12	Thyroid hormone receptor interactor 12
TSS	Transcription start site
tTA	Tetracycline transactivor
TUBE	Tandem ubiquitin binding entities IP lysis buffer
TUSC4	Tumour suppressor candidate 4
Tween-20	Polyoxyethylene sorbitan monolaureate
Ub	Ubiquitin
UBA	Ubiquitin associated domains
UBASH3B	Ubiquitin associated and SH3 domain containing B
UBB	Ubiquitin B
UBD	Ubiquitin binding domain
UBE3C	Ubiquitin protein ligase E3C
UbiCREST	Ubiquitin chain restriction analysis
UbiChEM-MS	Ubiquitin Chain Enrichment Middle-down Mass Spectrometry
UBR5	Ubiquitin protein ligase E3 component N-Recognin 5
UCH	Ubiquitin c-terminal hydrolase
UFD	Ubiquitin fusion degradation
UPS	Ubiquitin proteasome system
UCSC	University of California Santa Cruz
USP	Ubiquitin-specific protease
UTR	Untranslated region
VDAC1	Voltage-dependent anion channel 1
VME	Vinylmethylester
vOTU	viral OTU
VPRBP	Vpr-binding protein
WB	Western blot
Wnt	Wingless-type MMTV integration site family member
WT	Wild-type
WWP-1/-2	WW Domain Containing E3 Ubiquitin Protein Ligase 1
γTuRC	γ-tubulin ring complex

Table of contents

Table of figures

Table of tables

Chapter 1: Introduction

1.1. The cell cycle

The cell cycle is a fundamental process that needs to be tightly regulated. The discovery of key regulators of the cell cycle led to the Nobel Prize in Physiology or Medicine being awarded to Leland H Hartwell, Timothy Hunt, and Paul M Nurse in 2001. The cell cycle functions to yield two daughter cells that contain the same genetic information. This process is divided into two main stages, the phase in which the cell grows and duplicates its DNA (interphase) and the phase where the cell physically divides into two identical daughter cells (M phase) (Vermeulen, *et al*. 2003). Interphase is further subdivided into G1 (Gap 1), G2 (Gap 2), and S (synthesis) phase. The gap phases, so called as they represent the "gaps" between DNA replication and mitosis, function to gather information to determine the readiness of the cell to enter S or M phase (Figure 1.1) (Norbury, & Nurse. 1992; Vermeulen, *et al*. 2003). The first gap, G1 phase, is the stage of the cell cycle where the cell prepares for DNA synthesis, and precedes S phase, where 2N DNA content becomes 4N. The second gap phase, G2, prepares cells for mitosis, a process that is further divided into five stages (Figure 1.2) (Norbury, & Nurse. 1992).

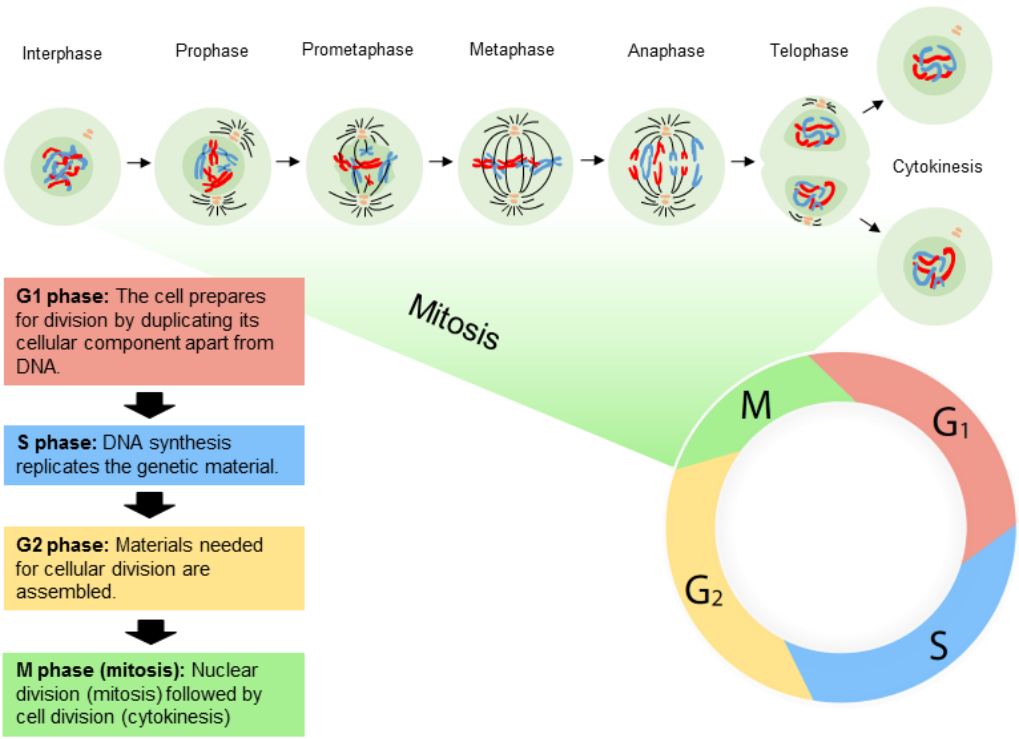

Figure 1.1. Diagram illustrating the main phases and events in the cell cycle. The cell cycle is subdivided into G1, S, G2, and M phase. M phase is then divided into 5 further stages allowing mechanical division of the DNA and the cellular components. Adapted from Vermeulen, *et al*. 2003 and Inside the Cell I Cellular Reproduction: Multiplication by Division, U.S. Department of health and human services. NIH Publication No. 05-1051, September 2005.

1.1.1. Mitotic stages

M phase comprises Prophase, Prometaphase, Metaphase, Anaphase, Telophase, and finally cytokinesis, where the cell physically divides into two daughter cells (Figure 1.2A). Mitosis is the most mechanical phase of the cell cycle; whereby large reorganisation of the cell is needed to mediate nuclear division and cellular division (Pines. 2006).

During prophase two main events occur, the condensation of mitotic chromosomes, mediated by a five-subunit complex called condensin, and the formation of the mitotic spindle (Sager, *et al.* 1986; Strunnikov. 2003). The breakdown of the nuclear envelope and movement of centrosomes to each pole marks the initiation of prometaphase, where chromosomes start to move towards the centre of the cell (Aubin, *et al.* 1980; Beaudouin, *et al.* 2002). During this time, the kinetochores begin to form around the centromeres, a central process in the joining of the sister chromatids and in linking chromosomes to the mitotic spindle (Hayden, *et al*. 1990). The kinetochore consists of two regions; the inner kinetochore, which is associated with the centromere and the outer kinetochore, which interacts with the microtubules (Brinkley & Stubblefield. 1966; Van Hooser & Heald. 2001). Microtubules originating from the centrosomes at either pole reach the chromosomes and attach to the kinetochores. Dynamic instability of the microtubules allows for the “search and capture” of the chromosomes with their plus ends (Hayden, *et al*. 1990; Holy & Leibler. 1994). Chromosomes are captured by the lateral surface of the microtubule rather than the tip, forming lateral attachments. Eventually kinetochores interact with more microtubules, where the plus ends become embedded into the kinetochore plate (Rieder & Alexander. 1990; Hayden, *et al*. 1990; Merdes & De May. 1990). Under normal attachment of the microtubules to the kinetochore, amphitelic attachment, the microtubules originate from opposite poles in a bipolar fashion (Figure 1.2B) (Musacchio & Salmon. 2007). However, because the microtubule-kinetochore attachment occurs via microtubules from one pole first and then from the other pole, monotelic, syntelic, or merotelic attachments often precede amphitelic attachments (Figure 1.2B) (Musacchio & Salmon. 2007). In the instance of monotelic and syntelic attachments, a “wait” signal is in place to prevent chromosome segregation, this is called the spindle assembly checkpoint (SAC) and is active until the centromeres are under sufficient tension (Stern & Murray. 2001; Uchida, *et al.* 2009).

During metaphase, once the chromosomes are attached to the microtubules, the chromosomes then move to align themselves in the middle of the cell (Rieder & Alexander. 1990). This alignment along the equatorial plane is aided by counterbalance forces that originate from the spindle microtubules and the kinetochores (Inoué & Salmon. 1995; Heald, *et al.* 1996). During metaphase, the spindle assembly checkpoint remains active, until all chromosomes are aligned along the equatorial plane and correct (“end-on”) kinetochore

attachment has occurred (Stern & Murray. 2001; Kuhn & Dumont. 2017). Anaphase begins only once the checkpoint has been satisfied, and results in the separation of sister chromatids (Rieder, *et al*. 1994). The process of anaphase occurs in two phases, Anaphase I, where the sister chromatids begin to segregate to opposite poles of the spindle, and Anaphase II, where elongation of the spindle and further separation of the sister chromatids occurs (Baskin & Cande. 1990; Pines. 2006). The fifth and final phase of mitosis, telophase, is the process that separates the chromatids into two daughter cells. It is during this phase that the nuclear envelope forms around each set of chromosomes in the daughter cells, and the chromosomes uncoil (Chaudhary & Courvalin.1993; Schwalm. 1969). Finally, the cleavage furrow develops at the location of the metaphase plate, and aides in final splitting of the membrane resulting in the physical separation of the daughter cells (Barr & Gruneberg. 2007).

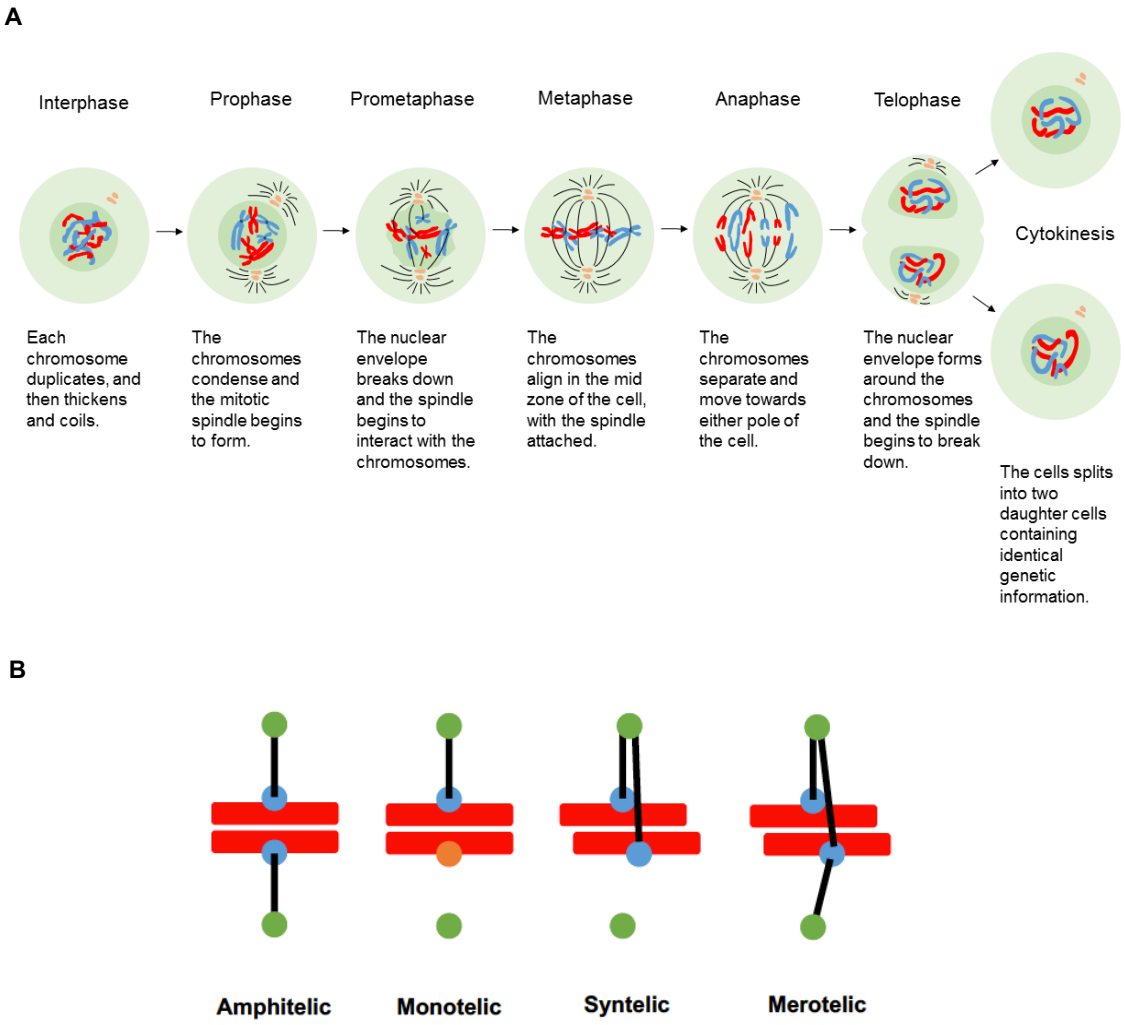

Figure 1.2. Diagram illustrating the stages of mitosis. A) Chromosomes condense, the nuclear envelope breaks down, chromosomes align in the centre of the cell, separate, nuclear envelope reforms resulting in cell division. Adapted from Inside the Cell I Cellular Reproduction: Multiplication by Division, U.S. Department of health and human services. NIH Publication No. 05-1051, September 2005. B) In the event of improper attachment of the mitotic spindle to the kinetochores (monotelic, syntelic), a "wait" signal known as the spindle assembly checkpoint (SAC), prevents anaphase onset. In amphitelic attachment the centromeres are under sufficient tension to remove the "wait' signal, SAC, allowing for proper division of the chromosomes. This is also true for merotelic attachment but in this case it will result in lagging chromosomes, and improper division of chromosomes. In both monotelic and syntelic attachments, neither create sufficient centromeric tension, therefore resulting in the "wait" signal persisting, preventing anaphase onset. Adapted from Musacchio & Salmon (2007).

1.1.2. Cell cycle checkpoints

Cell cycle checkpoints are supervision mechanisms that ensure the correct order, integrity, and fidelity of the cell cycle. Briefly, the three major cell cycle checkpoints are, the G1 checkpoint, the G2 checkpoint, and the spindle assembly checkpoint (SAC) (Murray. 1994) (Figure 1.3). The G1 checkpoint is the first checkpoint of the cell cycle, and controls entry into S phase. This checkpoint is also known as the restriction point, whereby cells ensure that there is the correct environment to divide, after which they are committed to the cell cycle (Johnson, & Skotheim. 2013). Two Cyclin-dependent kinases (CDKs), CDK4/6-Cyclin D and CDK2-Cyclin E, work to relieve inhibition of retinoblastoma protein (Rb) and E2F, allowing for transcription of genes required for DNA replication (Besson, *et al.* 2008). The checkpoint is active under TGF-β signalling, DNA damage, replicative senescence, and growth factor withdrawal (Murray. 1994). DNA damage activates response pathways mediated by ATM/ ATR and CHK1/2 kinases, which block CDK activity, therefore leading to cell cycle arrest because the G1 checkpoint is still active (Reinhardt & Yaffe. 2009). Furthermore, p53 is a critical component of DNA damage checkpoints, particularly in the G1 checkpoint (Giono & Manfredi. 2006).

The G2 checkpoint is known as the DNA damage checkpoint, specifically because it prevents cells with DNA damage from entering mitosis (Löbrich & Jeggo. 2007). Both WEE1 and MYT1 function to keep Cyclin B-CDK1 inactive because it is vital for ensuring the G2 to M phase transition (Takizawa & Morgan. 2000). Activation of CDK1 is thought to occur via the kinases Aurora A and PLK1 (Polo-like kinase 1) (Lens, *et al*. 2010). DNA damage results in the inhibition of CDK1 by the ATM/ ATR kinases, preventing the cells from entering mitosis (Nam & Cortez. 2011). Here, p53 is also important for regulating entry into mitosis, where CDK1 is inhibited simultaneously by three transcriptional targets of p53 GADD45, p21, and 14-3-3 (Taylor & Stark. 2001).

Finally, the SAC occurs during mitosis, and prevents anaphase onset until each kinetochore is attached to the mitotic spindle, ensuring proper chromosome segregation (Murray. 1994; Stern & Murray. 2001). The SAC comprises the serine/threonine kinases MPS1, and BUB1, as well as MAD1, MAD2, BUB3, and BUBR1 (Hoyt, *et al.* 1991; Li & Murray. 1991; Weiss & Wilney. 1996). Together, these proteins function to ensure proper chromosome segregation, by delaying anaphase onset until each kinetochore is attached to the mitotic spindle. This is achieved by the sequestering of CDC20 by these proteins to inactive the APC/C (Fang, *et al.* 1998; Hwang, *et al.* 1998; Kramer, *et al.* 1998). The APC/C ubiquitinates and therefore triggers proteasomal degradation of Cyclin B1 and securin, the separase inhibitor, triggering sister chromatid separation and exit from mitosis (Glotzer, *et al*. 1991; Holloway, *et al.* 1993; Cohen-Fix & Koshlan. 1999). The SAC is responsible for the

formation of the Mitotic Checkpoint Complex (MCC), an inhibitory complex, responsible for sequestering CDC20. The MCC is a heterotetramer composed of CDC20, MAD2, BUBR1, and BUB3 (Sudakin, *et al.* 2001). Kinetochores play a central role in SAC signalling, whereby the MCC forms at unattached kinetochores, sequestering and therefore inhibiting CDC20, preventing anaphase onset. Furthermore, it has been suggested that the APC/C degrades CDC20 to maintain the checkpoint, not to release CDC20 from the MCC (Nilsson, *et al*. 2008). Upon microtubule binding, the SAC is satisfied and CDC20 is released (Rieder, *et al.* 1995). The exact mechanism by which this occurs is still largely unknown however, the APC/C subunit APC15 has been shown to be required for SAC deactivation and release of the MCC in response to microtubule attachment (Mansfeld, *et al.* 2011). A lack of inter-kinetochore tension has been associated with activation of the SAC in budding yeast cells, in contrast stretching of the kinetochores results in SAC inactivation (Stern & Murray. 2001; Uchida, *et al.* 2009). Therefore, it can be assumed that microtubule tension creates sufficient inter-kinetochore tension to satisfy the checkpoint.

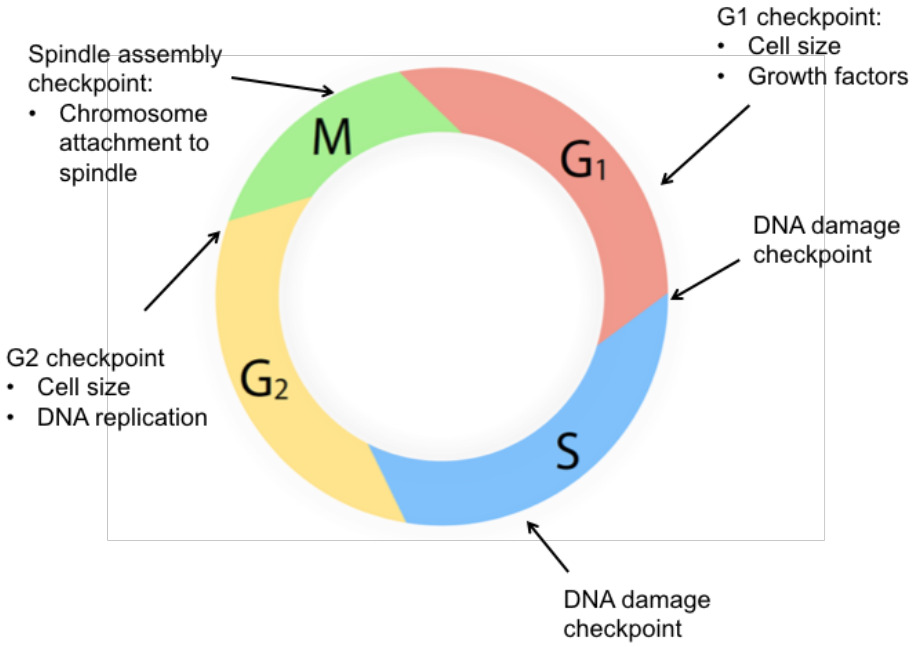

Figure 1.3. Cell cycle checkpoints. The G1 checkpoint ensures that the cell is in the right environment to divide, after which point the cell is committed to the cell cycle. This is followed by DNA damage checkpoints at the G1/S border and in S phase. The G2 checkpoint prevents cells with damaged DNA from entering mitosis, and the spindle assembly checkpoint ensures that the chromosomes are attached to the spindle before anaphase onset can occur (Murray. 1994). Own figure.

1.2. Regulation of the cell cycle by post-translational modifications

Protein post-translational modifications (PTMs) such as phosphorylation and ubiquitination play key roles in driving cells through the different phases of the cell cycle. Phosphorylation is the best characterised PTM, and in the cell cycle it is conferred by serine/threonine-specific kinases, called CDKs. These kinases are activated at different stages of the cell cycle and ensure the faithful progression of the cell cycle (Lim & Kaldis. 2013). CDK/Cyclin complexes were first discovered as cell cycle regulators from work carried out in yeast. A single CDK, Cdc28 in *S. Cerevisiae* and Cdc2 in *S. Pombe*, was found to promote transitions between different cell cycle phases (Nurse, *et al.* 1976; Nurse & Thuriaux; Beach, *et al.* 1982; Reed, *et al.* 1982). CDKs control the cell cycle through oscillation of activity mediated by proteins called Cyclins (Pines. 2011; Lim & Kaldis. 2013). They are expressed constitutively in cells but their activity is controlled by the availability of their binding partner, Cyclins. Therefore, the turnover of Cyclins is fundamental for the temporal regulation of CDKs' activity and the control of cell cycle (Evans, *et al*. 1983; Shaik, *et al.* 2012). Using sea urchin embryos as a model system, Cyclin B1 was found to accumulate and disappear suggesting for the first time protein turnover was key to cell division (Evans, *et al.* 1983). The work carried out in Tim Hunt's lab led to the hypothesis that synthesis of Cyclin B1 drove cells into mitosis, and its destruction allowed cells to complete cell division (Murray. 2004). Cyclin B1 was later described to complex with CDC2 (CDK1) to initiate mitotic onset (Pines & Hunt. 1987; Draetta & Beach. 1988). Importantly, the destruction of Cyclin B1 was later found to be mediated by the ubiquitin proteasome system (UPS) (Glotzer, *et al.* 1991). Defining how Cyclin B1 is regulated and the machinery driving protein degradation was pivotal to our understanding of the molecular mechanisms driving cell division.

1.3. Ubiquitination

Protein turnover is essential to maintain cell homeostasis. However, it was not until the early 1980s that the molecular mechanisms mediating protein turnover were uncovered. The discovery of the UPS as a pathway for protein degradation led to the Nobel Prize in Chemistry being awarded to Aaron Ciechanover, Avram Hershko, and Irwin Rose in 2004. Ubiquitin was first identified as a polypeptide, which had lymphocyte-differentiating properties (Goldstein, *et al.* 1975). It was characterised as an 8.5kDa protein, 76 amino acids in length, that was speculated to be found universally in all living cells (Schlesinger, *et al.* 1975). Experiments carried out in reticulocytes found that ubiquitin-mediated proteolysis was ATP-dependent (Ciechanover, *et al.* 1978) and, more specifically, that the formation of a ubiquitin-substrate isopeptide bond was ATP-dependent (Hershko, *et al.* 1980; Ciechanover, *et al.* 1981). The isopeptide bond forms via the C-terminal glycine

residue (G76) of ubiquitin and the ε-amino group of a substrate lysine residue (Pickart. 2001) (Figure 1.4).

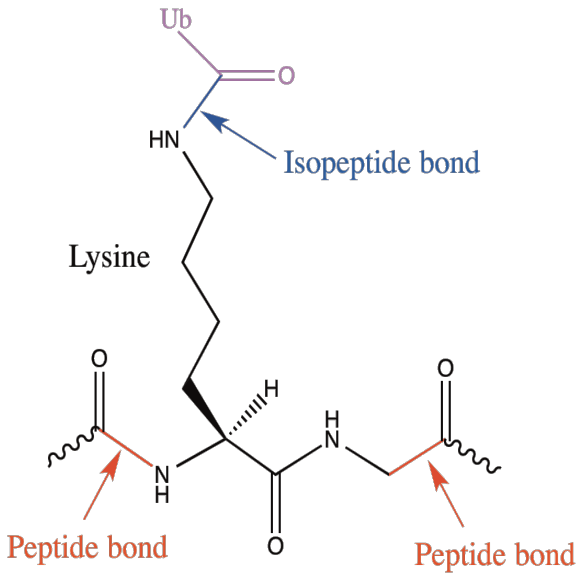

Figure 1.4. Isopeptide bond in lysine ubiquitination. Ubiquitin is attached via its C-terminal glycine residue (G76) and the ε-amino group of the side chain of a substrate lysine residue forming an isopeptide bond. Own figure.

The conjugation of ubiquitin to a target protein requires a cascade of three enzymes, an E1 ubiquitin-activating enzyme (Ciechanover, *et al.* 1982; Haas, *et al.* 1982), E2 ubiquitin-conjugating enzyme, and E3 ubiquitin-protein ligases (Hershko, *et al.* 1983) (Figure 1.5). The E1 enzyme uses ATP in the presence of Mg^{2+} to form an intermediary ubiquitin-adenylate (activated ubiquitin), which is then bound to the catalytic cysteine of the E1 via a thioester bond (Ciechanover, *et al.* 1981; Ciechanover, *et al.* 1982). The activated ubiquitin is transferred from the E1 enzyme to a catalytic cysteine on the E2 enzyme, again forming a thioester bond. The final stage of ubiquitin transfer is mediated by an E3 ligase, which transfers ubiquitin onto a lysine residue on the substrate forming a isopeptide bond with its ε-amino group (Hershko, *et al.* 1983). The E3 ligase can either behave as a scaffold to bring the E2 into close proximity to the substrate to aid ubiquitin transfer (e.g. RING ligases), or can go via an intermediate step where ubiquitin is accepted onto the E3 ligase via the formation of a thioester bond, before transferring the ubiquitin to the substrate (e.g. HECT ligases) (You & Pickart. 2001; Wang, *et al*. 2006; Kim & Huibregtse. 2009). Ubiquitin-conjugated substrates are degraded in an ATP-dependent manner, by a protein complex known as the 26S proteasome, which is conserved from archeabacteria to all eukaryotes (Hershko, *et al.* 1984; Dahlmann, *et al.* 1989).

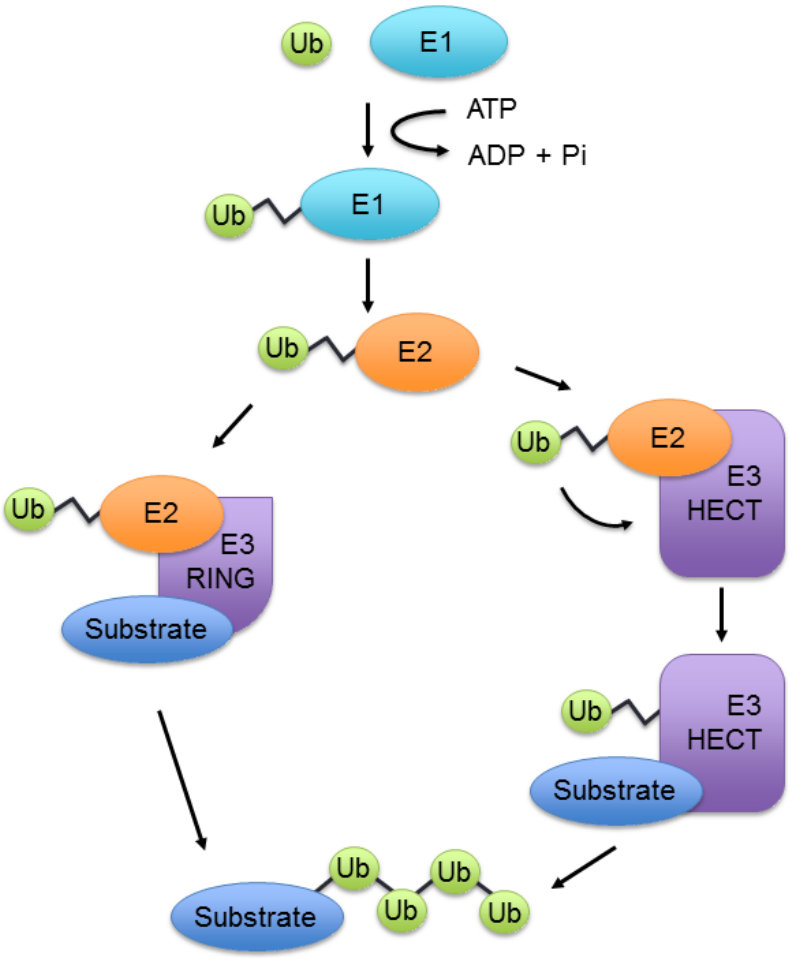

Figure 1.5. Protein ubiquitination cascade. Ubiquitination of a substrate is achieved via an enzymatic cascade. First, the E1 ubiquitin-activating enzyme, in an ATP-dependent mechanism, forms an activated intermediary ubiquitin-adenylate. This intermediary ubiquitin-adenylate is then bound to the catalytic cysteine of the E1 enzyme. The E1 then transfers the activated ubiquitin to the E2 conjugating enzyme. Finally, the ubiquitin is transferred from the E2 to the substrate lysine facilitated by an E3 ubiquitin ligase to form an isopeptide bond with the lysine ε-amino group. This can be facilitated by the E3 by the formation of an E3-ubiquitin intermediate or it can indirectly attach the ubiquitin to the substrate. The diagram shows the mechanism of RING E3 ligases compared to HECT E3 ligases, which results in ubiquitin conjugation to the substrate. Adapted from Di Fiore, *et al.* (2003).

Ubiquitin is a highly conserved and diverse protein modifier. It can either be conjugated to a substrate as a monomer (mono-ubiquitination) or as polymers (polyubiquitination), forming ubiquitin chains. Ubiquitin contains seven lysine residues K6, K11, K27, K29, K33, K48 and K63 (Figure 1.6), which are able to form an isopeptide bond with the C-terminus of another ubiquitin molecule. In addition, linear ubiquitin chains can form through the N-

terminal Met1 residue on ubiquitin forming linear ubiquitin chains (Kirisako, *et al.* 2006). Therefore, two ubiquitin molecules can assemble through 8 linkages in order to form a chain (see section 2.3) (Komander. 2009). The substrate selectivity of this pathway is conferred through the enzymatic cascade in which there are many more E3 enzymes than E1 and E2 enzymes. The human genome encodes two E1-activating enzymes, 37 E2-conjugating enzymes and >600 E3 ligases (Deshaies & Joazeiro. 2009). Ubiquitination is a reversible modification, and substrates can indeed be deubiquitinated by proteases known as deubiquitinases (DUBs) (Nijman, *et al.* 2005). The human genome encodes around 100 DUBs, which function to mediate the removal and processing of ubiquitin (Nijman, *et al.* 2005; Clague, *et al.* 2013). DUBs were initially subdivided into five families: ubiquitin C-terminal hydrolases (UCHs), ubiquitin-specific proteases (USPs), ovarian tumour proteases (OTUs), Josephins, and JAB1/ MPN/ MOV34 metalloenzymes (JAMMs). While the UCHs, USPs, Josephins and OTU are cysteine proteases, the JAMM DUBs are zinc metalloproteases (Komander, *et al.* 2009; Clague, *et al.* 2013). However, more recently, a new family of DUBs have been identified known as motif interacting with Ub-containing novel DUB family (MINDY) (Abdul Rehman, *et al*. 2016).

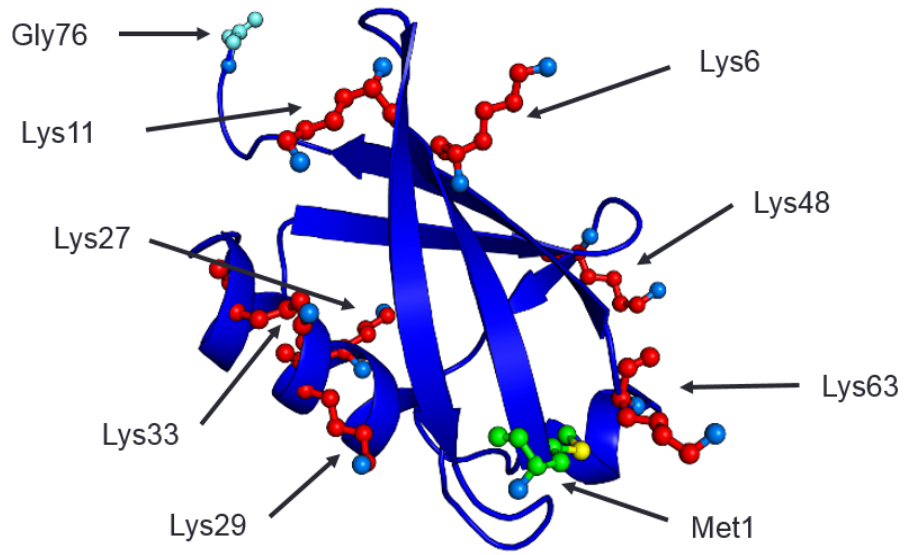

Figure 1.6. The structure of ubiquitin. Ubiquitin contains 7 lysine residues that facilitate the formation of an isopeptide bond; K(Lys)6, 11, 27, 29, 33, 48, and 63. In addition, ubiquitin can form a peptide bond via the N-terminal Met1. The isopeptide and peptide bonds are formed via the C-terminal Gly76. Annotated figure from the Protein Data Bank (PDB) 1UBQ.

1.3.1. E3 ubiquitin ligases

E3 ubiquitin ligases are classified into four classes: Really Interesting New Gene (RING), Homologous to E6-AP Carboxyl Terminus (HECT), Ring Between Ring (RBR), and U box ligases. Each class is characterised by conserved functional and structural features (Table 1.1).

Table 1.1. The different families of E3 ligases. Domain features, including the presence of a catalytic cysteine, alongside the estimated number of each family in mammals (Ardley & Robinson. 2005).

	Domain features	Catalytic cysteine?	Estimated number in mammals	References
RING	RING: Zn^{2+} coordinating binding domain, recruits the Ub-charged E2.	No	600	Borden. 2000; Pickart. (2001); Satija, *et al*. (2013).
HECT	Bilobed. N lobe: Ub-charged E2 binding. C lobe: Catalytic Cys. With a flexible hinge domain in-between.	Yes	28	Rotin & Kumar. (2009); Grau-Bove, *et al.* (2013).
RBR	RING 1: domain recruits Ub-charged E2. IBR: In-between RING domain. RING 2: contains catalytic Cys. Functional hybrid of RING and HECT.	Yes	12	Marín, *et al.* (2004); Spratt, *et al*. (2014).
U-box	Similar fold to RING domain without Zn^{2+} coordination.	No	6	Hatakeyama, *et al.* (2001).

RING ligases have the highest number of family members, followed by the HECT family (Ardley & Robinson. 2005; Grau-Bove, *et al.* 2013; Satija, *et al*. 2013). The main difference between the RING and HECT E3 ligases is their mechanism of ubiquitination (Figure 1.5). RING E3 ligases act as a scaffold protein whereby the type of polyubiquitin chain formed is usually determined by their partner E2. In contrast, HECT E3 ligases transfer ubiquitin from the E2 onto their catalytic cysteine located in the C-terminal HECT domain, via a thioester bond. HECT ligases have been shown to provide specificity for the chain type they synthesise (You & Pickart. 2001; Wang, *et al*. 2006; Kim & Huibregtse. 2009).

RING type ubiquitin ligases are conserved from yeast to humans, and form the largest family compared to the HECT family, containing over 600 ligases in mammals (Satija, *et al*. 2013). RING E3 ligases are further subdivided into; monomeric RING ligases such as GRAIL (gene related to anergy in lymphocytes), homodimeric RINGs for example RNF4, heterdimeric RINGs such as BRCA1-BARD1, the Cullin RING ligase SCF (SKP1-Cullin-F-box protein), and the multisubunit RING ligase, the APC/C (Brzovic, *et al*. 2001; Pickart. 2001; Lineberry, *et al.* 2008; Plechanovová, *et al.* 2011). RINGs are cysteine rich, zinc-binding domains characterised by several defining features. They are defined by a pattern of conserved cysteine and histidine residues, the binding of two atoms of zinc, and finally that zinc ligation is required for domain folding (Borden. 2000). RING E3 ligases can be seen as more of scaffold to support ubiquitin transfer rather than having a catalytic function (Pickart. 2001) (Huibregtse, *et al.* 1995) (Figure 1.5). The HECT ligase family, features and functions are further discussed in section 1.4.

RBR ligases directly catalyse ubiquitin transfer via a catalytic cysteine present in the RING2 domain, whilst ubiquitin-charged E2 binding is conferred by the RING1 domain. This group of multidomain enzymes includes the ligase PARKIN, a regulator of mitophagy, which its dysfunction has been linked to autosomal recessive juvenile parkinsonism (Shimura, *et al.* 2000; Spratt, *et al*. 2014). Finally, the smallest group of ligases comprises the U-box ligases, which are characterised by a domain structurally similar to the RING domain that does not coordinate Zn^{2+}. Given their structural similarity they display similar modes of activity to RING ligases, and can function as a monomer or part of a larger complex of proteins (Ardley & Robinson. 2005). CHIP (also known as STUB1) is the best characterised U-box ligase, and has been shown to interact with molecular chaperones such as HSP70 and HSP90 (Jiang, *et al.* 2001; Zhang, *et al*. 2005).

1.4. HECT ligases

The HECT family of E3 ligases were first discovered when investigating the function of E6-AP. This E3 ubiquitin ligase forms a complex with E6, a protein of the cancer related human papillomavirus (HPV) types 16 and 18 and was shown to function in targeting the p53 tumour-suppressor protein for degradation by the UPS (Scheffner, *et al*. 1993). HECT ligases are defined by the conserved C-terminal HECT domain, composed of ~350 amino acids. It contains a N-lobe, C-lobe, catalytic cysteine, hinge glycine, and an interface for E2 and ubiquitin binding (Huibregtse, *et al.* 1995; Buetow & Huang. 2016). The HECT family of E3 ligases is now known to contain 28 members in humans and 5 members in yeast (Li, *et al.* 2008). The family has typically been subdivided into 3 groups based on N-terminal

domain architecture; the neural precursor cell-expressed developmentally downregulated 4 (NEDD4) family containing 9 members, the HERC family contains 6 members, and the other HECTs which contains 13 members (Rotin & Kumar. 2009). The NEDD4 subfamily contains E3 ligases, which have a C2 domain, three or four WW domains, and a HECT domain (Kumar, *et al.* 1992). The WW domain comprises two conserved tryptophan residues that are spaced 20-22 amino acids apart. The domain forms a hydrophobic ligand-binding groove by three stranded antiparallel beta-sheets (Huang, *et al*. 2000; Verdecia, *et al.* 2000). The C2 domain is a conserved lipid- and protein- binding domain, which can be regulated by calcium in some cases (Nalefski & Falke. 1996).

The HERC subfamily of E3 ligases contains RLDs (RCC1 like domains). This subfamily can be further subdivided into large and small HERCs; the regulator of chromosome condensation 1 (RCC1)-like domains are present multiple times in large HERCs, but only once in small HERCs (Ohtsubo, *et al.* 1987; Rotin & Kumar. 2009). The RLD is characterised by a seven-bladed β-propeller fold, each blade made up of 51-68 amino acids. This seven-bladed β-propeller fold acts as a guanine exchange factor (GEF) for the GTP binding protein Ran (Renault, *et al.* 1998; Renault, *et al.* 2001). The third and final subfamily is called the “other” HECTs and contains all the HECTs that contain neither WW repeats or RLDs (Scheffner & Kumar. 2014). This subfamily contains HECT E3 ligases with many different domains these include ankyrin repeats; WWE domains, zinc fingers, PHD or RING domains, ubiquitin associated domains (UBA), as well as domain which are yet to be characterised, showing a high degree of diversity across this subfamily (Rotin & Kumar. 2009).

However, this widely accepted classification of the HECT family of E3 ligases into 3 subfamilies has been said to be fundamentally incorrect from a phylogenetic viewpoint (Marín. 2010). Insights into the evolution of HECT E3 ligases has revealed that the family of 28 can in fact be subdivided into 16 subfamilies in humans based on structural data. In this investigation into the evolution of the HECT E3 ligases in animals, it was found that most of these 16 subfamilies predate or coincide with the evolution of animals (Marín. 2010). Whilst in eukaryotes as a whole the HECT family can be subdivided into 6 classes, based on phylogenetic analysis based on the last eukaryotic common ancestor (LECA) (Grau-Bove, *et al.* 2013). The HECT system has evolved acquiring diversity through two parallel mechanisms, the first being through protein duplication, and the second by domain shuffling yielding new protein domains used to target substrates. This domain shuffling occurs predominantly at the N-terminus of the protein because the HECT domain being located in the C-terminus. This led to the diversification and expansion of the HECT family especially

in animals providing the substrate specificity needed to conduct diverse cellular functions (Grau-Bove, *et al.* 2013; Scheffner & Kumar. 2014).

1.4.1. Mechanism of ubiquitin transfer by HECT ligases

In order to elucidate the mechanism of action of HECT E3 ubiquitin ligases, the structures of HECT domains of 8 HECT E3 ligases have been solved (E6AP, WWP1, SMURF2, NEDD4-L, HUWE1, yeast Rsp5, NEDD4, and WWP2) (Huang, *et* al. 1999; Verdecia, *et al.* 2003; Ogunjimi, *et al.* 2005; Kamadurai, *et al.* 2009; Pandya, *et al.* 2010; Kim, *et al.* 2011; Maspero, *et al.* 2011; Gong, *et al.* 2015). The HECT domain contains an N-terminal lobe that binds the E2, a flexible linker, and a C-terminal lobe harbouring the catalytic cysteine (Figure 1.7) (Huang, *et* al. 1999). The catalytic core is completed by a conserved C-terminal phenylalanine residue, which mediates the inter-lobe contacts, as seen with Phe896 in NEDD4 (Maspero, *et al.* 2013). In the absence of a ubiquitin-loaded E2, the distance between the catalytic Cys of the HECT domain and that of the unloaded E2 is large (as seen in E6AP 41Å, and WWP1 16Å) (Huang, *et al*. 1999; Verdecia, *et al.* 2003). Indeed, the reported distance of 8Å between the E2-Cys and E3-Cys is not close enough for trans-thioesterification to occur, and it has been proposed that the C-lobe is able to rotate to shorten the distance further (Kamadurai, *et al.* 2009). Therefore, conformational flexibility between the N- and C- lobes is essential for ubiquitin transfer as shown in the crystal structure of the complex between $HECT^{NEDD4L}$ and Ub-loaded UBCH5B complex (Kamadurai, *et al.* 2009).

HECTs use a two-step mechanism to conjugate ubiquitin to the substrate (Figure 1.7). The first step involves the transfer of ubiquitin from an E2 enzyme to the HECT domain forming a thioester-bonded HECT-ubiquitin intermediate (Berndsen & Wolberger. 2014; Buetow & Huang. 2016). The mechanism of the second step where the HECT-ubiquitin intermediate transfers ubiquitin was elucidated by structural studies into the NEDD4 family of HECT E3 ligases. Both studies suggest that after the HECT-ubiquitin intermediate is formed, the C-lobe remains associated with its thioester-linked ubiquitin (Maspero, *et al.* 2013; Kamadurai, *et al.* 2013). The crystal structure of yeast Rsp5 revealed that the C-lobe and ubiquitin together rotate ~130° to face the substrate bound the N-terminal WW domain (Kamadurai, *et al.* 2013). Due to steric hindrance, a ubiquitin-loaded E2 enzyme is unable to access the ubiquitin-binding site of the C-lobe until the E3 transfers the donor ubiquitin to the substrate (Maspero, *et al.* 2013). Therefore, the reloading of ubiquitin, for the next addition of ubiquitin has been theorised to be stimulated by the discharge of ubiquitin from the HECT domain onto the substrate (as described in Section 1.5).

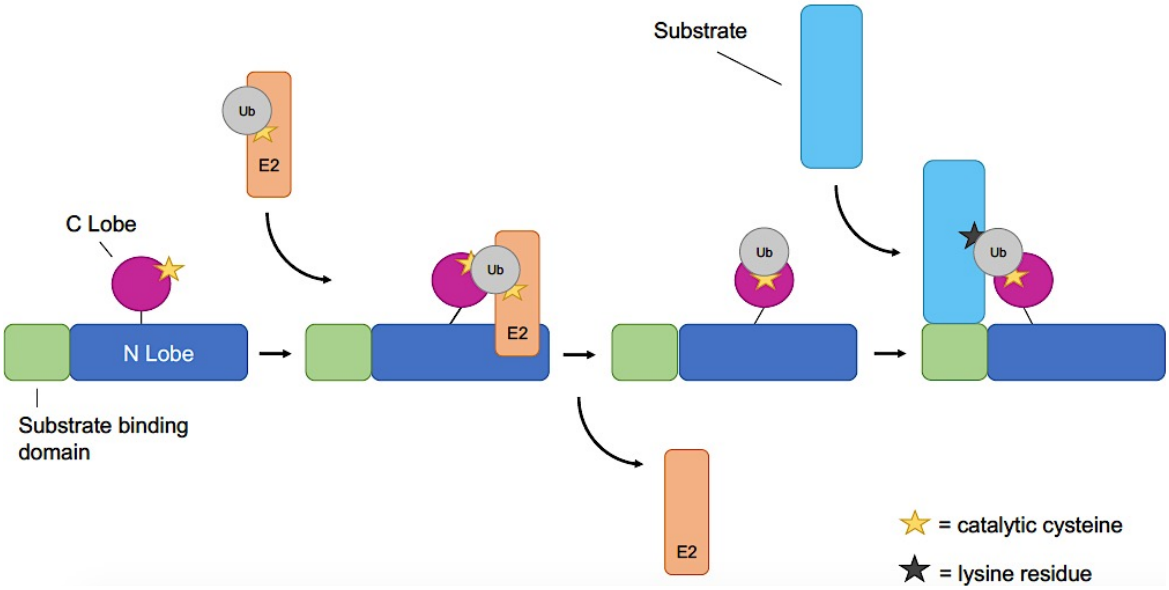

Figure 1.7. Ubiquitin transfer by HECT E3 ligases. Cartoon schematic demonstrating the mechanism of ubiquitin transfer by HECT ligases. The C-lobe of the protein is flexible relative to the N-lobe of the catalytic domain. The N-lobe binds the ubiquitin charged E2 and the C-lobe is able to rotate to bind ubiquitin. Ubiquitin is then transferred from the catalytic cysteine of the E2 to the catalytic cysteine of the C-lobe, in a transthioesterification reaction. Once ubiquitin has been transferred, the E2 enzyme is then released. The substrate binds to the E3 via the substrate binding domain, and the C-lobe rotates so that the catalytic cysteine of the E3 and the lysine residue of the substrate are bought into close proximity for ligation. Adapted from Buetow & Huang (2016).

The catalytic cysteine of HECT E3 ligases is vital for enzyme activity. HECT E3 ligases determine the chain type that is conjugated to the substrate, with different HECTs shown to synthesise different polyubiquitin chains. For example, E6AP forms K48 chains, UBE3C forms K48 and K29 chains, NEDD4 and ITCH form K63 chains and more recently AREL1 (apoptosis-resistant E3 Ub protein ligase 1) was found to assemble K33-linked ubiquitin chains (Wang & Pickart. 2005; Wang, *et al.* 2006; Kim, *et al.* 2007; Scialpi, *et al.* 2008; Kristariyanto, *et al.* 2015). Ubiquitin chain specificity of HECTs is thought to be a function of the C-lobe of the HECT domain, and not determined by the cognate E2 (Kim & Huibregtse. 2009). Indeed, analysis of chimeric and truncated HECTs, containing the N-terminus of yeast Rsp5 and the C-terminal lobes of other HECT E3 ligases showed different ubiquitin-chain linkage specificity compared to that of wild-type Rsp5. Therefore, the C-lobe determines the chain type by the different orientations of the thioester-bound ubiquitin molecule imposed. The last few amino acids present in the C-terminal tail of HECTs may influence chain type specificity together with the determinants of the C-lobe. The last four residues of NEDD4 were replaced with the last three of E6AP, and interestingly, this hybrid HECT switched its activity from synthesising K63 to K48 (Maspero, *et al.* 2013).

Further to what determines chain specificity in HECTs, the mechanism by which the polyubiquitin chains are formed on the substrate is still under debate. The two predominant theories are the sequential addition of ubiquitin to the substrate forming a chain on the substrate, or the formation of the *en-bloc* chain on the catalytic cysteine of the HECT domain, which is then transferred to the substrate (Wang & Pickart. 2005). Early work suggested that both mechanisms were plausible, indicating that E6AP builds up K48 linked chains on the HECT cysteine, whilst UBE3C generated K48 and K29 chains as free entities (Verdecia, *et al.* 2003; Wang & Pickart. 2005; Wang, *et al.* 2006). However, more recent studies favour the sequential addition mechanism (Kim & Huibregtse. 2009; Kim, *et al.* 2011; Maspero, *et al.* 2013). The NEDD4 ligase, WWP1, catalyses the formation of ubiquitin chains by sequential addition. In the first phase, chains are synthesised in a unidirectional manner and linked via K63, and in the second phase the chains are elongated in a multidirectional manner by the formation of K11 and K48 mixed and branched linkages (French, *et al*. 2017). This demonstrates the ability of HECT ligases to synthesise heterotypic ubiquitin chains.

1.4.2. Regulation of HECT ligase activity

Regulation of HECT ligases can either occur via regulation of the N-terminal domains, influencing localisation and substrate binding, and/or by the regulation of the HECT domain, preventing E2 binding and catalysis (Rotin & Kumar. 2009; Scheffner & Kumar. 2014).

Targeting of HECT ligase activity by N-terminal domains

While the HECT domain is responsible for the enzymatic activity of the protein, the N-terminus of the ligase contains domains that target the activity of the ligase, either directly or via adapters, to specific complexes or organelles. For example, WW domains are found in a number of NEDD4 family members and mediate interaction with PPXY motifs that have a high affinity for WW domains (Chen & Sudol. 1995). The adapter protein, N4WBP5 (also known as NDFIP2), regulates NEDD4 ligase activity through this ability to bind the NEDD4 WW domain via two PPXY motifs. NDFIP2 localises to intracellular membranes where it acts as an adapter for NEDD4-like proteins and regulates the sorting and trafficking of ubiquitinated cargoes (Harvey, *et al*. 2002; Shearwin-Whyatt, *et al.* 2004). Similarly, the PY motifs in α- and β- arrestins have been shown to interact with the WW domains of NEDD4 mediating recruitment of the ligase to 7 transmembrane receptors such as, β_2 adrenergic receptor. This recruitment allows for the ubiquitination and subsequent lysosomal trafficking or degradation of the receptor (Shea, *et al.* 2012; Han, *et al.* 2013). Adapter proteins also can bind the C2 domain of NEDD4 family proteins. For example, the C2 domain of NEDD4 interacts with annexin XIIIb resulting in localisation to apical membranes (Plant, *et al.* 2000).

While, the SH2 domain of GRB10 associates with the C2 domain of NEDD4, promoting IGF1R (insulin-like growth factor 1 receptor) ubiquitin-mediated internalisation, and degradation (Huang & Szebenyi. 2010).

Interestingly, adapter proteins can also mediate inhibition of the ligase. For example, the adaptor protein 14-3-3 is recruited to NEDD4-2 upon phosphorylation by AKT1 and SGK1 (serum and glucocorticoid regulated kinase 1) kinases, which are activated by hormones such as insulin and aldosterone. The binding of 14-3-3 prevents dephosphorylation of NEDD4-2 rendering it unable to ubiquitinate the epithelial sodium channel ENaC, needed for transepithelial Na^+ transport. 14-3-3 functions to maintain NEDD4-2 inhibition preventing degradation of ENaC, allowing Na^+ absorption to increase (Debonneville, *et al.* 2001; Ichimura, *et al.* 2005; Bhalla, *et al.* 2005; Lee, *et al.* 2007). This inhibition occurs by the disruption of the interaction between the WW domains of NEDD4-2 and the PY motif of ENaC (Nagaki, *et al*. 2006). In addition, the adapter protein N4BP1 binds the WW domains of ITCH to inhibit its activity through a poorly understood domain that lacks a PPXY motif. This interaction interferes with substrate binding including p73 and c-JUN (Oberst, *et al.* 2007).

Regulation of HECT domain

The regulation the HECT domain, controlling catalysis and E2 binding, is another way to regulate HECT ligase activity. For example, the HECT domain of SMURF2 is suboptimal for binding of its E2, UBCH7. In TGFβ signalling, the inhibitory protein SMAD7 recruits SMURF2 to the TGFβ receptor complex to facilitate receptor degradation. The N-terminus of SMAD7 stimulates SMURF2 activity by recruiting UBCH7 to the HECT domain (Ogunjimi, *et al*. 2005). Regulation SMURF2 exhibits intramolecular regulation, whereby interaction between the C2 and HECT domains inhibits SMURF2 activity, and the HECT binding domain of SMAD7 antagonises this inhibitory interaction. This interaction between C2 and HECT domains autoinhibits the degradation of SMURF2 and its substrates because the catalytic cysteine of SMURF2 is not accessible to UBCH7 (Wiesner, *et al.* 2007). This intramolecular interaction is not uncommon among the NEDD4 subfamily of HECTs. Small PY-containing membrane proteins, NDFIP1 and NDFIP2 also bind to release ITCH from its autoinhibitory intramolecular interaction, exposing the HECT domain and allowing ubiquitination of JUN proteins (Mund, & Pelham. 2009). The Wnt signalling protein dishevelled contains a PPXY, WW binding motif, which is able to bind WWP2 and relieve the autoinhibition by C2-HECT, WW-HECT interactions. This is dependent on DVL2 (Dishevelled) polymerisation resulting in WWP2 activation in Wnt signalosomes (Mund, *et al.* 2015). In NEDD4L, the C2 domain binds Ca^{2+} and inositol 1,4,5-trisphosphate (IP_3), using the same autoinhibitory interface that is used to bind to the HECT domain. The

concentration of Ca^{2+} therefore acts as a switch to modulate NEDD4L activation, as well as its intracellular localisation (Wang, *et al.* 2010; Escobedo, *et al.* 2014).

Phosphorylation is also important in disrupting this autoinhibitory mechanism of some HECT ligases. For instance, JNK1 mediates phosphorylation of two serine residues and a tyrosine residue (S199, S232, and T222) in ITCH to disrupt the inhibitory intramolecular interaction between the WW domain and the HECT domain, enhancing catalytic activity (Gallagher, *et al.* 2006). Phosphorylation is also important in relieving the autoinhibitory interaction of the C2 and HECT domains of NEDD4. The receptor tyrosine kinase fibroblast growth factor receptor 1 (FGFR1) is degraded by NEDD4. Activation of FGFR1 leads to activated c-SRC mediated phosphorylation of NEDD4 enhancing its activity (Persaud, *et al.* 2014). Recently, it was found that peptide linkers between the WW domains found in NEDD4 family proteins, such as WWP1, WWP2, and ITCH are important for their catalytic regulation. These linkers were found to function to lock the ligase in an inactive conformation and that tyrosine phosphorylation was found to relieve this autoinhibition (Chen, *et al*. 2017).

More recently the oligomerisation state of the HECT domain has emerged as a mechanism to regulate enzyme activity by locking the HECT domain in a closed conformation (Sander, *et al.* 2017; Attali, *et al*. 2017). In the case of HUWE1, the HECT domain forms an autoinhibitory dimer which locks the C-Lobe of HUWE1 in a position that prevents catalysis. This homo-dimerised form of HUWE1 is stabilised by the binding of the tumour suppressor, p14ARF. This provides a mechanistic explanation for the inhibition of HUWE1 activity in cancer (Sander, *et al.* 2017). Both Rsp5 and its mammalian orthologue NEDD4 also oligomerise into ligase-inactive trimers and hexamers, and in contrast to HUWE1 these mechanisms are ubiquitin-dependent. Here, ubiquitination of the α-1 helix in Rsp5 HECT domain resulted in trimerisation by the binding of the Ub-α-1 helix to the UBD in the HECT domain, and inhibition of HECT ligase activity (Attali, *et al*. 2017). Together these studies highlight that the regulation of HECT ligase activity is complex and suggest that most likely, other mechanisms may yet be uncovered.

1.5. Ubiquitin chains

Substrates can be mono-ubiquitinated or polyubiquitinated. Mono-ubiquitination can take two forms, this can be either on one lysine residue (mono-ubiquitination) or on multiple lysine residues (multi-mono-ubiquitination) (Komander. 2009) (Figure 1.8). Mono-ubiquitination has been associated with proteasomal degradation and also proteasome-independent cellular functions, an example of which is intracellular protein movement. It

was found that multi-mono-ubiquitination of receptor tyrosine kinases (RTKs), led to the internalisation and degradation of the cell surface receptors in the lysosome, or recycling to the cell surface (Haglund, *et al.* 2003). DNA damage has been shown to induce mono-ubiquitination of histone H2A close to DNA lesions (Bergink, *et al*. 2006). Furthermore, in some cases mono-ubiquitination has also been implicated in acting as a crucial priming event for the assembly of polyubiquitin chains (Rodrgio-Brenni & Morgan. 2007).

Polyubiquitin chains are formed by the sequential addition of ubiquitin to the substrate (Mastrandrea, *et al*. 1999; Kim & Huibregtse. 2009). The polyubiquitin chains formed can be homotypic, exclusively of one chain type, or heterotypic, of different chain types (Figure 1.8). Polyubiquitin chains are divided into typical ubiquitin chains and atypical ubiquitin chains (Kulathu & Komander. 2012). Ubiquitination is a diverse modification with different polyubiquitin linkages conferring different functions within a cell. This is because the different types of linkages have different 3-dimensional structures, which therefore affects the recognition by different ubiquitin-binding proteins (Tenno, *et al.* 2004; Komander, *et al*. 2009). Furthermore, the conformations that these different ubiquitin linkages take, affects the recognition and activity of interacting proteins and downstream effectors. Interestingly, K63, and Met-1 linkages have been shown by single-molecule fluorescence resonance energy transfer to exist in an equilibrium between extended “open” conformations and compact “closed” conformations (Ye, *et al.* 2012). The fact that the conformation of ubiquitin chains is dynamic may suggest an additional level of regulation.

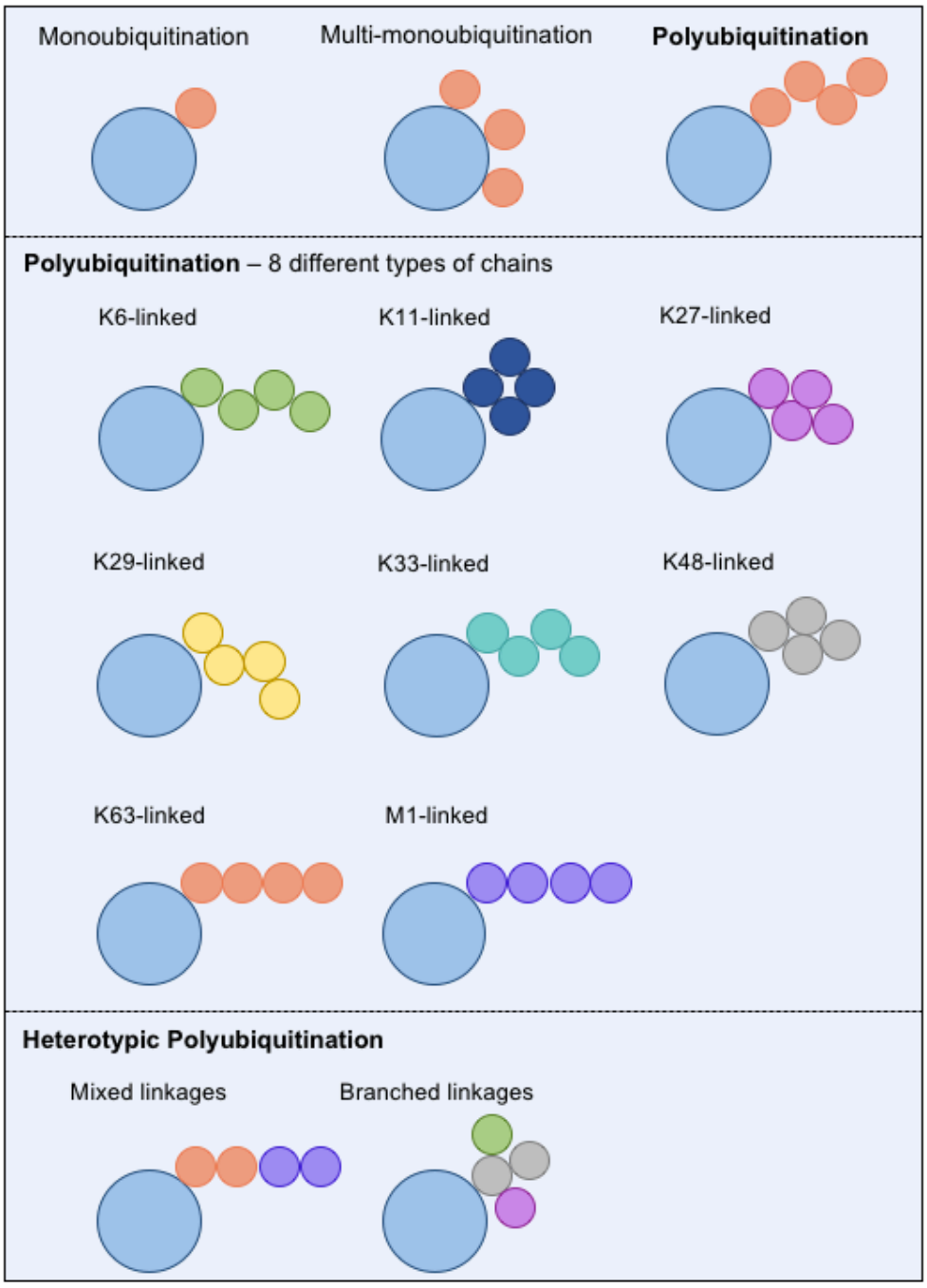

Figure 1.8. Diversity of ubiquitin linkages. Ubiquitin is a diverse modification, with different linkages conferring different functions by their different structures. Ubiquitin can be added to substrates as monoubiquitin, multi-monoubiquitin, and polyubiquitin. Polyubiquitination can occur via 7 lysine residues (K6, 11, 27, 29, 33, 48, and 63) or via the N-terminal residue M1. Heterotypic polyubiquitination occurs as either mixed or branched chains of different linkages. Known branched ubiquitin chains include K11/K48 and K48/K63 linkages. Adapted from Komander. (2009) and Yau & Rape. (2016).

1.5.1. Canonical ubiquitin chains

Typical ubiquitin chains are considered to be K48 and K63-linked chains, which are the most characterised and abundant type of ubiquitin linkage (Xu, *et al.* 2009; Dammer, *et al.* 2011; Kulathu & Komander. 2012) (Table 1.2). K48-linked ubiquitin chains were first discovered as a polyubiquitin chain that formed on proteasomal substrates required for degradation (Chau, *et al*. 1989). Later work showed that mutation of K48 on ubiquitin prevented chain assembly, inhibiting proteolysis and cell cycle progression in *Saccharomyces cerevisiae* (Finley, *et al*. 1994). K48 chains form tetramers that act as the recognition motif for the 26S proteasome, responsible for the ATP-dependent degradation of target substrates (Pickart. 1997; Thrower, *et al.* 2000). DUBs present on the proteasome (RPN11, UCH37, and USP14), cleave ubiquitin from the substrate, leaving the ubiquitin to be recycled (Komander, *et al*. 2009; Lee, *et al*. 2011).

K63 linkages have been implicated in DNA repair, where mutation of K63 resulted in defects in DNA repair (Spence, *et al*. 1995; Hoffman & Pickart. 1999). K63 has been shown to have a more open extended structure compared to K48, with more of ubiquitin surface exposed (Figure 1.8) (Sayto, *et al.* 2008; Weeks, *et al.* 2009). Furthermore, in contrast to K48, it is widely accepted that K63 linkages do not target substrates to the proteasome (Komander. 2009; Nathan, *et al.* 2013). Whilst, K63 linked ubiquitin chains have been implicated in signal transduction rather than degradation, with roles in autophagy (Ferreira, *et al.* 2015), endocytosis (McCullough, *et al*. 2004), and Wnt signalling (Tran, *et al.* 2008). In NFκB signalling, IκB kinase (IKK) is activated by the E3 ligase, TRAF6, through the addition K63-linked polyubiquitin chains (Deng, *et al.* 2000). CYLD, a USP family DUB family member, functions as a tumour suppressor. CYLD antagonises NF-κB signalling by cleaving K63 linked ubiquitin chains, therefore preventing interactions between the signalling components, further demonstrating the degradation-independent role of K63 chains in signal transduction (Kovalenko, *et al.* 2003).

Table 1.2. Abundance of polyubiquitin chains in Yeast and Mammalian cells. Abundance generated from AQUA (absolute quantification)-mass spectrometry in Yeast (Xu, *et al.* 2009), and in Mammalian cells (Dammer, *et al*. 2011).

Chain type	Abundance in Yeast	Abundance in Mammalian cells (HEK293)
K6	11%	≤0.5%
K11	28%	2%
K27	9%	≤0.5%
K29	3%	8%
K33	3%	≤0.5%
K48	29%	52%
K63	16%	38%

1.5.2. Atypical ubiquitin chains

Atypical ubiquitin chains are linkages through K6, K11, K27, K29, K33, or M1, which by comparison to K48 and K63 are not as well studied (Kulathu & Komander. 2012). These chain types tend to be less abundant in yeast and mammalian cells, with the exception of K11 in yeast (Xu, *et al.* 2009; Dammer, *et al.* 2011) (Table 1.2).

K6 linked ubiquitin chains have been shown to be produced by a heterodimeric RING E3 ligase complex consisting of the breast cancer-susceptibility protein BRCA1 and BARD1 (Nishikawa, *et al*. 2004). Furthermore, BRCA1 is involved in the DNA damage response indicating a potential role for K6. Whilst the more abundant K11, has been reported to be involved in proteasomal degradation and endoplasmic reticulum-associated degradation (ERAD) (Xu, *et al*. 2009). K11 have most notably been shown to have a role in mammalian cell cycle regulation. The anaphase promoting complex/ cyclosome (APC/C), conjugates K11 chains to cell cycle substrates such as Cyclin B1, which targets it for degradation (Jin, *et al*. 2008). Since, it has been demonstrated that branched chains of K11 with K48 and/or K63 are synthesised by the ACP/C and UBE2S, leading to enhanced proteasomal degradation of cell cycle substrates (Figure 1.8) (Meyer & Rape. 2014). Interestingly, it has been demonstrated that pure homotypic K11-linked ubiquitin chains do not bind strongly to the proteasome and instead heterotypic K11/K48-linked ubiquitin chains bind strongly to the proteasome and stimulate degradation of Cyclin B1 (Grice, *et al*. 2015). In addition, quantitative mass spectrometry revealed that mixed chains of K11 and K63 have been shown to be required for efficient internalisation of MHC class 1 (Boname, *et al.* 2010). Nevertheless, in contrast to homotypic chains, the composition, function and regulation of heterotypic polyubiquitin chains are poorly understood.

K27 accounts for around 10% of all ubiquitin chains in yeast (Xu, *et al*. 2009), however only accounts for ≤0.5% in HEK293 mammalian cells (Dammer, *et al*. 2011), potentially indicating less of a role in mammalian cells, compared to yeast. K27 has been shown to function in mitophagy, where it is conjugated on VDAC1 (voltage-dependent anion channel 1) by PARKIN, functioning in the regulation of a mitochondrial trafficking protein, MIRO (Geisler, *et al*. 2010; Birsa, *et al*. 2014). More recently mitochondrial damage has been shown to induce PARKIN to assemble K6, K11, and K63 chains on mitochondria. The deubiquitinase USP30 was shown to have a strong preference for cleaving K6 and K11, counteracting PARKIN and preventing apoptotic cell death (Cunningham, *et al.* 2015; Liang, *et al*. 2015). This suggests that although K27 has been implicated in the regulation of mitochondria, it is not the only chain type involved, and others may be involved.

Of the atypical ubiquitin chains, K29 is the most abundant in resting mammalian cells (Dammer, *et al.* 2011). The HECT ligase, ITCH, has been shown to assemble K29 linked chains on Deltex, a regulator of Notch signalling, leading to its lysosomal degradation (Chastagner, *et al.* 2006). Furthermore, K29 has been shown to exist as heterotypic polyubiquitin chains, mainly containing K48 linkages that are produced by the HECT E3 ligase, UBE3C (You & Pickart. 2001). Interestingly, K29 linked chains have been implicated in the ubiquitin fusion degradation (UFD) pathway, which was first discovered to involve a HECT E3 ligase called Ufd5 found in *S. cerevisiae* (Johnson, *et al*. 1995). The UFD pathway is a proteolytic system that is conserved from yeast to mammals. The system involves an uncleavable ubiquitin moiety fused to the N-terminus of a protein during translation, which serves to function as a degradation signal. This contrasts with the canonical pathway or the N-end rule pathway where ubiquitin is added post-translationally onto Lys residues (Chau, *et al*. 1989) or onto the first N-terminal residue (i.e. Arg, Leu, Phe, Asp and Lys) (Bachmair, *et al.* 1986).

This ubiquitin fusion protein is formed from the translation of a ubiquitin fusion gene. Only a handful of proteins have been found to have a fused ubiquitin moiety at their N-terminus including ribosomal proteins L40 and S27a in yeast (Ozkaynak, *et al*. 1987; Redman & Rechsteiner. 1989) and ribosomal protein P1, and interestingly actin in chlorarachinophyte algae (Archibald, *et al*. 2003). This fused ubiquitin acts as a platform for further K29 or K48 ubiquitin chain conjugation, resulting in degradation of the substrate (Johnson, *et al*. 1995). Mutant ubiquitin (UBB+1), which was first discovered in the brain of patients with Alzheimer's Disease (van Leeuwen, *et al.* 1998), is the only mammalian UFD substrate identified to date. A numbered of studies have tried to identify the E3 ligase and DUBs responsible for the regulation of UFD substrates. The HECT ligase TRIP12 was shown to ubiquitinate UBB^{+1} (Park, *et al*. 2009), while other studies have confirmed this suggesting that TRIP12 is a UFD ligase (Poulsen, *et al.* 2012). Interestingly, Hecd1 has also been implicated as UFD E3 ligase in a *Caenorhabditis elegans* genetic screen using the artificial UFD substrate UbG76V-GFP as readout, suggesting that the HECT family is the main ligase family implicated in the UFD pathway (Segref, *et al.* 2014).

Ubiquitin chains are also formed via the C-terminal Gly76 of one ubiquitin and the N-terminal Met1 of another ubiquitin, forming a 'head-to-tail' linear chain. This chain type is made by LUBAC (linear ubiquitin chain assembly complex), a complex consisting of two RING finger proteins, HOIL-1L and HOIP, and was show to target substrates to the proteasome (Kirisako, *et al.* 2006). These Met1-linked linear ubiquitin have been shown to be involved in the canonical NF-κB pathway. LUBAC activates the canonical NF-κB pathway by binding to NEMO and forming linear polyubiquitin chains (Tokunaga, *et al.* 2009). Recently the

deubiquitinase OTULIN has been shown to act antagonistically to LUBAC, having specificity for Met1 linear chains, regulating NF-κB pathway signaling (Keusekotten, *et al.* 2013). Together this highlights the increasing knowledge into the study of atypical ubiquitin chains, and the complexity they exhibit. Finally, very little is known about K33, some members of the AMP-activated protein kinases (AMPK)-related family of protein kinases are ubiquitinated with K29 and/or K33 linked ubiquitin chains (Al-Hakim, *et al*. 2008). Interestingly ubiquitination of these kinases resulted in blocking their kinase activation (Al-Hakim, *et al*. 2008).

1.6. E3 ligases and cell cycle regulation

1.6.1 APC/C and SCF

Ubiquitination is a key process in cell cycle regulation where ubiquitination and deubiquitination of substrates ensures unidirectionality (Hershko. 1997). Many DUBs have been implicated in cell cycle regulation, such as CYLD, which regulates the mitotic spindle, and USP15, which is required for restoring protein levels of REI silencing transcription factor (REST) at mitotic exit (Faronato, *et al*. 2013; Li, *et al*. 2014; Darling, *et al*. 2017). Equally, many E3 ligases have been demonstrated to regulate the cell cycle (Teixeira & Reed. 2013). The two most characterised E3 ligases in cell cycle regulation are the multi-subunit RING E3 ligases; the APC/C and SCF (Figure 1.9). These E3 ligase complexes are involved at key stages of cell division. For example, the APC/C controls the progression through mitosis and the subsequent G1 phase (Pines. 2011), whereas the SCF regulates the G1/S and G2/M transitions (Peters. 1998).

The APC/C complex regulates the metaphase to anaphase transition through the ubiquitin-dependent degradation of Cyclin A, Cyclin B, securin, and the mitotic Aurora kinase (Pines. 2011). The APC/C E3 ligase, is a multiprotein complex which includes the APC11 RING finger subunit that interacts with the E2 enzyme, UBE2S (Acquaviva & Pines. 2006). Recent studies have defined the biochemical properties of APC/C and in particular its activity for the synthesis of K11 ubiquitin chains and branched K11 and K48 ubiquitin chains (Jin, *et al*. 2008; Meyer & Rape. 2014). From prophase to metaphase, the APC/C binds CDC20, while during anaphase it is tightly associated with CDH1 and remains bound until the next round of mitosis is initiated at prophase (Matsusaka, *et al*. 2014; Sivakumar & Gorbsky. 2015). Depending on whether it is bound by different regulatory proteins, CDC20 or CDH1, the APC/C regulates different substrates and therefore exerts different functions during cell cycle progression (Pfleger, *et al.* 2001). The function of the APC/C is tightly regulated by phosphorylation as well as autoubiquitination of its E2 enzyme (Kraft, *et al.* 2003; Rape &

Kirschner 2004). Furthermore, as discussed previously, the cell cycle checkpoint, SAC, functions to inhibit the activation of the APC/C during metaphase, preventing the separation of sister chromatids until all of the chromosomes are attached to the mitotic spindle (Hagting, *et al.* 2002; Nilsson, *et al.* 2008).

In contrast to the APC/C, the SCF^{SKP2} ligase complex controls entry into S phase and mitosis, by the degradation of G1 and S phase Cyclins, Cdk inhibitors and cell cycle kinases (Peters. 1998). This complex is composed of three primary subunits including SKP1 (S-phase kinase associated 1), CUL1 (also known as Cdc53), and RBX1/ROC1 (also known as ROC1 and HRT1) (Kipreos, *et al*. 1996; Teixeira & Reed. 2013). The SCF complex relies on the F-box, which interacts with SKP1, for its substrate specificity (Cardozo & Pangano. 2004). The SCF regulates the G1/S and G2/M transitions by the degradation of substrates such as Cyclin D, Cyclin E, the Cyclin/CDK inhibitor p27, CDC6 and the mitotic kinase WEE1 (Peters. 1998). The SCF^{SKP2} mediates substrate degradation by K48 linked polyubiquitination of its substrates, which target them for the proteasome (Petroski & Deshaies. 2005). The focus of ubiquitin in the cell cycle has primarily been on the function of RING E3 ligases, however recent discoveries are starting to shed light on the role that the smaller family of HECT E3 ligases has in the cell cycle.

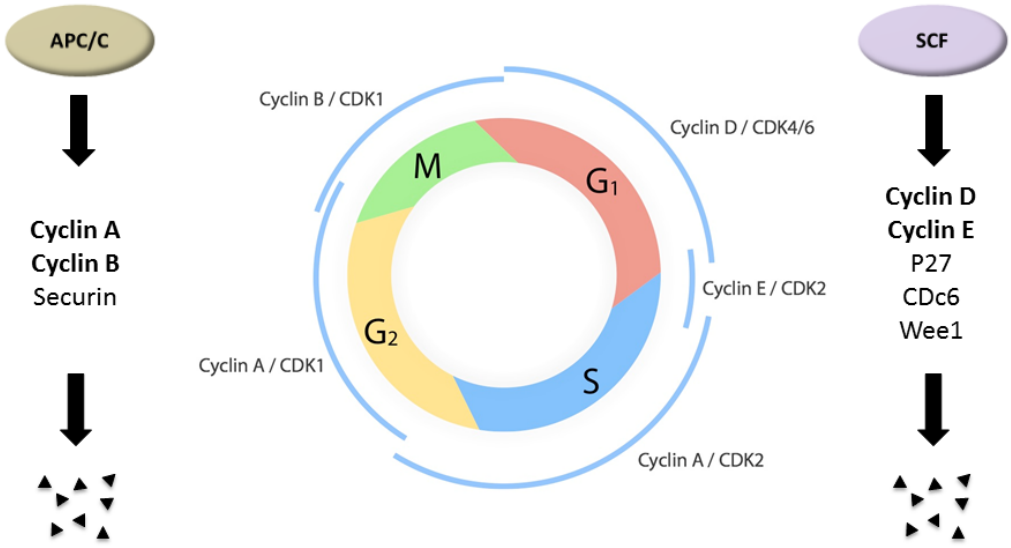

Figure 1.9. Ubiquitination in the cell cycle. Examples of ubiquitination during the cell cycle. APC/C and SCF mediated degradation of cell cycle specific substrates. The degradation of the substrates provides directionality ensuring that the cell cycle progresses in one direction towards cell division. The CDKs with their partner Cyclin are active during specific stages of the cell cycle. Own figure.

1.6.2 HECT ligases and the cell cycle

Yeast HECT ligases and cell cycle regulation

The HECT domain is highly conserved, and has been identified in 879 sequences from 101 species, ranging from yeast to humans, according to the Sanger Protein Domain Database (Rotin & Kumar. 2009). The fungal HECT family is small and very limited in N-terminal domain diversification, compared to mammalian HECTs, limiting the diversity of the ligases (Grau-Bove, *et al.* 2013). The HECT family of E3 ligases contains 5 members in yeast (*Saccharomyces cerevisiae)* (Li, *et al.* 2008). Furthermore, yeast HECT ligases have been implicated in cell cycle functions. In *S. cerevisiae,* the HECT E3 ligase Temperature-dependent Organisation in Mitotic nucleus (Tom1) has been implicated in cell cycle progression. In a *tom1* mutant, at high temperatures, cells were arrested at G2/M, with a dumbbell morphology, a single large nucleus, and short spindles, suggesting the Tom1 is required for mitosis and cell cycle exit (Utsugi, *et al*. 1999). More recently Tom1 was shown to target Cdc6, an AAA+-ATPase involved in the establishment of pre-replicative complexes at replication origins through the loading of the Mcm2-7 replicative helicase complex at replication during G1 phase of the cell cycle (Kim. *et al.* 2012b). The SCF protein adaptor Dia2 also play key roles in this process, although early evidence suggesting that Tom1 and Dia2 contribute to Cdc6 ubiquitination and degradation during the G1 phase of the cell cycle. Deletion of Dia2 partially suppressed the temperature sensitive phenotype of *tom1* mutants, suggesting that Tom1 and Dia2 act independently of SCF^{Cdc4}, the only other known E3 ligase complex that regulates Cdc6 levels (Drury, *et al.* 1997; Kim. *et al.* 2012b). Tom1 also targets Dia2 for degradation by the UPS through a degradation/ NLS domain, however the significance of this regulation in the context of Cdc6 regulation during G1 remains to be established (Kim & Koepp. 2012a).

In the fission yeast *Schizosaccharomyces pombe,* Pub1 and Pub2, two members of the Rsp5/ NEDD4 (mammalian homologue) family of HECT E3 ligases (Tamai & Shimoda. 2002), have been shown to target the mitotic phosphatase Cdc25p for UPS-mediated degradation, allowing for the timely regulation of G2/M transition (Nefsky & Beach. 1996). Overexpression of the functionally similar Pub2p led to repression of cell division suggesting that although functionally similar, Pub1 and Pub2 exert distinct functions (Tamai & Shimoda. 2002). A more recent study revealed that the serine-threonine phosphatase Flp1p in conjunction Pub1p/2p is responsible for the degradation of Cdc25p. Flp1p was shown to interact *in vivo* with Pub2p, a Pub1p-redundant ligase, suggesting that the phosphatase may regulate Pub1p/2p's function (Esteban, *et al*. 2008). Taken together, this demonstrates the importance of yeast HECT ligases in the yeast cell cycle.

Mammalian HECT ligases and cell cycle regulation

The mammalian family of HECT E3 ligases is more diverse than in yeast with 28 members, 10 of which have been shown to function in the cell cycle. The evolutionary acquisition of N-terminal domains, allowed for greater diversification of the HECT family of ligases in mammals (Grau-Bove, *et al.* 2013). The increase and diversification of mammalian HECTs in cell cycle regulation mirrors the increased complexity of the cell cycle in mammals. Having multiple HECTs involved in cell cycle regulation allows for increased regulation, and many in turn have been shown to be regulated themselves in a cell cycle dependent manner. Some of the HECT ligases have been implicated in multiple roles, such as in DNA damage signalling, p53 signalling, and the SAC. However, other ligases have only one known role in cell cycle progression, for example in centrosome architecture, or the regulation of Golgi dynamics during mitosis (Table 1.3). Interestingly, the majority of HECT ligases function in the regulation of cell cycle checkpoints, maintaining the integrity of the cell cycle.

Table 1.3. HECT E3 ligases in cell cycle regulation. The substrate specificity and function for each HECT E3 ligase implicated in cell cycle regulation. Where known the ubiquitin chain type is specified.

HECT E3 ligase name(s)	Substrates/ Interactors	Cell cycle stage/ Function	Mechanism (and chain type where known)	References
HUWE1/ MULE/ ARF-BP1/ UREB1/ HECTH9	CDC6	Prevents DNA replication, G1/ S phase.	Degradation of CDC6.	Hall, *et al.* (2007).
	p53	DNA damage induced cell cycle arrest, G1/S and G2/M transitions.	Degradation of p53.	Chen, *et al.* (2005); Yoon, *et al.* (2005).
	TopBP1	DNA damage induced cell cycle arrest, G1 phase.	Degradation of TopBP1.	Herold, *et al.* (2008).
	MYC	Release from DNA damage arrest.	Signalling via K63.	Adhikary, *et al.* (2005).
	BRCA1	DNA damage checkpoint? G1/S checkpoint.	Degradation.	Wang, *et al.* (2014).
	RASSF1C	DNA damage checkpoint? G1/S checkpoint.	Degradation.	Zhou, *et al.* (2012).
HERC2	BRCA1	Cell cycle arrest, S phase.	BRCA1 degradation.	Wu, *et al.* (2010).
	Claspin, MCM2	G2/M checkpoint.	Facilitates MCM2 phosphorylation.	Izawa, *et al.* (2011).
	USP20	DNA damage checkpoint, G1/ S checkpoint.	Degradation.	Yuan, *et al.* (2014).
	RNF8	DNA damage checkpoint, G1/ S checkpoint.	Facilitates interaction of RNF8 with UBC13.	Bekker-Jensen, *et al.* (2010).
	p53	DNA damage checkpoint, G1/ checkpoint.	Induces p53 oligomerisation.	Cubillos-Rojas, *et al.* (2014).

	CP110 and NEURL4	Centrosome amplification.	Association with NEURL4? via K48.	Al-Hakim, *et al.* (2012).
	USP33	Centrosome amplification.	Degradation.	Chan, *et al.* (2014).
EDD	TopBP1	Coordination of DNA damage, G1/S checkpoint.	Degradation.	Honda, *et al.* (2002).
	CHK2	DNA integrity, G1/S and G2/M checkpoints.	Modulation of the kinase.	Henderson, *et al.* (2005); Munoz, *et al.* (2007).
	p53	G1/S transition.	Processing of miRNAs involved in p53 regulation.	Smits, *et al.* (2012).
	Katanin p60	M phase progression.	Degradation of Kataninp60.	Maddika & Chen. (2009).
	MSP58	All phases.	Degradation, modulating Cyclin expression.	Benavides, *et al*. (2013).
	BUB3 and BUBR1	SAC regulation, M phase.	Interacts with BUB3 and BUBR1. Mechanism unknown.	Scialpi, *et al.* (2015).
ITCH	p73	DNA damage cell cycle arrest.	Degradation.	Rossi, *et al.* (2005).
	p63	DNA damage cell cycle arrest.	Degradation.	Rossi, *et al.* (2006).
	RASSF5	G1/ S checkpoint.	Degradation of RASSF5.	Suryaraja, *et al.* (2013).
HECTD3	TARA	Mitotic spindle regulation, M phase.	Degradation of TARA.	Yu, *et al.* (2008).
SMURF1	WEE1	S phase progression.	Degradation of WEE1.	Wei, *et al.* (2017).
SMURF2	MAD2	SAC regulation, M phase.	Preventing degradation, by K63 ubiquitin chains?	Osmundson, *et al.* (2008).
HACE1	Rab proteins	Postmitotic Golgi membrane fusion.	Interaction with Rab proteins.	Tang, *et al.* (2011); Mizuno-Yamasaki, *et al.* (2012).
	Cyclin D1	Cell Cycle arrest at G1 phase.	Degradation of Cyclin D1 (no direct evidence).	Zhang, *et al.* (2007).
NEDL2	p73	Unknown.	Stabilisation.	Miyazaki, *et al.* (2003).
	Unknown	M phase.	Recquired for metaphase to anaphase transition.	Lu, *et al.* (2013).
G2E3	Unknown (localised to the nucleus)	Cell cycle regulation and DNA damage response, G2/M phase.	Unknown, catalytically inactive HECT domain.	Brooks, *et al.* (2006); Brooks, *et al.* (2008).

HUWE1

HUWE1, also known as MULE1, HECTH9, ARF-BP1, and UREB1, is the human homolog of yeast Tom1, and has been shown to have a conserved role in the cell cycle. Similar to the function in yeast for Tom1, HUWE1 polyubiquitinates and degrades CDC6, and is associated with release of CDC6 from chromatin, therefore preventing DNA replication (Hall, *et al.* 2007). Specifically, upon DNA damage in G1 or S phase, CDC6 is degraded by HUWE1 and p53 is stabilised, resulting in cell cycle arrest (Hall, *et al.* 2007). In addition, HUWE1 has been shown to directly regulate p53 stability (Chen, *et al.* 2005; Yoon, *et al.* 2005). The ARF tumour suppressor was shown to inhibit ligase function and thus prevent ubiquitination and inactivation of p53, resulting in p53 stabilisation and cell growth suppression (Chen, *et al.* 2005). Furthermore, mutation of the HECT domain in HUWE1 also stabilised p53, in colorectal cell lines, further demonstrating the role of HUWE1 ubiquitination in p53 regulation (Yoon, *et al.* 2005). Loss of HUWE1 has also been shown to induce DNA damage-dependent cell cycle arrest, independent of CDC6 degradation (Herold, *et al.* 2008). This demonstrates the diverse roles that HUWE1 has in cell cycle regulation.

HERC2

HERC2 belongs to the large HERC subfamily of HECT E3 ligases, which are over 500kDa in size, and contains a HECT domain and more than one RLD (Sánchez-Tena, *et al.* 2016). HERC2 has been implicated in many functions in the cell cycle including the DNA damage response. HERC2 has been shown to interact with the breast cancer suppressor, breast cancer 1 (BRCA1), leading to its degradation. The HERC2-BRCA1 interaction peaks in S phase of the cell cycle but rapidly reduces during G2/M, when BRCA1 associates with BARDI, and is stabilised (Wu, *et al.* 2010). The HERC2-BRCA1 interaction can be disrupted by the tumour suppressor protein tumour suppressor candidate 4 (TUSC4), which physically interacts with BRCA1 to prevent degradation by HERC2, therefore stabilising it (Peng, *et al.* 2015). The function of BRCA1 needs to be tightly regulated as it maintains genomic stability by DNA damage repair and cell cycle checkpoint activation in S phase and G2/M transitions (Venkitaraman. 2002; Deng. 2006). Further to this, in the presence of BRCA1, HERC2 interacts with Claspin, a protein essential for G2/M checkpoint activation and replication fork stability, and MCM2 a component of the pre-replication complex. HERC2 was shown to facilitate MCM2 phosphorylation, regulating DNA replication progression and origin firing, however the mechanism for this is not certain (Izawa, *et al.* 2011).

HERC2 has also been implicated in p53 activity and centrosome regulation highlighting its function as a multitasked cell cycle regulator. HERC2 has been shown to regulate the DNA damage checkpoint and DNA damage response, via ATR-CHK1 mediated signalling (Yuan,

et al. 2014), and facilitates formation of a complex with the RING E3 ligase RNF8 and UBC13, facilitating K63 polyubiquitination of γH2AX at sites of DNA damage (Bekker-Jensen, *et al.* 2010). Furthermore, HERC2 facilitates the recruitment of repair factors such as 53BP1, RAP80 and BRCA1 (Bekker-Jensen, *et al.* 2010). HERC2 has been demonstrated as a cell growth regulator through regulation of p53 activity, independent of the proteasome. HERC2 increases p53 transcriptional activity by inducing p53 oligomerisation, initiating p53 signalling (Cubillos-Rojas, *et al.* 2014), and therefore inhibition of the G1/S transition. In addition, HERC2 has been identified in centrosome regulation, where together with neuralised homologue NEURL4 it binds to the centrosome protein CP110, to maintain normal centrosome architecture. CP110 controls centrosome duplication during the cell cycle. HERC2 was shown to ubiquitinate NEURL4 with K48 chains, however it was shown that NEURL4 was stabilised by HERC2 when present in a complex, suggesting that the ubiquitylation may serve another function than regulating protein levels (Al-Hakim, *et al.* 2012). Furthermore, the deubiquitinating enzyme USP33 was shown to deubiquitinate CP110 during centrosome duplication (Li, *et al.* 2013a). USP33 itself was shown to be polyubiquitinated and regulated by HERC2, followed by proteolysis mediated by p97 and its adapter protein UFD1-NLP4, further demonstrating its role in centrosome amplification (Chan, *et al.* 2014).

EDD

In addition to HUWE1, E3 identified by differential display (EDD; hHYD in Drosophila; UBR5 in Human) has also been shown to interact with the DNA topoisomerase II binding protein 1 (TopBP1) (Honda, *et al.* 2002). EDD ubiquitinates TopBP1, which is then degraded by the proteasome. However, during DNA damage TopBP1 is ubiquitinated resulting in localisation with γH2AX at DNA breaks, suggesting a role in EDD coordination of TopBP1 in the DNA damage response (Honda, *et al.* 2002) and DNA damage checkpoint. Furthermore, EDD has been reported to modulate activity of the DNA damage checkpoint kinase, CHK2, resulting in phosphorylation of downstream targets leading to cell cycle arrest, DNA repair, and apoptosis (Henderson, *et al.* 2006). EDD depletion led to decreased CHK2 activation and altered expression of the key cell cycle regulators CDC25A/C and E2F1, resulting in polyploidy and cell death via mitotic catastrophe. Furthermore, EDD is necessary for the maintenance of G2/M arrest after double strand breaks, in addition to its roles in G1/S and S-phase DNA damage checkpoint activation (Munoz, *et al.* 2007). EDD has also been suggested to regulate G1/S transition by regulation of p53 (Ling & Lin. 2011). It is suggested that EDD regulates p53 by controlling or processing one or more microRNAs (miRNAs) involved in negative regulation of p53 (Smits. 2012). This is further supported by the study that demonstrated that EDD is a key component in gene silencing mediated by miRNAs (Su, *et al.* 2011).

EDD has also been implicated in M phase through formation of the DYRK2-EDVP complex. The EDVP complex (composed of EDD, DDB1, and VPRBP) is responsible for the phosphorylation-dependent ubiquitination of katanin p60, and this is implicated in mitotic progression (Maddika & Chen J. 2009). Whilst EDD together with microspherule protein 58 (MSP58) have been shown to control cell cycle progression, depletion of EDD leads to an increase of MSP58 protein level. This indicates that EDD controls MSP58 turnover by the UPS. Knockdown of either MSP58 or EDD in human lung fibroblast cells affects the levels of Cyclin B, D, and E as well as cell cycle progression (Benavides, *et al.* 2013) strongly indicating that EDD plays key role in the cell cycle. Finally, EDD has been shown to function in the SAC. EDD depletion abrogated the accumulation of cells in G2/M in response to SAC activation caused by Nocodazole treatment. This led to reduced mitotic cell viability, and increased expression of CDC20. Furthermore, EDD was shown to physically interact with BUB3 and BUBR1 which are components of the SAC, indicating that EDD helps to maintain the SAC (Scialpi, *et al.* 2015). The DNA damage checkpoint and the SAC have been shown to be linked in an ATR/ATM dependent manner (Kim & Burke. 2008). Due to that fact that EDD had been shown to function in DNA damage and the SAC, this led the author to speculate that EDD may act as a caretaker of genomic integrity through its ability to regulate cell cycle arrest in metaphase, and in interphase, in response to cellular stress (Scialpi. *et al.* 2015).

ITCH

The NEDD4 family E3 ligase, ITCH, binds and degrades the p53 family proteins, p63 and p73, but not p53 itself. ITCH is involved in the MDM2-independent ubiquitination and degradation of p73, a transcription factor that is upregulated in response to DNA damage, inducing cell cycle arrest and apoptosis. During DNA damage ITCH is downregulated, resulting in an increase in p73, to allow cell cycle arrest or apoptosis (Rossi, *et al.* 2005). ITCH also ubiquitinates and degrades p63, important in regulating both cell cycle and apoptosis. In ITCH knockout keratinocytes, the levels of p63 were significantly increased, showing a role for ITCH in p63 turnover (Rossi, *et al.* 2006). PY motifs are located near to the sterile alpha motif (SAM) domains in p63 and p73, but not in p53, hence why ITCH can bind via its WW domains and facilitate ubiquitination and degradation of the transcription factors (Rossi, *et al.* 2005; Rossi, *et al.* 2006; Bellomaria, *et al.* 2012). In addition to control of p63 and p73, ITCH was found to associate with and regulate Ras association (RalGDS/AF-6) domain family member RASSF5, which is a non-enzymatic RAS effector super family protein, involved in cell division. ITCH interacts with the RASSF5 PPxY motif via its WW domains, to cause its polyubiquitination and degradation via the 26S proteasome. ITCH overexpression showed a strong inhibitory effect on RASSF5-mediated G1 phase arrest, and apoptosis, indicating that ITCH is a regulator of RASSF5, which controls cell cycle arrest (Suryaraja, *et al*. 2013).

HECTD3

HECTD3 was found to be a regulator of Trio-associated repeat on actin (TARA), which was originally identified as a Trio-binding protein (Seipel, *et al.* 2001; Yu, *et al.* 2008). Trio is a Rho guanine nucleotide exchange factor that regulates actin cytoskeletal reorganization, cell motility and cell growth (Seipel, *et al.* 1999). It was found that TARA also binds TRF1, which plays a role in regulation of the mitotic spindle (Nakamura, *et al.* 2002). It was found that overexpression of HECTD3 promotes the degradation of TARA *in vivo*, and inhibition leads to TARA stability. The depletion of HECTD3 resulted in an increased number of cells with multipolar spindles, suggesting that HECTD3 facilitates mitotic progression, and spindle regulation by the degradation of TARA (Yu, *et al.* 2008). HECTD3 has more recently been shown to conjugate K63 ubiquitin chains in the context of cancer cell survival, where polyubiquitination of caspase 8 decreases its activation, and apoptotic signalling (Li, *et al.* 2013). However, K63 has not been shown to be relevant in the context of HECTD3 and cell cycle regulation, especially as it has a degradative role, suggesting another chain type may be involved.

SMURF1

The NEDD4 subfamily E3 ligase, SMAD ubiquitination regulatory factor 1 (SMURF1), has been implicated in S phase progression by the degradation of WEE1 kinase (Wei, *et al.* 2017). It was observed that silencing of SMURF1 resulted in S phase arrest, and that progression through S phase was dependent of the ubiquitin-dependent degradation of WEE1. Interestingly, WEE1 was shown to interact to SMURF1 through both the WW and HECT domains, not just the WW domains alone. However, the exact mechanism by which this occurs remains unknown (Wei, *et al.* 2017).

SMURF2

The NEDD4 subfamily E3 ligase SMURF2 has been shown to function in the spindle assembly checkpoint. The spindle assembly checkpoint (SAC) prevents the separation of sister chromatids until all of the chromosomes are attached to the mitotic spindle, by inhibiting the APC/C recognition of key substrates such a Cyclin B1 and securin required for anaphase (Nilsson, *et al.* 2008). Depletion of SMURF2 resulted in misaligned and lagging chromosomes, premature anaphase onset, and defective cytokinesis. SMURF2 depletion led to degradation of MAD2, a component of the SAC, by the UPS. As a result, SMURF2-depleted cells have defective SAC, indicating that SMURF2 is a novel mitotic regulator. Interestingly, it has been suggested that SMURF2 mediates this effect via the synthesis of K63-linked ubiquitin chains, although biochemical evidence are lacking (Osmundson, *et al.* 2008)

HACE1

During mitosis, the Golgi apparatus needs to be divided between daughter cells, this process occurs by disassembly and reassembly of the Golgi. At the onset of mitosis, the Golgi is fragmented, dispersing the stacks, leading to vesiculation resulting in vesicles disturbed throughout the cytoplasm (Acharya, *et al.* 1995). These vesicles are then evenly disrupted between the two daughter cells during telophase. Post-mitotic Golgi reassembly is mediated by membrane fusion controlled by two ATPases associated with various cellular Activities (AAA) ATPases, *N*-ethylmaleimide-sensitive factor (NSF), and p97 (Rabouille, *et al.* 1998). It was shown that HACE1 is targeted to the Golgi membrane through interactions with Rab proteins, a GTPase that is involved in membrane trafficking (Mizuno-Yamasaki, *et al.* 2012). Therefore, the ubiquitin ligase activity of HACE1 is required post-mitotic Golgi membrane fusion. Knockdown of HACE1, or expression of a catalytic mutant resulted in impaired post-mitotic Golgi membrane fusion. Conversely the expression of Rab1 inactive mutant caused the dissociation of HACE1 from the Golgi membranes and Golgi fragmentation, indicating a role for ubiquitin in Golgi biogenesis during the cell cycle (Tang, *et al.* 2011). Finally, HACE1 has been characterised as being a critical tumour suppressor in multiple cancers such as Wilm's Tumour, pancreatic, and gastric carcinomas to name a few. At the molecular level, HACE1 appears to modulate cell proliferation by Cyclin D1 degradation, causing cycle arrest in G1. However, there is no evidence to suggest that Cyclin D1 is directly targeted by HACE1 (Zhang, *et al*. 2007).

NEDL2

NEDD4-like ubiquitin ligase 2 (NEDL2) was shown to enhance p73-dependent transcriptional activation, by increasing p73 stability. Expression of p73, a p53 family member is important in the regulation of cell growth and apoptosis, and its expression is maintained at low levels in mammalian cells. NEDL2 binds p73 PY motifs, and is ubiquitinated and stabilized, reducing the degradation rate (Miyazaki, *et al.* 2003). NEDL2 has been shown to be a substrate of APC/C-CDH1 complex as cells exit mitosis, regulating the metaphase to anaphase transition. CDH1 recognises the NEDL2 destruction box ($R^{740}GSL^{743}$) and targets it for degradation during mitotic exit. NEDL2 was shown to associate with the mitotic spindle, having a protein level maximum in mitosis, indicating it has an essential function in mitosis. This was supported by NEDL2 depletion which led to prolonged metaphase, and when overexpressed caused lagging chromosomes (Lu, *et al.* 2013).

G2E3

G2E3, is a dual function E3 ligase, containing both a HECT domain and three PHD/RING domains, catalyses the conjugation of K48 polyubiquitin chains. Interestingly, the HECT domain of G2E3 is reported to be catalytically inactive (Brooks, *et al.* 2008). G2E3 was

shown to localise to the DNA in a DNA damage response dependent manner, and was reported to contain a nucleolar localisation signal (NLS) in its amino terminus and a nuclear export domain within the HECT domain (Brooks, *et al.* 2006). The nuclear export domain was shown to be regulated by another region of the HECT domain that has been shown to suppress the function of the NES, an NES inhibitor (Brooks, *et al.* 2006). This function of nuclear export within the HECT domain has not been previously reported and is atypical in HECT ligases. However, the cell cycle specific expression and its regulated nuclear localisation suggest a role in cell cycle regulation and DNA damage (Brooks, *et al.* 2006).

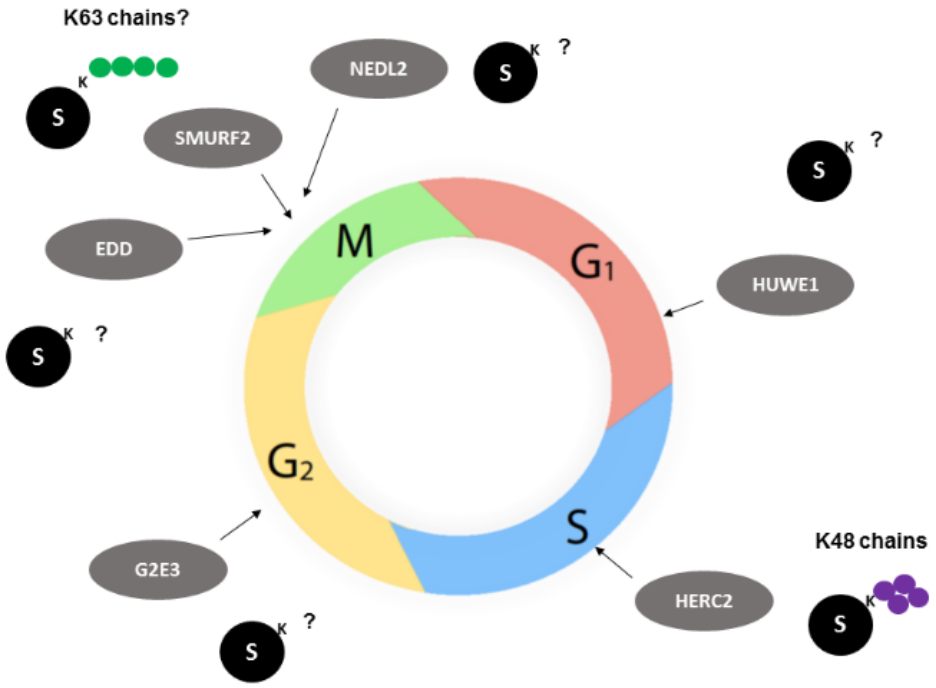

Figure 1.10. HECT ligases in cell cycle regulation. Summary of HECT ligases that have been characterised in cell cycle related functions. Where known the ubiquitin chain type has been included. Own figure.

1.6.3. Ubiquitin chain types and HECT function in cell cycle regulation

The majority of the HECT E3 ligases involved in cell cycle regulation appear to mediate protein degradation by the UPS via K48-linked ubiquitin chains (Al-Hakim, *et al.* 2012). K63 chains have also been shown to function in the cell cycle although in this case this ubiquitin signal would prevent degradation of MAD2 (Osmundson, *et al*. 2008). However, for the majority of the HECT E3 ligases shown to regulate the cell cycle, the chain type has not been defined. Recent work by the Rape lab has provided exciting insights into the role and function of branched/mixed chains in the cell cycle (see section 1.5.2) (Meyer, *et al.* 2014) and therefore identifying other linkages involved will improve our understanding on the role of ubiquitin in the cell cycle.

1.7. HECTD1 domain containing 1 (HECTD1)

Preliminary data from the lab show that HECTD1 synthesises K29 and K48-linked ubiquitin chains. In addition, immunofluorescence studies suggested that HECTD1 might localise to the mitotic spindle, opening up the exciting possibility that a novel ubiquitin chain type might have a role in the cell cycle. *HECTD1* is located on chromosome 14 (14q2) and encodes a HECT domain containing E3 ubiquitin ligase (Zohn, *et al*. 2007). Human HECTD1 consists of 2610 amino acid residues, containing an ankyrin repeat domain, a central MIB/HERC2 domain, and a C terminal HECT domain (NCBI) (Figure 1.11).

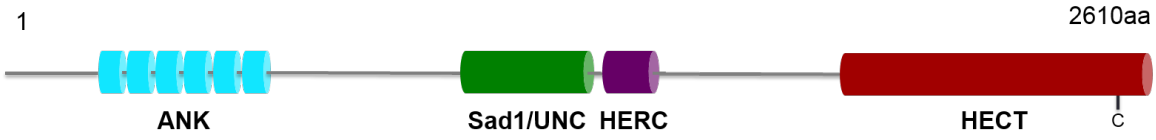

Figure 1.11. Annotated domains of HECTD1. HECTD1 contains an ankyrin repeat domain, Sad1/UNC domain, HERC domain and the HECT domain which contains a catalytic cysteine (shown), which is required for HECTD1 E3 ligase functionality. Adapted from the domains annotated in NCBI.

The C-terminal HECT domain of HECTD1 contains a conserved catalytic cysteine (Cys2579) that is required for ubiquitin conjugation to the substrate (Huibregtse, *et al.* 1995; Sarkar, *et al.* 2012). However, the function of the other domains of HECTD1 are less understood. The ankyrin repeat domain is a very common amino acid motif that has been

identified as a scaffold for protein-protein interactions (Mosavi, *et al*. 2004). Interestingly, the Sad1/UNC domain can be found in proteins that reside in the inner nuclear envelope forming a molecular bridge in the nuclear envelope despite HECTD1 being expressed throughout the cell, and not exclusively found at the nuclear envelope (own findings) (Zhou, *et al*. 2012). Finally, the MIB/HERC2 domain is not well characterised, and is so called as it is present in Mind bomb-2 (MIB2) and HECT- and RCC1-like domains 2 (HERC2) E3 ligase, suggesting that this domain is involved in protein interaction with HERC2, or has interactions similar to HERC2 (Stempin, *et al.* 2011; Cubillos-Rojas, *et al*. 2014).

In mammals, HECTD1 has diverse functions within the cell, from the cytosol to the nucleus, as well as being important for development (Zohn, *et al.* 2007; Tran, *et al.* 2013; Li, *et al.* 2013b; Sarkar, *et al.* 2014; Li, *et al*. 2015). HECTD1 was first shown to be involved in the process that leads to the closure of the dorsal neural tube. *Hectd1* mutant mouse embryos display exencephaly, which is caused by the failure of the anterior neural tube to close completely during embryonic development (Zohn, *et al.* 2007). Investigation into the molecular basis of the abnormal behaviour of *Hectd1* mutant cranial mesenchyme revealed heat shock protein 90 (HSP90) as one of HECTD1's substrates (Sarkar, *et al.* 2012). HSP90 is a chaperone protein, which is vital for maintaining the stability of its client proteins, such as the oncogenic tyrosine kinase, v-Src (Tsutsumi & Neckers. 2007). It was suggested that HECTD1-dependent K63 ubiquitination of HSP90 influences its intracellular localisation and negatively regulates its secretion, leading to the migration of the cranial mesenchyme and therefore the closure of the dorsal neural tube (Sarkar, *et al.* 2012).

HECTD1 has also been implicated as a negative regulator in the Wnt signalling pathway, therefore playing a role in cell fate and cell homeostasis (Tran, *et al.* 2013). HECTD1 associates with the OTU family DUB, TRABID, to modulate the K63 polyubiquitination of Adenomatous Polyposis Coli (APC) (Tran, *et al.* 2008; Tran, *et al*. 2013) as well as cell migration, where it functions in the regulation of the focal adhesion (FA) sites of cells (Li, *et al.* 2013b). Recently, HECTD1 has also been implicated in the regulation of IQGAP1, a scaffold protein, regulating cell migration and the formation of FA sites, further demonstrating the role HECTD1 has in cell migration (Shen, *et al*. 2017).

Finally, HECTD1 was shown to be involved in transcriptional activation, where, during interphase of human breast cancer cells, upon activation with oestrogen, HECTD1 recruits transcriptional coactivators by removing the corepressor, RIP40 (Li, *et al*. 2015). Condensin I and condensin II subunits, which play nonredundant differing roles in organising mitotic chromosomes, were found to be strongly recruited to oestrogen receptor α (ER-α)-bound functionally active enhancers (Green, *et al.* 2012; Li, *et al*. 2015). It was found that the condensins positively regulate ligand-dependent enhancer activation by recruiting

HECTD1. The degradation of RIP40 by the recruited HECTD1 allows for eRNA transcription, formation of enhancer:promoter looping, and therefore the activation of the coding gene (Li, *et al*. 2015).

Biochemical data for HECTD1 are still lacking for these studies and although K63 chains have been suggested in previous functions of HECTD1, the evidence for HECTD1 synthesising K63 remain weak. In these experiments, K63 has only been implicated by immunoprecipitation assays and an anti-K63 antibody in cell lysates (Sarkar, *et al.* 2012; Tran, *et al.* 2013). Interestingly, data from our lab support that, at least in vitro, HECTD1 preferentially makes K29 and K48-linked ubiquitin chains.

1.8. Aims and objectives

The HECT ligase HECTD1, has been shown to synthesise atypical ubiquitin chains linked via K29 and K48 (Licchesi JDF, unpublished data). Previous observations in our lab have suggested that HECTD1 might localise to the mitotic spindle. Therefore, the overall aim of this thesis was to determine whether HECTD1 regulates the cell cycle and to implicate heterotypic K29 and K48 for the first time in mitosis. The key objectives of this thesis were to:

1. Determine the effect of transient depletion and knock out of HECTD1 in mammalian cells (HEK293ET, HEK293T, and HeLa) using cell proliferation and cell cycle assays. This was achieved using siRNA knockdown, CRISPR/Cas9 cells, rescue assays, cell synchronisation and protein densitometry of western blots. (Chapter1)

2. Determine whether the effect of HECTD1 depletion on cell proliferation is through an effect of the cell cycle. This was explored by flow cytometry, immunofluorescence and confocal microscopy, time-lapse microscopy, and rescue assays using WT and catalytically mutant mHectd1 constructs. (Chapter 2)

3. Further define the cell cycle phenotype associated with HECTD1 depletion using pHistone H3 and Cyclin B1 as established molecular markers of mitosis. This was achieved through cell synchronisation, immunofluorescence and confocal microscopy, as well as western blotting. In this chapter, it was also addressed whether the ubiquitin chains synthesised by HECTD1 are found in the cell cycle, in particular during mitosis. To this end, pull-down assays with a ubiquitin binding domain specific to K29 aimed to demonstrate, for the first time, the presence of these chains in mitosis. (Chapter 3)

4. Examine the evidence that HECTD1 might be contributing to cancer development. This was determined by investigating HECTD1 expression in lung cancer cell lines, analysis of mutation and expression status from available databases including Oncomine^{TM} and CBioPortal. In addition, the effect of overexpression and knockdown of HECTD1 on glioblastoma cell proliferation was determined. Finally, HECTD1 expression in a small cohort of glioblastoma samples was assessed in order to explore the potential for this E3 ubiquitin ligase as a new diagnostic marker for brain tumours. (Chapter 4)

Chapter 2: Materials and Methods

2.1. Materials

All general laboratory chemicals stated below were purchased from Sigma-Aldrich or Fisher Scientific unless otherwise stated.

2.1.1 Buffers and solutions

- *Agar Plates (with ampicillin)*
  LB Broth with Agar (Lennox) (Sigma-Aldrich, L2897), with 50µg/ml ampicillin (Sigma-Aldrich, A0166).
- *Agar Plates (with kanamycin)*
  LB Broth with Agar (Lennox) (Sigma-Aldrich, L2897), with 30µg/ml kanamycin (Sigma-Aldrich, K1377).
- *Colony Formation Assay Fixing Solution*
  0.27% (v/v) Formaldehyde 37% solution (Sigma-Aldrich, F15587), 1% (v/v) Methanol, 10% (v/v) 10X PBS, made up to 100ml with ddH_2O.
- *Colony Formation Assay Staining Solution*
  0.1g Crystal Violet (Sigma-Aldrich, C3886) in 1L ddH_2O.
- *FACS Staining Buffer*
  100mM Tris, pH7.4, 150mM NaCl, 1mM $CaCl_2$, 0.5mM $MgCl_2$, 0.1% Nonidet P-40 (Sigma-Aldrich, 9016-45-9).
- *Immunofluorescence Blocking Buffer (BSA)*
  3% Bovine Serum Albumin (BSA) (Sigma-Aldrich, A9418) (w/v) in PBS.
- *Lysogeny broth (LB)*
  LB broth (Sigma-Aldrich, L3022)
- *Membrane Blocking Buffer (BSA)*
  3% Bovine Serum Albumin (BSA) (Sigma-Aldrich, A9418) (w/v) in PBS-Tween.
- *Membrane Blocking Buffer (milk)*
  5% Oxoid™ skim milk powder (w/v) (Thermo Fisher, LP0013B) in PBS-Tween.
- *Phosphate-buffered saline (PBS)*
  Oxoid™ PBS Tablets (Thermo Fisher, BR0014).
- *PBS-Tween*
- *Paraformaldehyde (PFA)*
  4% PFA (Sigma-Aldrich, P6148) in ddH_2O.
- Oxoid™ PBS Tablets (Thermo Fisher, BR0014) with 0.1% Tween-20.
- *RIPA Lysis Buffer*
  150mM NaCl, 20mM Tris.Cl, pH7.5, 1mM Na_2EDTA, 1mM EGTA, 1% (v/v) NP-40 (Sigma-Aldrich, 9016-45-9), 1% (w/v) sodium deoxycholate.

- *SDS-PAGE Running Buffer*
  25mM Tris.Cl, pH6.3, 0.2M glycine, 0.1% (w/v) SDS.
  Dilute to 0.5X, plus 10% (v/v) Methanol to make Wet Transfer Buffer.
- *Triton Lysis Buffer*
  150mM NaCl, 50mM Tris.Cl, pH8.0, 1% (v/v) Triton X-100.
- *1X Tris-Acetate-EDTA (TAE) buffer*
  40mM Tris.Cl, pH7.6, 20mM Acetic Acid, 1mM EDTA.
- *TRABID$_{1-200}$ IP Lysis Buffer*
  150mM NaCl, 50mM Tris.Cl, pH7.4, 5mM Dithiothreitol (Sigma-Aldrich, DTT-RO ROCHE), 2mM *N*-Ethylmaleimide (Sigma-Aldrich, E3876), 10mM Iodoacetimidine (Sigma-Aldrich, I6709), 1% (v/v) Triton X-100.
- *TRABID$_{1-200}$ IP Pull-Down Buffer*
  150mM NaCl, 50mM Tris.Cl, pH7.4, 5mM Dithiothreitol (Sigma-Aldrich, DTT-RO ROCHE), 2mM *N*-Ehthylmaleimide (Sigma-Aldrich, E3876), 10mM Iodoacetimidine (Sigma-Aldrich, I6709), 0.5mg/ml BSA (Sigma-Aldrich, A9418), 100µM $ZnCl_2$, 0.1% (v/v) Nonidet P-40 (Sigma-Aldrich, 9016-45-9).
- *TRABID$_{1-200}$ IP Wash Buffer*
  250mM NaCl, 50mM Tris.Cl, pH7.4, 5mM Dithiothreitol (Sigma-Aldrich, DTT-RO ROCHE), 0.1% (v/v) Nonidet P-40 (Sigma-Aldrich, 9016-45-9).
- *Wet Transfer Buffer*
  0.5X SDS-PAGE Running Buffer, 10% Methanol.

2.1.2. Antibodies

Antibody suppliers, product code, species, and dilutions are summarised in Table 2.1 for primary antibodies and Table 2.2 for secondary antibodies. For immunoblotting, primary and secondary antibodies were diluted in either 3% (w/v) BSA in PBS-Tween or 5% (w/v) Oxoid™ skim milk powder in PBS-Tween according to the manufacturer's instructions. For immunofluorescence staining, primary and secondary antibodies were diluted in 3% (w/v) BSA in PBS.

Table 2.1. Primary antibodies. Antibody name, supplier, product code, species, and the dilution of primary antibodies used. Abbreviations: WB = western blot, and IF = immunofluorescence, pAb = polyclonal antibody, mAb = monoclonal antibody.

Antibody name	Supplier	Code	Species	Dilution	Reference for use of antibody
Anti-beta-actin	Sigma-Aldrich	A5441	Mouse mAb	1:10000 (WB)	Fortungo, *et al*. (2002).
Anti-BUB3	Abcam	ab133699	Rabbit pAb	1:1000 (WB)	n/a
Anti-BUBR1	Abcam	ab215351	Rabbit pAb	1:500 (IF)	n/a
Anti-Cyclin B1	Santa Cruz Biotechnology	sc-245	Mouse mAb	1:1000 (WB)	Vassilev, *et al.* (2006).
Anti-GST	Roche	27-4577-01	Goat pAb	1:5000 (WB)	n/a
Anti-HA	Roche	HA3F10	Rat pAb	1:1000 (WB)	n/a
Anti-HECTD1 (N terminus)	Abcam	ab101992	Rabbit pAb	1:2500 (WB) 1:200 (IF)	Flack, *et al.* (2017).
Anti-HECTD1 (C terminus)	Abcam	ab101993	Rabbit pAb	1:2500 (WB) 1:200 (IF)	n/a
Anti-phospho-Histone H3 (Ser28)	Abcam	ab10543	Rat pAb	1:1000 (WB) 1:200 (IF)	Xu, *et al.* (2009).
Anti-α-tubulin	Abcam	ab7291	Mouse mAb	1:1000 (IF)	Prins, *et al.* (2009).
Anti-Ubiquitin (Ubi-1)	Abcam	ab7254	Mouse mAb	1:1000 (WB)	Castiel, *et al.* (2011).
Anti-Ubiquitin	Millipore	07-375	Rabbit pAb	1:1000 (WB)	Komander, *et al.* (2009).
Anti-Ubiquitin (P4D1)	Enzo	BML-PW0930	Mouse mAb	1:1000 (WB)	Sokolova, *et al.* (2015).

Table 2.2. Secondary antibodies. Antibody name, supplier, product code, species, dilution of primary antibodies used, and application. Abbreviations: WB = western blot, and IF = immunofluorescence.

Antibody name	Supplier	Code	Species	Dilution	Application
Goat anti-mouse IgG HRP	Santa Cruz Biotechnology	sc-2054	Goat	1:5000	WB
Goat anti-rabbit IgG HRP	Santa Cruz Biotechnology	sc-2005	Goat	1:5000	WB
Goat anti-rat IgG HRP	Santa Cruz Biotechnology	sc-2006	Goat	1:5000	WB
Rabbit anti-goat IgG HRP	Thermo Fisher	31402	Rabbit	1:5000	WB
Alexa Fluor488 Goat anti-mouse	Life Technologies	A11029	Goat	1:500	IF
Alexa Fluor546 Donkey anti-rabbit	Life Technologies	A10040	Donkey	1:500	IF
Alexa Fluor456 Goat anti-rat	Life Technologies	A11081	Goat	1:500	IF

2.1.3. Plasmids

Plasmid DNA was stored at -20ºC.

Table 2.3. Plasmids. Plasmid name and source.

Plasmid name	Source
Mouse HA tagged full length Hectd1^{WT}	Dr M Bienz, LMB Cambridge, UK
Mouse HA tagged full length Hectd1^{C2579G}	Dr M Bienz, LMB Cambridge, UK

2.1.4. siRNA oligonucleotides

All siRNA were resuspended in RNase-free 1x siRNA buffer (GE Dharmacon) at 100µM and the stock solution stored at -20ºC. A working solution of siRNA at 10µM was aliquoted and stored also at -20ºC.

Table 2.4. siRNA oligonucleotide sequences. siRNA name, supplier, product code, and sequences used. Abbreviations: siRNA = small interfering RNA

Name	Supplier	Catalogue	Oligo sequence (5' -> 3')
On-Target Plus Non Targeting Pool siRNA	GE Dharmacon	D-001810-10-05	UGGUUUACAUGUCGACUAA UGGUUUACAUGUUGUGUGA UGGUUUACAUGUUUUCUGA UGGUUUACAUGUUUUCCUA
On-Target Plus HECTD1 Individual #06 siRNA	GE Dharmacon	J-007188-06	GUUAAUAGCUGUACUAGAA
On-Target Plus HECTD1 Individual #07 siRNA	GE Dharmacon	J-007188-07	GCUCAUAGCUGCAUAUAAG
On-Target Plus HECTD1 Individual #08 siRNA	GE Dharmacon	J-007188-08	CAUAGAGGAUUUAGGUUUA
On-Target Plus HECTD1 Individual #09 siRNA	GE Dharmacon	J-007188-09	GAAAGGGACAUGCAACUAA
On-Target Plus HECTD1 SMARTPool siRNA	GE Dharmacon	J-007188-00	GUUAAUAGCUGUACUAGAA GCUCAUAGCUGCAUAUAAG CAUAGAGGAUUUAGGUUUA GAAAGGGACAUGCAACUAA

2.1.5. RT-PCR primers

All primers were resuspended in DNase-free and RNase-free ddH_2O at 100µM and the stock solution stored at -20ºC. A working solution of 10µM was aliquoted and also stored at -20ºC.

Table 2.5. RT-PCR primer sequences. Target, primer sequence, and product size. * = primer sequences previously reported in Valtente V, *et al.* 2009.

Target (human)	**Primer sequence (5' -> 3')**	**Product size (bp)**
HECTD1 (JL 1+2)	Forward: GAATTAGTAAACCCACACAGAGCCAGA Reverse: CATCAAATCCACATATTCTTCTGCATTATCC	300
HECTD1 (JL 3+4)	Forward: TATCCTCTGCTGCCCAGGATGGTGACTGG Reverse: GAAGACTTTGAATTAGTAAACCCACACAGAGC	459
HECTD1 (JL 6+7)	Forward: GAAATACCACCCCCAGGGAC Reverse: TCACGAGTCGTTCCAAGACC	113
RNA Pol IIA	Forward: TTGTGCAGGACACACTCACA Reverse: CAGGAGGTTCATCACTTCACC	83
GAPDH	Forward: GAAGGTCGGAGTCAACGGATTT Reverse: ATGGGTGGAATCATATTGGAAC	147
RPS18	Forward: TGGACAACAAGCTCCGTGAA Reverse: GGGCCCGAATCTTCTTCAGT	53
HPRT1 *	Forward: TGACACTGGCAAAACAATGCA Reverse: GGTCCTTTTCACCAGCAAGCT	94
TBP *	Forward: GAGCTGTGATGTGAAGTTTCC Reverse: TCTGGGTTTGATCATTCTGTAG	117

2.1.6. Cell cycle synchronisers

All synchronisers were stored at -20ºC. Working concentrations of cell cycle synchronisers can be found in section 2.2.1 of Chapter 2.

Table 2.6. Cell cycle synchronisers. Cell cycle synchroniser, resuspension, and stock concentrations.

Cell cycle synchroniser	Resuspension solution	Stock concentration	References
Aphidicolin	DMSO	1mg/ml	Pedrali-Noy, *et al.* (1980). Krokan, *et al.* (1981).
2'-Deoxycytidine	ddH_2O	1M	Thomas & Lingwood. (1975).
Nocodazole	DMSO	1mg/ml	Zieve, *et al*. (1980).
RO-3306	DMSO	5mg/ml	Vassilev, *et al.* (2006).
Thymidine	ddH_2O	100mM	Xeros. (1962).

2.2. Methods

2.2.1. Mammalian cell culture

Human embryonic kidney (HEK) cells, HEK293T HECTD1 knock out cells (Dr Bienz, LMB Cambridge, UK) and HEK293ET cells (American Type Culture Collection, ATCC, USA) were cultured in Dulbecco's modified minimum essential medium (DMEM) with GlutaMAX supplement (Life Technologies, 10566016), supplemented with 10% (v/v) Fetal Bovine Serum (Heat-inactivated FBS, 10270106) (Life Technologies) and 1% (v/v) 10,000 units Penicillin-10mg/ml Streptomycin (Sigma Aldrich, P4333), at 37°C in a humidified incubator with 5% CO_2. Cells were passaged when confluent by incubating with sterile 0.05% EDTA-PBS for 5mins at 37°C, followed by pelleting the cells at 150 x g for 3mins. Cells were then resuspended in supplemented DMEM (+GlutaMAX) and seeded (1/10) in a Nunclon^{TM} Delta surface-treated (Nunc^{TM}) 10cm dish (Thermo Scientific, 150350). Human embryonic kidney (HEK) cells, specifically HEK293ET, offers the possibility to obtain high levels of recombinant protein expression, as well as high transfection efficiency for future studies in this project, and has been used previously in cell cycle studies (Lu, *et al.* 2013). The high recombinant protein expression of HEK293**ET** is attributed to two stably transfected transgenes, **E**BNA-1 and the large **T** antigen, which promote plasmid replication (Durocher, *et al.* 2002). For experiments, HECTD1 knock out cells were cultured from passage 4 to passage 35. Both HEK293T HECTD1 KO1 and KO2 have been generated using the same gRNA and these are confirmed individual clones (and not pools). Sequencing carried out by Dr Bienz's lab on HEK293T HECTD1 KO2 confirms that the mutation induces a frame shift and premature stop codon leading to nonsense mediated decay (Figure A.1). The gRNA is as published in (Flack, *et al*. 2017).

HeLa cells (cervical cancer cell line) (American Type Culture Collection, ATCC, USA) were cultured in DMEM, supplemented with 10% (v/v) FBS and 1% (v/v) 10,000 units Penicillin-10mg/ml Streptomycin. HeLa cells were passaged when confluent by washing with sterile PBS, incubating with sterile 0.05% Trypsin-EDTA (Life Technologies, 25300054) for 5mins at 37°C, followed by pelleting the cells at 150 x g for 3mins. Cells were resuspended in supplemented DMEM and seeded (1/5) in a Nunclon^{TM} Delta surface-treated (Nunc^{TM}) 10cm dish.

Glioblastoma cell lines U87 and U251 (Dr H Haynes, Bristol Southmead Hospital, University of Bristol) were cultured in Eagle's Minimum Essential Media (EMEM) (Sigma, M2279), supplemented with 10% (v/v) Fetal Bovine Serum (Heat-inactivated FBS), 2mM L-glutamine (Thermo Fisher, 25030081), MEM 1% (v/v) non-essential amino acids (Thermo Fisher, 11140050), 1mM sodium pyruvate (Thermo Fisher, 11360070), and 1%(v/v) 10,000 units Penicillin-10mg/ml Streptomycin, at 37°C in a humidified incubator with 5% CO_2. U87 and

U251 cell lines were passaged when confluent by washing with sterile PBS, incubating with sterile 0.25% Trypsin-EDTA (Life Technologies, 25200056) for 5mins at 37°C, followed by pelleting the cells at 150 x g for 3mins. Cell were then resuspended in supplemented EMEM and seeded (1/5) in a Nunclon™ Delta surface-treated (Nunc™) 10cm dish. U87 are of likely glioblastoma origin and U251 are glioblastoma astrocytoma cells. Finally, all cell lines were tested for Mycoplasma contamination, using the MycoAlert™ Mycoplasma Detection Kit (Lonza), as per manufacturer's instructions.

Cell synchronisation

To synchronise the cells with RO-3306, cells were treated with 9μM RO-3306 (Caymen, 872573-93-8) for 20hrs, washed three times in PBS, and released into fresh media for synchronous progression of the cell cycle from the G2/M transition. For synchronisation using Aphidicolin, cells were cultured in medium with reduced serum (0.5% FBS (v/v)), for 48hrs before treatment with 11.8μM Aphidicolin (Fisher Scientific, 38966-21-1) for 15hrs. Cells were washed three times in PBS, and released in fresh media for synchronous progression of the cell cycle from the G1/S transition. For synchronisation with Nocodazole (Sigma-Aldrich, M1404), cells were treated with 50ng/ml Nocodazole for 20hrs, before collection of mitotic cells via mitotic shake off. The cells were centrifuged at 150 x g for 3mins, washed with PBS three times, then released into fresh media and plated into a 6 well plate, for synchronous progression of the cell cycle from metaphase. For a double thymidine block, cells were treated with 2mM thymidine (Sigma-Aldrich, T9250) for 18hrs, and then washed with PBS once, before adding fresh media containing 25μM 2'-deoxycytidine (Sigma-Aldrich, D3897) for 9hrs. After 9hrs, 2mM thymidine was added for 15hrs. Cells were washed three times in PBS, and released in fresh media containing 25μM deoxycytidine for synchronous progression of the cell cycle from the G1/S transition.

2.2.2. Transfection and gene silencing

Transfection of siRNA oligonucleotides

HEK293ET were seeded into an appropriately sized plate one day prior to transfection into DMEM + 10% (v/v) FBS, without antibiotics present. 24hrs later the knockdown mix was made by combining siRNA and Lipofectamine® 2000 diluted in OptiMEM (Life Technologies, 31985062). For HEK293ET cells, in a 24-well plate, 20pmol of siRNA RNA and 1μl of Lipofectamine® 2000 (Thermo Fisher, 11668027) was used, according to the manufacturer's protocol (see Table 2.7 for more details). Lipofectamine® 2000 was added to OptiMEM and left to incubate for 5mins, before being added to OptiMEM containing the appropriate siRNA and left to incubate for a further 20mins at room temperature. During this time, all media was removed from the wells, so that only the knock down mix covered the

cells. 4-6hrs later DMEM + 10% (v/v) FBS was added to each well to make it the appropriate total volume for each well.

HeLa cells were seeded into an appropriately sized plate one day prior to transfection into DMEM + 10% (v/v) FBS, without antibiotics present. Again, 24hrs later the knockdown mix was made by combining siRNA and Lipofectamine 2000 diluted in OptiMEM. For HeLa cells, in a 24-well plate, 25pmol of siRNA RNA and 0.5µl of Lipofectamine® 2000 was used, according to the manufacturer's protocol (see Table 2.8 for more details). Lipofectamine® 2000 was added to OptiMEM and left to incubate for 15mins, before being added to OptiMEM containing the appropriate siRNA and left to incubate for a further 15mins at room temperature. Again, during this time all media was removed from the wells, so that only the knock down mix covered the cells. 4-6hrs later DMEM + 10% (v/v) FBS was added to each well to make it the appropriate total volume for each well.

U87 and U251 cells were seeded into an appropriately sized plate one day prior to transfection into supplemented EMEM, without antibiotics present. 24hrs later, Lipofectamine® RNAiMAX (Thermo Fisher, 13778-075) was diluted in OptiMEM and incubated for 5mins before being added to the appropriate volume of siRNA (Table 2.9), and incubated for a further 5mins at room temperature. All media was removed from the wells, and then knock down mix was added. 4-6hrs later supplemented EMEM was added to each well to make it the appropriate total volume for each well. All samples were then harvested for the appropriate assay.

Table 2.7. HEK293ET knockdown mix. Volumes of siRNA, Lipofectamine® 2000, and OptiMEM provided for each size plate format.

	24 well plate	**12 well plate**	**6 well plate**
siRNA (20µM)	1µl	2µl	5µl
Lipofectamine® 2000	1µl	2µl	5µl
OptiMEM	50µl of each (100µl in total)	100µl of each (200µl in total)	250µl of each (500µl in total)

Table 2.8. HeLa knockdown mix. Volumes of siRNA, Lipofectamine® 2000, and OptiMEM provided for each size plate format.

	24 well plate	**12 well plate**	**6 well plate**
siRNA (20µM)	1.25µl	2.5µl	6.25µl
Lipofectamine® 2000	0.5µl	1µl	2.5µl
OptiMEM	50µl of each (100µl in total)	100µl of each (200µl in total)	250µl of each (500µl in total)

Table 2.9. U87 and U251 knockdown mix. Volumes of siRNA, Lipofectamine® RNAiMAX, and OptiMEM provided for each size plate format.

	24 well plate	12 well plate	6 well plate
siRNA (20μM)	1μl	2μl	5μl
Lipofectamine® RNAiMAX	1.5μl	3μl	7.5μl
OptiMEM	50μl of each (100μl in total)	100μl of each (200μl in total)	250μl of each (500μl in total)

Plasmid transfection

HEK293ET and HEK293T cells were seeded into an appropriately sized plate one day prior to transfection into DMEM + 10% (v/v) FBS, without antibiotics present. 24hrs later, the transfection mix was made by combining branched PEI (MW ~25000) (Sigma, 408727) and DNA at a ratio of 3:1 diluted into 150mM NaCl. For example, in 24 well plate, 250ng of DNA was combined with 750ng of PEI (Table 2.10). The PEI and DNA were individually diluted in 150mM NaCl, left for 5mins before being combined and then incubated for 15mins at room temperature. The mix was then added to cells that had been placed in OptiMEM, and left before a media change into DMEM + 10% (v/v) FBS 24hrs later (this step was optional depending on the assay).

Table 2.10. HEK293ET and HEK293T knockdown mix. Volumes of DNA, PEI, and NaCl provided for each size plate format. Concentration (x) depends on the DNA.

	24 well plate	12 well plate	6 well plate
DNA	250ng	500ng	1-1.25μg
PEI (1mg/ml)	3:1	3:1	3:1
NaCl (150mM)	50μl per tube (100μl in total)	100μl per tube (200μl in total)	250μl per tube (500μl in total)

2.2.3. Microscopy

Immunofluorescence

For confocal imaging, cells were plated at an experiment specific density onto Poly-L-Lysine (mol wt 30,000 – 70,000) (Sigma-Aldrich, 9155) coated Nunc™ Thermanox™ 13mm coverslips (Thermo Fisher, 1749500) in 12well plates (Corning, CLS3513). Asynchronous or synchronous cells were then fixed with 300μl/well 4% (w/v) paraformaldehyde, washed three times with 1ml PBS 100mM glycine, then permeabilised with 0.1% (v/v) Triton PBS for 5mins at room temperature. Cells were washed three times with 1ml PBS and then blocked with 3% (w/v) BSA in PBS for 1hr at room temperature. Cells were then incubated with 100μl/coverslip primary antibody for 1hr at room temperature. Cells were washed three

times with PBS and then incubated with 100µl/coverslip secondary antibody for 1hr at room temperature. Cells were washed twice with PBS and then counterstained with 100µl/coverslip Hoechst 33342 (Thermo Fisher, H1399), 1µg/ml in PBS, followed by two more washes in PBS. VectaShield Antifade Mounting Medium (Vector Laboratories, H-1000) was used as the mounting media. Samples were then imaged on the LSM Meta 510 confocal microscope (Zeiss).

Microtubule regrowth assay

HEK293ET and HEK293T cells were seeded at 150,000 cells per well on Poly-Lysine coated coverslips before the addition of 300ng/ml of Nocodazole (Sigma M1404) in DMEM for 1hr at 37ºC. Cells were then shifted on ice for 30mins, followed by two 3min washes in ice cold PBS. The treated cells were released into DMEM at 37ºC before then fixing the cells in 4% (w/v) PFA at 15mins post-release. Cells were then stained for immunofluorescence with the microtubule marker, α-tubulin (to enable visualisation of microtubules at different time points), in addition to the DNA stain, Hoechst 33342 (Thermo Fisher, H1399), 1µg/ml in PBS.

Spindle Assembly Checkpoint marker staining

HEK293ET and HEK293T cells were seeded at 150,000 cells per well on Poly-Lysine coated coverslips before the addition of 9µM RO-3306 (Caymen, 872573-93-8) for 20hrs. After the incubation cells were washed three times with warm PBS for 5mins, and released into DMEM at 37ºC before then fixing the cells in 4% (w/v) PFA at 0, 10, 30, 60, and 120mins post-release. Cells were then stained for immunofluorescence with the spindle assembly checkpoint marker, BuBR1, and the microtubule marker, α-tubulin, in addition to the DNA stain Hoechst.

Live cell imaging

For live cell imaging, HEK293ET and HEK293T cells were seeded at 30,000 cells per ml onto Poly-L-Lysine (mol wt 30,000 – 70,000) (Sigma-Aldrich 9155) coated plastic Ibidi 8-well chamber slides (Ibidi IB-80826). Cells were left overnight in 300µl/well DMEM + 10% (v/v) FBS, before exchanging the media the following day for Leibovitz's L-15 media (no phenol red) (Life Technologies 21083027), with 10% (v/v) FBS. Cells were then filmed over the course of hours at either 2, 3, or 5min intervals using an Olympus IX81 microscope with a 40X oil immersion objective lens and Hammatsu ORCA-ET Camera for imaging at 37ºC. Micro-Manager (Edelstein, *et al.* 2014) was used to acquire and manage the images. Only the DIC channel was used for imaging. A binning of 2 was used for image acquisition, and images were acquired as a stacked TIFF format for downstream analysis. Images were then processed using ImageJ software (National Institutes of Health).

2.2.4. Flow Cytometry: cell cycle profiling

HeLa cells were seeded at 300,000 cells per well and HEK293ET cells at 500,000 cells per well in a 6 well plate (Corning, 3516), cultured as normal, then treated with an appropriate cell synchroniser. At each time point samples were harvested in the following manner. The culture media was removed and saved in an eppendorf, the cells were then rinsed with PBS, before being treated with 300µl of 0.05% Trypsin-EDTA (Life Technologies, 25200056). Once the cells were fully trypsinised the media was added back to generate a single cell suspension. Cells were pelleted at 500 x g for 5mins, supernatant discarded, then washed with PBS, by centrifugation and removing the supernatant. Cells were fixed in 69% ethanol, 400µl ice-cold PBS with 900µl ice-cold 100% ethanol. Samples were then stored at 4ºC for at least 2hrs before staining. Samples were stained the same day as collecting the data. 2µg/ml Propidium Iodide (PI) (Life Technologies, P3566) and 100µg/ml RNase A (Life Technologies, EN0531) were diluted in 500µl FACS Staining Buffer. The samples were then incubated at 37ºC for 30mins before being placed on ice in the dark, just before running the samples on the BD FACSCanto (BD Biosciences). Data were analysed using BD FACSDIVA™ software V.8.0.1. For cell cycle analysis, histograms were gated at 50 PI-A to calculate the percentage of cells in G1 and 100 PI-A to calculate the % of cells in G2.

2.2.5. Cell proliferation assay

Trypan Blue counting

HEK293ET and HEK293T cells were seeded at 60,000 cells per well in a Poly-L-Lysine coated 24 well plate (Corning, 3524). At each time point cells were trypsinised and resuspended in DMEM + 10% (v/v) FBS, before being mixed in a 1:1 ratio with Trypan Blue solution 0.4% (Thermo Fisher, 15250061). Cells were then counted under a light microscope using a haemocytometer. Cells that are dead appear blue and cells that are living appear white. Counts were carried out in triplicate for each sample over three independent experiments. If appropriate some of the sample was kept and stored for Western Blot analysis. Total number of viable cells and percentage viability were calculated using the equations below.

$$Viable\ Cells = Number\ of\ blue\ cells - Total\ number\ of\ cells$$

$$\%\ Viability = \left[1 - \left(\frac{Number\ of\ blue\ cells}{Total\ number\ of\ cells}\right)\right] \times 100$$

CellTiter-Glo assay

HEK293T cells were seeded at 4000 cells per well into a Poly-L-Lysine coated 96 well clear-bottomed white walled plate (Corning, 3903) in DMEM + 10% (v/v) without antibiotics. 48hrs later cells were transfected with either empty vector (eV), full length HA-HECTD1^{WT}, or HA-HECTD1^{C2579G} vector (see 2.2.2 for transfection protocol), then left for 48hrs before measuring the ATP content using CellTiter-Glo assay kit (Promega, G7570). The assay was carried out according to the manufacturer's protocol for a 96 well format, and measured in the GloMax Multi Plate Reader (Promega).

Colony formation assay

HEK293T cells were seeded at 500 cells per well in 5mL of DMEM + 10% (v/v) FBS of a 6 well plate. The cells were left to grow over a period of 9 days before fixing in Colony Formation Assay Fixing Solution for 30mins at room temperature. The Colony Formation Assay Fixing Solution was removed and replaced with Colony Formation Assay Staining Solution for 1hr at room temperature. Cells were then washed with water and left to air dry before being imaged with a commercial camera (adapted from Haloom, *et al*. 2011).

2.2.6. Western blotting

Protein assays

Control asynchronous or synchronised cells were grown in an appropriately sized plate depending on the assay type, then lysed in Triton X-100 lysis buffer with the addition of Pierce^{TM} Protease Inhibitor Mini Tablets (Thermo Fisher, 86665) and Pierce^{TM} Phosphatase Mini Tablets (Thermo Fisher, 88667). Cell lysates were clarified by centrifugation and total protein concentration was determined using Pierce^{TM} Coomassie Plus Bradford assay kit (Life Technologies, 23236), according to manufacturer's instructions for 96 well format. For cells that were lysed in RIPA buffer, protein quantification had to be carried out by using the Pierce^{TM} Bicinchoninic Acid (BCA) protein assay kit (Thermo Fisher, 23225). A standard curve was generated according to the protocol and using the BSA protein standard provided (Thermo Fisher, 23236). A BCA working solution was prepared by mixing Reagent A and Reagent B together at a ratio of 50:1. In a 96 well plate, 10µl of each standard was plated in triplicate, followed by each sample in triplicate. 200µl of working solution was then added to each well before the plate was incubated at 37°C for 30mins. The absorbance at 565nm was taken using a Spectra Rainbow microplate spectrophotometer (Thermo Fisher). Protein concentrations were calculated from the BSA standard curve in Microsoft Excel. Protein values were normalised between samples based from the BCA assay by the addition of lysis buffer to yield the same protein concentration across the samples.

SDS-PAGE

Samples were prepared using NuPage 4X LDS sample buffer (Life Technologies, NP0007), reduced in 100mM Dithiothreitol (DTT) (Sigma-Aldrich, DTT-RO ROCHE) and denatured at 95°C for 5mins. Samples were run on NuPAGE® Novex® 4-12% Bis-Tris Protein Gels, 1.0mm gels (Life Technologies, NP0322BOX) for 100mins at 140V in 1X NuPAGE® MOPS SDS Running Buffer (Life Technologies, NP0001). Samples were run alongside the PageRuler^{TM} Prestained Protein Ladder (Thermo Fisher, 26616).

Wet transfer

Samples were transferred from the protein gel to a Whatman® Westran® PVDF membrane 0.45µm (Sigma-Aldrich, Z671088) using the Bio-Rad Mini Trans-Blot® Wet Transfer System (Bio-Rad), for 60mins at 100V in Wet Transfer Buffer (see section 2.1.1).

Membrane boiling

For detection of ubiquitin, samples were placed in sample buffer and were frozen without boiling. Prior to blocking membranes are boiled in the microwave for 10mins in ddH_2O sandwiched between glass plates, to ensure even boiling (adapted from Emmerich, & Cohen. 2015).

Immunoblotting

PVDF membrane was blocked in 3% BSA-PBS-Tween (0.1%) for 1hr at room temperature. Primary antibody was diluted in 3% BSA-PBS-Tween (0.1%) as described in Table 2.2 and incubated either over-night at 4°C or for 1hr at room temperature. Membranes were then washed three times for 5mins in PBS-Tween (0.1%) before the addition of species-specific horseradish-peroxidase (HRP)-conjugated secondary antibody diluted as described in Table 2.2. in 3% BSA-PBS-Tween (0.1%) for 1hr at room temperature. Membranes were washed a further three times for 5mins before three quick washes with ddH_20 to remove any excess Tween. Proteins were detected by incubating membranes for 1min using Pierce^{TM} ECL Western Blotting Substrate (Life Technologies, 32106). Chemiluminescence was detected using Fusion SL Chemiluminescence and Fluorescence Imager, Vilber Lourmat. Quantification of detected bands was carried out using ImageJ software (http:// rsb.info.nih.gov/ij/; W. Rasband, National Institutes of Health, Bethesda, USA).

2.2.7. Pull-down assays

NZF1 pull-down assay

For the enrichment of K29/K33 ubiquitin chains, GST-TRABID$_{1-200}$, GST-NZF1, and GST-NZF1 LV/TY domains expressed in *E. Coli* were used (contributed by Dr Licchesi). For each

10cm^3 dish, 100ug of trapping protein was used. 10µg of GST tagged protein was conjugated to Pierce™ Glutathione Magnetic Agarose Beads (Thermo Fisher, 78602), for 1hr at room temperature. Cells in 10cm^3 dishes were lysed in 500µl of TRABID$_{1-200}$ IP Lysis Buffer for 20mins, before being clarified by centrifugation (13,000 x g for 15mins at 4°C). 60µl of lysate was collected for the input sample. 110µl of lysate was added to 50µl of conjugated beads in 500µl TRABID$_{1-200}$ IP Pull-Down Buffer and left overnight at 4ºC. Beads were then washed four times in TRABID$_{1-200}$ IP Wash Buffer for 5mins, before the addition of 2X LDS sample buffer with 100mM DTT.

2.2.8. Molecular biology

DNA agarose gel electrophoresis

PCR products were combined with bromophenol blue loading buffer (1% v/v). Samples were then loaded onto 0.8 – 3% (w/v) agarose Tris-Acetate-EDTA (TAE) gels containing GelStar™ Nucleic Acid Stain 0.2X (Lonza, S9430), alongside 5µl of 1Kb Plus DNA Ladder (Invitrogen, 10787018). DNA gels were run at approximately 10V/cm of gel until the gel front approached the end of the gel. DNA on the gel was visualised using a non-UV Darker Reader Transilluminator (Clare Chemical Research). Gels were imaged using the UV filter in the GelDoc-It™ Imaging System (UVP).

Transformation of chemically competent cells

One Shot™ TOP-10 Chemically Competent *E. Coli* (Thermo Fisher, C404010) were thawed on ice and dispensed into 25µl aliquots. 2µl of plasmid DNA was added to each aliquot and incubated on ice for 30mins. Negative, no DNA, and positive pUC19 vector control transformations were included according to the manufacturer's instructions. Samples were then heat-shocked at 42°C for 30secs and placed on ice for a further 2mins, before 250µl of pre-warmed S.O.C medium (2% tryptone, 0.5% yeast extract, 10mM NaCl, 2.5mM KCl, 10mM $MgCl_2$, 10mM $MgSO_4$, and 20mM glucose) (Thermo Fisher, 15544034) was added. Samples were then left at 37°C with vigorous shaking for 1hr to allow outgrowth. Between 20 and 200µl was then plated onto LB Agar selective plates and left at 37°C overnight to allow colony formation.

Plasmid purification

Colonies from the desired plasmid product were expanded by picking a single colony with a pipette tip and adding it to prewarmed selective media, 5ml for miniprep and 50ml for midiprep cultures. Cultures were grown overnight at 37°C with vigorous shaking. Plasmids were purified from overnight cultures using QIAGEN Midi/ Maxi-Prep Kits (Qiagen, 12163) according to the manufacturer's instructions. DNA was eluted using Buffer EB.

2.2.9. RT-PCR

Lung cell line RNA was contributed by Dr Licchesi (University of Bath). Glioblastoma cDNA was contributed by Dr Kurian (University of Bristol). Reverse transcription was performed using the High Capacity RNA-to-cDNA Kit™ (Applied Biosystems, 4387406). 1µg of RNA was used per 20µl reaction, according to manufacturer's instructions. The quality of the RNA was checked using an agarose gel and the RNA was quantified using a NanoDrop (Thermo Fisher).

RT-PCR

PCR reactions were set up with a total volume of 100µl, at a final concentration, containing 1 X PCR buffer, 20µM dNTPs (each), 1.5mM $MgCl_2$, 0.5µM Forward Primer, 0.5µM Reverse Primer, 1U Taq Polymerase (Thermo Fisher, EP0404), and 2µl cDNA. Reactions were carried out in a Bio-Rad Thermocycler (Bio-Rad) using the following cycling protocol: initial denaturation at 94ºC for 5mins, then 25 cycles of denaturation at 94ºC for 45secs, annealing at 55ºC for 30secs, and extension at 72ºC for 30secs, followed by a final extension at 72ºC for 10mins. A low number of PCR cycle was selected to provide semi-quantitative analysis of expression. For each reaction, a negative RT control with no reverse transcriptase present was used to confirm the absence of contaminating genomic DNA and water control were ran as negative controls on a 3% (w/v) agarose TAE gel containing GelStar™ Nucleic Acid Stain 0.2X, alongside 5µl of 1Kb Plus DNA Ladder, to assess HECTD1 expression in the cancer cell lines.

Real time quantitative PCR (RT-qPCR)

The standard reaction used in all the RT–PCR performed was as follows; 1X Power SYBR Green PCR Master Mix (Applied Biosystems, 4368577), 100nM reverse and forward primer, 100ng cDNA and nuclease–free water made up to 20µl (according to the manufacturer's instructions). Primers shown in Table 2.5. PCR reactions were loaded into MicroAmp fast 96–well reaction plates (Applied Biosystems, 4349606) and the plates were sealed with MicroAmp Optical adhesive film (Applied Biosystems, 4311971). The cycling conditions for all reactions were as follows: initial denaturation at 95ºC for 10mins, then 40 cycles of denaturation at 95ºC for 15secs and annealing at 55ºC for 1min. Reactions were carried out using the StepOnePlus RealTime PCR System (Applied Biosystems) and threshold cycles (C_T) were calculated using the instrument software. Control reactions without reverse transcriptase confirmed the absence of contaminating genomic DNA. Primer efficiency was validated by Dr Licchesi and amplified with an efficiency of 2. C_T values were normalised to RNA Pol II and RPS18 housekeeping genes. These ΔCT values were used to calculate the relative change in mRNA expression as the ratio of mRNA expression in treated cells versus

mRNA expression in the control condition, using the Livak method (Livak & Schmittgen. 2001).

The final normalised ratio was calculated by the following formula:

$$Normalised\ relative\ ratio = 2^{-\Delta\Delta CT}$$

Where,

$$\Delta C_T = C_T\ (target) - C_T\ (reference)$$

$$\Delta\Delta C_T = \Delta C_T\ (sample) - \Delta C_T\ (calibrator)$$

Data are presented as mean ratio values ±SEM from three biological repeats.

2.2.10. Statistical analysis

All data were analysed using GraphPad software (Prism, La Jolla, CA, USA), including mean, standard error values and statistical analysis. Standard error of the mean (S.E.M.) was calculated to quantify the precision of the mean and to compare differences in the means between conditions. S.E.M. was used to take into account both the value of the standard deviation and the sample size. Statistical analysis was carried out either using a one-way ANOVA with a Dunnett's post-test, or a paired student's t-test. A one-way ANOVA with a Dunnett's post-test was used when comparing a series of conditions to a single control condition. A paired student's t-test was used when comparing two conditions. Relevant p-values are indicated where relevant by * $p < 0.05$, ** $p < 0.01$ and *** $p < 0.001$. A p-value of less than 0.05 was considered to be significant.

Chapter 3: Is HECTD1 a novel cell cycle regulator?

3.1. Introduction:

HECTD1, a member of the class II family of HECT E3 ubiquitin ligases, was first demonstrated to function in dorsal neural tube closure in mice, where it is required for the migration of cranial mesenchyme migration (Zohn, *et al.* 2007; Sarkar, *et al.* 2012; Grau-Bove, *et al*. 2013). The mechanism put forward suggested that HSP90 was ubiquitinated with K63-linked ubiquitin chains by HECTD1, although clear evidence on the chain type involved and the fate of ubiquitinated HSP90 are still lacking (Sarkar, *et al.* 2012). HECTD1 also appears to function as a negative regulator of Wnt signalling, a key signal transduction pathway that regulates stem cell homeostasis (Tran, *et al.* 2013). Here, HECTD1 was reported to ubiquitinate APC with K63 chains and in doing so facilitate the binding of the APC to Axin, an inhibitor of the Wnt signalling pathway (Nakamura, *et al*. 1998; Tran, *et al.* 2013). Therefore, HECTD1-mediated K63 ubiquitination might regulate the assembly of the β-catenin destruction complex (Tran, *et al.* 2013). Other roles for HECTD1 involve substrate degradation, for example, the regulation of focal adhesion sites where HECTD1 is responsible for the degradation of PIPKIγ90, and its role in oestrogen-regulated enhancer activation mediated by the degradation of RIP40 (Li, *et al.* 2013b; Li, *et al*. 2015). Additionally, HECTD1 functions in placenta development, the mechanism by which this occurs is unknown (Chapter 1) (Sarkar, *et al.* 2014; Sarkar, *et al.* 2016; Shen, *et al.* 2017).

Whilst synthesis of K63 chains by HECTD1 has been suggested in previous studies mentioned above, there are a lack of *in vitro* biochemical experiments to directly support this conclusion. Unpublished *in vitro* biochemical data from the lab, suggests that HECTD1 synthesises mixed K29 and K48 ubiquitin chains (Figure 3.1A). Ubiquitin-absolute quantification (AQUA) mass spectrometry (Kettenbach, *et al*. 2011) was carried out on *in vitro* synthesised wild-type polyubiquitin ubiquitin to determine the abundance of different ubiquitin linkages. It was revealed that K29 and K48 linkages were the most abundant, and that K63 linkage only accounted for 13% of the ubiquitin synthesised by the catalytic domain of HECTD1 (Figure 3.1B) (Licchesi, unpublished data). HECTD1 is only the second ubiquitin ligase, in addition to UBE3C, to assemble mixed K29/K48 chains. However, the function of this chain type has not been investigated beyond the ubiquitin fusion degradation (UFD) pathway. Additionally, their role in signal transduction and in the regulation of cellular processes such as the cell cycle regulation remains unknown.

Interestingly, mixed K29/K48 ubiquitin chains have been linked to proteasomal degradation via the UFD pathway. The UFD pathway is a proteolytic system that involves an uncleavable ubiquitin moiety fused to the N-terminus of a protein during translation, which serves to function as a degradation signal (Johnson, *et al*. 1995). Recently, it was shown in *S. cerevisiae*, that the HECTD1 orthologue, Ufd4p, has been demonstrated to be a UFD ligase.

Together with Ufd2p, Ufd4p is able to conjugate branched ubiquitin chains of K29 and K48 that are synthesised on UFD substrates resulting in proteasome degradation (Liu, *et al.* 2017). Therefore, this suggests that the atypical K29/K49 ubiquitin chains synthesised by HECTD1 may function in the UFD pathway in mammalian cells. Furthermore, data in multicellular organisms such as *C.elegans* also suggests that HECTD1 is a UFD pathway E3 ligase, where it functions to regulate mitochondrial proteins (Segref, *et al.* 2014). Nevertheless, the function of this chain type beyond the UFD pathway has until now not been investigated. It was initially considered that branched chains seem to be less effective at promoting proteasome degradation compared to a single linkage (Kim, *et al.* 2007; Kim, *et al.* 2009). However, a role for branched ubiquitin chains in protein degradation is starting to emerge. For instance, recent evidence suggests that K11/K48 branched chains, synthesised by the APC/C together with UBE2S and UBE2C, enhances UPS-mediated degradation (Meyer & Rape. 2014; Grice, *et al.* 2015; Yau, *et al.* 2017). Additionally, K48 branching of K29-linked ubiquitin chains, has been identified as a better degradation signal than K29 alone (Liu, *et al*. 2017).

Indeed, mixed ubiquitin chains have been demonstrated as having an important role in cell cycle regulation. Using a K11/48 bispecific antibody, *in cellulo,* it was confirmed that APC/C substrates Cyclin A, CDC20, and NEK2A were indeed modified with branched K11/K48-linked ubiquitin chains (Yau, *et al.* 2017). Furthermore, in synchronised cells, the abundance of these chains were measured by immunofluorescence using a specific antibody and this revealed that the abundance of K11/K48-linked ubiquitin chains increases during mitosis (Yau, *et al.* 2017). This further suggests that branched chains containing K48 are degradation signals.

A

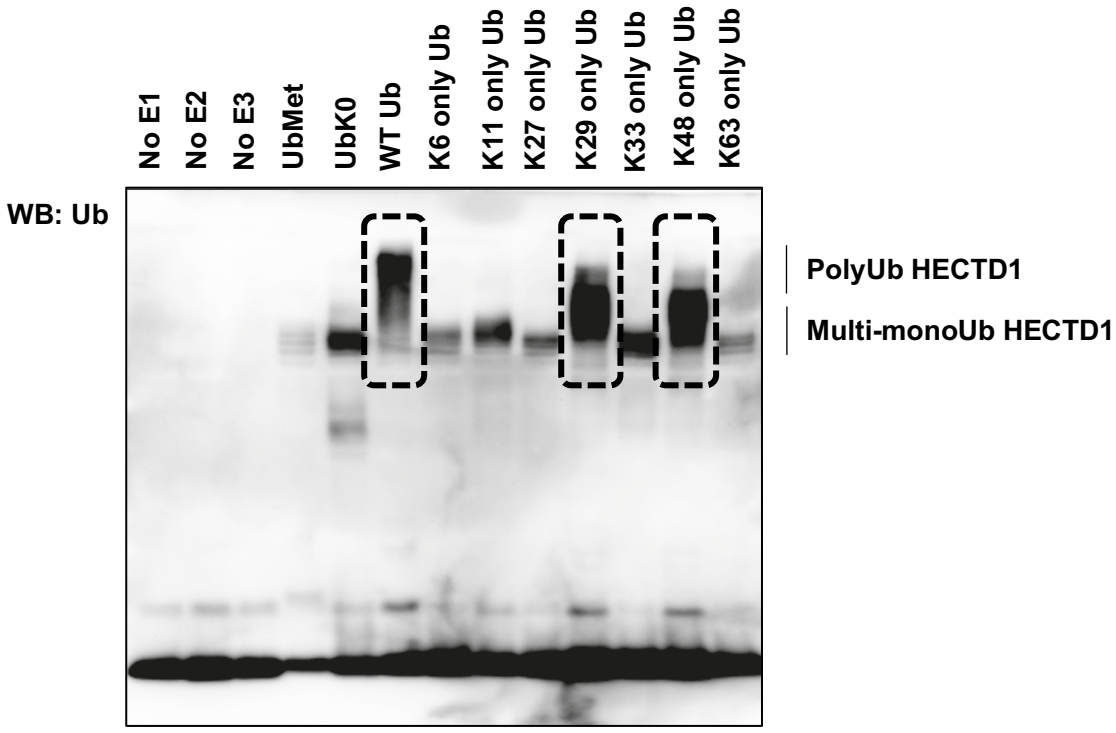
No E1
No E2
No E3
UbMet
UbK0
WT Ub
K6 only Ub
K11 only Ub
K27 only Ub
K29 only Ub
K33 only Ub
K48 only Ub
K63 only Ub
WB: Ub
PolyUb HECTD1
Multi-monoUb HECTD1

B

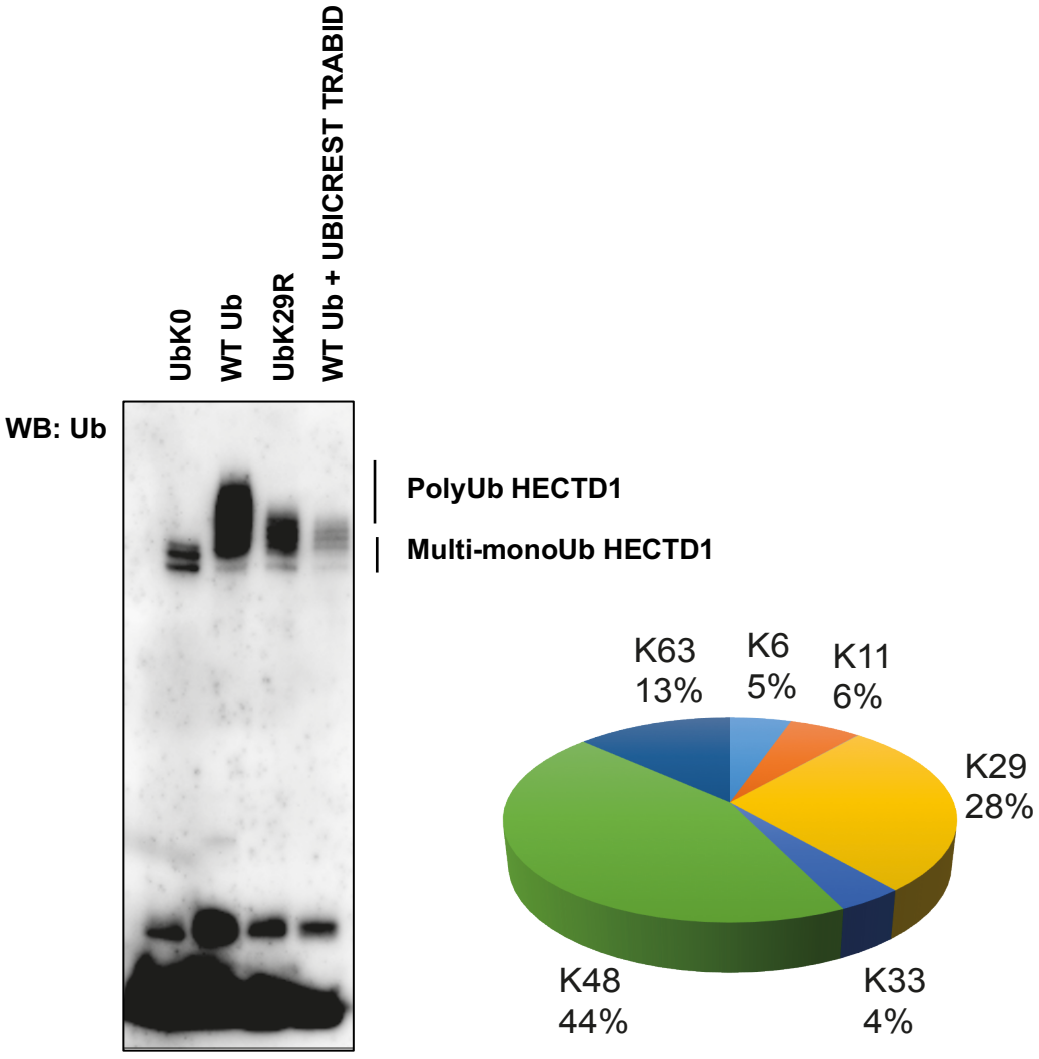
UbK0
WT Ub
UbK29R
WT Ub + UBICREST TRABID
WB: Ub
PolyUb HECTD1
Multi-monoUb HECTD1
K63
13%
K6
5%
K11
6%
K29
28%
K48
44%
K33
4%

Figure 3.1. HECTD1 synthesises atypical K29 and K48 ubiquitin chains *in vitro*. A) *In vitro* autoubiquitination assay using wild-type or mutant ubiquitin to assess the linkage specificity of HECTD1 conducted by Dr Licchesi. No E1, E2 and E3 controls, to show that ubiquitin conjugation requires E1, E2 and E3 activity. The methylated ubiquitin, UbMet, is unable to form polyubiquitin chains and can be used to visualise multi-monoubiquitination events. Ub-K0 is a mutant form of Ub, in which all Ks are replaced with Rs: Ub-K6R, K11R, K27R, K29R, K33R, K48R, and K63R are mutant forms of Ub with Lysines on residue 6, 11, 27, 29, 33, 48, and 63, respectively, replaced with Arginine, so therefore is also not able to form polyubiquitin chains. The following ubiquitin mutants K6, K11, K27, K29, K33, K48, and K63- only ubiquitin prevent the formation of a ubiquitin chain through any lysine residue other than non-mutated residue named, so for example the K6 only mutant can only form K6 ubiquitin chains. Interestingly, other than the WT ubiquitin, only the K29-only and K48-only mutants were able to produce a polyubiquitin smear. However, compared to the WT polyubiquitin smear both the K29 only and K48 only ubiquitin cannot fully constitute the signal of the WT ubiquitin. This suggests that HECTD1 conjugates mixed ubiquitin chains of K29 and K48. B) To confirm the presence of atypical chains, ubiquitin-AQUA Mass spectrometry was carried out on the polyubiquitin smear made with wild type ubiquitin. Left: western blot, showing the wild-type ubiquitin smear analysed by ubiquitin-AQUA, alongside a K29R ubiquitin mutant and a UbiCREST TRABID sample. The K29R ubiquitin mutant prevents ubiquitin linkages through K29, and therefore this sample shows the extent of chain formation without K29, again highlighting that K29 is required to recover the full ubiquitin smear of the wild type ubiquitin, but is not the only linkage present. Furthermore, the UbiCREST TRABID sample demonstrates that the wild-type smear can be digested by the K29/K33 specific DUB, however a small polyubiquitin smear remained. This further demonstrates that K29 linkages form part of the polyubiquitin conjugates that can be assembled by HECTD1. Right: pie chart showing the representation of the different lysine residue linkages present in the wild type ubiquitin smear. K48 and K29 are the most abundant chain types, again demonstrating that HECTD1 is a E3 ubiquitin ligase synthesising atypical ubiquitin chains assembled via K29 and K48.

3.1.1. Aims

Unpublished data from the lab suggests that HECTD1 is a E3 ubiquitin ligase synthesising atypical ubiquitin chains assembled via K29 and K48. Furthermore, previous observations in our lab have suggested that HECTD1 might localise to the mitotic spindle. Therefore, the aim of this chapter was to search for a cell cycle-related phenotype upon HECTD1 depletion by initially focusing on cell proliferation, and then characterising the role that these atypical chains K29/K48 chains have in its cellular function. To achieve this the following objectives were addressed:

1. To determine whether HECTD1 transient depletion or genetic knockout led to reduced cell proliferation in HEK293T, HEK293ET and HeLa cells. This was achieved using trypan blue cell counting and the CellTiter-Glo assay kit (Promega).

2. To optimise the transient knock down of HECTD1 with the view to validate the cell proliferation findings using transient depletion and knockout of HECTD1. Optimisation was carried out in HEK293ET cells using both HECTD1 SMARTpool siRNA and individual HECTD1 siRNAs.

3. To establish protocols for the cell synchronisation of different cell cycle populations using propidium iodide staining and flow cytometry, with the view to study HECTD1 function in the cell cycle. Both HEK293ET and HeLa cells were synchronised with four different cell synchronisers (RO-3306, Nocodazole, Aphidicolin and double Thymidine block).

4. To quantify HECTD1 expression at the protein level in the different stages of the cell cycle in HEK293ET and HeLa cells by densitometry using western blotting. Cells were synchronised and the levels of HECTD1 protein were quantified relative to beta actin (housekeeping protein) over the different stages of the cell cycle.

3.2. Results:

3.2.1. Decrease in cell proliferation observed in HECTD1 knockout cell lines

A previous observation in the Licchesi lab was that HECTD1 was shown by immunofluorescence to localise to the mitotic spindle during mitosis. Furthermore, a cellular function for the atypical K29/K48 ubiquitin chains synthesised by HECTD1 had not been established. Therefore, to establish a role for HECTD1 in the cell cycle, and to characterise a functional role for these atypical chains, the effect of HECTD1 depletion on cell proliferation was first characterised. The cell cycle and cell proliferation are directly linked (Duronio & Xiong. 2013), so it was deemed appropriate to first characterise the effect of HECTD1-depletion on cell proliferation as an simple read-out of any potential cell cycle function of HECTD1. The hypothesis being that if HECTD1 regulates the cell cycle, it may result in changes in overall cell proliferation.

To this end, two CRISPR/Cas9 knockout clones were manually counted over 6 days using trypan blue staining and compared to wild type cells. Interestingly, trypan blue cell counting revealed a significant reduction in proliferation in HECTD1 KO1 and KO2 cell lines compared to the WT control (Figure 3.2A, C-D). By day 6 there was a 23.6% reduction in KO1 cells and a 24.9% reduction in KO2 cells. Furthermore, in both cell lines there was no observable change in viability between conditions (Figure 3.2B), indicating that the reduced cell number is due to cells proliferating slower compared to the wild type cells. Furthermore, this decrease in proliferation is observed in both HECTD1 knock out clones, indicating that this observation is not as a result of clonal selection. This decrease in cell proliferation was also visualised in the colony formation assay (Figure 3.1E), where the colonies formed by KO1 cells were fewer and smaller than the WT control. This was also observed with the KO2 cells but to a lesser extent. Taken together these results suggest that upon HECTD1 knockout, cells proliferate at a slower rate, with no change in viability over time in culture.

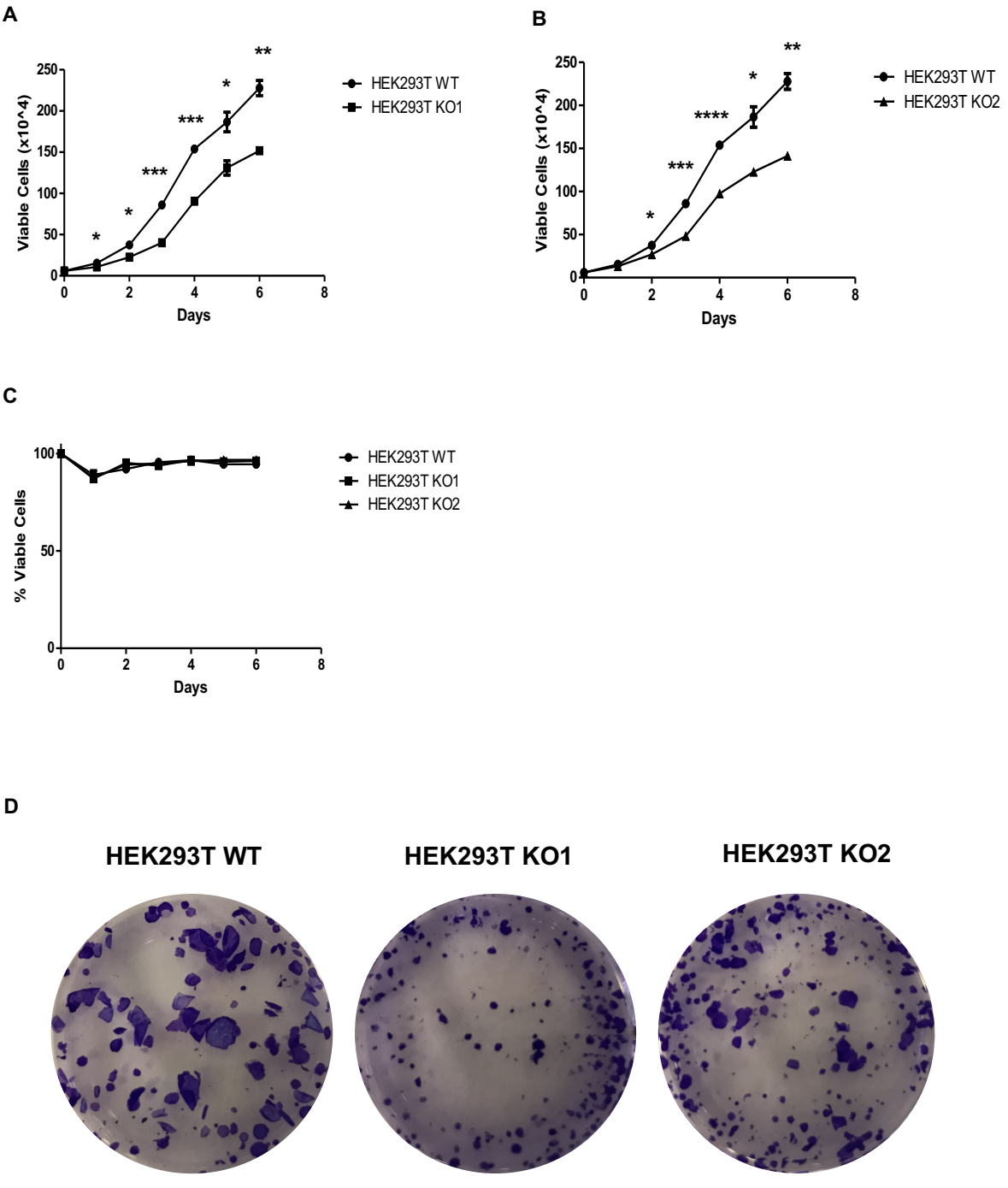

Figure 3.2. Reduced cell proliferation in HECTD1 knock out cells but no effect on cell viability. A) Viable cell count (x10^4) for HEK293T WT compared with HECTD1 KO1. B) Viable cell count (x10^4) for HEK293T WT compared with HECTD1 KO2. C) Viability (%) for HEK293T WT, HECTD1 KO1 and HECTD1 KO2. Cells were counted using trypan blue to assess the viability of the cells. Data plotted as mean with error bars that represent ±S.E.M., over three independent experiments (n=3). ****p<0.001, ***p<0.001, **p<0.01, *p<0.05 by paired student's t-test. D) Colony formation assay comparing WT with HECTD1 KO1 and HECTD1 KO2, cells were stained with crystal violet for visualisation (n=1).

3.2.2. Decrease in cell proliferation observed in HECTD1-depleted cells

To confirm the observations seen in the HECTD1 CRISPR/Cas9 knockout cells, HECTD1 was transiently depleted in HEK293ET cells and HeLa cells. To this end, HECTD1 transient depletion was optimised using small-interfering RNAs (siRNA) oligomers (Fire, *et al.* 1998) and Lipofectamine 2000 in HEK293ET cells. In order to transiently deplete HECTD1, 4 individual siRNAs that target 6 of the 8 protein encoding isoforms of HECTD1 (Appendix Table A.1), and a SMARTpool (Dharmacon) that contains a combination of the 4 individual siRNAs were screened in HEK293ET cells (Figure 3.3). The SMARTpool and all individual siRNAs were able to knock down HECTD1, but the efficiency of the knock down varied. The HECTD1 SMARTpool showed a 60% knockdown efficiency and HECTD1 #06 gave the best knockdown efficiency out of the individual siRNAs at around 80%. HECTD1 #07, #08, #09, gave a 65%, 70%, and 25% knockdown efficiency, respectively. Based on this preliminary data, SMARTpool and individual HECTD1 oligomers #06 and #08 were used for downstream experiments. In particular, SMARTpool oligomers were used in most experiments while the individual siRNAs were used alongside whenever appropriate to discount any off-target effects and provide more confidence when characterising the cellular phenotype. In addition, the amount of siRNA was optimised in order to establish the lowest concentration with the most efficient HECTD1 knockdown (Figure 3.4). For this optimisation experiment, HEK293ET cells were treated with varying amounts of HECTD1 SMARTpool siRNA, maintaining the same concentration of Lipofectamine 2000 for each condition. This revealed that the 20pmol condition of siRNA produced around a 75% knockdown efficiency compared to the control. Therefore, the 20pmol condition was selected since it also showed no obvious cell toxicity in contrast to the 40pmol condition.

Given that HECTD1 was successfully depleted using siRNA, HECTD1-depleted HEK293ET and HeLa cells were counted over 4 days post knockdown to assess proliferation and viability over time in culture (Figure 3.5). Similar to the knockout cell lines, transient depletion of HECTD1 with HECTD1 SMARTpool siRNA in HEK293ET and HeLa cells resulted in reduced cell proliferation over time in culture. In HECTD1 transiently depleted HEK293ET cells, by day 4 there was a 26.9% reduction in viable cell number (Figure 3.5A). Again, there was no observable change in viability between conditions (Figure 3.5B), suggesting slower proliferation compared to the control. Strikingly, this was again observed in HECTD1 transiently depleted HeLa cells where by day 4 there was a 43.6% reduction in viable cell number (Figure 3.5C). The reduction in the number viable cells was to a greater extent to those seen in both HEK293T and HEK293ET cells (Figure 3.2A and Figure 3.5A). Consistently, the statistically significant reduction in cell number was associated with no observable change in viability (Figure 3.5D). Interestingly, in both HECTD1 knockout cells and HECTD1 depleted cells there was a decrease in proliferation with no change in viability.

Taken together this suggests that HECTD1 has a role in cell proliferation, although it is not essential as HECTD1-depleted cells are viable.

Throughout the project HECTD1 was depleted using HECTD1 SMARTpool siRNA, and two individual siRNA #06 and #08 as per the optimisation. This was carried out to ensure that any observations made were not as a result of an off-target effect of one of the individual siRNAs. However, despite the optimisation, the knockdown efficiency was variable and therefore experiments were also carried out using a knockout system to observe any phenotype without questioning the extent of HECTD1 depletion. Use of a CRISPR/Cas9 system (Cong, *et al.* 2013; Mali, *et al.* 2013) for studying the role of HECTD1 does have drawbacks in that any observations in the phenotype could be related to clonal selection as opposed to HECTD1 knockout (Graham & Root. 2015). Clonal selection occurs in the process of generating the CRISPR/Cas9 genome-edited cell lines, where cells undergo phenotypic changes. To overcome this, and where possible, two knockout clones (KO1 and KO2) were used for future assays (contributed by Mariann Bienz, MRC-LMB, Cambridge UK).

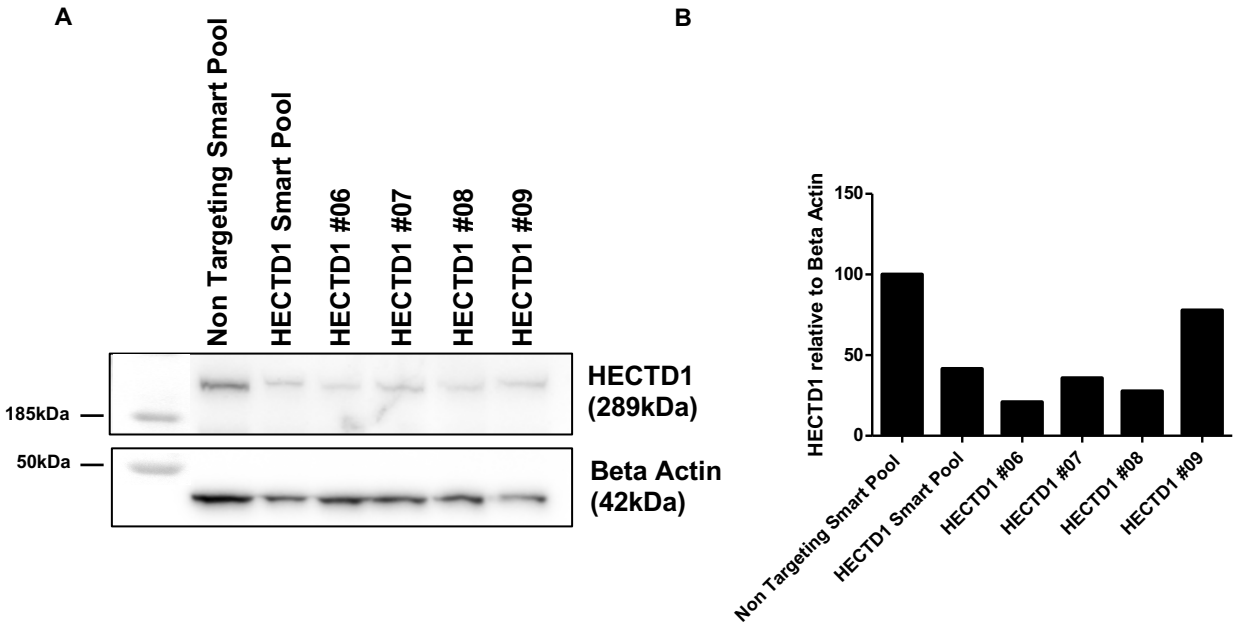

Figure 3.3. Efficiency of HECTD1 knockdown by SMARTpool and individual oligonucleotides. HEK293ET cells were transiently transfected using 20pmol of HECTD1 SMARTpool (smart pool) siRNA and individual HECTD1 siRNA with Lipofectamine 2000. Following 72hrs incubation, cells were harvested, lysed in RIPA buffer and HECTD1 proteins levels were analysed on a 4-12% SDS PAGE. Following western blotting on PVDF, the membrane was blocked in 3%-BSA-PBST and incubated overnight with anti-HECTD1 antibody (ab101992) followed by detection with a secondary HRP antibody. Anti-beta-actin (A5441) was used as loading control. For validation of HECTD1 (ab101992) antibody see Figure 4.4 (Chapter 4). A) Western blot of HECTD1 and loading control beta actin. Molecular weight markers are superimposed on the left-hand side of the immunoblot. B) quantification of HECTD1 normalised to beta actin (n=1). Data from one biological repeat.

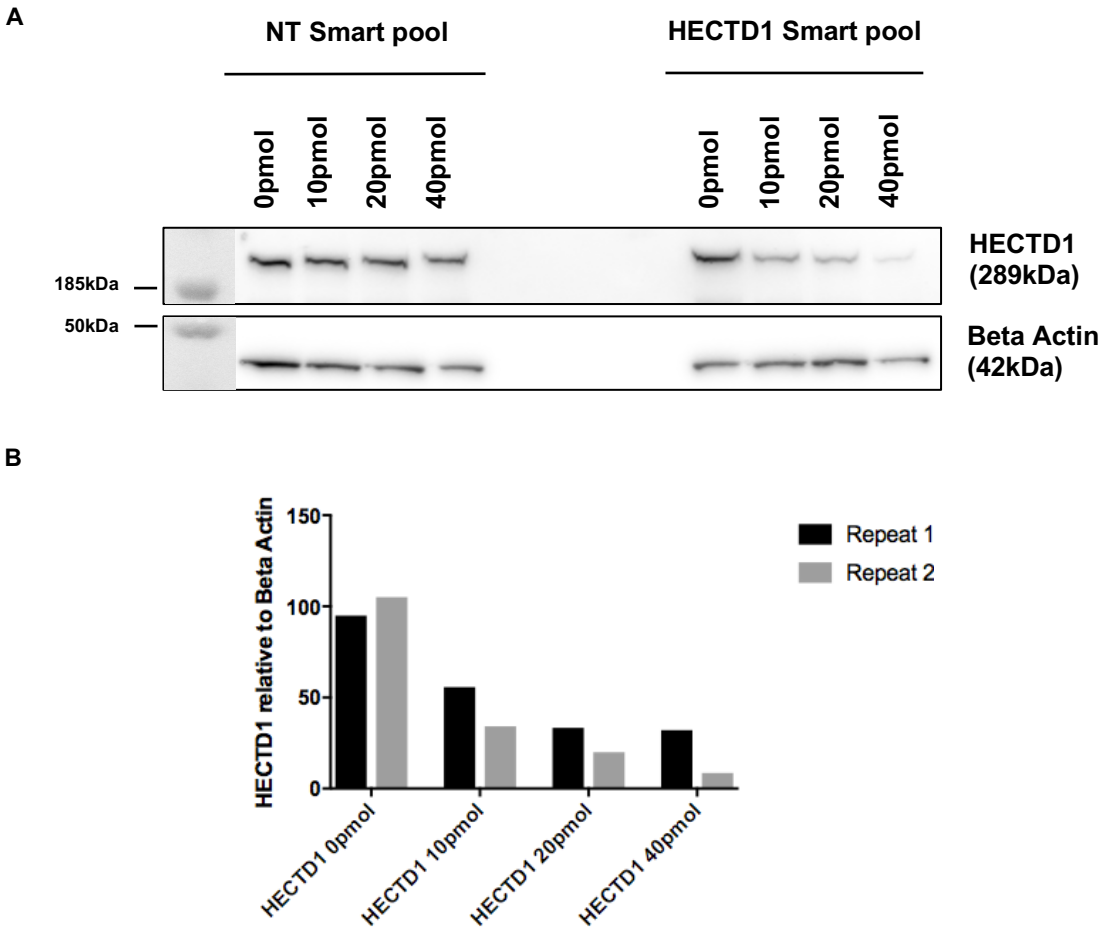

Figure 3.4. Efficiency of HECTD1 knockdown by different concentrations of SMARTpool oligonucleotides. HEK293ET cells were transiently transfected using 0pmol, 10pmol, 20pmol, and 40pmol siRNA with Lipofectamine 2000. Following 72hrs incubation, cells were harvested, lysed in RIPA buffer and HECTD1 proteins levels were analysed on a 4-12% SDS PAGE. Following western blotting on PVDF, the membrane was blocked in 3%-BSA-PBST and incubated overnight with anti-HECTD1 antibody (ab101992) followed by detection with a secondary HRP antibody. Anti-beta-actin (A5441) was used as loading control. A) Western blot of HECTD1 and loading control beta actin. Molecular weight markers are superimposed on the left-hand side of the immunoblot. B) quantification of HECTD1 normalised to beta actin.

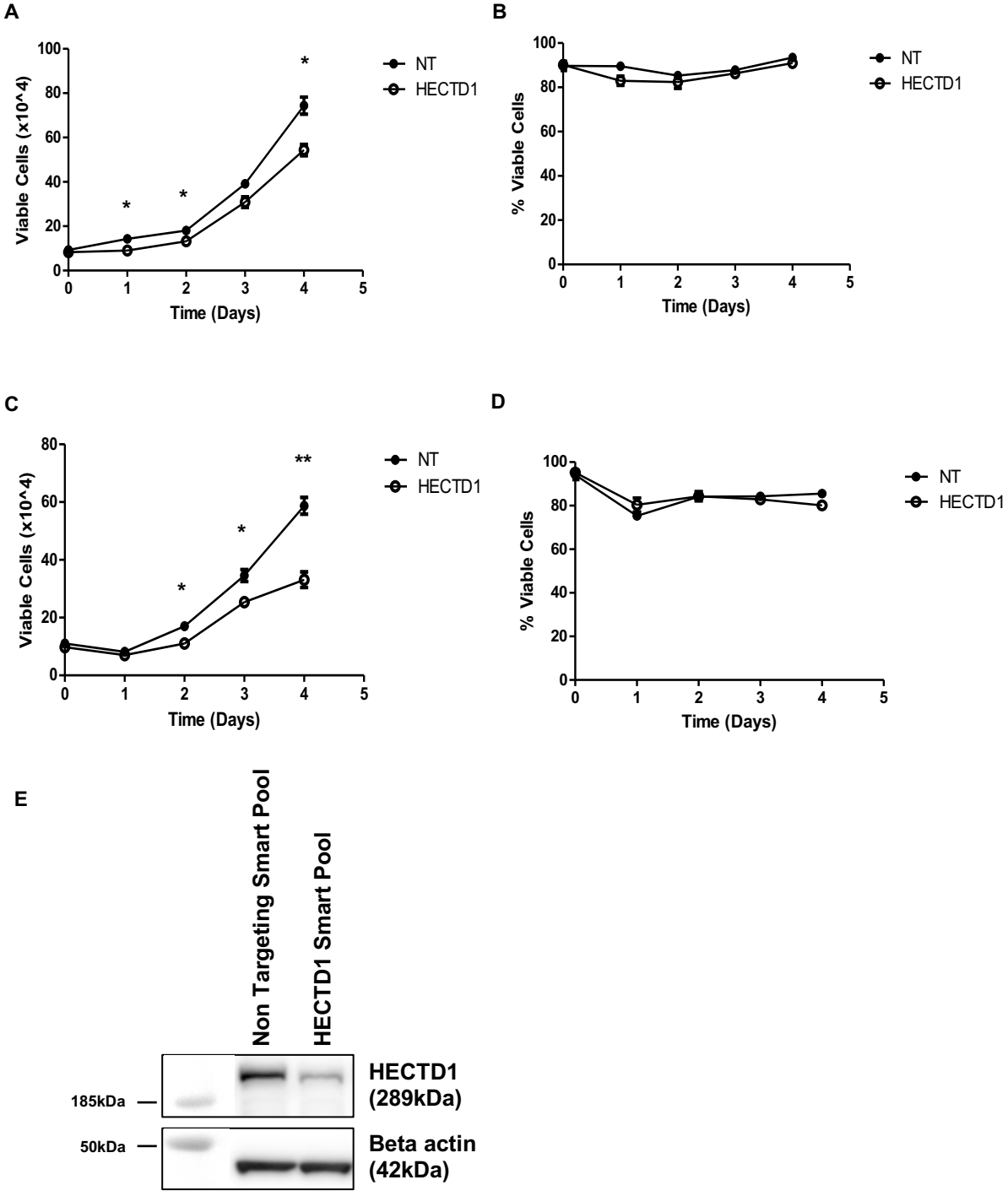

Figure 3.5. Reduced cell proliferation upon HECTD1 transient depletion but no effect on cell viability. HEK293ET and HeLa cells knocked down with 20pmol HECTD1 SMARTpool (smart pool) siRNA and Lipofectamine 2000/ RNAiMAX, on day 0. Viable cell count (x10^4) for HEK293ET A) and HeLa C) and cell viability (%) for HEK293ET B) and HeLa D), which have been treated with non-targeting siRNA and HECTD1 SMARTpool (smart pool) siRNA. E) Western blot showing HeLa knockdown with 20pmol HECTD1 SMARTpool (smart pool) siRNA and RNAiMAX. Cells were counted using trypan blue to assess the viability of the cells. Molecular weight markers are superimposed on the left-hand side of the immunoblot. Data plotted as mean with error bars that represent ±S.E.M., over three independent experiments (n=3) defined as three separate transfections. **p<0.01, *p<0.05 by paired student's t-test.

3.2.3. The E3 ligase activity of HECTD1 is needed to rescue the decrease in cell proliferation

To further demonstrate the requirement of HECTD1 ubiquitin ligase activity in the decrease in proliferation phenotype, rescue assays were performed (Figure 3.6-7). To understand the role HECTD1 plays in the decrease in proliferation observed in Figure 3.2 in HECTD1 CRISPR/Cas9 knock out cells were transfected with *HA-FL-mHectd1*^{WT} and the catalytically-dead version of this construct, *HA-FL-mHectd1*^{C2579G}. In Figure 3.6A HEK293T HECTD1 KO1 cells were transfected with empty vector (eV), *HA-FL-mHectd1*^{WT}, and *HA-FL-Hectd1*^{C2579G}, then viable cell number was calculated by counting cells in the presence of trypan blue. It can be seen that 48hrs post-transfection HEK293T HECTD1 KO1 cells transfected with *HA-FL-mHectd1*^{WT} showed a 19.9% increase compared to cells transfected with eV. However, this increase was not comparable to the proliferation observed in the HEK293T WT cells. By day 5, the increase in viable cells in HEK293T HECTD1 KO1 transfected with *HA-FL-mHectd1*^{WT} was comparable to the number of viable cells seen in HEK293T WT cells (Figure 3.6A), showing rescue of the reduced proliferation phenotype. In HEK293T HECTD1 KO1 cells transfected with *HA-FL-mHectd1*^{C2579G}, there was a 21.4% reduction in viable cells compared to HEK293 WT cells. This indicates that the catalytic mutant was not able to rescue the proliferation defect. Confirmation of expression of HA-FL-mHectd1 was carried out by western blot (Figure 3.6B).

Furthermore, the rescue of the phenotype seen with cell counting was confirmed using an alternative assay, an ATP-assay, for both knock out clones; KO1 and KO2. ATP-assays are regularly used as an alternative to MTT assays (a colorimetric assay using 3-(4,5-dimethylthiazol-2-yl)-2,5-diphenyltetrazolium bromide) as a more sensitive method to assess cell viability and proliferation (Maehara, *et al.* 1987; Petty, *et al*. 1995). CellTiter-Glo assay (Promega) was used for both HEK293T KO1 and HEK293T KO2 at 48hrs post-transfection, to see if in both clones the phenotype could be rescued. It can be seen that in both HEK293T KO1 and HEK293T KO2 the phenotype could be significantly rescued by HA-FL-mHectd1^{WT} but not HA-FL-mHectd1^{CM} (Figure 3.7). Indeed, in KO1 cells transfected with *HA-FL-mHectd1*^{WT}, the relative luminescence was comparable to the parental HEK293T cells (98.8% KO1 + WT; 100% WT), indicating rescue. Similar data were also observed for the KO2 cells, which showed cells transfected with *HA-FL-mHectd1*^{C2579G}, growing at a similar rate to the KO2 cells transfected with the empty vector (78.0% KO2 + CM; 85.7% KO2 + eV). In agreement with this, KO2 cells transfected with *HA-FL-mHectd1*^{WT} showed a higher relative luminescence than that of the WT cells (121.5% KO2 + CM; 100% WT), suggesting that whilst wild type mHectd1 was able to rescue the decrease in proliferation seen in both knockout cells. In summary, the growth defects observed in both of the KO cell lines can be rescued by HA-FL-mHectd1^{WT} but not HA-FL-

mHectd1^{C2579G}. Further demonstrating that the E3 ubiquitin ligase activity of HECTD1 is needed for optimum cell proliferation. Therefore, HECTD1 may regulate cell proliferation by regulating the cell cycle. For example, depletion of the cell cycle regulator NuMA, was associated with a decreased proliferation phenotype (Haren, *et al*. 2009). In NuMA-depleted HeLa cells, an enrichment of cells in early mitosis coincided with a decrease in proliferation compared to non-targeting controls (Haren, *et al*. 2009). Therefore, this may indicate that the role of HECTD1 in regulating cell proliferation, is similar to that of the cell cycle regulator, NuMA.

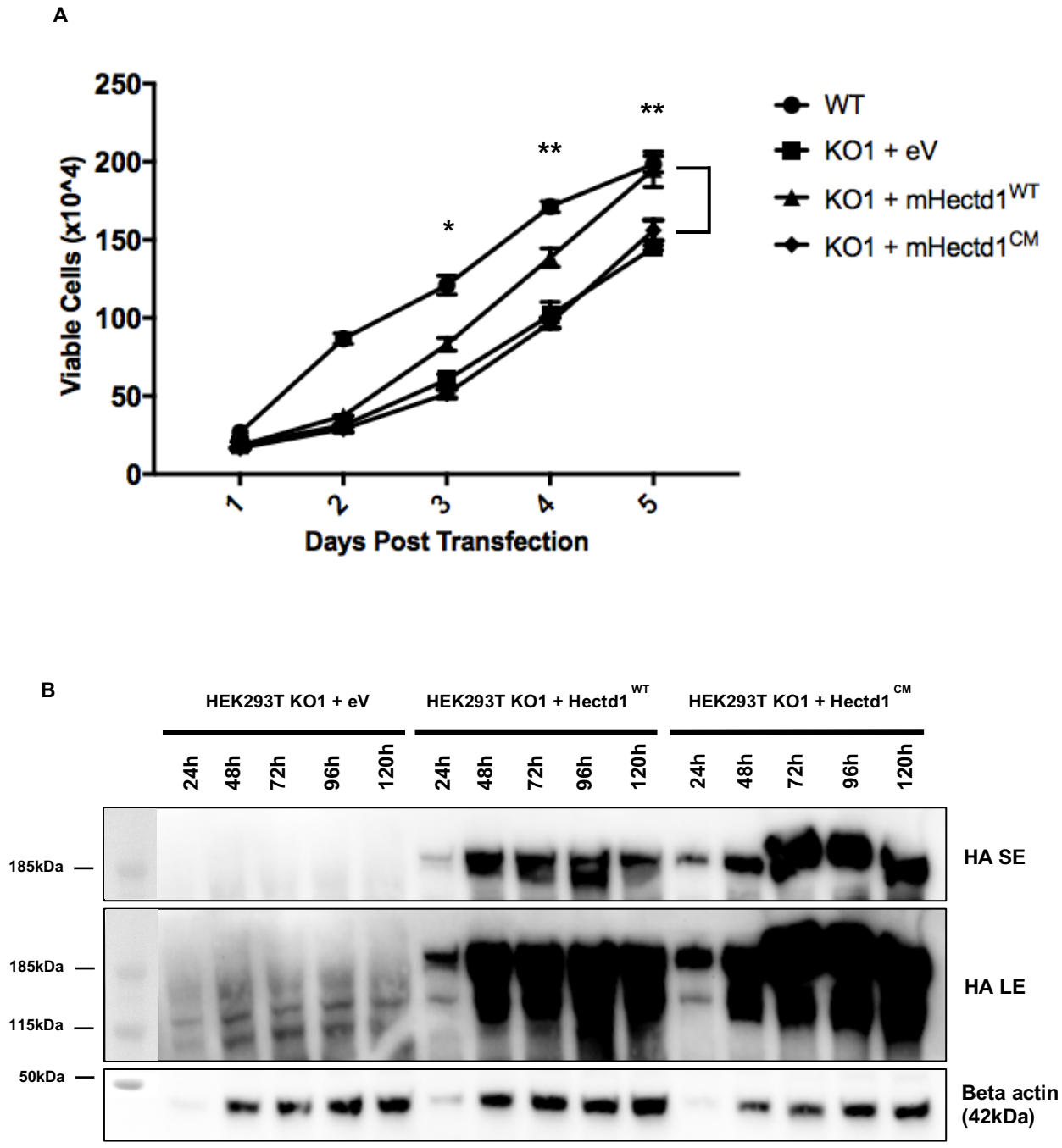

Figure 3.6. HA-FL-mHectd1^{WT} but not HA-FL-mHectd1^{CM} rescues the decrease in proliferation phenotype. HEK293T KO1 cells were transfected with empty vector (eV), *HA-FL-mHectd1^{WT}* (Hectd1^{WT} on figure) and *HA-FL-mHectd1^{CM}* (Hectd1^{CM} on figure) vectors with PEI. Samples were harvested at 1, 2, 3, 4, and 5 days post-transfection and lysed in RIPA buffer. A) Cell proliferation count (Viable cells) measured by trypan blue staining. B) Western blot showing HA-FL-mHectd1 expression in HEK293T KO1 cells. Samples were analysed on a 4-12% SDS PAGE, followed by western blotting on PVDF, the membrane was blocked in 3%-BSA-PBST and incubated overnight with anti-HA antibody (HA3F10) followed by detection with a secondary HRP antibody. Anti-beta-actin (A5441) was used as loading control. SE = short exposure and LE = long exposure. Molecular weight markers are superimposed on the left-hand side of the immunoblot. Data plotted as mean with error bars that represent ±S.E.M., over three independent experiments (n=3) defined as three separate transfections, **p<0.01, *p<0.05 by a one-way ANOVA with Dunnett's post-test. Significant when KO1 + eV and KO1 + mHectd1^{WT} are compared.

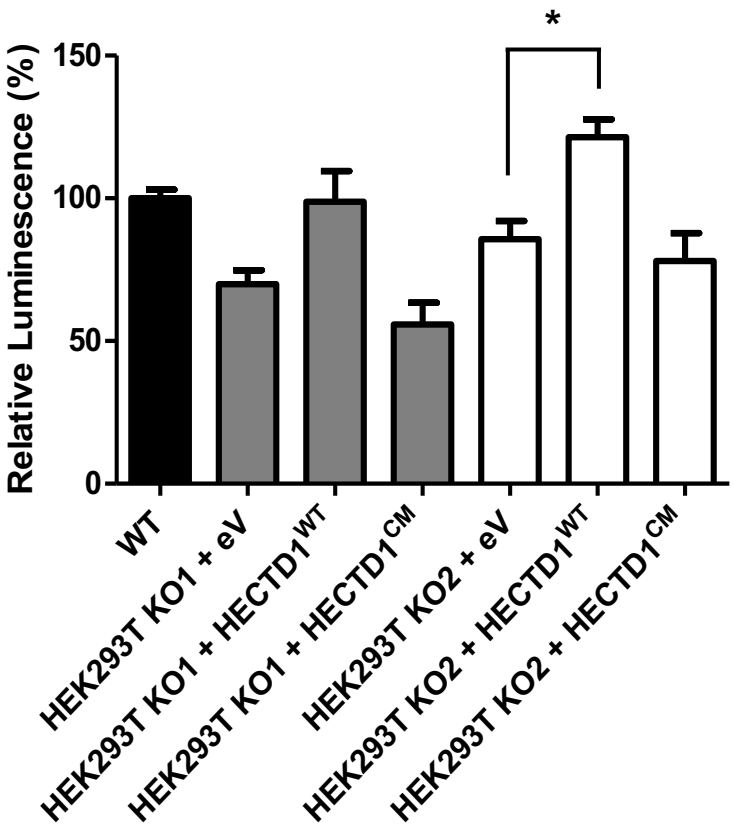

Figure 3.7. HA-FL-mHectd1^{WT} but not HA-FL-mHectd1^{CM} can rescue the decrease in proliferation in HEK293T KO2 at 48hrs post-transfection. HEK293T KO1 and KO2 cells were transfected with empty vector (eV), *HA-FL-mHectd1^{WT}* (mHectd1^{WT} on figure), or *HA-FL-mHectd1^{C2579G}* (mHectd1^{CM} on figure) vectors. Samples were taken at 48hrs post-transfection. Cell proliferation count (relative luminescence) measured by CellTiter-Glo assay. Data plotted as mean with error bars that represent ±S.E.M., over three independent experiments (n=3) defined as three separate transfections, *p<0.05 by a one-way ANOVA with Dunnett's post-test.

3.2.4. Characterisation of cell synchronisers

Having established that HECTD1 is required for optimum cell proliferation, protocols for cell cycle synchronisation were optimised in order to help determine whether the phenotype observed is due to a defect in the cell cycle. Cell synchronisers are chemical compounds that inhibit the progression of the cell cycle at a specific stage, therefore allowing enrichment of stage-specific cell populations. To this end, four synchronisation agents (i.e. RO-3306, nocodazole, aphidicolin, and thymidine) were used (Figure 3.8). RO-3306, a quinolinyl thiazolinone derivative, is a selective small-molecule inhibitor of human cyclin dependent kinase 1 (CDK1), which arrests cells at the G2/M border (Vassilev, *et al.* 2006). CDK1 is non-redundant in the cell cycle, and together with Cyclin B1 minimally forms the mitosis promoting factor, which allows for mitotic onset (Draetta & Beach. 1988; Sherr & Roberts. 2004; Vassilev, *et al.* 2006). Nocodazole binds to α-tubulin and inhibits the assembly of microtubules, the main constituent of the mitotic spindle (Hoebeke, *et al.* 1976; Kline-Smith & Walczak. 2004). Nocodazole is therefore, a mitotic spindle poison that reversibly arrests cells in M-phase (Zieve, *et al*. 1980). Aphidicolin synchronises cells in G1, preventing cells from entering S phase by the inhibition of DNA polymerase α (Pedrali-Noy, *et al.* 1980; Krokan, *et al.* 1981). Finally, treatment of cells with excess thymidine prevents DNA synthesis by the inhibition of the formation of deoxycytidine, arresting cells in S phase (Xeros. 1962). To achieve greater synchronisation, a double thymidine block can be used, which includes two treatments of thymidine to accumulate cells at the G1/S boundary prior to the final release (Puck. 1964; Bootsma, *et al*. 1964). The arrested cells are released by multiple washes to remove the synchroniser, then they are replaced in fresh media. Release from the thymidine block is aided by the addition of deoxycytidine, which replenishes the depleted pools (Thomas & Lingwood. 1975). The released cells are then harvested at time points post-release to capture synchronous cells.

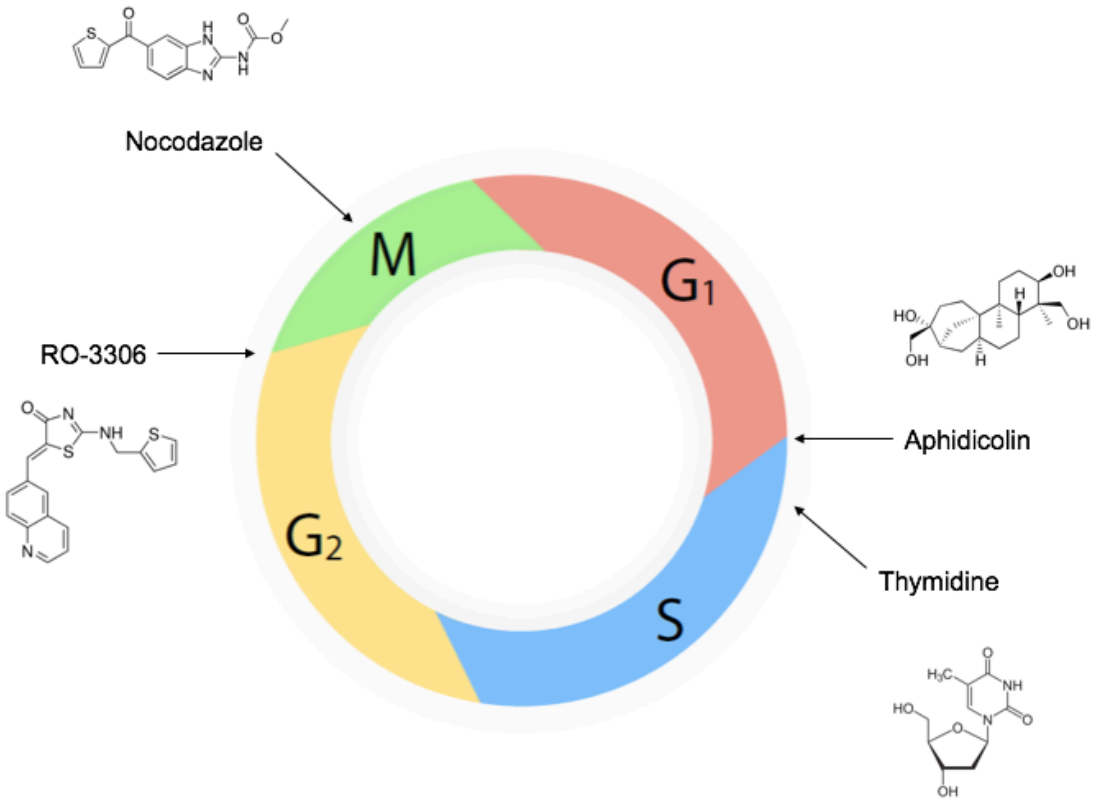

Figure 3.8. Diagram illustrating where RO-3306, nocodazole, aphidicolin, and thymidine block cell cycle progression. RO-3306 blocks cells at the G2/M transition, nocodazole in metaphase, aphidicolin at the G1/S transition, and thymidine in early S phase.

The efficacy of RO-3306, nocodazole, aphidicolin and thymidine in enriching specific cell populations was determined by cell cycle profiles generated by using propidium iodide staining and flow cytometry (Figures 3.9-12). PI is a nucleic acid stain, which is used to label the DNA content of each cell (Pollack & Ciancio. 1990). Although, a limitation when using PI staining and flow cytometry is that the G2 and M populations cannot be separated, it is the simplest method to assess the cell cycle profile (Ormerod & Kubbies. 1992). Human epithelial cervical cancer cells, HeLa cells, were used for synchroniser characterisation because they are extensively used for cell cycle assays, for example, in the characterisation of the APC/C in human cells (Geley, *et al*. 2001; Sudakin, *et al.* 2001).

Synchronisation of cells at the G2/M boundary was achieved using the CDK1 inhibitor RO-3306 for 20 hours (t=0). This led to an enrichment of cells at the G2/M stage (42.2% HeLa; 67.9% HEK293ET) compared to asynchronous untreated cells (14.3% HeLa; 21.8% HEK293ET). Cells were then released into mitosis through washes and a media change. As expected, G2/M population was enriched at 30mins (54.2% HeLa; 61.6% HEK293ET) and 1hr post-release (54.1% HeLa; 66.8% HEK293ET). In HEK239ET cells samples

collected 6hrs post-release show that most cells had exited mitosis (26.0% HEK293ET), however a large proportion of HeLa cells were still in mitosis (33.8% HeLa) (Figure 3.9). The extent of synchronisation seen in the HeLa cells was not to the same extent as seen in Vassilev, *et al.* (2006), where most cells are in the G2/M peak after treatment with RO-3306 for 20hrs (t=0).

In order to test whether greater synchronisation of the G2/M population could be obtained in both cell lines, nocodazole was used. Synchronisation of HeLa and HEK293ET following treatment with 50ng/ml of nocodazole for 20hrs (t=0), led to an enrichment of cells in the G2/M population (79.0% Hela; 44.2% HEK293ET). In contrast to RO-3306, after 30mins most HeLa cells had exited mitosis, unlike HEK293ET cells (27.4% HeLa; 36.9% HEK293ET), which were seen to exit mitosis after 1hr (28.7% HEK293ET) (Figure 3.10). RO-3306 synchronises cells at the G2/M border, whereas nocodazole synchronises cells in metaphase, therefore it is expected that cells synchronised with nocodazole will exit mitosis before those synchronised with RO-3306. In addition, the extent of synchronisation achieved using nocodazole in HeLa cells was comparable to that seen in Neganova, *et al.* (2009), where 67.5% of hESCs (human embryonic stem cells) were synchronised using nocodazole.

In contrast to RO-3306 and nocodazole, aphidicolin is often used to arrest cells in G1, preventing them from entering S phase (Pedrali-Noy, *et al.* 1980; Krokan, *et al.* 1981). In agreement with this both HeLa and HEK293ET cells were synchronised in G1 after 48hrs serum starvation, followed by 15hrs of treatment with 4µg/ml aphidicolin (74.5% HeLa; 69.3% HEK293ET), compared to the asynchronous population (70.8% HeLa; 67.6% HEK293ET). HeLa cells around 4hrs post-release were seen to enter S phase, in contrast to HEK293ET, which entered S phase at 6hrs post-release. This complements the HeLa synchronisation with aphidicolin seen in Pedrali-Noy, *et al.* (1980), where after 4.5hrs post-release, cells were in S phase. 12hrs post-release, cells were present in the G2/M population (53.7% HeLa; 39.1% HEK293ET) (Figure 3.11), although this enrichment in G2/M was not to the same extent of RO-3306 and nocodazole, aphidicolin could be used to track cells from G1 through to G2/M phase.

Double thymidine block, as a method of synchronisation, has already been used for the characterisation of HECT ligases in the cell cycle (Osmundson, *et al.* 2008; Lu, *et al.* 2013). Two rounds of treatment with 2mM thymidine arrest cells at the G1/S boundary (Puck. 1964; Bootsma, *et al*. 1964), as seen in HeLa and HEK293ET (Figure 3.12). At t=0, HeLa cells were in G1, whereas HEK293ET cells entered S phase, as seen in the G1 peak (68.0% HeLa; 31.3% HEK293ET) at 0hrs compared to the asynchronous G1 peak (72.8% HeLa;

63.8% HEK293ET). In accordance with Lu, *et al.* (2013), HeLa cells were seen to be in S phase at 4hrs post-release, before entering G2/M at 8hrs post-release from the double thymidine block (65.7% HeLa; 39.3% HEK293ET). By contrast, the largest G2/M peak observed in HEK293ET cells was seen at 4hrs post-release (42.4% HeLa; 52.3% HEK293ET). 12hrs post-release most cells have exited mitosis with the G2 peak returning to near asynchronous levels (28.4% HeLa; 11.2% HEK293ET). In comparison to aphidicolin, cells synchronised using a double thymidine block, entered S phase earlier post- release, resulting in mitotic entry and exit being captured. However, like aphidicolin, the enrichment of cells in G2/M was not as efficient as using RO-3306 or nocodazole.

A

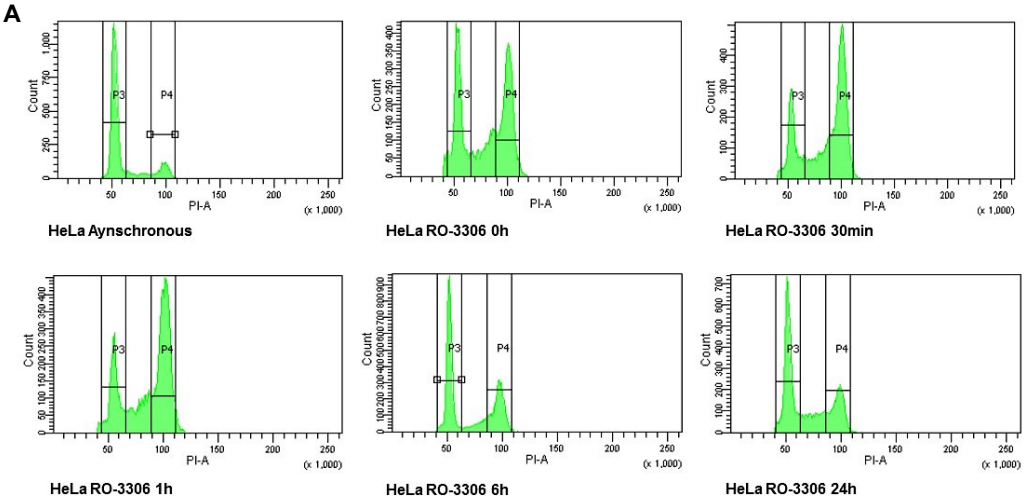

B

HeLa Time points	G1 population (P3)	G2/M population (P4)
Asynchronous	75.2%	14.3%
0h	34.5%	42.2%
30min	25.1%	54.2%
1h	21.4%	54.1%
6h	53.1%	33.8%
24h	51.4%	27.2%

C

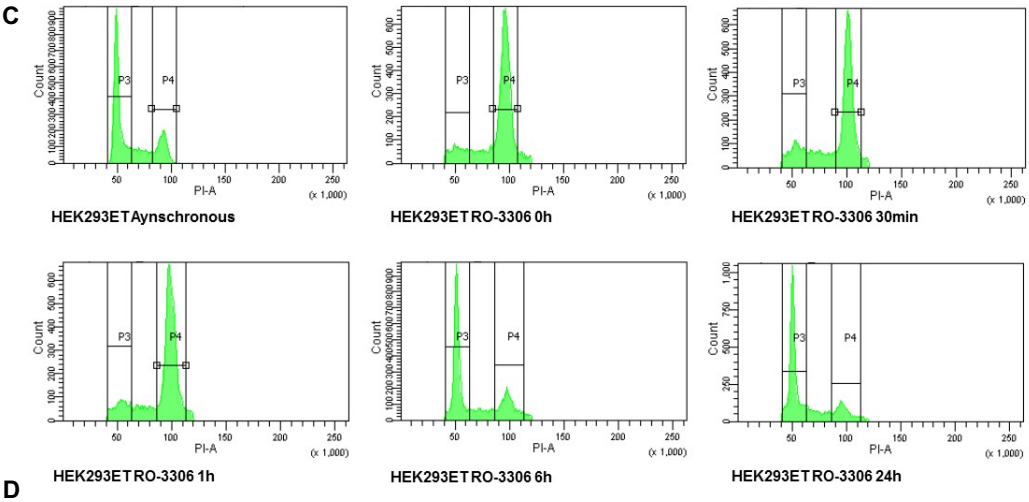

D

HEK293ET Time points	G1 population (P3)	G2/M population (P4)
Asynchronous	61.5%	21,8%
0h	14.0%	67.9%
30min	17.6%	61.6%
1h	14.7%	68.8%
6h	55.69%	26.0%
24h	61.9%	18.9%

Figure 3.9. Synchronisation of HeLa and HEK293ET with RO-3306. HeLa and HEK293ET cells were treated with 9μM RO-3306 for 20hrs, before releasing and harvesting time points. 0hrs time point was taken before releasing the cells. Cells were fixed using 70% ethanol, cells were stained using 2μg/ml PI, with 100μg/ml RNase A, for 30mins at room temperature. Stained samples were then analysed immediately by flow cytometry. Histograms for each time point, A) HeLa and C) HEK293ET. Gated population percentages shown in tables B) Hela and D) HEK293ET. PI-A of 50 is equivalent to 2N (G1 population), and PI-A of 100 is equivalent to 4N (G2/M population).

A

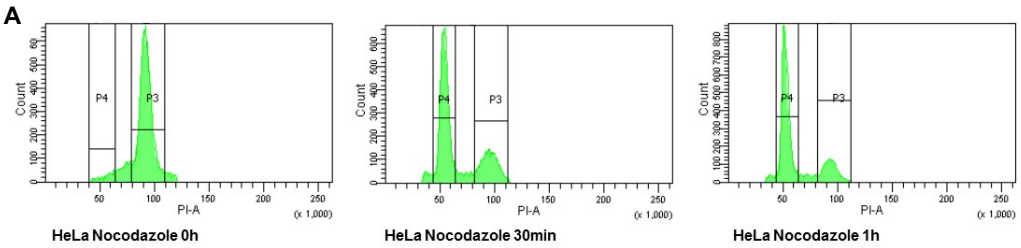

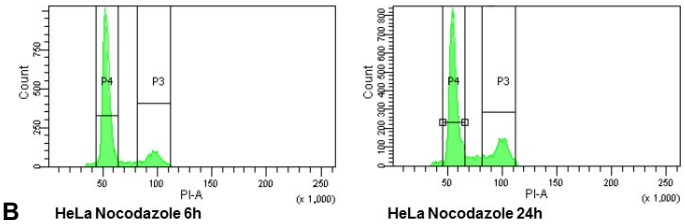

B

HeLa Time points	G1 population (P3)	G2/M population (P4)
0h	6.8%	79.0%
30min	60.1%	27.4%
1h	66.3%	21,7%
6h	73.7%	17.2%
24h	63.1%	25.7%

C

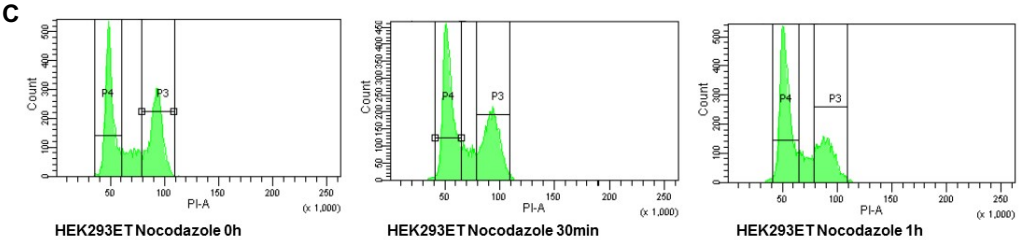

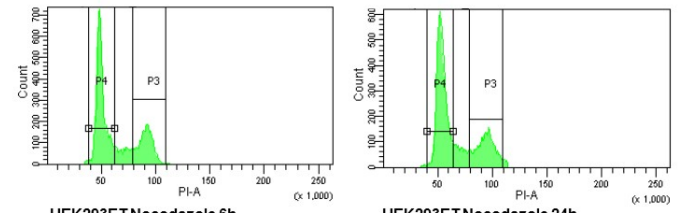

D

HEK293ET Time points	G1 population (P3)	G2/M population (P4)
0h	39.7%	44.2%
30min	50.2%	36.9%
1h	57.4%	28,7%
6h	59.0%	27.6%
24h	59.8%	26.8%

Figure 3.10. Synchronisation of HeLa and HEK293ET with nocodazole. HeLa and HEK293ET cells were treated with 50ng/ml nocodazole for 20hrs, before releasing and harvesting time points. 0hrs time point was taken before releasing the cells. Cells were fixed using 70% ethanol, cells were stained using 2µg/ml PI, with 100µg/ml RNase A, for 30mins at room temperature. Stained samples were then analysed immediately by flow cytometry. Histograms for each time point, A) HeLa and C) HEK293ET. Gated population percentages shown in tables B) Hela and D) HEK293ET. PI-A of 50 is equivalent to 2N (G1 population), and PI-A of 100 is equivalent to 4N (G2/M population).

A

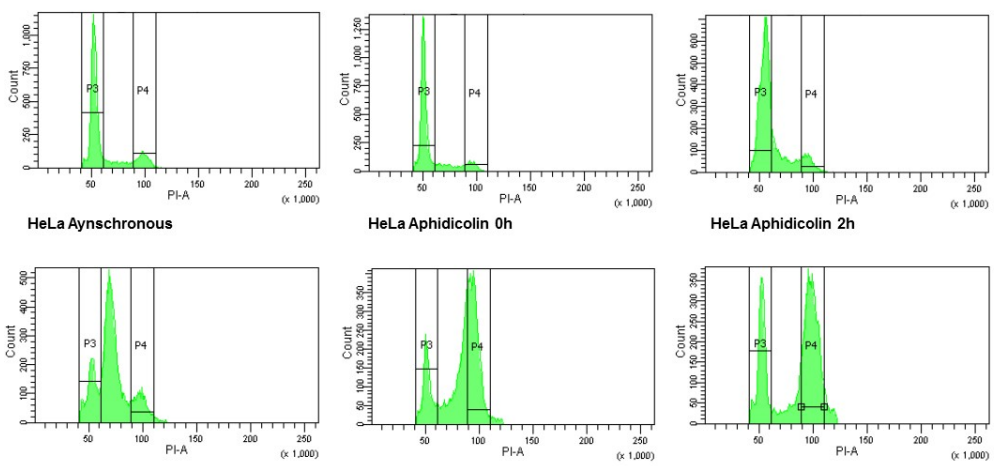

B

HeLa Time points	G1 population (P3)	G2/M population (P4)
Asynchronous	70.8%	15.3%
0h	74.5%	10.0%
2h	70.3%	9.4%
4h	23.6%	14.3%
8h	19.6%	42.5%
12h	27.8%	53.7%

C

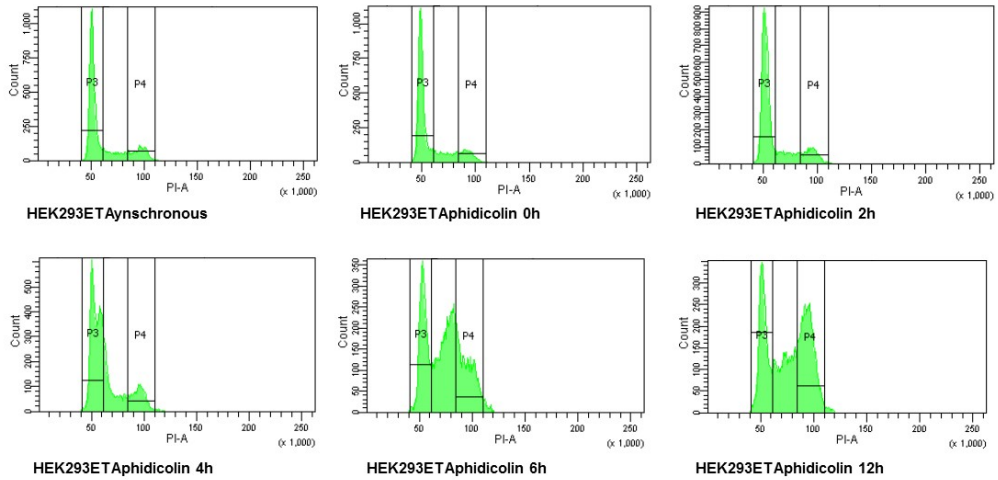

D

HEK293ET Time points	G1 population (P3)	G2/M population (P4)
Asynchronous	67.6%	16.8%
0h	69.3%	13.8%
2h	68.6%	15.0%
4h	62.4%	16.1%
8h	30.8%	27.0%
12h	31.6%	39.1%

Figure 3.11. Synchronisation of HeLa and HEK293ET with aphidicolin. HeLa and HEK293ET cells were treated with 48hrs of serum starvation, followed by 4µg/ml aphidicolin for 15hrs, before releasing and harvesting time points. 0hrs time point was taken before releasing the cells. Cells were fixed using 70% ethanol, cells were stained using 2µg/ml PI, with 100µg/ml RNase A, for 30mins at room temperature. Stained samples were then analysed immediately by flow cytometry. Histograms for each time point, A) HeLa and C) HEK293ET. Gated population percentages shown in tables B) Hela and D) HEK293ET.PI-A of 50 is equivalent to 2N (G1 population), and PI-A of 100 is equivalent to 4N (G2/M population).

A

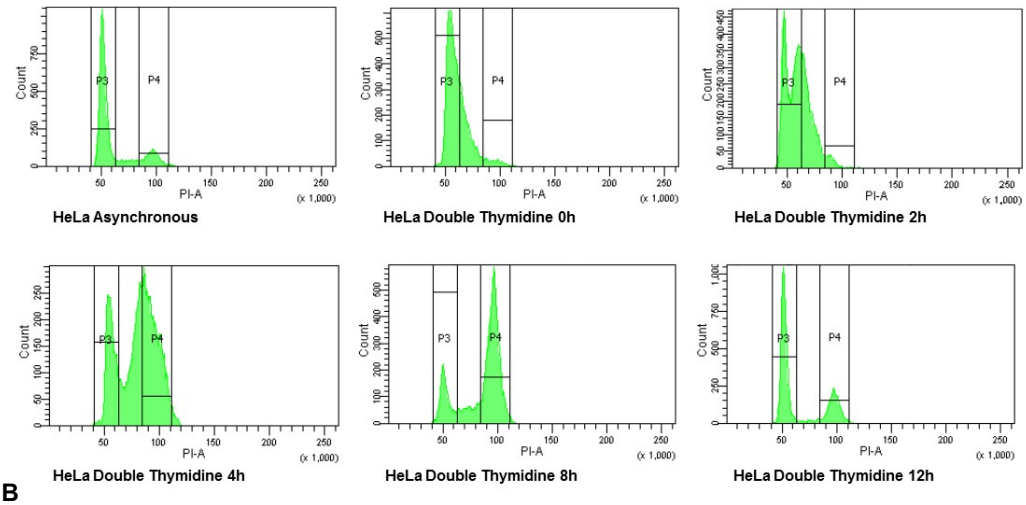

B

HeLa Time points	G1 population (P3)	G2/M population (P4)
Asynchronous	72.8%	17.0%
0h	68.0%	5.5%
2h	63.7%	4.1%
4h	23.9%	43.4%
8h	20.1%	65.7%
12h	65.6%	28.4%

C

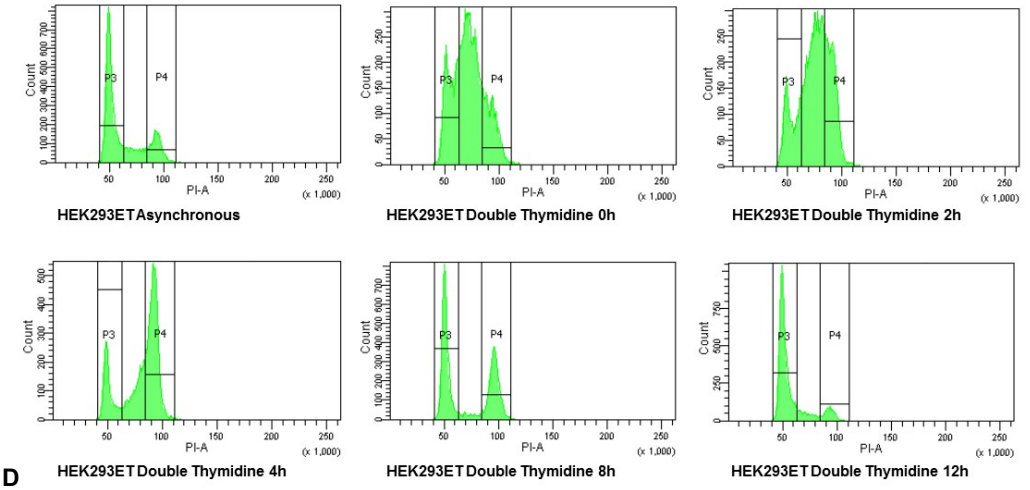

D

HEK293ET Time points	G1 population (P3)	G2/M population (P4)
Asynchronous	63.8%	19.9%
0h	31.3%	18.6%
2h	21.2%	28.0%
4h	21.5%	52.3%
8h	53.4%	39.3%
12h	77.2%	11.2%

Figure 3.12. Synchronisation of HeLa and HEK293ET with double thymidine block. HeLa and HEK293ET cells were treated with 2mM thymidine for 18hrs, followed by a 9hrs release. Then an additional 2mM thymidine for 15hrs, before releasing and harvesting time points. 0hrs time point was taken before releasing the cells. Cells were fixed using 70% ethanol, cells were stained using 2µg/ml PI, with 100µg/ml RNase A, for 30mins at room temperature. Stained samples were then analysed immediately by flow cytometry. Histograms for each time point, A) HeLa and C) HEK293ET. Gated population percentages shown in tables B) Hela and D) HEK293ET. PI-A of 50 is equivalent to 2N (G1 population), and PI-A of 100 is equivalent to 4N (G2/M population).

3.2.5. HECTD1 protein levels throughout the cell cycle

To establish a link between the cell proliferation phenotype and the cell cycle, it was next established whether HECTD1 itself is regulated by the cell cycle. Interestingly, sequence analysis revealed that HECTD1 has a predicted KEN box and 10 potential D boxes based on the RxxL motif (none following the RxxLxxxxN motif) (data in Appendix Figure A.3). Therefore, making HECTD1 a potential APC/C substrate. The hypothesis was that HECTD1 may be a target of the APC/C, as both the D box and KEN are well established degradation motifs in APC/C substrates (Glozter, *et al.* 1991; Pfleger & Kirschner. 2000). Interestingly, NEDL2, a HECT E3 ligase was found to be degraded by the APC/C^{CDH1} upon mitotic exit (Lu, *et al.* 2013). Therefore, to establish whether HECTD1 is cell cycle regulated given the cell proliferation phenotype, HeLa and HEK293ET cells were synchronised in M-phase and in G1 and HECTD1 protein levels were determined.

To establish whether HECTD1 is degraded during mitosis or mitotic exit, HeLa cells were synchronised using 50ng/ml nocodazole for 20hrs (Figure 3.12A) (Zieve, *et al*. 1980). From the characterisation of the synchronisers (Figure 3.10), the greatest enrichment of G2/M phase HeLa cells was achieved using nocodazole. However, both visually and from the quantification of HECTD1 protein from the western blot (Figure 3.13B), the relative HECTD1 levels remained constant throughout the cell cycle. Taking into consideration the large variability between replicates, there appeared to be no overall loss of HECTD1 protein level between metaphase and mitotic exit (60secs and 90secs time points) or subsequent G1 phase (3hrs and 5hrs time points). However, nocodazole synchronises cells in metaphase and therefore does not allow for mitotic entry to be monitored (Zieve, *et al*. 1980). To overcome this, HEK293ET cells were synchronised in G2/M phase by RO-3306 (Figure 3.13C). HEK293ET cells were synchronised using our optimised and also published conditions of 9μM RO-3306 for 20hrs (Vassilev, *et al.* 2006). Again, synchronisation using RO-3306 revealed no overall consistent change in HECTD1 levels in the 28hrs following release. The quantification of HECTD1 shows that upon mitotic exit (5hrs time point), there was no loss of HECTD1 (Figure 3.13D). However, because RO-3306 synchronises cells at the G2/M transition by CDK1 inhibition (Vassilev, *et al.* 2006), the later time points did not capture G1 phase. In addition, as shown in the synchroniser characterisation (Figure 3.9-10), the degree of synchronisation was lost over time.

To overcome the limitations of using nocodazole and RO-3306 to capture cells in G1, both HeLa and HEK293ET cells were synchronised using aphidicolin. From the synchronisation characterisation (Figure 3.11), use of aphidicolin resulted in the greatest enrichment of cells in G1. HEK293ET and HeLa cells (Figure 3.14) were synchronised using serum starvation followed by aphidicolin treatment and released into the G1/S transition (Pedrali-Noy, *et al.*

1980; Krokan, *et al.* 1981). In agreement with Figure 3.13, there was no consistent and repeated observable change in HECTD1 protein levels in HeLa relative to beta actin during cell cycle progression. Due to the fact that the data did was not consistent between repeats, this experiment should be repeated using additional APC/C substrates to rule out that HECTD1 is an APC/C substrate. The data currently are inconclusive and therefore, it is not possible to determine whether HECTD1 is degraded during the cell cycle by the APC/C.

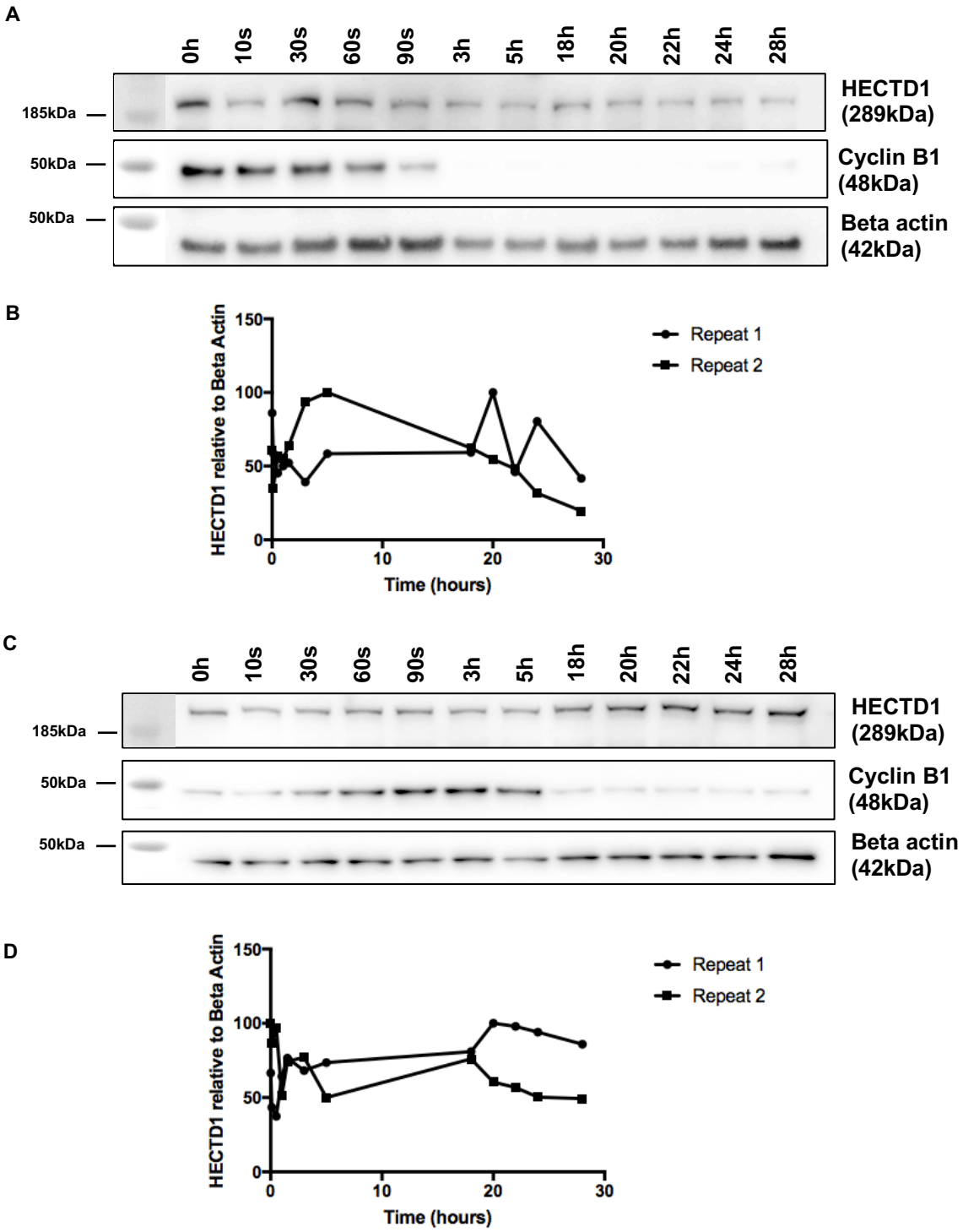

Figure 3.13. HECTD1 protein levels in G2/M phase synchronised cells. A) Representative western blot of HeLa cells synchronised with 50ng/ml Nocodazole for 20hrs. B) Quantification of HECTD1 expression relative to the loading control, beta actin (n=2). C) Representative western blot of HEK293ET cells synchronised with 9μM RO-3306 for 20hrs. D) Quantification of HECTD1 expression relative to the loading control, beta actin (n=2). HeLa and HEK293ET cells were synchronised then harvested and lysed in RIPA buffer at the following time points collected at 0hrs, 10secs, 30secs, 60secs, 90secs, 3hrs, 5hrs, 18hrs, 20hrs, 22hrs, 24hrs, and 28hrs post release. Samples were analysed on a 4-12% SDS PAGE and following western blotting on PVDF, the membrane was blocked in 3%-BSA-PBST and incubated overnight with anti-HECTD1 antibody (ab101992) and anti-Cyclin B1 (sc-245), followed by detection with a secondary HRP antibody. Anti-beta-actin (A5441) was used as loading control. Molecular weight markers are superimposed on the left-hand side of the immunoblot.

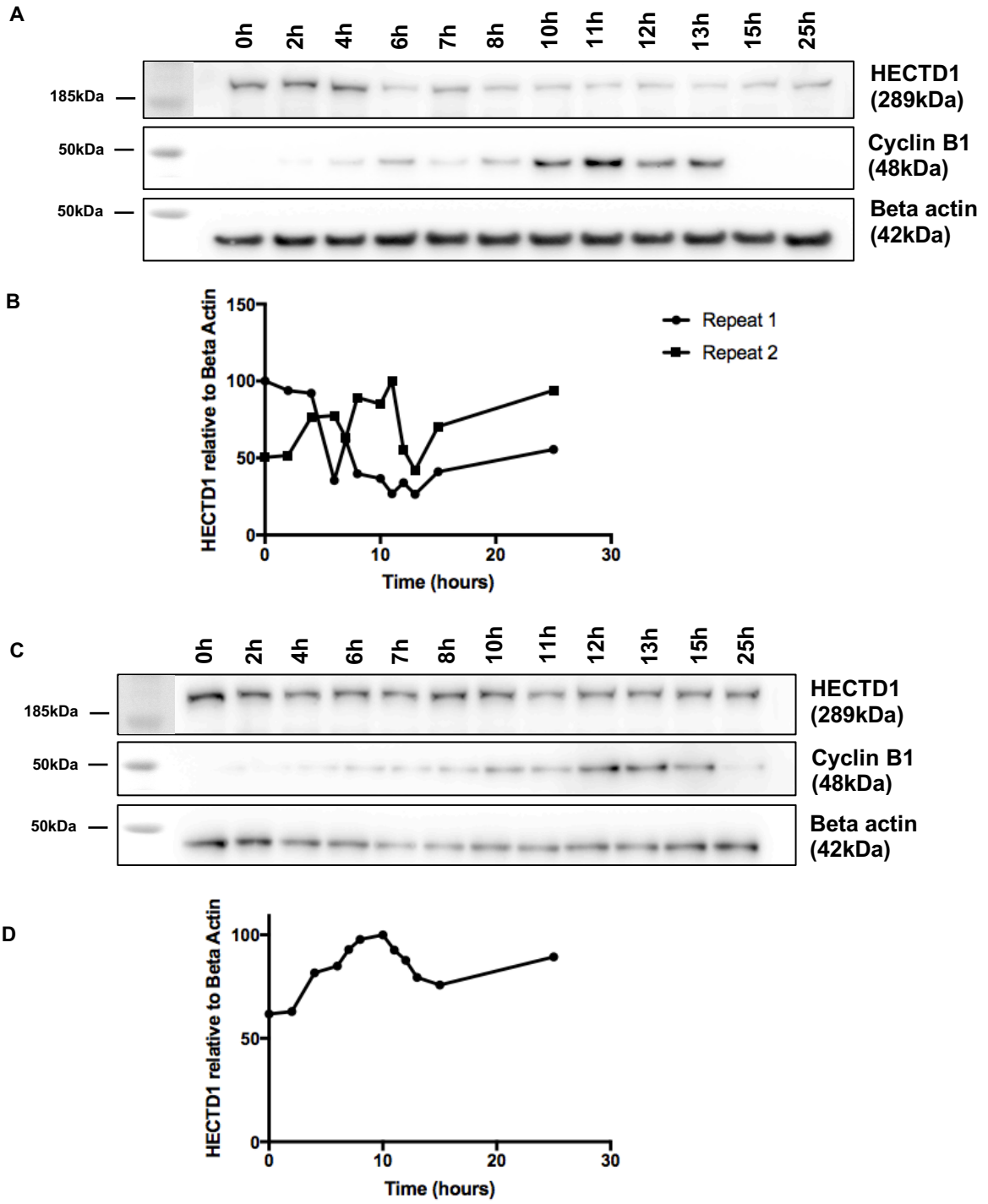

Figure 3.14. HECTD1 protein levels in G1 phase synchronised cells. A) Representative western blot of HeLa cells synchronised by serum starvation for 48hrs before treatment with 4µg/ml Aphidicolin for 15hrs. B) Quantification of HECTD1 expression relative to the loading control, beta actin (n=2). C) Representative western blot of HEK293ET cells synchronised by serum starvation for 48hrs before treatment with 4µg/ml Aphidicolin for 15hrs. D) Quantification of HECTD1 expression relative to the loading control, beta actin (n=1). HeLa and HEK293ET cells were synchronised then harvested and lysed in RIPA buffer at the following time points collected at 0, 2, 4, 6, 7, 8, 10, 11, 12, 13, 15 and 25hrs post-release. Samples were analysed on a 4-12% SDS PAGE and following western blotting on PVDF, the membrane was blocked in 3%-BSA-PBST and incubated overnight with anti-HECTD1 antibody (ab101992) and anti-Cyclin B1 (sc-245), followed by detection with a secondary HRP antibody. Anti-beta-actin (A5441) was used as loading control. Molecular weight markers are superimposed on the left-hand side of the immunoblot.

3.3. Discussion:

In this chapter, HECTD1 has been identified as a regulator of cell proliferation. The decrease in cell proliferation seen in HEK293T HECTD1 knock out cells was also seen in HECTD1-depelted HEK293ET and HeLa cell lines. Furthermore, this decrease in proliferation can only be rescued by wild type mHectd1 and not the catalytic mutant. This strongly indicates that the ubiquitin ligase activity of HECTD1 is required for optimum cell proliferation. To investigate the mechanisms involved, and given that many proteins involved in the cell cycle are cell-cycle regulated at the protein level, HECTD1 levels were assessed. To this end, synchronising agents were fully characterised across two cell lines allowing the enrichment of specific cell cycle populations. HECTD1 protein levels were assessed in synchronised cell population, however the data is inconclusive at this stage and would require further work to demonstrate whether HECTD1 is cell cycle regulated.

3.3.1. Decrease in proliferation as a result of HECTD1-depletion or knockout

In an attempt to determine the cellular functions of HECTD1 more rigorously, it was determined whether HECTD1 depletion resulted in any obvious cellular phenotype. Specifically, cell proliferation was assessed to determine if it was affected in HECTD1 knockout or HECTD1-depleted cells using trypan blue and cell counting as a readout. It was observed that over time, the number of proliferating cells were reduced in the knockout compared to the wild type cells. Furthermore, this was also observed in cells treated with HECTD1 siRNA in both HEK293ET and HeLa, indicating that the robustness of this effect. Transient overexpression of HA-FL-mHectd1^{WT} resulted in the rescue of the reduced proliferation observed in the KO cell lines indicating that indeed HECTD1 was required for cell proliferation. In contrast, overexpression of HA-FL-mHectd1^{C2579G} was not able to rescue this decreased proliferation suggesting that the E3 ligase activity is required for optimum cell proliferation. Therefore, this suggests that the atypical activity of HECTD1 in synthesising K29/K48 ubiquitin chains may function in regulating cell proliferation. This is a novel and exciting observation because to date, depletion of HECTD1 has not been shown to result in a reduced cell proliferation phenotype. This regulation of cell proliferation alongside the previous observation that HECTD1 colocalises to the mitotic spindle, may together indicate the HECTD1 has a role in cell cycle regulation, this will be explored at a greater depth in Chapter 4.

An important consideration is that the cell proliferation phenotype associated with HECTD1-depletion may not be linked to a role the cell cycle. For example, HECTD1 has been previously reported to function in the Wnt signalling pathway however, it acts as a negative regulator (Tran, *et al*. 2013). In this scenario, increased HECTD1 leads to reduced Wnt

signalling, which results in reduced proliferation. Therefore, reduced HECTD1 would result in increased cell proliferation and so, the observed phenotype of reduced proliferation upon HECTD1-depletion is not due to the role HECTD1 has in Wnt signalling. Furthermore, HECD-1, the HECTD1 orthologue, has been implicated in mitochondrial metabolism in *C. elegans* (Segref, *et al.* 2014). Therefore, aberrant regulation of the mitochondria by HECTD1-depletion may result in reduced proliferation as a result of reduced metabolic output. Dysregulation of the mitochondria often results in cell death through ATP depletion and Ca^{2+} dysregulation (Di Lisa, & Bernardi. 1998). The viability of HECTD1 depleted or knockout cells did not reduce over time in culture, therefore suggesting that the reduction in cell proliferation was not as a result of cell death, suggesting that changes in proliferation were not as a result of mitochondrial regulation. Therefore, the observed reduction in proliferating cells may be as a result of cell cycle regulation associated with HECTD1 and not a previously published role of HECTD1. To implicate HECTD1 in the cell cycle, further work will be needed to see if the phenotype is cell cycle related (Chapter 4).

3.3.2. Optimisation of cell synchronisation protocol to study HECTD1 in the cell cycle

In contrast to nocodazole, RO-3306 is able to capture the whole of mitosis due the inhibition at the G2/M transition (Zieve, *et al*. 1980; Vassilev, *et al.* 2006). For HeLa cells synchronised with nocodazole, 79.0% of cells were in G2/M and HEK293ET cell synchronised with RO-3306 yielded a comparable 67.9%. However, HEK293ET cells synchronised with nocodazole, and HeLa synchronised with RO-3306 enriched less than 45% of cells in G2/M. The poor synchronisation of HEK293ET cells synchronised with nocodazole may be explained by the semi-adherent nature of the cells. The harvesting of mitotic cells synchronised with nocodazole, included a mitotic shake-off, therefore, non-mitotic cells may be collected additionally. HeLa in comparison are much more adherent, making the mitotic shake-off less likely to include non-mitotic cells. The poor enrichment of HeLa cells using RO-3306 is unexpected given that the synchroniser was initially characterised using HeLa cells, and in their data, shows greater enrichment in G2/M (Vassilev, *et al.* 2006). This may be as a result of the characterisation only being carried out once, therefore for future experiments the extent of synchronisation should be measured. Synchronisation using aphidicolin releases cells into G1, therefore allowing G1 to be monitored up to (4hrs-6hrs) post-release. However, when synchronised using a double thymidine block, HEK293ET are released straight into S phase and HeLa cells enter S phase 1 hr post-release. Therefore, when selecting which synchroniser to use for future experiments, this characterisation will help in experimental design to ensure that the cells are enriched in the desired cell cycle phase.

Chemical synchronisation reagents such as RO-3306, nocodazole, aphidicolin, and thymidine do have important drawbacks and limitations to consider. For instance, their mechanism of action is not fully understood, with possible pleiotropic side effects such as stress, and apoptosis. In contrast to chemical synchronisation, mitotic shake-off, counter-current centrifugal elutriation, and cell sorting via flow cytometry all provide a physical way of enriching for cells in a distinct cell cycle phase, potentially negating the side effects seen with chemical synchronisers. Mitotic shake-off, the simplest method of synchronisation, relies on the detachment of rounded mitotic cells under agitation. Chemical synchronisation before mitotic shake-off functions to enrich the mitotic population prior to agitation, however this is not necessary (Elvin, *et al.* 1983). The main limitation of this method being that only M-phase cells can be synchronised. Cell synchronisation by way of cell sorting separates cells according to antibody-, ligand-, and dye-mediated fluorescence in a flow cytometer, the benefit of which allows cells to be sorted on a single-cell basis (Rosner, *et al.* 2013). However, this method tends to be limited by the inability of cell cycle profiling by DNA staining to distinguish G2 phase from M phase (Ormerod & Kubbies. 1992). Finally, cells can be synchronised by separation by their physical size, by counter-current centrifugal elutriation. This method separates cells in 12 fractions by their sedimentation velocity in a gravitational field, which yields cells in each stage of the cell cycle. The liquid containing the cells flows against the centrifugal force, resulting in the sedimentation rate of the cells being proportional to their size (Lindahl. 1948). Importantly, this method ensures that cells are not metabolically perturbed, however the cells as a result of the elutriation process can enter quiescence, G0 (Kauffman, *et al.* 1990; Zickert, *et al*. 1993).

3.3.3. HECTD1 protein levels during cell cycle progression

Given the presence of both a KEN box and several D boxes predicted in the sequence of HECTD1 (data in Appendix Figure A.3), it was hypothesised that it may be a substrate of the APC/C. Using nocodazole, RO-3306, and aphidicolin, mitotic exit and G1 phase were captured, where APC/C^{CDH1} is active (Wei, *et al.* 2004; Lu, *et al.* 2013). Furthermore, early mitosis was captured by synchronisation using RO-3306 where APC/C^{CDC20} is active (Kramer, *et al*. 2000). However, both cell lines, synchronised in G2/M and G1, showed large variability in the protein levels of HECTD1 both visually and by quantification. Therefore, it was not possible to conclude whether HECTD1 protein levels are cell cycle regulated. This experiment would need to be repeated, and for completeness blotted for APC/C substrate other than Cyclin B1, such as Cyclin A, NEK2A, securin, and PLK1. If HECTD1 was degraded by the APC/C, one would expect to see a visible loss of the HECTD1 protein band as seen in western blots of other E3 ligases, NEDL2, SKP2, and SMURF1 (Wei, *et al.* 2004; Kannan, *et al.* 2012; Lu, *et al.* 2013). The HECT E3 ligase, EDD, involved in SAC

regulation, was shown not to be cell cycle regulated in the 180mins following release from nocodazole (Scialpi, *et al.* 2014). Therefore, not all regulators of the cell cycle are cell cycle regulated and therefore it is possible that HECTD1 enzymatic activity, rather than HECTD1 protein levels might be regulated during the cell cycle. Indeed, recent data indicate that some HECT ligases are constitutively inactive and regulated by complex intra- and intermolecular mechanisms. For example, the NEDD4 family of HECT ligases have an auto-inhibitory C2 domain which can be released upon binding to Ca^{2+} or small PY-containing membrane proteins, NDFIP1 and NDFIP2 (Mund & Pelham. 2009; Wang, *et al.* 2010). In addition, the HECT ligase HUWE1 has been described as being regulated by the formation of an auto-inhibitory dimer that is stabilised by the tumour suppressor p14ARF (Sander, *et al.* 2017). Recently it was found that peptide linkers between the WW domains found in NEDD4 family proteins, such as WWP1, WWP2, and ITCH are important for their catalytic regulation. These linkers were found to function to lock the ligase in an inactive conformation and that tyrosine phosphorylation was found to relieve this autoinhibition (Chen, *et al*. 2017). However, it is currently unknown how the ligase activity of endogenous HECTD1 is regulated.

A potential solution to studying the ligase activity of endogenous HECTD1 is by using Activity-Based Probes (ABP). ABPs are chemical probes that direct the active site of enzymes, to profile their activity within complex mixtures of proteins (Love, *et al.* 2007). To specifically target E3 ligases, novel E2-based ABPs have been recently developed in order to monitor ubiquitin ligase activity (Pao, *et al*. 2016). E2-based ABPs, mimic a ubiquitin-charged E2 with a C-terminal electrophilic warhead that is able to label RBR and HECT E3 ubiquitin ligases. This allows for specific labelling of RBR and HECT ligases, as only active sites with an E2 binding site will result in covalent modification of the cysteine, thus excluding labelling of deubiquitinases (Pao, *et al.* 2016). These C-terminal warheads comprise aldehyde, vinyl sulfone, vinylmethylester (VME), and propargylamide (PA) (Hershko & Rose. 1987; Palmer, *et al*. 1995; Borodovsky, *et al.* 2001; Borodovsky, *et al.* 2002; Ekkebus, *et al.* 2013). The use of novel ABPs could therefore help decipher whether HECTD1 ligase activity changes during cell cycle progression and how loss of this activity can impact on cell proliferation (Further discussed in 3.4. Future Work).

3.4. Future work:

The use of trypan blue to count the number of viable cells for growth curves, is a simple experiment, however is subject to human error or bias when counting. Therefore, to overcome this, cellular assays, such as MTT or ATP assays can be used to calculate cell viability, and the number of viable cells, which are not subject to bias (Riss, *et al*. 2004). Only one of the cell proliferation analyses was carried out using an ATP proliferation assay, which largely repeated the observation seen with manual cell counting. However, for future work this metabolic readout should be used as a more reliable and high-throughput method to assay cell proliferation and viability.

The use of propidium iodide staining to assess the cell cycle profile is a quick and simple method. However, due to the nature of the technique whereby the DNA content is measured, it is not possible to quantify the proportion of cells in S-phase, or separate out the G2 population from the M population (Ormerod & Kubbies. 1992). The S-phase population is assumed to be the population of cells that exists between G1 and M phase populations. However, a more accurate way of measuring this is using BrdU (bromodeoxyuridine) staining. BrdU, a synthetic nucleoside that is an analogue of thymidine, is incorporated into newly synthesised DNA. S-phase cells are detected by using an antibody against BrdU (Gratzner. 1982), and this can be adapted to flow cytometry or high-content microscopy to quantify this population (Ormerod & Kubbies. 1992; Massey A. 2015). In addition, the use of mitotic specific antibodies such as cyclin B1 and pHistone H3 (ser28) can be used for flow cytometry or high content microscopy to visualise the mitotic population (Chapter 4).

One limitation of using western blotting to characterise HECTD1 protein levels throughout the cell cycle, is that the technique is exposed to uneven loading of the sample, and that it is only ever semi-quantitative. Therefore, any subtle change in protein levels would be difficult to detect. To overcome hits, endogenous GFP-tagged HECTD1 signal could be measured and tracked over time in synchronised cells transfected with the GFP-tagged protein. This measurement and tracking of the localisation could be carried out using high-content microscopy. For example, Liberali, *et al.* 2014, used high-content microscopy to conduct an RNAi screen on single-cells to measure endocytic tracking, where fluorescently labelled cargo were tracked and measured quantitatively. Another limitation to be considered is the use of only one cell cycle maker, Cyclin B1, which only identifies cells that are in G2/M (Pines & Hunt. 1987; Murray & Kirschner. 1989). To identify cell cycle populations, flow cytometry or high-content microscopy, as discussed, could be used to show the cell cycle stage at each time point alongside the western blot.

Finally, expanding on the idea that HECTD1 ligase activity rather than the stability of the ligase might be regulated during cell cycle progression, synchronised cell lysates could be treated with an E2-Ub-ABP (Byrne, *et al*. 2017). Previously, using ABPs our laboratory showed that in unstimulated HeLa and HEK cells, HECTD1 is either inactive or that its activity is below the threshold of detection for the assay, in experiments carried out in asynchronised cells (Byrne, *et al.* 2017). Preliminary data using ABPs on frozen cell lysates obtained from synchronised cells did not result in the labelling of endogenous HECTD1. Since frozen samples might be an issue for labelling, cells have been lysed by sonication as described in Pao, *et al.* (2016). This was also unsuccessful at labelling HECTD1 in RO-3306 synchronised cell lysates at 0hrs, 20mins, 2hrs and 20hrs post-release. However, this was only carried out once, and by western blot the cell lysis appears to be incomplete, suggesting that an initial optimisation of this experiment would be to improve the lysis protocol. Based on optimisation from previous experiments, the ABP probe is always in excess, therefore the availability of HECTD1 may be a limiting factor. The anticipated results would be that whilst the ABP would not covalently label HECTD1 in basal unstimulated cells, it may do so at a specific cell cycle stage when the enzymatic activity of HECTD1 is activated.

Chapter 4: HECTD1 is required for the timely progression through mitosis

4.1. Introduction:

Transient and genetic depletion of HECTD1 resulted in a reduction in cell proliferation in HEK293T, HEK293ET and Hela cells (Chapter 3). The cell cycle and cell proliferation are tightly and directly connected and reduced cell proliferation phenotypes have been observed for cell cycle regulators such as NuMA (Haren, *et al*. 2009). Therefore, it was hypothesised that the observed reduction in proliferating cells may be due to a novel role of HECTD1 in the cell cycle. The control of cell proliferation is regulated in late G1, where, activation of G1/S- and S-CDKs triggers an irreversible commitment to a new cell cycle. This point of commitment is known as the restriction point (Zetterberg, *et al.* 1995; Johnson & Skotheim. 2013). The activation of G1/S- and S-CDKs is regulated by extracellular factors known as mitogens, which ensure that cells proliferate only when needed (Zetterberg, *et al.* 1995; Hengstschläger, *et al*. 1999). Interestingly, it has been observed that cells, which undergo prolonged prometaphase, result in the inhibition of daughter cell proliferation despite normal completion of mitosis (Uetake & Sluder. 2010). It was subsequently revealed that a mechanism exists that senses prometaphase duration in cells. For instance, a delay in prometaphase for more than 1.5hrs triggered a durable p38- and p53- dependent G1 arrest of the daughter cells despite normal division of the parent cell (Uetake & Sluder. 2010).

Most of what is known about ubiquitin signalling in the cell cycle relates to RING E3 ligases such as the APC/C and the SCF complexes, where the mechanisms, substrates, and ubiquitin chain types have been studied over the last 15 years, by many different research groups (Vordermaier. 2004; Petroski, *et al*. 2005; Jin, *et al.* 2008). In contrast, HECT E3 ligases have diverse roles in cell cycle regulation and for the majority of ligases, their substrates and chain type are yet to be fully characterised (Table 1.3). These proposed roles include, regulation of DNA replication, centrosome amplification, and regulation of the spindle assembly checkpoint. HUWE1 the human ortholog of the yeast Tom1, was shown to be responsible for the degradation of CDC6, a cell cycle protein responsible for DNA replication (Hall, *et al.* 2007; Kim, *et al.* 2012b). HERC2, together with NEURL4 and CP110, was identified as a regulator of centrosome amplification (Al-Hakim, *et al.* 2012). Interestingly, both SMURF2 and EDD, have been implicated in the regulation of the spindle assembly checkpoint. SMURF2 prevents ubiquitination and degradation of MAD2, a SAC component, permitting the checkpoint to be active. Therefore, depletion of SMURF2 resulted in premature anaphase onset, a phenotype associated with a defective SAC (Osmundson, *et al.* 2008). Finally, EDD was shown to physically interact with the SAC components BUB3 and BUBR1, although its precise mechanism of regulation is unknown (Scialpi, *et al.* 2015).

Importantly, the cell proliferation defect observed upon HECTD1 depletion was rescued by expression of HA-FL-mHectd1^{WT} but not HA-FL-mHectd1^{C2579G} (Chapter 3). This suggests that the E3 ligase activity of HECTD1 is required for cell proliferation. Therefore, the atypical ubiquitin ligase activity of HECTD1 in synthesising K29/K48 ubiquitin chains, (Licchesi, personal communication), may function as a novel signal in cell proliferation and perhaps the cell cycle. To date, the best characterised chain type in cell cycle regulation is K11-linked ubiquitin chains, which are conjugated onto substrates by the APC/C (Jin, *et al.* 2008). More recently, branched K11 ubiquitin chains synthesised by the APC/C and UBE2S, have been shown to enhance proteasomal degradation of the cell cycle substrates NEK2A and p21 (Meyer & Rape. 2014). Furthermore, the APC/C was also recently shown to synthesise K11/K48 ubiquitin chains on similar mitotic substrates (NEK2A and Cyclin A) (Yau, *et al.* 2017). The HECT E3 ligase HERC2 has been shown to conjugate K48 onto NEURL4 in its role in regulating centrosome duplication (Al-Hakim, *et al.* 2012). In mitosis, the HECT ligase SMURF2 conjugates K63 in the regulation of the mitotic protein MAD2, however there is currently no biochemical evidence to support this chain type specificity (Osmundson, *et al*. 2008). Together these studies emphasise that the type of ubiquitin chains synthesised by HECT ligases in the context of the cell cycle is still poorly understood. Therefore, the discovery that HECTD1, which *in vitro* appears to synthesise K29/K48 chains, is important for optimum cell proliferation is exciting. Indeed, this suggests that a novel type of ubiquitin chain might be implicated in cell cycle regulation, through HECTD1 ubiquitin ligase activity.

4.1.1. Aims

Given that HECTD1 depletion leads to reduced cell proliferation, this next chapter aims to identify the cellular process affected by the loss of HECTD1 function. Since, the cell cycle is tightly connected to cell proliferation (Duronio & Xiong. 2013), the aim was to determine whether HECTD1 depletion affects cell cycle progression. Therefore, the following objectives were to:

1. Measure DNA content by flow cytometry as a readout for cell cycle stage, to determine the effect of HECTD1 depletion on the cell cycle in HeLa and HEK293ET cells.

2. Use immunofluorescence and confocal microscopy to determine the localisation of HA-FL-mHectd1 during the cell cycle in HEK293ET cells.

3. Use immunofluorescence and confocal microscopy to quantify the number of cells in each stage of mitosis, to determine the effect of HECTD1-depletion in both HeLa and HEK293ET cells. Mitotic and nuclear defects were also quantified.

4. Compare the length of mitosis in both wild-type and HECTD1-depeleted cells by synchronising cells and probing western blots for cell cycle markers. Additionally, by measuring the DNA content by flow cytometry as a readout for cell cycle stage in synchronised cells. Finally, by measuring the time taken from Nuclear Envelope Breakdown (NEBD) to anaphase onset by using time lapse microscopy.

5. Determine whether the observed phenotypes are due to HECTD1 ubiquitin ligase activity through rescue assays using plasmids encoding *HA-FL-mHectd1*^{WT}, *HA-FL-mHectd1*^{C2579G}, and an empty vector control.

4.2. Results:

4.2.1. HECTD1 depletion results in no change in the G2/M population

In Chapter 3, HECTD1 depletion was shown to result in a decrease in cell proliferation and interestingly this phenotype was rescued by HA-FL-mHectd1^{WT}. Therefore, it was hypothesised that this decrease in proliferation could be mediated by an effect on the cell cycle. Flow cytometry alongside propidium iodide staining is a useful technique to determine the cell cycle stages of individual cells in an asynchronous population, with the limitation that it is not possible to quantify the proportion of cells in S phase, or separate out the G2 population from the M population (Ormerod & Kubbies. 1992). However, propidium iodide staining was used here to determine whether HECTD1-depleted cells may show any obvious defects in their ability to cycle through the different stages of the cell cycle.

The cell cycle profiles shown in Figure 4.1, show similar sized G1 peaks, and similar G2/M peaks. This therefore suggests that there is no change in G2/M population in cells depleted of HECTD1. PI staining and flow cytometry can be used to assess the presence of 8N populations as a result of cells being unable to complete mitosis, as seen with the ligase SMURF2 (Osmundson, *et al*. 2008). Therefore, PI staining was used to establish whether HECTD1-depleted cells could induce chromosomal instability. However, there were no 8N cells present (data not shown), indicating that cells were successful in completing mitosis.

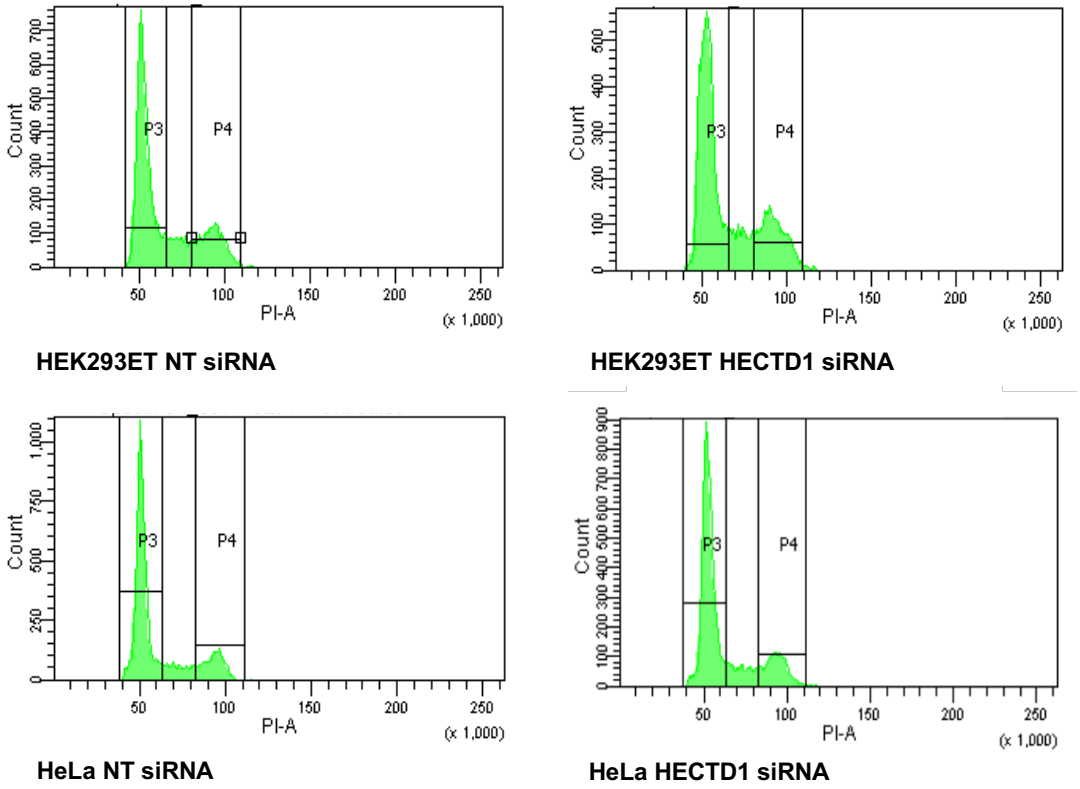

Figure 4.1. No change in G2/M population upon HECTD1-depletion in HEK293ET and HeLa cells. Cell cycle profile was characterised by using flow cytometry and propidium iodide staining. HEK293ET and HeLa cells were knocked down with either 20pmol Non-targeting siRNA (NT) or HECTD1 SMARTpool siRNA (HECTD1) and Lipofectamine 2000/ RNAiMAX, then analysed asynchronously after 72hrs. Cells were fixed using 70% ethanol and stained using 2µg/ml PI, with 100µg/ml RNase A, for 30mins at room temperature prior to analysis. Histograms for HEK293ET and HeLa, gate P3 = G1 population and gate P4 = G2/M population to quantify cell populations (HEK293ET, n=3 and HeLa, n=3). PI-A of 50 is equivalent to 2N (G1 population), and PI-A of 100 is equivalent to 4N (G2/M population).

4.2.2. HA-FL-mHectd1 localises to the mitotic spindle during mitosis

To characterise the previously observed mitotic spindle staining, the localisation of HECTD1 throughout the cell cycle was explored. To this end, two HECTD1 antibodies were tested for their ability to detect endogenous HECTD1 by immunofluorescence in HEK293ET cells and two HECTD1 CRISPR/Cas9 KO cell lines (kindly contributed by Mariann Bienz, MRC-LMB, Cambridge) (Figure 4.2). The antibody ab101992 was raised against the N-terminal amino acids 1-50 of hHECTD1 while ab101993, also from Abcam, was raised against the C-terminal region of hHECTD1 (AA2100-2150). Staining with the N-terminal HECTD1 antibody revealed a strong signal, almost exclusively cytosolic in interphase cells and at the mitotic spindle of mitotic HEK293T cells (Figure 4.2A). However, this signal was also present in two CRISPR/Cas9 clones derived from HEK293T cells suggesting that the observed staining is non-specific (Figure 4.2B). In contrast, the C-terminal specific HECTD1 antibody showed a dissimilar staining pattern in interphase cells, where a nuclear staining was observed, and a weak signal was observed in mitotic cells (Figure 4.2A). In addition, with this antibody the signal was reduced in HECTD1 KO cell lines, suggesting that the epitope was more specific towards endogenous HECTD1 (Figure 4.2B). However, the signal in cells stained with ab101993 was overall weak compared to the background signal, making this antibody unsuitable. Therefore, neither antibody was suitable for immunofluorescent staining of mitotic cells. In contrast, both antibodies could be used to detect full-length HECTD1 by western blotting, with ab101992 yielding fewer background bands compared to ab101993 (Figure 4.3). This validates and confirms the previous observations carried out in Chapter 3 using ab101992, therefore, ab101992 was deemed appropriate for further western blotting experiments.

The limitation of using the endogenous HECTD1 antibodies for immunofluorescence was overcome by the use of an overexpression assay. Although overexpression can lead to artefacts, expression of HECTD1 labelled with a HA- epitope tag, allows for more specific detection of the protein compared to antibodies raised against the endogenous protein. HEK293ET cells were transiently transfected with *HA-FL-mHectd1* (kindly contributed by Mariann Bienz, MRC-LMB, Cambridge) and cells were imaged by IF detection using anti-HA antibody in interphase and mitotic cells. Both HA-FL-mHectd1^{WT} and HA-FL-mHectd1^{C2579G} during interphase showed diffuse staining in the cytoplasm and exclusion from the nucleus (Figure 4.4). Interestingly, HA-FL-mHectd1^{WT} was found to localise with the mitotic spindle marker, α-tubulin (Mandelkow & Mandelkow. 1989), in prometaphase and metaphase, suggesting that HECTD1 may function in mitosis. Furthermore, as cells progress from anaphase I to telophase, the staining of HA-FL-mHectd1 at the mitotic spindle (α-tubulin), became gradually weaker and more diffuse until no colocalisation was observed in anaphase II and telophase (Figure 4.5). To elucidate whether the E3 ligase activity of

HECTD1 was required for its mitotic localisation, the catalytic mutant of HECTD1 (C2579G) (Sarkar, *et al.* 2012) was overexpressed in HEK293ET cells, and imaged throughout mitosis. HA-FL-mHectd1^{C2579G} was seen to localise to the mitotic spindle (α-tubulin) during prometaphase and metaphase, as seen with the wild-type protein. Again, the localisation, and potentially the staining for HECTD1, was reduced as cells progressed from anaphase I to telophase (Figure 4.6). This indicates that the E3 ligase activity of the HECTD1 is not required for its localisation during mitosis. Importantly, to validate this assay, an empty vector control was also carried out and showed absence of staining, including spindle staining, suggesting that the observed staining was not due to non-specific binding of the anti-HA antibody (Figure 4.4-6). Taken together, this suggests a potential function for HECTD1 during M phase and not G2 phase.

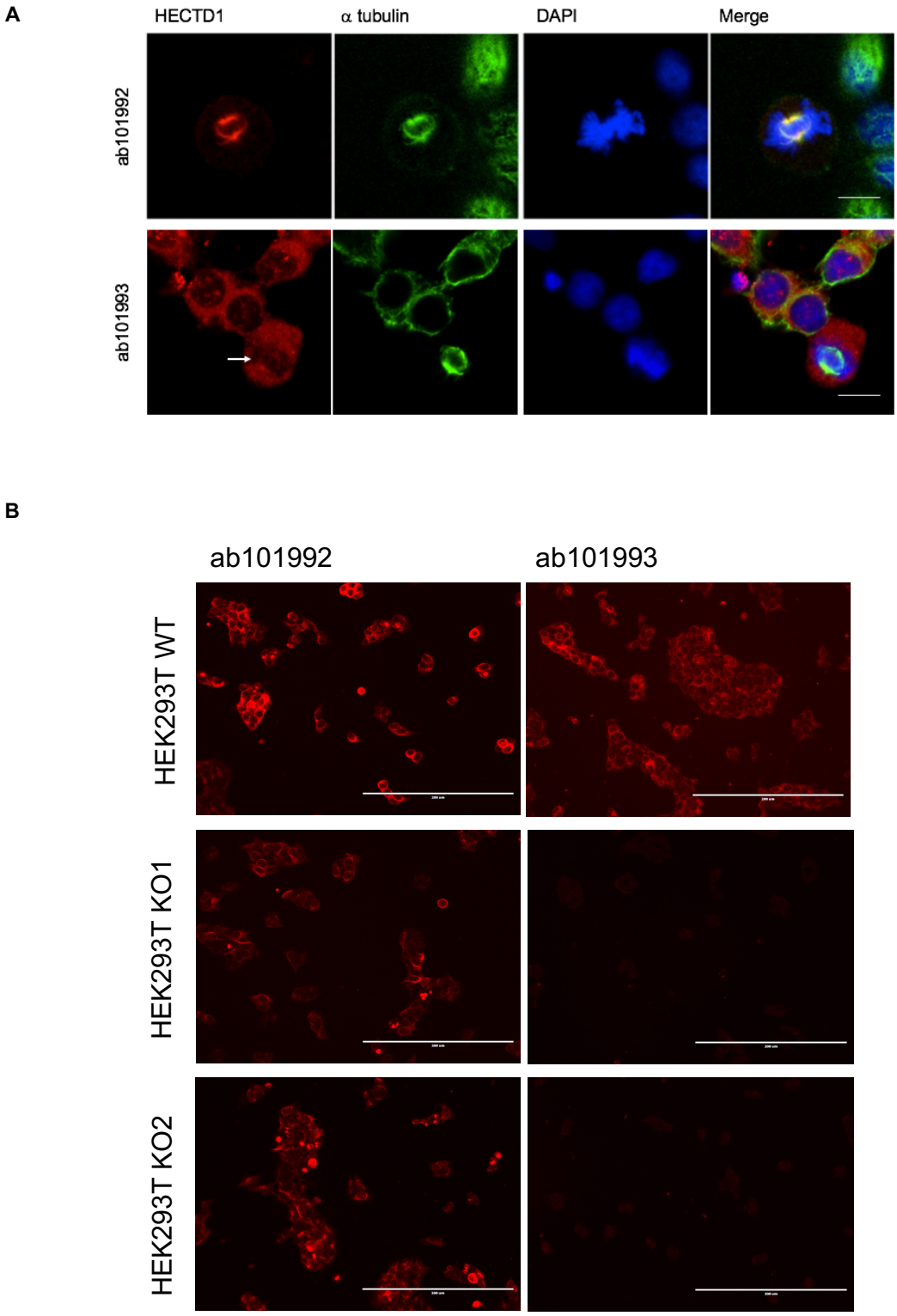

Figure 4.2. Validation of HECTD1 antibodies for immunofluorescent staining. A) Confocal images of HEK293ET mitotic cells stained with ab101992 or ab101993 (1 in 200 dilution). Cells were fixed using 4% PFA, and imaged using the LSM 510 Meta Confocal Microscope. Scale bar represents 10μm. White arrow indicates weak mitotic spindle staining using C terminal antibody. B) HEK293T HECTD1 knockout cells were stained with either a HECTD1 N-terminal antibody (ab101992) or a HECTD1 C-terminal antibody (ab101993), at a 1 in 200 dilution. Cells were fixed using 4% PFA, and imaged using the EVOS FL Cell Imaging System. Scale bar represents 200μm.

A

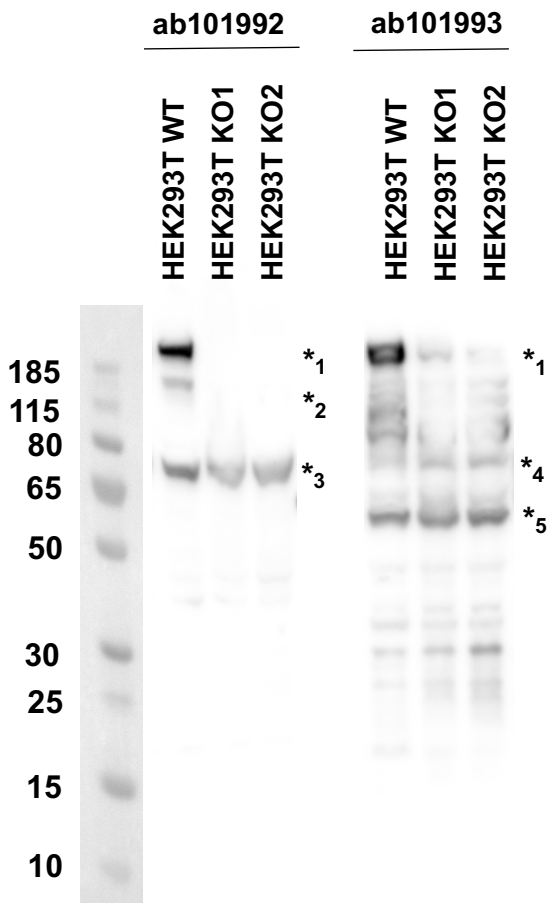

B

Name	Molecular weight (kDa)
HECTD1-201	289.368
HECTD1-001	289.368
HECTD1-202	289.632
HECTD1-005	163.187
HECTD1-006	110.496
HECTD1-003	102.012
HECTD1-010	22.548
HECTD1-012	20.058

Figure 4.3. Validation of HECTD1 antibodies for western blotting. A) Western blot showing the antibody staining for ab101992 and ab101993 in HEK239T HECTD1 knockout cells, labelled with the molecular weight marker on the left-hand side. Based on the molecular weight, the band indicated by $*_1$ represents full length HECTD1 and $*_2$ represents HECTD1 005, $*_3$, $*_4$, and $*_5$ do not correspond to known splice variants of HECTD1. Cells were lysed in RIPA buffer and samples were analysed on a 4-12% SDS PAGE. Following western blotting on PVDF, the membrane was blocked in 3%-BSA-PBST and incubated overnight with anti-HECTD1 antibody (ab101992) and anti-pHistone H3 (ser28) (ab10543), followed by detection with a secondary HRP antibody. Anti-beta-actin (A5441) was used as loading control. B) Predicted molecular weights of protein coding variants of hHECTD1, using Ensembl Gene Browser 90, https://www.ensembl.org, (accessed 09/10/17).

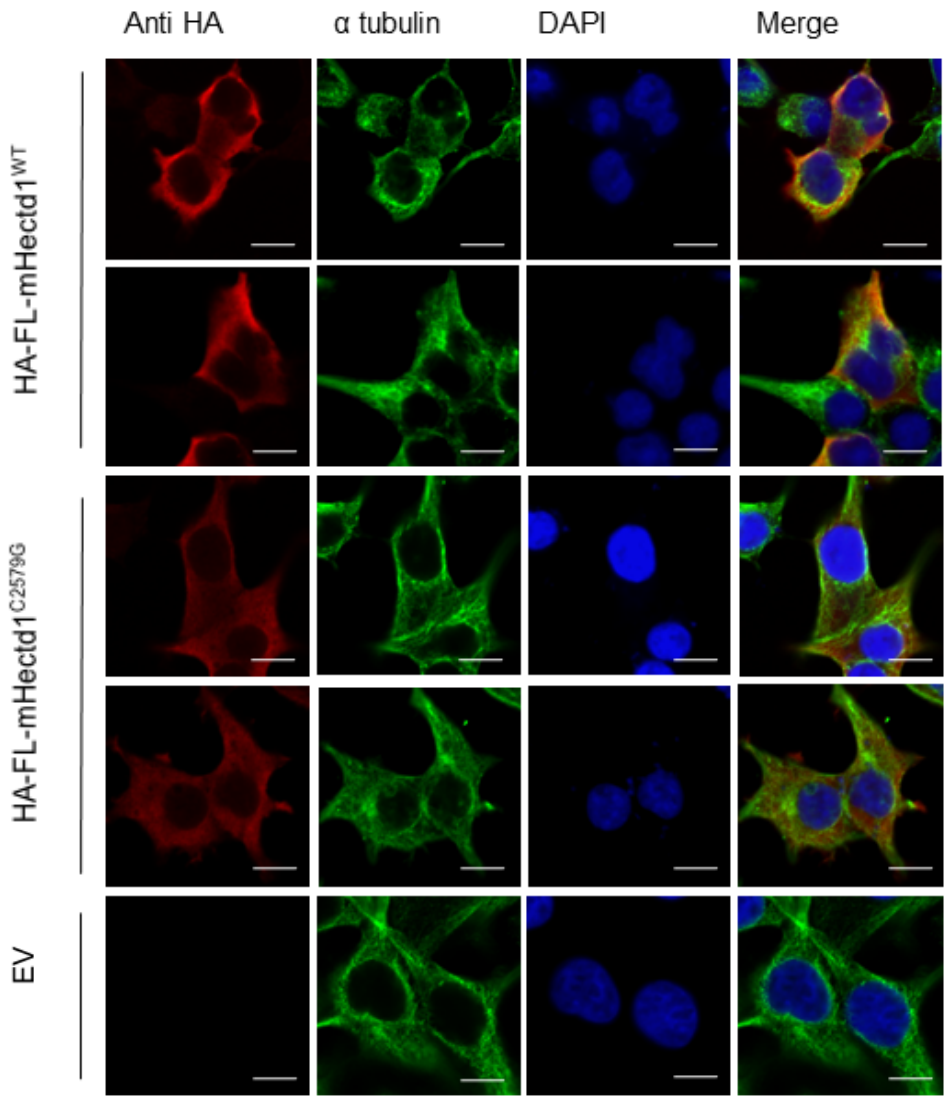

Figure 4.4. Diffuse localisation of mHectd1^{WT} and mHectd1^{C2579G} in human cell lines during interphase. Representative images of HA-FL-mHectd1^{WT} and HA-FL-mHectd1^{C2579G} staining in interphase HEK cells. HEK293ET cells were transfected with 500ng of *HA-FL-mHectd1^{WT}*, *HA-FL-mHectd1^{C2579G}* and an HA-tagged empty vector (EV) using PEI, in a 12 well format. 24hrs post-transfection cells were fixed using 4% PFA, then stained with anti-HA, anti-α-tubulin and Hoechst. Images were taken using the LSM Meta 510 Confocal Microscope. Scale bar represents 10μm.

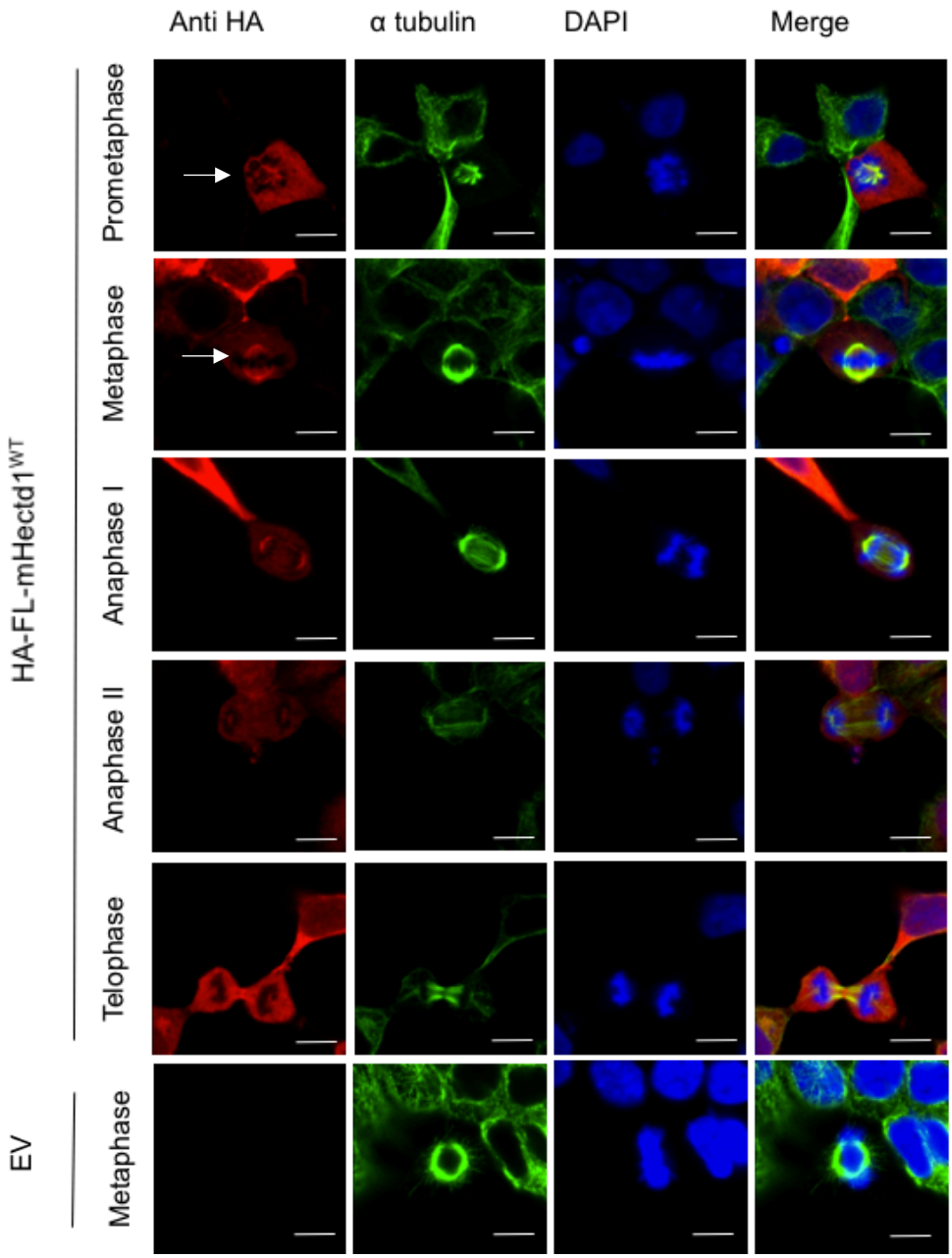

Figure 4.5. HA-FL-mHectd1^{WT} is localised to the mitotic spindle in HEK293ET cells during mitosis. Representative images of HA-FL-mHectd1^{WT} in mitotic HEK cells. HEK293ET cells were transfected with 500ng of *HA-mHectd1^{WT}* and an HA-tagged empty vector (EV) using PEI, in a 12 well format. 24hrs post-transfection cells were fixed using 4% PFA, then stained with anti-HA, anti-α-tubulin and Hoechst. Images were taken using the LSM Meta 510 Confocal Microscope. Scale bar represents 10μm. Images were taken of cells in prometaphase, metaphase, anaphase I, anaphase II, and telophase. Anaphase was subdivided into anaphase I, and anaphase II; anaphase I denotes early anaphase, where the sister chromatids begins to segregate to opposite poles of the spindle, and anaphase II denotes late anaphase where elongation of the spindle occurs (Pines. 2006). White arrows indicate cells with the strongest colocalisation to α-tubulin, seen during prometaphase and metaphase.

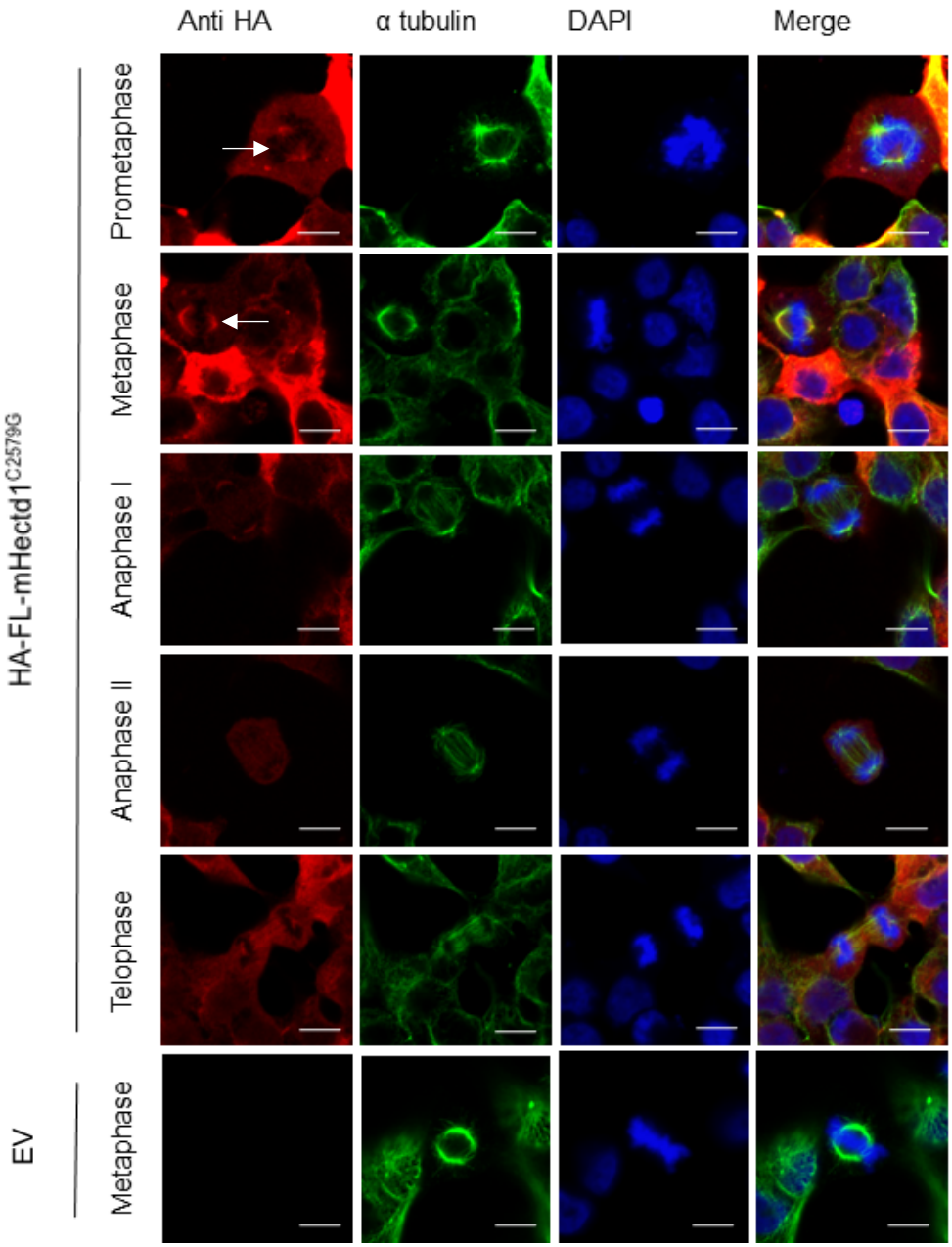

Figure 4.6. HA-FL-mHectd1^{C2579G} is localised to the mitotic spindle in HEK293ET cells during mitosis. Representative images of HA-FL-mHectd1^{C2579G} in mitotic HEK cells. HEK293ET cells were transfected with 500ng *HA-mHectd1^{C2579G}* and an HA-tagged empty vector (EV) using PEI, in a 12-well format. 24hrs post-transfection cells were fixed using 4% PFA, then stained with anti-HA, anti-α-tubulin and Hoechst. Images were taken using the LSM Meta 510 Confocal Microscope Scale bar represents 10μm. Images were taken of cells in prometaphase, metaphase, anaphase I, anaphase II, and telophase. Anaphase was subdivided into anaphase I, and anaphase II; anaphase I denotes early anaphase, where the sister chromatids begins to segregate to opposite poles of the spindle, and anaphase II denotes late anaphase where elongation of the spindle occurs (Pines. 2006). White arrows indicate cells with the strongest colocalisation to α tubulin, seen during prometaphase and metaphase.

4.2.3. HECTD1 depletion results in an enrichment of metaphase cells

Given the limitation of the PI staining in reporting a change in the G2/M population of cells upon HECTD1 depletion, and the apparent localisation of HECTD1 during mitosis, cells were scored based on their mitotic stage following confocal imaging. This is an established phenotypic assay successfully used to identify JMJD5 and NuMA as mitotic regulators (Haren, *et al*. 2009; He, *et al.* 2015). Here, HECTD1 was transiently depleted in HEK293ET and HeLa cells, and stained with anti-α-tubulin antibody and Hoechst. Cells were scored at prophase, prometaphase, metaphase, anaphase, and telophase based on the morphology of the microtubules and the DNA. Cells in prophase were defined as cells with condensed chromosomes (Sager, *et al.* 1986; Strunnikov. 2003) and cells in prometaphase were defined by centrosomes at each pole, with chromosomes that begin to align into the centre of the cell (Aubin, *et al.* 1980; Beaudouin, *et al.* 2002). Metaphase cells were defined by chromosomes aligned along the equatorial plane (Rieder & Alexander. 1990), followed by anaphase cells where sister chromatids begin to segregate to opposite poles (Baskin, & Cande. 1990; Pines. 2006), and finally telophase cells where the nuclear envelope forms around each set of chromosomes in the daughter cells, and the chromosomes uncoil (Chaudhary, & Courvalin. 1993; Schwalm. 1969). A representative image of each stage of mitosis scored is shown in Figure 4.7C.

In HEK293ET that were transiently depleted of HECTD1, there was a significant increase in the number of metaphase cells compared to control. Specifically, 40% of cells in the non-targeting control were in metaphase, compared to 58.1% seen with cells treated with HECTD1 siRNA #06, and 57.7% for the HECTD1 SMARTpool (SP) siRNA (Figure 4.7A). Similarly, this effect was also observed in Hela cells, where 35.7% of cells in the non-targeting condition were scored as being in metaphase, compared to 50.4% (SMARTPool), 48.8% (#06), and 51.7% (#08). (Figure 4.7B). In summary, cells depleted for HECTD1 showed an 18% increase in HEK239ET and a 15% increase in HeLa of cells in metaphase compared to the non-targeting siRNA control. This therefore indicates that HECTD1 depletion results in an enrichment of cells in metaphase.

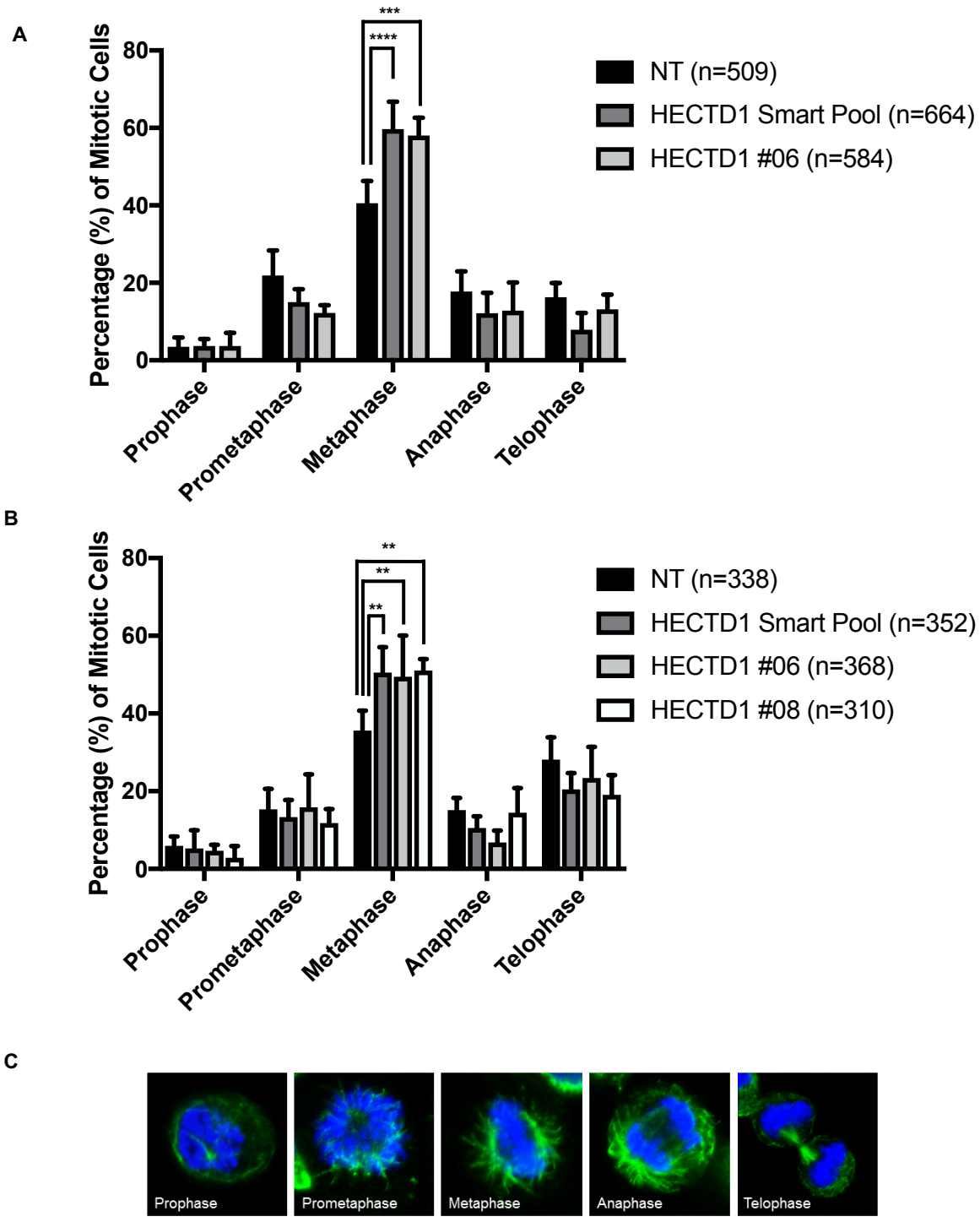

Figure 4.7. Scored mitotic stage upon HECTD1 depletion in HEK293ET and HeLa cells. Asynchronous A) HEK293ET cells and B) HeLa cells were scored according to chromatin morphology or spindle morphology based on Hoechst (blue) and α-tubulin (green) staining following knockdown using NT (non-targeting), HECTD1 SMARTpool (smart pool), #06, and #08 siRNA, and Lipofectamine-2000 or -RNAiMAX for 48hrs. Data plotted as mean with error bars that represent ±S.E.M., over 6 biological repeats (individual transfections). **p<0.01, ***p<0.001, and ****p<0.0001 using a one-way ANOVA with a Dunnett's post-test. Each HECTD1 siRNA condition was significant when compared to the NT control. C) Image stills of HEK293ET cells at each mitotic phase scored.

4.2.4. HECTD1 depletion does not induce mitotic spindle or nuclear defects

Having shown that HECTD1 depletion resulted in a significant enrichment of metaphase cells. The next question was to establish whether this could be due to an increase in abnormal mitosis and perhaps increased defects including multipolar spindles, misaligned metaphase plates or lagging chromosomes. For instance, cells depleted of NuMA were found to be enriched in early mitosis coinciding with chromosome alignment defects and spindle abnormalities (Haren, *et al.* 2009). Multipolar spindles are defined by cells that have more than two spindle poles (Yan, *et al.* 2015) and cells with a misaligned metaphase plate are cells that have a number of unattached kinetochores (Haren, *et al.* 2009; Chapard, *et al*. 2014; Yan, *et al.* 2015) (Figure 4.8C). Cells with lagging chromosomes exhibit chromosomes that do not move at the same rate as the other chromosomes during anaphase (Chapard, *et al*. 2014; Yan, *et al.* 2015). Finally, normal mitotic cells are cells that have no observable mitotic defects. Again, HECTD1 was transiently knocked down in HEK293ET and HeLa cells and stained with anti-α-tubulin antibody and Hoechst, to score their morphologies. In both cell lines, there was no change in the number of cells with multipolar spindles, misaligned metaphase plates, and lagging chromosomes (Figure 4.8). Taken together this suggests that the observed enrichment of metaphase cells in HECTD1-depleted cells does not translate into mitotic defects for most cells.

Nuclear defect phenotypes generally refer to cells with abnormal spindles. For example, depletion of MISU, identified as being required for mitotic spindle stability, results in unstructured and multipolar spindles, resulting in chromosome missegregation and therefore leading to multinucleated cells (Hussain, *et al* 2009). To establish whether HECTD1 depletion resulted chromosome missegregation, and therefore abnormal nuclei, interphase cells were scored based on their nuclear morphology to identify any abnormal nuclear phenotypes. Multinucleated cells were defined as cells with more than one nuclei, cells with enlarged nuclei were defined as possessing 2X the mean diameter of nuclei, 14.5μm, at the widest point, and finally multilobed nuclei were nuclei that had an irregular shape comprising 2 or more defined lobes (Hussain, *et al* 2009; Jevtić, *et al.* 2015) (Figure 4.9C). In both cell types, there were no differences in the number of multinucleated cells, cells with enlarged nuclei, multilobed nuclei in the compared to the control (Figure 4.9) (Hussain, *et al* 2009; Jevtić, *et al.* 2015). Therefore, indicating that HECTD1 depletion does not lead to large increases in nuclear defects.

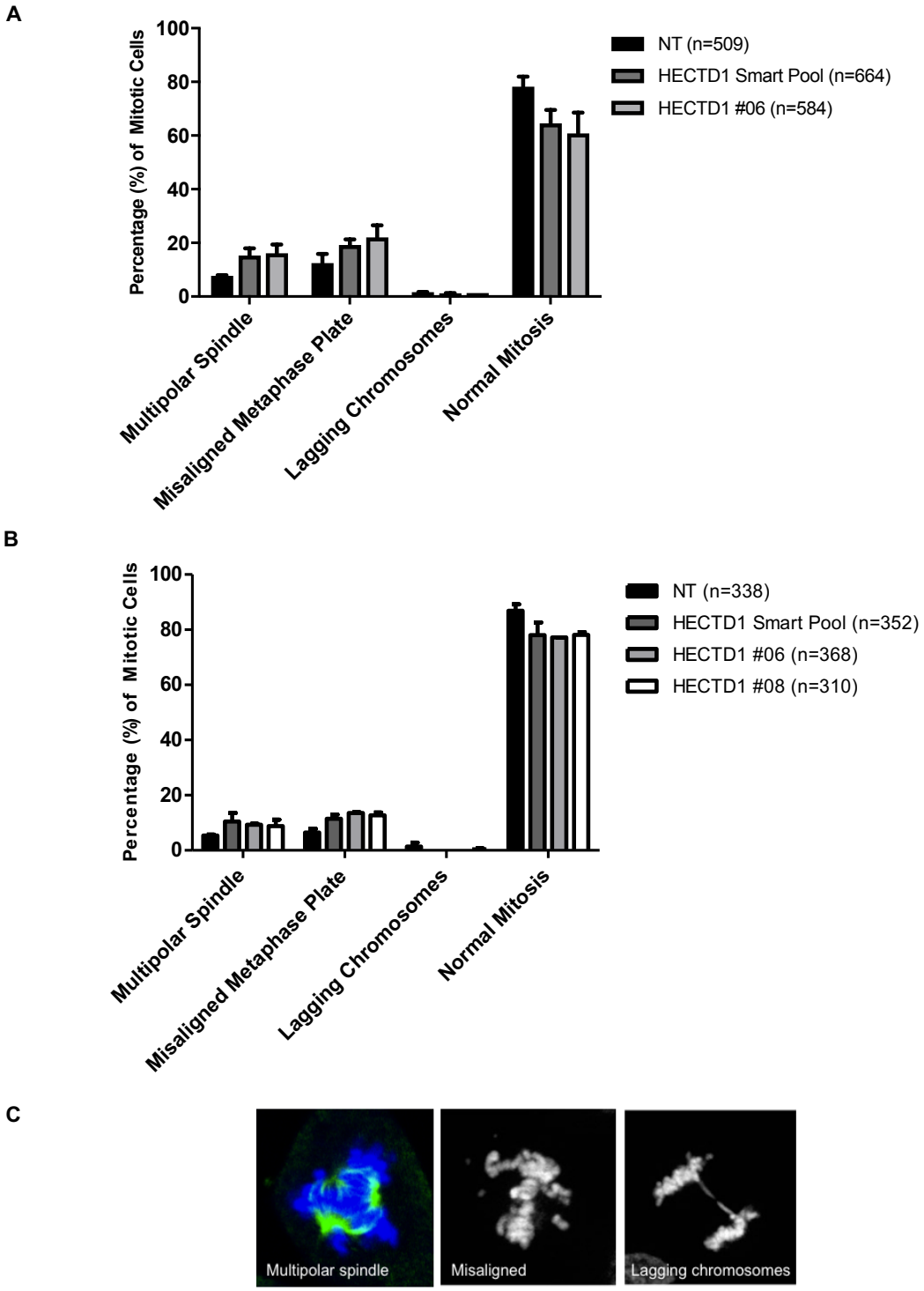

Figure 4.8. Scored mitotic defects upon HECTD1 depletion in HEK293ET and HeLa cells. Asynchronous A) HEK293ET cells and B) HeLa cells were scored according to chromatin morphology or spindle morphology based on Hoechst (blue or white) and α-tubulin (green) staining following knockdown using NT (non-targeting), HECTD1 SMARTpool (smart pool), #06, and #08 siRNA, and Lipofectamine-2000 or -RNAiMAX for 48hrs. Cells were categorised into three mitotic defect phenotypes: multipolar spindle, misaligned metaphase plate, or lagging chromosomes. Cells with no observable mitotic defects were scored as cells that were in normal mitosis. Data plotted as mean with error bars that represent ±S.E.M., over 6 biological repeats. Average increase in multipolar spindle = HECTD1 siRNA of 8.0% HEK293ET; 4.1% HeLa. Average misaligned metaphase plate = HECTD1 siRNA of 7.1% HEK293ET; 6.2% HeLa. C) Representative images of each mitotic defect scored. No statistical significance was found using a one-way ANOVA test.

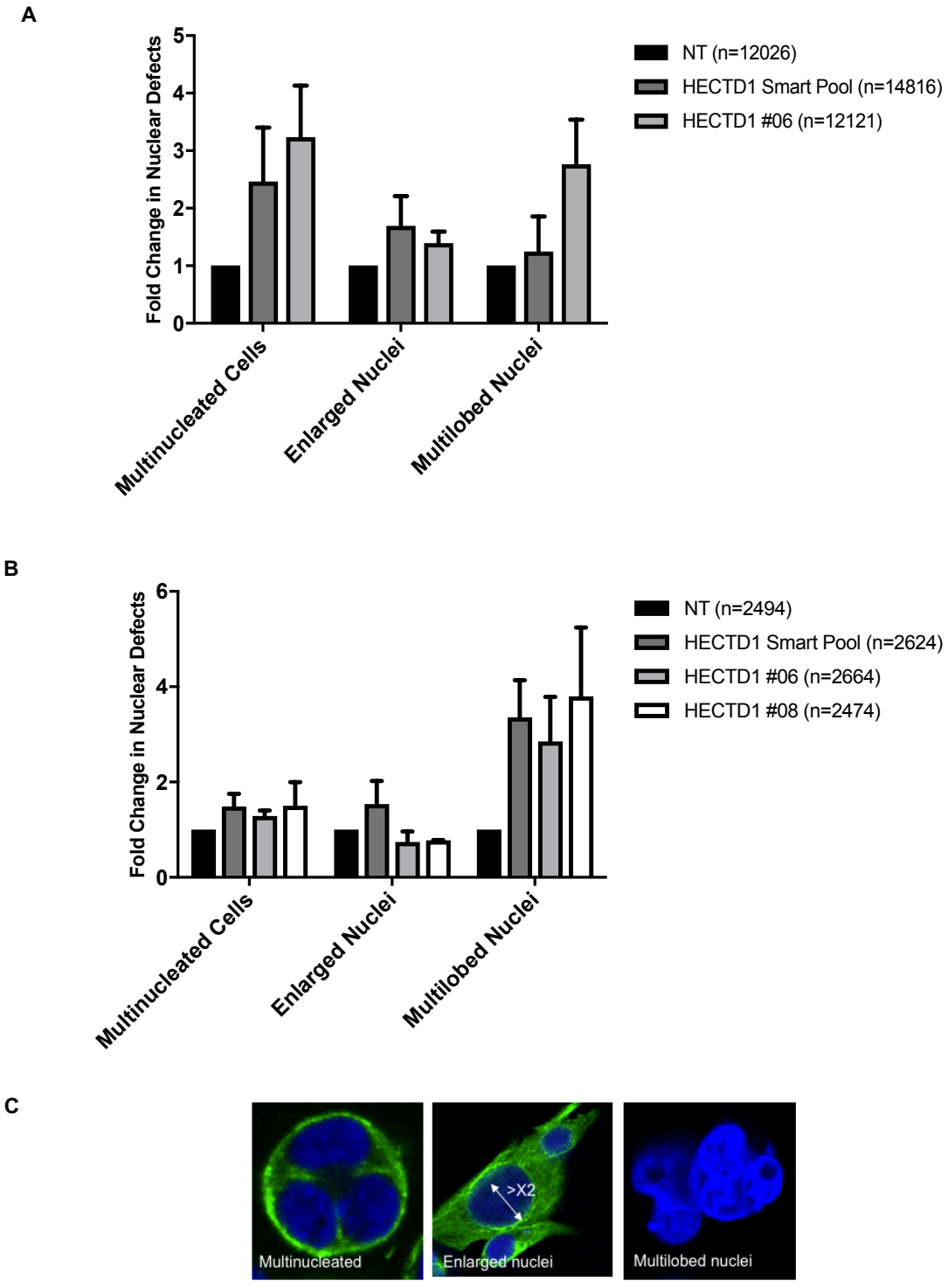

Figure 4.9. Scored nuclear morphology upon HECTD1 depletion in HEK293ET and HeLa cells. A) HEK293ET cells and B) HeLa cells were scored according to nuclear morphology based on Hoechst (blue) staining of interphase cells following knockdown using NT (non-targeting), HECTD1 SMARTpool (smart pool), #06, and #08 siRNA, and Lipofectamine-2000 or -RNAiMAX for 48hrs. Cells were categorised into three nuclear defect phenotypes: multinucleated cells, enlarged nuclei, or multilobed nuclei. Data plotted as mean with error bars that represent ±S.E.M., over 6 biological repeats. HEK293ET HECTD1 08 siRNA represents one independent experiment. C) Representative images of each nuclear defect scored, cells were stained with Hoechst (blue) and α-tubulin (green). No statistical significance was found using a one-way ANOVA test.

4.2.5. Mitotic delay observed in HECTD1-depleted and knockout cells

Given the enrichment of metaphase cells observed in Figure 4.7, it was hypothesised that this enrichment may lead to an increase in the time taken for cells to progress through mitosis. For example, with depletion of JMJD5, the enrichment of cells in early mitosis coincided with an increase in the length of mitosis (He, *et al.* 2015). Therefore, expression of pHistone H3 (Ser28) was used as a molecular marker to track mitotic entry and anaphase onset in order to time the length of mitosis in synchronised cells either WT or depleted for HECTD1.

Cells synchronised with a double thymidine block and released into fresh media were harvested at 0hrs, 3hrs, 6hrs, 8hrs, 10hrs, 12hrs, and 14hrs post-release to capture mitotic entry and exit. As seen by the presence of a 15kDa band on the western blot, mitotic entry occurred at 8hrs for both the non-targeting and HECTD1 SMARTpool siRNA treated samples, indicating that there was no delay in mitotic entry (Figure 4.10A). At the 12hr time-point, a strong signal for pHistone H3 (ser28) was present in HECTD1-depleted cells but not in the non-targeting control samples. Similarly, this was also seen at the 14hr time-point, suggesting that HECTD1-depletion leads to mitotic delay. A similar mitotic delay was also observed in HEK293T KO1 knock out cells, which further strengthen the data obtained by transient siRNA knock down.

To confirm this mitotic delay observed by western blotting, HEK293T KO1 and parental (i.e. WT) cells were synchronised using the CDK1 inhibitor RO-3306. Cells were released and the cell cycle profile was determined at time-points post-release by PI staining using the optimised conditions determined in Figure 3.8. RO-3306, a CDK1 inhibitor was used because of the ability to synchronise cells in G2/M, therefore allowing observation of mitosis from the G2/M border to mitotic exit (Vassilev, *et al.* 2006). At 0hrs, both samples showed a strong degree of synchronisation with RO-3306, with 90.2% synchronised in the WT condition (Figure 4.11A) and 88.8% of the KO1 cells (Figure 4.11B) in the G2/M peak (P4). At 2hrs post-release, 78.5% of KO1 cells were in the G2/M peak compared to 53.7% of HEK293T WT cells, further suggesting a delay in the completion of mitosis. Furthermore, at 4hrs, 66.0% of KO1 cells were in G2/M compared to 36.7% of WT cells. This therefore indicates that HECTD1 KO1 cells take longer to progress through mitosis compared to WT cells.

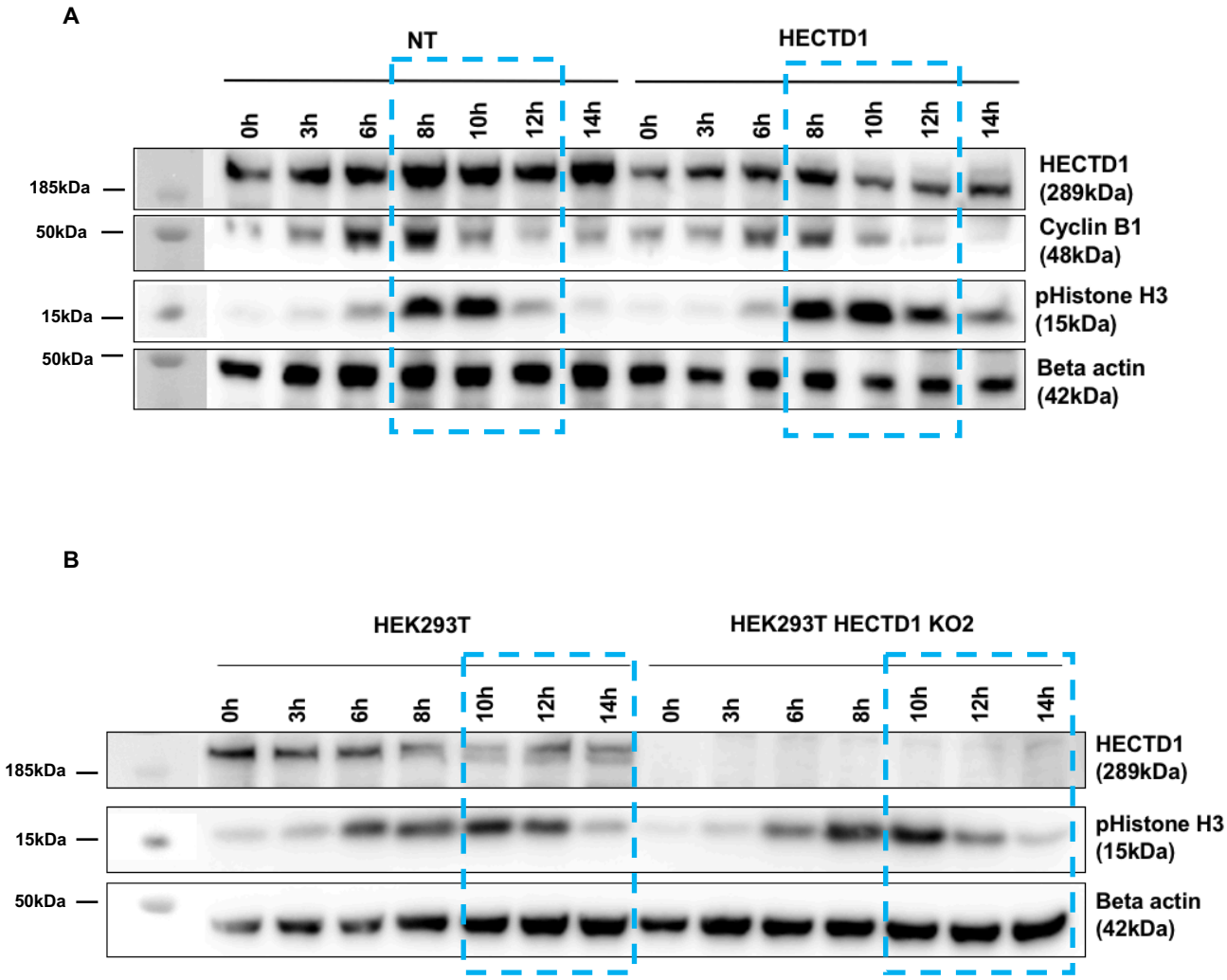

Figure 4.10. Delay in mitosis observed by a delay in pHistone H3 turnover. HEK293ET cells knocked down with 20pmol HECTD1 SMARTpool (smartpool) siRNA and Lipofectamine 2000. 24hrs later cells were then synchronised using a double thymidine block. Knockout cells were also synchronised using a double thymidine block. A) Representative blot showing HEK293ET cells treated with non-targeting and HECTD1 SMARTpool (smart pool) siRNA (n=2; independent transfections). B) Blot showing HEK293T WT compared with HEK293T KO1 cells (n=2). For the double thymidine block, cells were treated with 2mM Thymidine for 18hrs, followed by a 9hrs release. Then an additional 2mM Thymidine for 15hrs, before being released and harvested at 0hrs, 3hrs, 6hrs, 8hrs, 10hrs, 12hrs, and 14hrs post-release. Cells were lysed in RIPA buffer and samples were analysed on a 4-12% SDS PAGE. Following western blotting on PVDF, the membrane was blocked in 3%-BSA-PBST and incubated overnight with anti-HECTD1 antibody (ab101992) and anti-pHistone H3 (ser28) (ab10543), followed by detection with a secondary HRP antibody. Anti-beta-actin (A5441) was used as loading control. Molecular weight markers are superimposed on the left-hand side of the immunoblot.

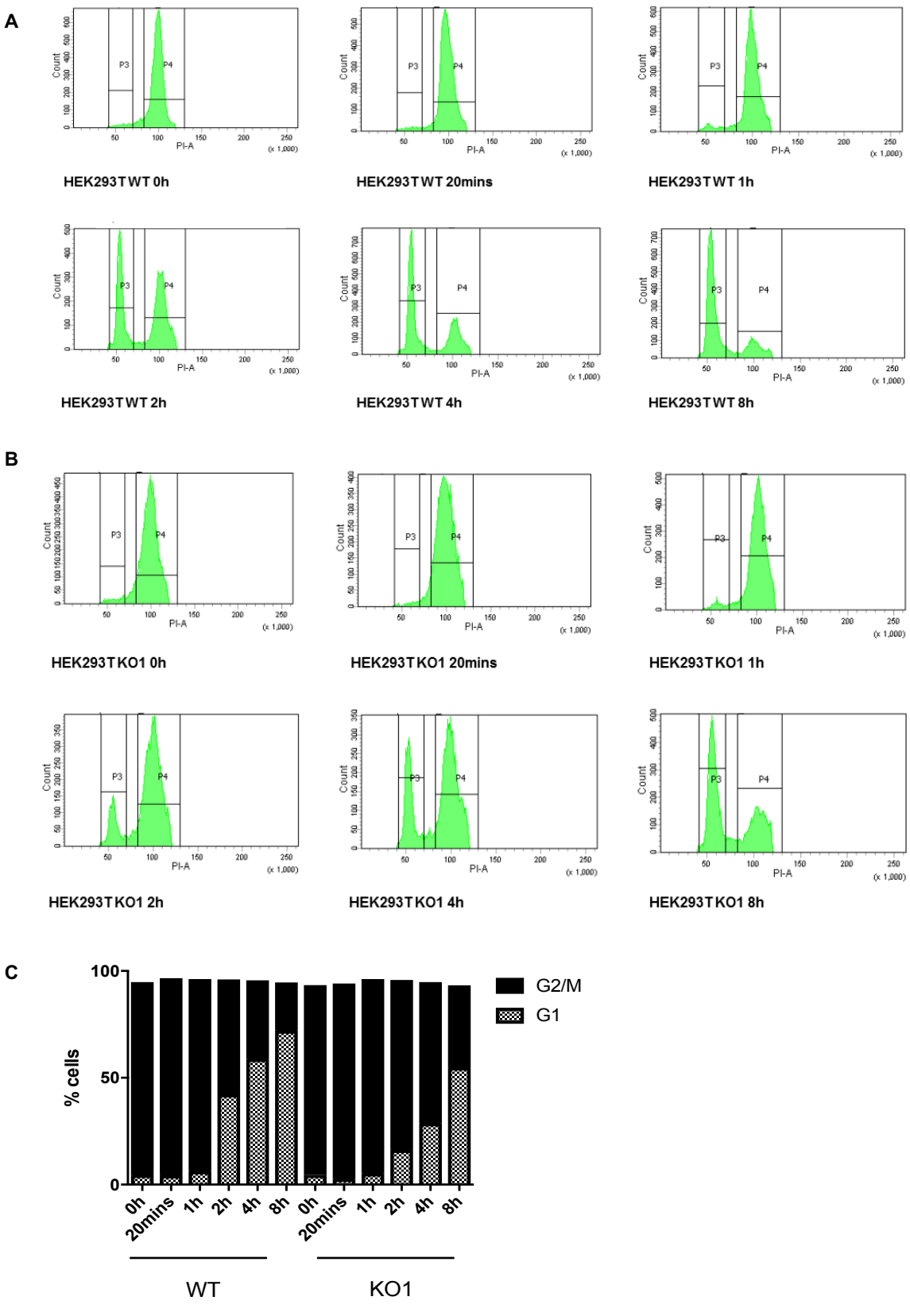

Figure 4.11. Delay in G2/M population observed in HEK293T knockout cells synchronised with RO-3306. HECTD1 knockout cells were treated with 9μM RO-3306 for 20hrs before being fixed using 70% ethanol. Cells were stained using 2μg/ml PI, with 100μg/ml RNase A, for 30mins at room temperature. A) Histograms for HEK293T WT cell line, B) histograms for HEK293T KO1 cell line. C) Graph showing quantification of G1 and G2/M populations in HEK293T WT and KO1 cell lines at each time point post RO-3306 release. Data from one independent experiment. PI-A of 50 is equivalent to 2N (G1 population), and PI-A of 100 is equivalent to 4N (G2/M population).

4.2.6. Increase in NEBD to anaphase onset in HECTD1-depleted and knockout cells

To understand whether the mitotic delay observed in cells depleted with HECTD1 and HECTD1 knock out cells is associated with the enrichment of metaphase cells, asynchronous HEK293T CRISPR/Cas9 knockout cells were filmed by time-lapse microscopy (Figure 4.12). The time taken for cells to progress from NEBD to anaphase onset is an established read out to measure mitotic progression and has been used to show the requirement of post translational modifications in regulation of CDC20 (Uzunova, *et al*. 2012; Hein, *et al*. 2017). Mitotic progression was analysed in HEK293T KO1 and KO2 HECTD1 knock out cell lines and the parental control cell line HEK293T. NEBD and anaphase onset were defined by visible loss of the nuclear membrane and the separation of chromosomes respectively by Differential Interference Contrast (DIC) (Beaudouin, *et al.* 2002; Pines. 2006) (Figure 4.12C). There was a significant delay in the time taken for cells to progress from NEBD to anaphase onset in HEK283T KO1 cells when compared to the WT control and this trend was also observed in KO2 cells (Figure 4.12A). Specifically, KO1 cells showed a mean delay of around 15.5mins and KO2 cells a mean delay of around 9mins compared to the WT control cell line. This indicates that the enrichment of metaphase cells seen in Figure 4.7, is due to a delayed NEBD to anaphase onset. Furthermore, cells can be observed with chromosomes aligned along the equatorial plane for longer before anaphase onset (Figure 4.12C), indicating that cells may be held by the spindle assembly checkpoint for longer.

To validate the data obtained with the knock out cells, mitotic progression was also analysed following transient HECTD1 knock down. HEK293ET cells were treated with non-targeting, HECTD1 SMARTpool (SP) HECTD1 #06, and #08 siRNA. Cells were visualised at 48hrs and 72hrs post knockdown. At 48hrs it can be seen that both HECTD1 SMARTpool and HECTD1 #08 showed a delay in the length of NEBD to anaphase onset compared to the non-targeting control (Figure 4.13A). HEK293T treated with HECTD1 SMARTpool siRNA showed a mean delay of around 28.3mins and 22.8mins for HECTD1 #08 siRNA compared to the non-targeting control (Figure 4.13B). At 72hrs the HECTD1 SMARTpool showed a mean delay of 21.6mins, and HECTD1 #06 siRNA showed a significant delay of 39.3mins compared to the non-targeting control. In contrast, the HECTD1 #08 treated sample was slightly faster than the non-targeting control in the time taken to progress from NEBD to anaphase onset. This is most likely due to the difficulty of targeting all cells transiently using siRNA. An important consideration is that the mean is only representative and in reality the data show that only a subset of cells are delayed for a long time (>200mins). Taken together, these results suggest that HECTD1 knockout or transient depletion results in a mitotic delay of around 15-30min on average, representing a 30-60 % increase in the length of mitosis in HEK293T and HEK293ET cells, which in our hands is around 50mins.

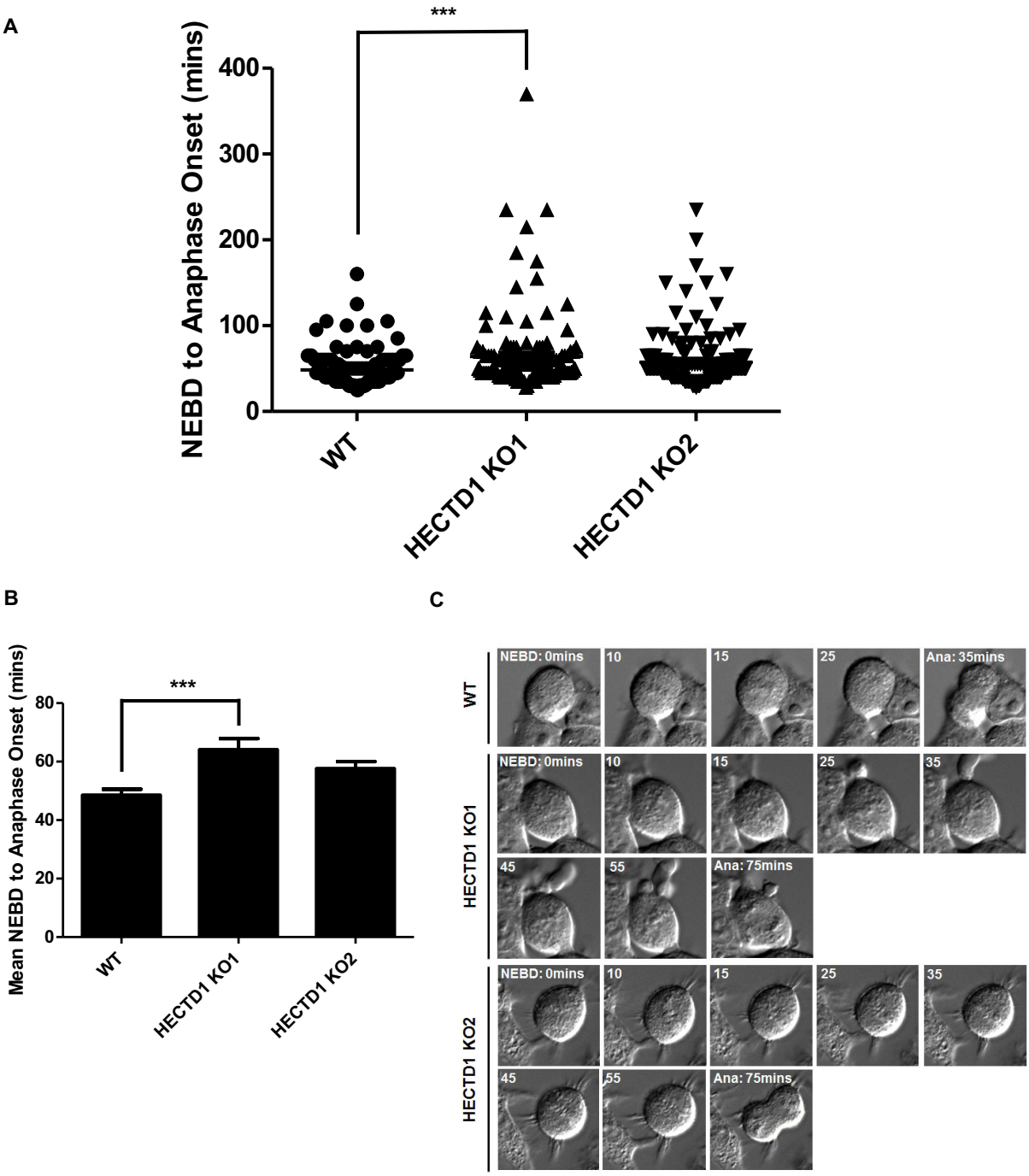

Figure 4.12. Delay in NEBD to anaphase onset in HECTD1 knockout cells. Duration of NEBD to anaphase onset was timed in asynchronous HEK293T WT and two HECTD1 CRISPR/Cas9 knockout cell lines. A) Vertical scatter plot showing the time taken for each cell to progress from NEBD to anaphase onset. B) Mean time taken for cells to progress from NEBD to anaphase onset. C) Representative images of cells scored in A). Error bars represent ±S.E.M., ***p<0.001, using a one-way ANOVA with a Dunnett's post-test. Number of cells filmed are as follows, WT = 116, KO1 = 136, and KO2 = 161, filmed over 4 independent experiments. Cells were imaged using an Olympus IX81 microscope with a 40X oil immersion objective lens and Hammatsu ORCA-ET Camera at 37ºC. Micro-Manager (Edelstein *et al.* 2014) was used to acquire and analyse the images.

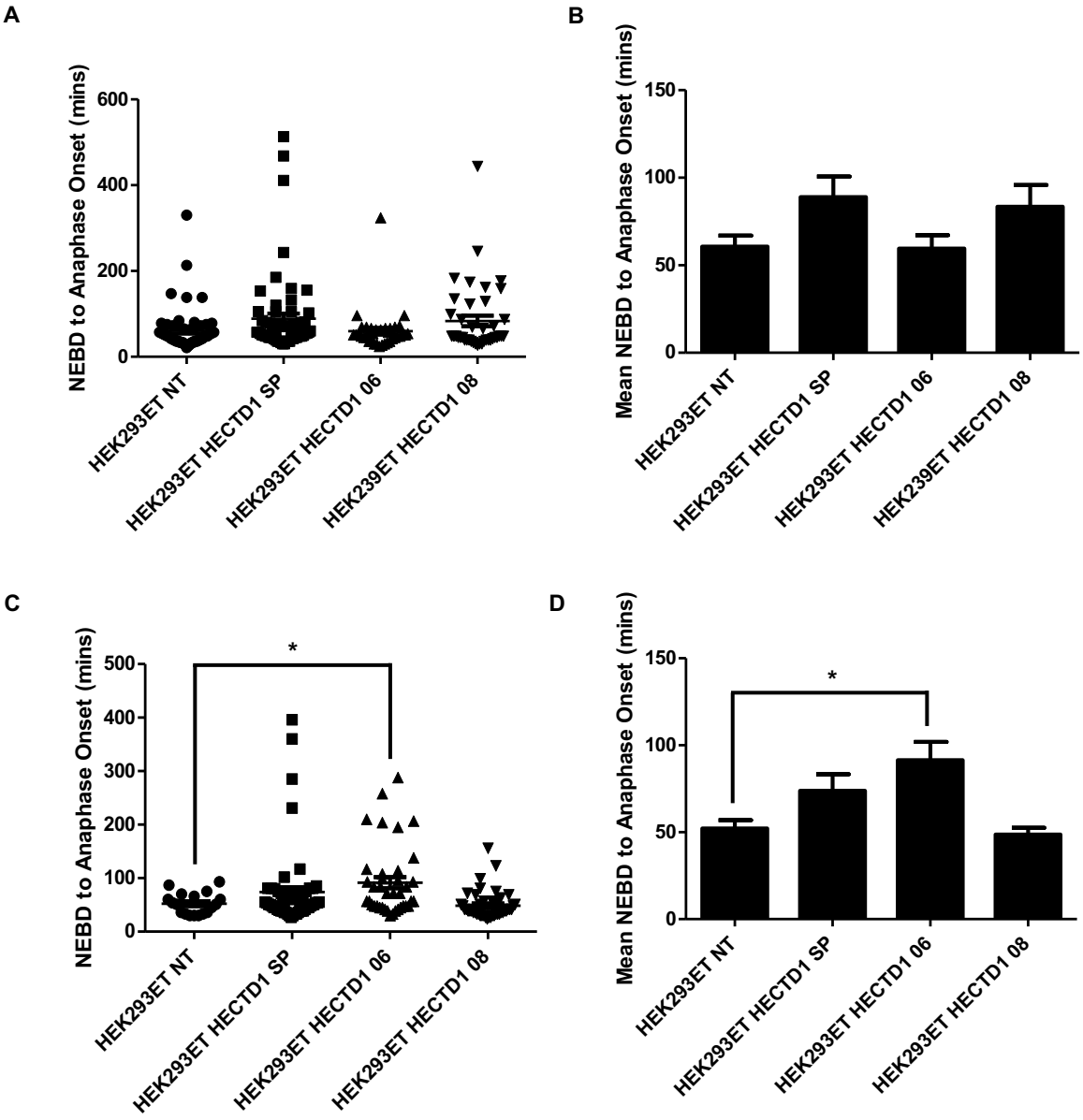

Figure 4.13. Delay in NEBD to anaphase onset in HECTD1-depleted HEK293ET cells. Duration of NEBD to anaphase onset was timed in HEK293ET cells treated with either NT (non-targeting), HECTD1 SP (SMARTpool), HECTD1 #06, and HECTD1 #08 siRNA, and Lipofectamine 2000 for either 48hrs and 72hrs. A) Vertical scatter plot showing the time taken for each cell to progress from NEBD to anaphase onset 48hrs post knockdown. B) Mean time taken for cells to progress from NEBD to anaphase onset for data shown in A). C) Vertical scatter plot showing the time taken for each cell to progress from NEBD to anaphase onset 72hrs post knockdown. D) Mean time taken for cells to progress from NEBD to anaphase onset for data shown in C). Error bars represent ±S.E.M., ***p<0.001, **p<0.01 by using a one-way ANOVA with a Dunnett's post-test. Number of cells filmed are as follows, NT (48h) = 60, HECTD1 SP (48h) = 64, HECTD1 #06 (48h) = 38, HECTD1 #08 (48h) = 41, NT (72h) = 18, HECTD1 SP (72h) = 57, HECTD1 #06 (72h) = 39, and HECTD1 #08 (72h) = 45, filmed over 3 independent experiments. Cells were imaged using an Olympus IX81 microscope with a 40X oil immersion objective lens and Hammatsu ORCA-ET Camera at 37ºC. Micro-Manager (Edelstein *et al.* 2014) was used to acquire and analyse the images.

4.2.7. The E3 ligase activity of HECTD1 is needed to rescue the NEBD to anaphase onset delay

To determine whether the mitotic delay phenotype associated with HECTD1 results from loss of its E3 ligases activity, asynchronous HEK293T KO1 cells transfected with either *HA-FL-mHectd1*^{WT} or *HA-FL-mHectd1*^{C2579G} were filmed by time-lapse microscopy (Figure 4.14). Interestingly, for most HECT ligases involved in cell cycle regulation the ligase activity is critical to their function (Chapter 1, Section 1.9.2). Although the HECT ligase G2E3, has been reported to contain a catalytically inactive HECT domain, the PHD/RING domains are able to catalyse the conjugation of Lys48-linked ubiquitin chains (Brooks, *et al.* 2006; Brooks, *et al.* 2008). In contrast, the HECT ligase EDD has been shown to regulate p53 independent of its ligase activity (Ling & Lin. 2011; Smits. 2012). For instance, EDD has been reported to regulate miRNA-mediated gene silencing independent of its E3 ligase activity (Su, *et al.* 2011). This demonstrates the ability of these HECT ligases to behave as multifunctional proteins, behaving in an E3 ligase-dependent or –independent manner. Therefore, the aim was to establish whether the role of HECTD1 in the cell cycle was dependent on its E3 ligase activity.

To assess whether the ligase activity of HECTD1 was needed to rescue the mitotic delay seen in Figure 4.14, the time taken for cells to progress from NEBD to anaphase onset was measured. This was compared between the parental HEK293T WT cell line and the two HECTD1 knock out cell lines transfected with either wild type mHectd1 (*HA-FL-mHectd1*^{WT}) or the catalytic mutant of mHectd1 (*HA-FL-mHectd1*^{c2579}) (Figure 4.14). As seen in Figure 14.4A, only HA-FL-mHectd1^{WT} was able to rescue the mitotic delay phenotype in both cell lines. Again, there was a significant delay in NEBD to anaphase onset in HECTD1 KO1 compared to WT, which was also seen with HECTD1 KO2 cells. The WT cells took on average 37.1mins to progress from NEBD to anaphase onset (Figure 4.14B). In comparison, both KO1 and KO2 cells showed an increase in the time taken to progress NEBD to anaphase onset, at 52.6mins and 52.9mins (on average) respectively. HA-FL-mHectd1^{WT} rescued the delay observed in HECTD1 KO1 and KO2 cells, reducing the time taken by around 14mins on average in both cell lines. Taken together this suggests that the E3 ligase activity of HECTD1 is required to rescue the observed delay in the progression from NEBD to anaphase onset, and positions the role of HECTD1 in the cell cycle specifically at mitosis.

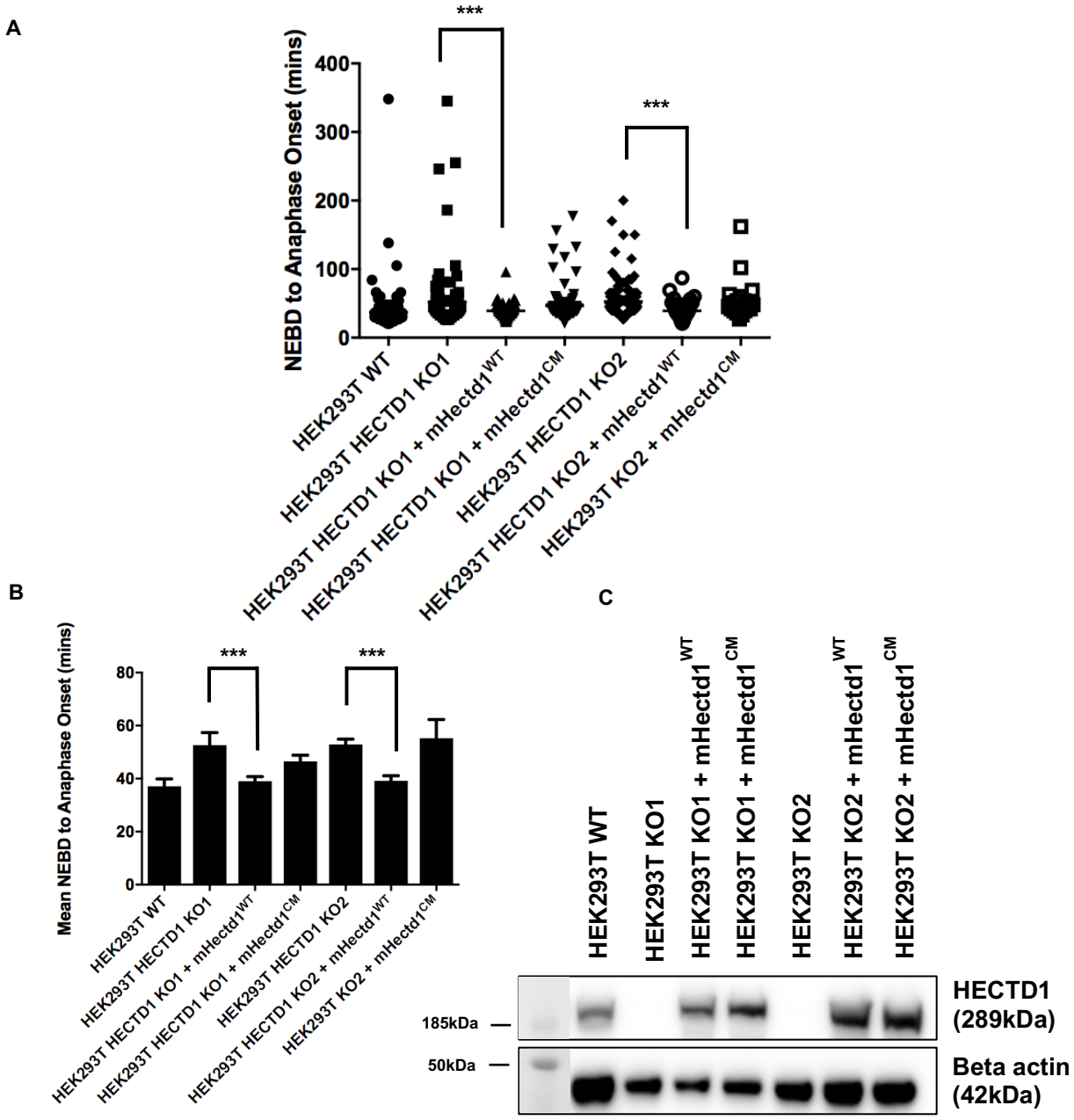

Figure 4.14. Rescue of delay in NEBD to anaphase onset in HEK293T knockout cells. Duration of NEBD to anaphase onset was timed in HEK293T knockout cells transfected with either *HA-FL-mHectd1*^{WT} (mHectd1^{WT} on figure), or *HA-FL-mHectd1*^{C2579G} (mHectd1^{CM} on figure) DNA and PEI. A) Vertical scatter plot showing the time taken for each cell to progress from NEBD to anaphase onset 48hrs post transfection. B) Mean time taken for cells to progress from NEBD to anaphase onset for data shown in A). Error bars represent ±S.E.M., ***p<0.001, **p<0.01 by a one-way ANOVA with a Dunnet's post-test. Number of cell filmed are as follows, WT = 127, KO1 = 97, KO1 + mHectd1^{WT} = 48, KO1 + mHectd1^{CM} = 108, KO2 = 153, KO2 + mHectd1^{WT} = 46, and KO2 + mHectd1^{CM} = 19, filmed over 3 independent experiments. Cells were imaged using an Olympus IX81 microscope with a 40X oil immersion objective lens and Hammatsu ORCA-ET Camera at 37ºC. Micro-Manager (Edelstein *et al.* 2014) was used to acquire and analyse the images. C) Western blot showing transfection of HECTD1 constructs in the knockout cells. Cells were lysed in RIPA buffer and samples were analysed on a 4-12% SDS PAGE. Following western blotting on PVDF, the membrane was blocked in 3%-BSA-PBST and incubated overnight with anti-HECTD1 antibody (ab101992) and anti-pHistone H3 (ser28) (ab10543), followed by detection with a secondary HRP antibody. Anti-beta-actin (A5441) was used as loading control. Molecular weight markers are superimposed on the left-hand side of the immunoblot.

4.3. Discussion:

In this chapter, using both transient HECTD1-depletion and HECTD1 knockout cells, HECTD1 has been shown to be required for the timely progression through mitosis. No change in the G2/M population in HECTD1 depleted cells was initially observed by flow cytometry. However, HA-FL-mHectd1 was expressed in HEK293ET cells to confirmed localisation to the mitotic spindle during metaphase. Interestingly, in HECTD1 transiently depleted cells, which were scored for different stages of mitosis, there was a significant enrichment of metaphase cells. Additionally, both HECTD1 knock down and knockout cells were shown to have a delayed mitotic exit by western blot compared to the control. This was further supported by the use of flow cytometry in the knockout cells, again revealing a prolonged mitosis. To understand how enrichment of metaphase cells and mitotic delay coincided, cells were filmed from NEBD to anaphase onset, to establish if the delay was occurring in early stages of mitosis. Indeed, in both HECTD1-depleted and HECTD1 knockout cells there was an increase in the time taken to progress from NEBD to anaphase onset. This therefore, indicates that HECTD1 is required for mitotic progression, and it is hypothesised that it functions specifically in metaphase to enable the timely progression through mitosis. Importantly, this phenotype was rescued using wild type full-length mHectd1, but not the catalytic inactive mutant. This strongly suggests that the ubiquitin ligase activity of HECTD1 is required for this cell cycle function. Taken together, data presented in this chapter are consistent with the observed reduced growth in HECTD1-depleted cells reported in Chapter 3.

4.3.1. No change in G2/M population upon HECTD1 depletion in HeLa and HEK293ET cells.

HECTD1-depleted HeLa and HEK293ET cells were first screened using flow cytometry to probe for a cell cycle associated phenotype. No change in the G2/M population in asynchronous cells was observed with HECTD1 depletion. This result is in stark contrast with, for example, cell depleted of CDH1 which resulted in a large increase in G2/M cells as well as chromosomal abnormalities (Wei, *et al.* 2004). This suggests, that the cell cycle related phenotype associated with HECTD1 is subtle. In addition, HECTD1 depletion did not yield 8N, tetraploid, cells suggesting that that the SAC checkpoint itself is not compromised in HECTD1 depleted cells. For example, SMURF2 depletion resulted in 8N cell populations, which is in line with its role as part of the SAC where it recruits MAD2 to unattached kinetochores (Osmundson, *et al.* 2008). Therefore, HECTD1 does not appear to be required for proper SAC function, and instead is associated with a prolonged SAC activation phenotype as seen with JMJD5, which will be discussed in Chapter 5.

An important consideration when using cell cycle profiling to study the phenotype associated with HECTD1 depletion is that it may be masked by an inability to distinguish between G2 and M populations. Propidium iodide staining is used to assess the cycle profile (as discussed in Chapter 3), by separating cells based on their DNA content. Indeed, G2 cells and M phase cells both have double the amount (4N) of DNA compared to G1 cells (2N), and therefore these different populations of cells with similar DNA content cannot be distinguished using flow cytometry and PI staining. Therefore, if the phenotype is subtle, as seen in further experiments, this may not be very apparent from looking at cell cycle profile alone. Additional experiments were carried out that could probe for the mitotic population independently.

4.3.2. HA-FL-mHectd1 localises to the mitotic spindle in cells during prometaphase and metaphase

HA-FL-mHectd1 was shown to colocalise with the mitotic spindle during mitosis, however the staining became more diffuse as cells progressed through the later stages of the cell cycle. This mitotic spindle staining confirms the previous observation that HECTD1 colocalised to the mitotic spindle. Additionally, these results indicate that the association to the spindle is metaphase specific, which implies that HECTD1 may only have a specific role during metaphase. Interestingly, cell cycle proteins such as JMJD5 and NuMA, show mitotic spindle staining and both function in spindle formation and orientation (Wong, *et al.* 2006; He, *et al*. 2016). JMJD5, was reported to regulate microtubule stability via α-tubulin acetylation. Depletion of the protein resulted in loss of inter-kinetochore tension, and failure to satisfy the SAC (He, *et al*. 2016). NuMA has been associated with the assembly and orientation of the spindle (Wong, *et al.* 2006; Haren, *et al.* 2009; Gallini, *et al*. 2016). This demonstrates a link between spindle localisation and mitotic spindle regulation. NEDL2 also colocalises to the spindle during mitosis, where it is speculated that the HECT ligase may regulate the SAC or activation of the APC/C, however no direct evidence was provided to show this (Lu, *et al.* 2013). Interestingly, SMURF2 and EDD which are known to regulate the SAC do not appear to show the same spindle localisation (Osmundson, *et al.* 2008; Scialpi, *et al.* 2015). This could potentially indicate that HECTD1 might regulate mitotic spindle formation rather than the SAC directly. Furthermore, two of the proposed substrates of HECTD1, Adenomatous Polyposis Coli (APC) and HSP90, have also been associated with the mitotic spindle (Sarkar, *et al.* 2012; Tran, *et al.* 2013). APC is a conventional microtubule associated protein, where it functions to stabilise microtubules, and together with EB1, has been implicated in spindle regulation (Berrueta, *et al.* 1998; Mimori-Kiyosue & Tsukita. 2003). Whilst the chaperone HSP90, has been shown to be required for Cyclin B1 localisation to the mitotic spindle (Basto, *et al.* 2007).

The catalytically-dead HA-FL-mHectd1^{C2579G} also localised to the mitotic spindle, suggesting that the ligase activity is not involved in the spindle localisation. HECTD1 has a number of predicted ankyrin repeats, and similar domains have been shown to be important for protein binding and substrate recognition (Mosavi, *et al*. 2004). It is therefore likely that HECTD1 ankyrin repeats direct the relocalisation of HECTD1 to the spindle during mitosis. An example of an ankyrin repeat domain protein is protein phosphatase 6 (PP6), an essential Ser/Thr phosphatase whose regulatory subunits are composed of ankyrin repeats (Stefansson, *et al.* 2008). PP6 has been implicated in the regulation of mitotic spindle formation and the ankyrin repeats were shown to be involved in its function (Zeng, *et al.* 2010). However, further work would be needed to understand the region of the HECTD1 responsible for localisation.

4.3.3. Enrichment of metaphase cells upon HECTD1 depletion and knockout

Having demonstrated that full-length HECTD1 localises to the mitotic spindle during metaphase, and that its depletion in cells results in enrichment of a G2/M population, HECTD1-depleted cells were next scored to see whether cells were enriched in a mitotic stage. To this end, HECTD1 transiently depleted HeLa and HEK293ET cells were scored in each mitotic stage, based on their morphology, using immunofluorescence. There was a significant increase of HeLa and HEK293ET cells in metaphase upon HECTD1 depletion using HECTD1 siRNA compared to the non-targeting control, indicating an enrichment of metaphase cells. Interestingly, at the metaphase to anaphase transition the mitotic checkpoint, known as the SAC functions to regulate mitotic progression (Murray. 1994). The SAC prevents the separation of sister chromatids until all of the chromosomes are attached to the mitotic spindle; only upon the checkpoint satisfaction can cell progress through to anaphase (Hagting, *et al.* 2002; Nilsson, *et al.* 2008). It is therefore possible that HECTD1 regulates the formation of the mitotic spindle, rather than regulating the SAC itself. Depletion of proteins that are involved in maintenance of the SAC result in a phenotype of increased progression through mitosis because of the checkpoint being compromised and therefore it cannot be “switched on” and prevent anaphase onset. This translates into no increase in the proportion of metaphase cells, because cells can progress to anaphase unmonitored. This is in contrast to the observed increase of G2/M cells, specifically metaphase cells, in HECTD1 knockout or transiently depleted cells. In addition, this may explain why there were no nuclear defect cells observed, because cells are not progressing through the checkpoint unmonitored they are accumulating at the checkpoint. This again complements the observation that no 8N populations are observed when using PI staining and flow cytometry. Through extensive microscopy, scoring, and analysis there was no change in the number of cells with mitotic defects, namely multipolar spindle and misaligned metaphase plate.

This observation may imply that HECTD1 does not regulate the SAC directly, or it may be due to a limitation of the assay, which is discussed in Section 4.4. Future Work.

4.3.4. Mitotic delay observed upon HECTD1 depletion or knockout

There are two main possible implications for the observed accumulation of mitotic cells upon HECTD1 depletion or knockout: shortening of premitotic processes (G1 phase, S phase or G2 phase) or prolongation of mitosis (He, *et al*. 2015). Interestingly, a recent study reported that the *C. elegans* ortholog of HECTD1, Hecd-1, cooperates with Ufd2 and Atx3, in response to DNA damage to activate apoptosis (Ackermann, *et al.* 2016), potentially implicating HECTD1 in the regulation of S phase. HECTD1 may regulate the DNA damage checkpoint, which may have knock-on effects in mitosis (Lawrence, *et al.* 2015). The western blot on HECTD1-depleted synchronised cells, showed that cells enter mitosis at the same time and the delay occurs in mitotic cells. Therefore, this suggests that the cells are not delayed in a premitotic process. When knockout cells were synchronised using the CKD1 inhibitor RO-3306, synchronising them at the G2/M transition, there was a delay in the decrease of the G2/M peak, further indicating that the delay was specific to mitosis and not premitotic. However, to confirm that the mitotic delay is not a results of HECTD1 regulation of DNA damage, further experiments would be required that induce DNA damage in cells and monitor their cell cycle progression.

To further demonstrate the second scenario, of prolongation of mitosis, the time taken from NEBD to anaphase onset was measured using live cell imaging. In both HECTD1-depleted cells and HECTD1 knockout cells, there was a delay in the time taken for the cells to progress from NEBD to anaphase onset. This period in mitosis was filmed based on the previous observation that HECTD1 depletion or knockout resulted in an enrichment of metaphase cells, and the implication that this may encompass the spindle assembly checkpoint. Therefore, any observed delay in NEBD to anaphase onset would further suggest that the phenotype is a result of the delayed SAC satisfaction, and not regulation of the checkpoint directly. As mentioned previously, this is in line with the observed phenotypes of mitotic spindle regulators, namely JMJD5 and BRISC, where depletion of either of these proteins results in an increased time taken for cells to progress from NEBD to anaphase onset (Yan, *et al.* 2015; He, *et al.* 2016). In contrast, cells depleted of the E3 ligase involved in SAC regulation, TRAIP, showed a decreased length of time to progress through NEBD to anaphase onset. Despite a deficient checkpoint, cells were able to progress through mitosis unchallenged resulting in a decrease in the length of time taken (Chapard, *et al.* 2014). This further suggests that HECTD1 is involved in mitotic spindle regulation, resulting in delayed spindle assembly checkpoint satisfaction.

Interestingly, no phenotype was associated with HECTD1 depletion in *Homo Sapiens*, in the Cellular Phenotype database (https://www.ebi.ac.uk/fg/sym, accessed 05/12/17), which provides phenotypic data derived from high throughput screening. Phenotypes screened included the mitocheck study, where by RNAi screens, mitotic proteins have been screened by microscopy to visualise their sub-cellular localisation at different stages of the cell cycle (Neumann, *et al.* 2010). The fact that HECTD1 RNAi did not correlate with a cellular phenotype, specifically a mitotic phenotype in these large high throughput screens, is not surprising based on the subtlety of the phenotype identified. In a large phenotype screen based on microscopy, a delay in mitotic progression that does not result in sustained cell cycle arrest or cell death may not be readily identifiable. In addition, the extent of HECTD1 depletion achieved in these screens cannot be readily assessed. The yeast orthologue of HECTD1, SPAC12B10.01c, was not identified in a systematic screen of new elements regulating at the G2/M control (Navarro & Nurse. 2012), indicating that the role of HECTD1 in cell cycle regulation might not be conserved in *S. pombe.*

4.3.5. HECTD1 catalytic activity is required to rescue the delay in NEBD to anaphase onset.

To implicate the novel activity of HECTD1 in synthesising K29/K48 ubiquitin chains in the delay observed when NEBD to anaphase onset was measured, HECTD1 KO1 cells were transfected with either *HA-FL-mHectd1*^{WT} or *HA-FL-mHectd1*^{C2579G}. Only HA-FL-mHectd1^{WT} was able to rescue the delay in NEBD to anaphase onset, which aligns with the rescue of the cell proliferation assay presented in Chapter 3. Therefore, this suggests that the E3 ligase activity of HECTD1 is also required for its function in mitosis. Additionally, this may implicate, for the first time, K29/K48 ubiquitin chains in mitosis. HERC2 has been shown to conjugate K48 ubiquitin chains in its role in centrosome amplification (Al-Hakim, *et al.* 2012). Furthermore, K63 has also been implicated with no direct evidence, in signalling and prevention of degradation in SAC regulation by SMURF2 (Osmundson, *et al*. 2008). Nevertheless, the composition and topology of the ubiquitin chain types through which these ligases may exert their effect in the cell cycle, specifically mitosis, remain poorly understood. Therefore, and given that the E3 ligase activity of HECTD1 is required to rescue the cell proliferation and mitotic phenotype identified, further work was carried out to try and establish whether the K29/K48 ubiquitin chains represent a novel signal in mitotic regulation (Chapter 5).

4.4. Future work:

To fully understand the localisation of HECTD1 during the cell cycle, experiments using endogenous GFP-tagged constructs of HECTD1 could be used. This would indeed facilitate characterisation by immunofluorescence and could limit the possibilities of artefacts associated with overexpression. Recent advances in genome editing have enabled the use of CRISPR/Cas9 genome editing, to generate a GFP knock-in cell line to produce GFP-tagged HECTD1 under the endogenous promoter thereby preventing any off-target effects usually associated with over-expression (Lackner, *et al.* 2015; Ratz, *et al.* 2015). Using fixed cells or live cell imaging, GFP-tagged HECTD1 localisation can be monitored during the cell cycle. Work conducted by Ratz, *et al.* 2015, generated CRISPR/Cas9 knock-in proteins and compared their expression to plasmid transfected cells, it was revealed that the knock-ins resulted in less variability in expression and localisation, and therefore less artefacts. Given that the E3 ligase activity has been shown to not be required for the localisation of HECTD1 to the spindle, the localisation of deletion constructs of HECTD1 protein could also be studied by immunofluorescence. This would help identify the region of the protein required for localisation to the mitotic spindle.

For a more high-throughput quantifiable method of showing mitotic enrichment, cell cycle staging of individual cells could be achieved by high-content microscopy and DAPI staining (Roukos, *et al*. 2015). This used in combination with fluorescent ubiquitin based cell cycle indicator (FUCCI) probes would provide a faster way of scoring cells that were enriched in certain phases of the cell cycle. The FUCCI method relies on proteasomal degradation of two fluorescently tagged cell cycle regulatory proteins: CDT1 and geminin (Sakaue-Sawano, *et al.* 2008). These proteins are fused to either a GFP or a RFP tag. Temporally regulated E3 ligases, APC/C^{CDH1} and SCF^{SKP2} are involved in degrading these proteins, which results in the inverse biphasic cycling of CDT1 and geminin. In G1, GFP-tagged geminin is degraded by ACP/C mediated ubiquitination leaving RFP-tagged CDT1 at the nuclei (McGarry & Kirschner. 1998). In S, G2, and M phases RFP-tagged CDT1 is degraded by SCF mediated ubiquitination resulting in GFP-geminin labelled cells (Li, *et al.* 2003). However, during the G1/S transition, when CDT1 levels are decreasing and geminin levels are increasing, both proteins are present, resulting in yellow cells, where the GFP and RFP signals are overlaid. These colour changes result in live tracking of cells in the cell cycle. However, a significant drawback to this technique and specifically to this project is that M phase is not easily defined in this method. Cells in mitosis are visualised as green as well as cells in S/G2 and G2 cells (Sakaue-Sawano, *et al.* 2008). One way to overcome the difficulty in identifying M phase cells it that because the GFP signal is visualised in the nucleus, upon NEBD the whole cell is visualised as green in accordance with a non-compartmentalised GFP signal, as demonstrated in the characterisation of the cell cycle in

HT1080 FUCCI cells (Marcus, *et al.* 2015). Therefore, the GFP signal could be measured using live cell imaging and quantified using software such as ImageJ, or high content microscopy to monitor enrichment of mitotic cells and length of mitosis.

Finally, to characterise abnormalities and defects in mitotic spindle formation, spindle dynamics in HECTD1 depleted cells could be measured and quantified by live cell imaging. Cell lines that stably express GFP-tagged α-tubulin could be imaged throughout the course of mitosis to visualise in unfixed cells the formation of the mitotic spindle (Rusan, *et al*. 2001). Furthermore, as outlined in the protocol by Decarreau, *et al*. (2014), the orientation of the mitotic spindle can be measured using MATLAB® in fixed cells by confocal microscopy. As part of the characterisation of the phenotype associated with NuMA phosphorylation by Aurora A, the orientation of the mitotic spindle was measured (Gallini, *et al*. 2016). This revealed that NuMA phosphorylation by Aurora A regulates spindle orientation, and therefore such studies could easily be applied to HECTD1 to determine whether it also has a role in mitotic spindle orientation. Additionally, recent advances in microscopy now mean that there are multiple types of super high-resolution microscopy available (Wegel, *et al*. 2016). For example, structured illumination microscopy (SIM), stimulated emission depletion (STED), and single molecule localisation microscopy (SMLM; also known as STORM microscopy). These different types of super high-resolution all have their advantages and drawbacks when imaging different cellular components, therefore it is important to consider, which type is the most appropriate for each experiment (Wegel, *et al*. 2016). Thus, to assess spindle defects using super high-resolution microscopy, either SIM or SMLM microscopy, would be the most appropriate, in comparison to STED, which gave a poor signal and lowest image contrast when imaging microtubules (Wegel, *et al*. 2016).

Chapter 5: Functional characterisation of the mitotic phenotype associated with HECTD1

5.1. Introduction:

Chapter 4 demonstrated that HECTD1 depletion resulted in a mitotic phenotype, specifically the enrichment of cells in metaphase, which was due to a delay in mitotic exit. Mitotic progression is monitored by the SAC. The SAC functions as a mitotic checkpoint to inhibit cells progressing from metaphase to anaphase until each kinetochore is attached to the mitotic spindle, safeguarding proper chromosome segregation (Murray. 1994; Stern & Murray. 2001). The accurate formation and orientation of mitotic spindle during prometaphase, is essential to enable cells to progress through the SAC (Stern & Murray. 2001; Uchida, *et al.* 2009; Tauchman, *et al*. 2015). Therefore, the mitotic phenotype associated with HECTD1 may be as a result of prolonged activation of the SAC. This chapter will investigate this hypothesis by looking at the effect of HECTD1 depletion on the SAC and spindle formation, as well as explore using $TRABID_{1-200}$ to identify mitotic proteins modified by K29-K48-linked ubiquitin chains, since our laboratory has shown that HECTD1 synthesises this chain type, at least *in vitro*.

5.1.1. Mitotic spindle formation

The mitotic spindle, composed of microtubules (MTs), is the macromolecular machinery responsible for the segregation of chromosomes into two daughter cells (Walczak & Heald. 2008). The mitotic spindle is thought to comprise three categories of microtubule, these are: kinetochore microtubules (K-MTs), non-kinetochore microtubules (nK-MTs), and astral microtubules (A-MTs) (Dumont & Mitchison. 2009). K-MTs are responsible for the attachment of the chromosomes to the poles where they have their plus-ends embedded in kinetochores and their minus-ends at or near poles (McDonald, *et al.* 1992; Dumont & Mitchison. 2009; Prosser & Pelletier. 2017). K fibres form by the attachment and stabilisation of K-MTs into morphologically distinct bundles at the kinetochore (Rieder & Salmon. 1998; Prosser & Pelletier. 2017). Correct attachment of K-MTs to the kinetochores is monitored by the SAC, and results in its satisfaction once all of the kinetochores are attached to the spindle (Tauchman, *et al*. 2015). nK-MTs, also known as interpolar microtubules, span the region from one spindle pole to the other, and help to stabilise K-MTs and separate the poles (Mastronarde, *et al.* 1993; Dumont & Mitchison. 2009). Finally, A-MTs radiate from spindle poles, which have their minus-ends attached to centrosomes and their plus-ends extending towards the cell cortex, are responsible for spindle positioning (Grill & Hyman. 2005; McNally. 2013).

Three pathways for spindle formation are used to explain how the mitotic spindle attaches to the chromosomes, these are centrosome-mediated MT nucleation, chromatin-mediated MT nucleation, and microtubule-mediated MT nucleation (Prosser & Pelletier. 2017).

Importantly, each pathway relies on γTuRC to initiate nucleation and MT motor proteins to aid the organisation of spindle formation (Gaglio, *et al*. 1996; Walczak, *et al*. 1998; Lüders, *et al*. 2005). The "search and capture" model stems from the principle of microtubules dynamic instability, where microtubules grow and shrink from centrosomes to "search" for chromosomes and upon "capture" this dynamic instability is suppressed, to facilitate attachment (Mitchison & Kirschner. 1984; Heald & Khodjakov. 2015). However, a limitation demonstrated by mathematic modelling, is that without any bias toward chromosomes, search and capture would not happen on the same time scale as prometaphase, and would take considerably more time (Wollman, *et al.* 2005). Chromatin facilitates spindle formation by the generation of a RanGTP gradient, which functions to promote spindle assembly directly around chromosomes by the local discharge of cargoes important in microtubule dynamics and organisation (Kalab, *et al.* 2002). RanGTP is also required for MT nucleation directly from kinetochores, where MTs grow from kinetochores forming K-fibres, which are then incorporated into the forming spindle (Maiato, *et al.* 2004; Meunier & Vernos. 2011). In addition, MTs nucleating from chromosomes can form independently of RanGTP by the formation of the chromosome passenger complex (CPC) (Carmena, *et al.* 2012). The CPC consists of Aurora B, INCENP, borealin, and survivin and functions to create an Aurora B gradient responsible for the inactivation of microtubule destabilising proteins; mitotic centromere-associated kinesin (MCAK) and stathmin 1 (STM1) (Lan, *et al.* 2004; Sampath, *et al*. 2004). Finally, in early prometaphase both centrosome and chromatin-mediated pathways drive MT nucleation facilitating the capture of chromosomes in the formation of a common spindle (Prosser & Pelletier. 2017). In late prometaphase, Augmin is recruited to MTs in an Aurora A and PLK1 dependent manner, and has been implicated in the nucleation of MTs from pre-existing MTs to further support spindle formation by K fibre formation and formation of a common spindle (Goshima, *et al.* 2008; Wainman, *et al*. 2009). This therefore demonstrates the complexity of spindle formation.

5.1.2. TRABID

TRABID is a DUB of the OTU family (Evans, *et al*. 2003), with roles suggested in Wnt signalling (Tran, *et al*. 2008) and innate immunity (Fernando, *et al*. 2014). The ovarian tumour (OTU) family of DUBs contain a papain-like catalytic core of around 180 amino acids (Komander, *et al.* 2009). TRABID was initially reported to cleave K63 linked-ubiquitin chains (Tran, *et al.* 2008), however more recent work identified TRABID as a K29-specific DUB, that could cleave K29 linked diubiquitin with a 40-fold higher efficiency compared to K63 linked diubiquitin (Virdee, *et al.* 2010). Furthermore, it was demonstrated by Licchesi, *et al.* (2012), that TRABID preferentially cleaved K29 and K33 over K63 linked ubiquitin chains, and cleaved no other chain type. This study also revealed that TRABID contains a UBD

based on an ankyrin-repeat fold (AnkUBD), which functions as a novel ubiquitin binding fold, which was essential for full DUB activity. The AnkUBD enables the positioning of the ubiquitin linkage connecting two ubiquitin molecules across the active site of the OTU domain and this restricts the linkage specificity of the TRABID OTU domain towards the cleavage of K29 and K33 linked ubiquitin chains. In addition to the AnkUBD domain, TRABID contains three NPL4 zinc finger (NZF) domains, which provide additional ubiquitin binding sites (Alam, *et al*. 2004; Licchesi, *et al*. 2012; Kristariyanto, *et al.* 2015a; Michel, *et al.* 2015) (Figure 5.1).

To study how NZF domains help to contribute to the specificity of TRABID, free K29 and K33 chains were synthesised using UBE3C and AREL1 E3 ubiquitin ligases, which have known activity for assembling K29/K48 and K29/K33 linked chains respectively, in combination with DUBs such a vOTU (Wang & Pickart. 2005; Kristariyanto, *et al.* 2015a; Kristariyanto, *et al.* 2015b; Michel, *et al.* 2015). Solution structures of both K29 and K33 revealed that these chains adopt open and dynamic conformations (Michel, *et al.* 2015). Furthermore, the crystal structure of K29 linked diubiquitin revealed an open extended conformation, with exposed hydrophobic patches on both ubiquitin moieties that were available for binding (Kristariyanto, *et al.* 2015a). The TRABID N-terminus, which contains three NZF UBDs was reported to specifically bind K29 and K33 linked diUb (Michel, *et al.* 2015; Kristariyanto, *et al.* 2015a). Pull-down experiments with individual NZF domains showed that K29/K33 specificity could be attributed entirely to the N-terminal NZF1 domain (aa 1–33) suggesting that NZF1 is the minimal module required for K29 binding (Michel, *et al.* 2015; Kristariyanto, *et al.* 2015a). The crystal structure of the NZF1 domain of TRABID in complex with K29 revealed that binding occurred through the hydrophobic patch of only one of the ubiquitin moieties and exploited the flexibility of the K29 chains to achieve linkage selective binding (Kristariyanto, *et al.* 2015a). These studies further support the possibility that ubiquitin binding domains such as NZF1 could be used to pulldown K29 and K33 linked polyubiquitin which might be relevant in specific cellular context, including the cell cycle (Kristariyanto, *et al.* 2015a).

The use of ubiquitin-binding domains and ubiquitin-associated domains as tools to capture (poly)ubiquitinated proteins has been widely reported (Scott, *et al*. 2015). For example, the ubiquitin-association domain (P2UBA) from ubiquilin-2, was used to capture total polyubiquitin chains from Huntington's disease models and patient samples (Bennett, *et al.* 2007). Furthermore, Tandem-repeated ubiquitin-binding entities (TUBEs) have been designed based on UBA domains to enhance that capture of polyubiquitinated proteins (Hjerpe, *et al.* 2009). These are designed with multiple UBAs to provide a higher affinity for

polyubiquitin providing an increased capture of polyubiquitin within cell lysates (Hjerpe, *et al.* 2009). Many TUBEs are now commercially available such as the NZF1 TUBE (UBPBio).

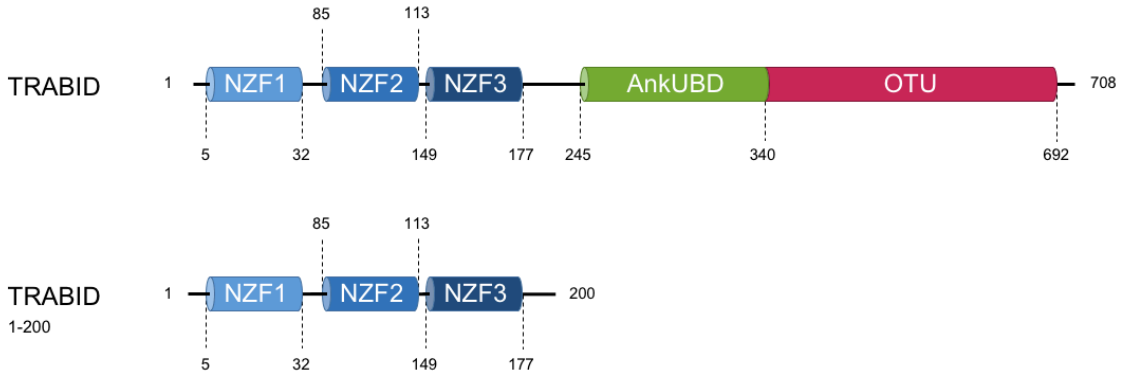

Figure 5.1. Domains of TRABID. Domains of full legnth TRABID and $TRABID_{1-200}$ (1-200 amino acids). Full length TRABID comprises three NZF domains, an AnkUBD and OTU domain. $TRABID_{1-200}$ comprises three NZF domains.

5.1.3. Aims

The mitotic phenotype associated with HECTD1 was characterised using cellular based techniques (Chapter 4). In this chapter molecular markers were used to validate this phenotype at the molecular level and to attempt to elucidate the mechanism by which HECTD1 regulates mitotic progression. In addition, $TRABID_{1-200}$ domain was used in synchronised cell lysates in an attempt to identify cell cycle proteins that have been modified with K29 ubiquitin chains, potentially representing HECTD1 substrates. This was achieved by the following objectives:

1. Validate the role of HECTD1 in mitosis by evaluating expression levels of early mitotic markers in cells transiently depleted of HECTD1 and HECTD1 knockout cells by western blot and immunofluorescence.

2. Establish whether HECTD1 is required for microtubule formation in HEK293T and HEK293ET cells through a microtubule regrowth assay in HECTD1-depleted and knockout cells.

3. Score HECTD1 knockout cells based on the spindle assembly checkpoint marker, BUBR1, to assess whether there is a delay in checkpoint satisfaction.

4. Optimise the use of GST-$TRABID_{1-200}$ to enrich for K29/K33 ubiquitin chains in HEK293T cell lysates.

5. Using GST-$TRABID_{1-200}$ to determine the presence of K29/K33 ubiquitin chains throughout the cell cycle and mitosis in HEK293T cell lysates.

5.2. Results:

5.2.1. HECTD1 depletion results in increase of an early mitotic marker

To confirm the increase in metaphase cells observed in the microscopy study (Chapter 4) using molecular markers, early mitotic markers were selected including Cyclin B1 and pHistone H3 (Ser28). Cyclin B1 levels increase during G2, before peaking in early mitosis, followed by the degradation of the protein at anaphase onset (Pines & Hunt. 1987; Murray & Kirschner. 1989). In contrast, pHistone H3 (ser28) was found to be phosphorylated during prophase, and dephosphorylated during exit from anaphase (Gurley, *et al*. 1978) (Figure 5.15), making them both suitable markers of early mitosis.

First, HECTD1 was transiently depleted in HEK293ET cells that were stained post-fixation with anti-Cyclin B1, anti-pHistone H3 (ser28) antibodies, and Hoechst. The number of Cyclin B1 positive cells (Figure 5.2) and pHistone H3 (ser28) (Figure 5.3) relative to the total number of cells was determined. The number of Cyclin B1 positive cells in HEK293ET showed no increase in cells treated with HECTD1 SMARTpool siRNA compared to the non-targeting control (Figure 5.2B). However, there was a significant increase in the proportion of pHistone H3 (ser28) positively stained cells between the non-targeting control and cells depleted of HECTD1 using HECTD1 SMARTpool siRNA in HEK293ET cells (Figure 5.3B), indicating an enrichment of cells in early mitosis. Here, the percentage of positive cells increased from 2.5% (±0.2%) in the non-targeting to 3.3% (±0.3%) in the HECTD1-treated condition. This was also seen in the image panel for HEK293ET cells (Figure 5.3A).

Cyclin B1 and pHistone H3 (ser28) were also scored in HEK293T knockout cells, however there was no increase in either Cyclin B1 or pHistone H3 (ser28) (Figure 5.4). The lack of an increase in pHistone H3 in the knockout cells compared to the transiently depleted cells may be because the knockout cells may have become adapted to the lack of HECTD1 protein, whereas the HECTD1-depleted cells do not have this adaptation. Another consideration is that the increase in pHistone H3 seen with HECTD1-depletion was carried out using only HECTD1 SMARTpool siRNA, therefore this result could be as a result of off-target effects. It is important in the future to repeat these experiments using individual siRNA.

Finally, the increase in pHistone H3 (ser28) seen by immunofluorescence in the transiently depleted cells was also determined by western blot (Figure 5.5). Figure 5.5A showed an increase in pHistone H3 (ser28) seen when HEK293ET cells were treated HECTD1 SMARTpool siRNA. Quantification, over three independent experiments, showed a 52% increase in signal compared to the control (Figure 5.5B). This indicates that the levels of pHistone H3 (ser28) significantly increased when HECTD1 is depleted. This was repeated

in the HEK293T knockout cells and a representative western blot shows that in both the KO1 and KO2 cell lines there was an increase in pHistone H3 (ser28) staining (Figure 5.5C). Taken together, this data suggest that there is an enrichment of cells in early mitosis following HECTD1 knockout. The use of molecular markers, rather than morphology, appears to confirm the phenotype observed in Chapter 4.

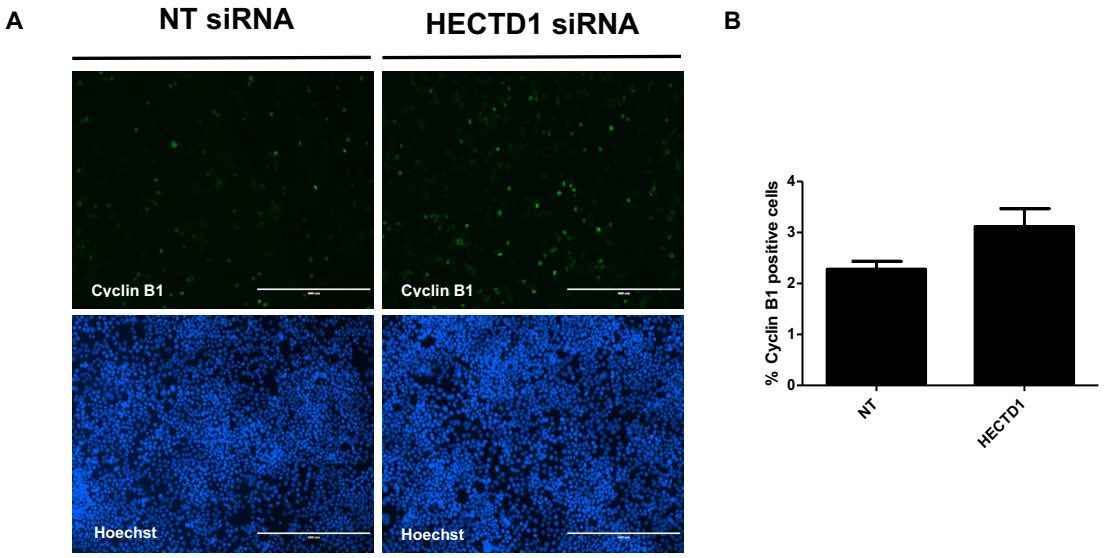

Figure 5.2. No change in Cyclin B1 positive cells in HEK293ET cells depleted with HECTD1. HEK293ET cells with HECTD1 knocked down using 20pmol HECTD1 SMARTpool (smart pool) siRNA and Lipofectamine-2000, then fixed with 4% PFA after 48hrs. 4% PFA, Cells were permeabilised with Triton X-100, and stained for Cyclin B1 and imaged using the EVOS FL Cell Imaging System. A) HEK293ET cells immunofluorescence images showing a representative field of view per condition. Cyclin B1 (green) and Hoechst (Blue). Scale bar represents 400µm. B) Quantification of Cyclin B1 positive cells in HEK293ET (n=3). For quantification 15 fields of view were imaged. Data plotted as mean with error bars that represent ±S.E.M., independent experiments, n, defined by number of separate transfections.

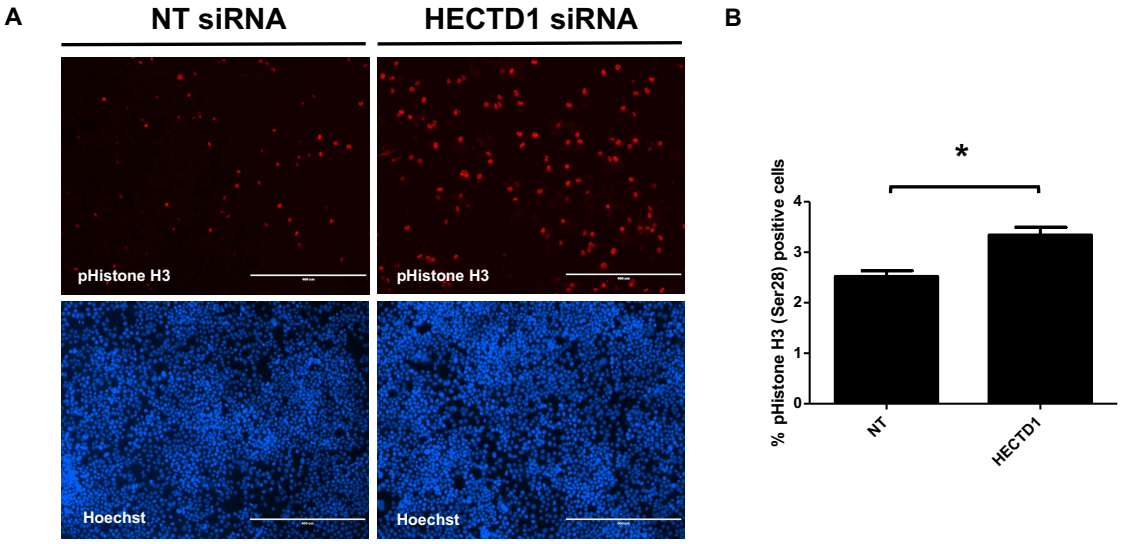

Figure 5.3. Increase in pHistone H3 (ser28) positive cells in HEK293ET cells depleted with HECTD1. HEK293ET cells with HECTD1 knocked down using 20pmol HECTD1 SMARTpool (smart pool) siRNA and Lipofectamine-2000, then fixed with 4% PFA after 48hrs. Cells were permeabilised with Triton X-100, and stained for pHistone H3 (ser28) and imaged using the EVOS FL Cell Imaging System. A) HEK293ET cells immunofluorescence images showing a representative field of view per condition. pHistone H3 (red) and Hoechst (Blue). Scale bar represents 400µm. B) Quantification of pHistone H3 (Ser28) positive cells in HEK293ET (n=3). For quantification 15 fields of view were imaged. Data plotted as mean with error bars that represent ±S.E.M., *p<0.05 by paired student's t-test. Independent experiments, n, defined by number of separate transfections.

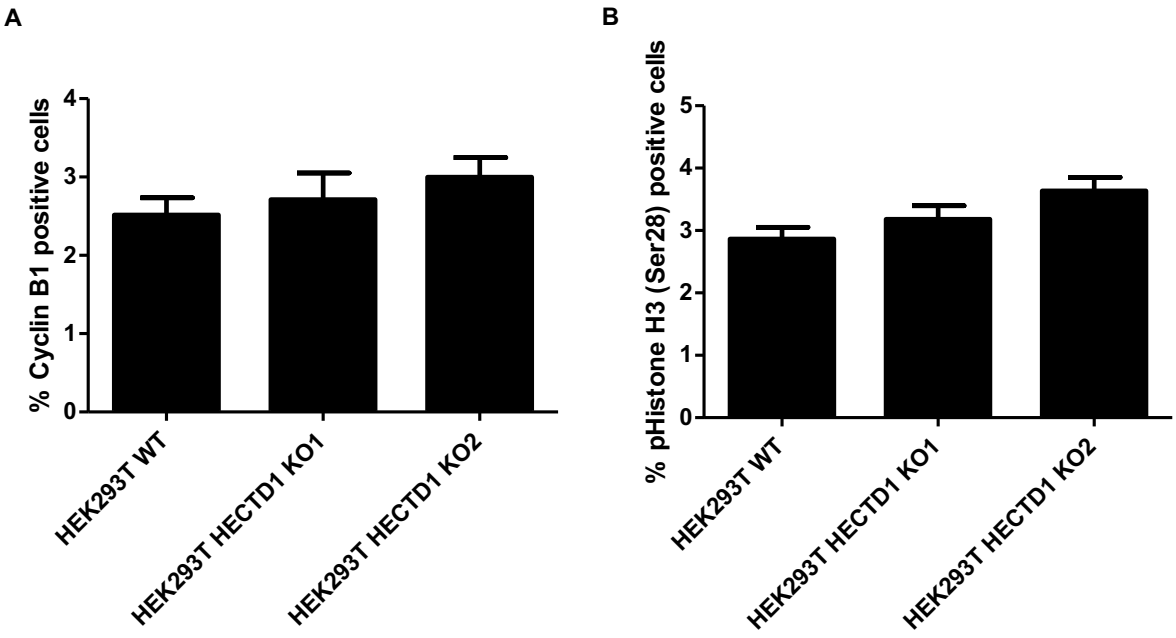

Figure 5.4. No change in the number of Cyclin B1 and pHistone H3 (ser28) positive cells in HECTD1 knockout cell lines. Asynchronous HECTD1 CRISPR/Cas9 knockout cells were fixed with 4% PFA, permeabilised with Triton X-100, and stained for Cyclin B1 and pHistone H3 and imaged using the EVOS FL Cell Imaging System. A) Quantification of pHistone H3 (Ser28) positive cells in HEK293T (n=3). B) Quantification of pHistone H3 (Ser28) positive cells in HEK293T (n=3). For quantification 15 fields of view were imaged, over three independent experiments, defined as separate seeding and staining of cells. Data plotted as mean with error bars that represent ±S.E.M.

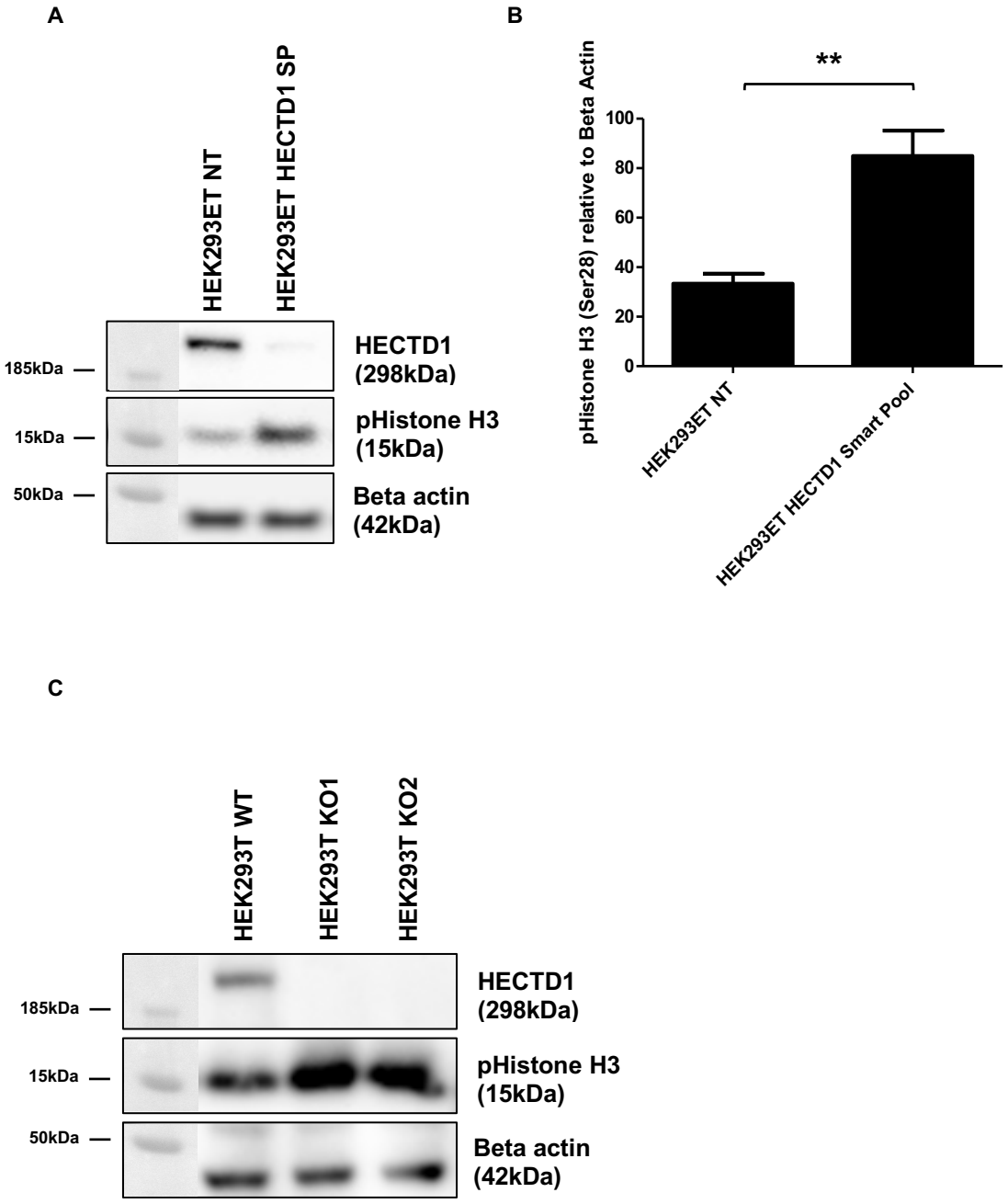

Figure 5.5. pHistone H3 (ser28) protein levels are increased in HECTD1-depleted cells. HEK293ET cells with HECTD1 knocked down using 20pmol HECTD1 SMARTpool (smart pool on figure) siRNA and Lipofectamine 2000, then analysed asynchronously after 72hrs. Knockout cells were harvested asynchronously. Cells were lysed in RIPA buffer and proteins levels were analysed on a 4-12% SDS PAGE. Following western blotting on PVDF, the membrane was blocked in 3%-BSA-PBST and incubated overnight with anti-HECTD1 (ab101992) and anti-pHistone H3 (ser28) followed by detection with an appropriate secondary HRP antibody. Anti-beta-actin (A5441) was used as loading control. A) Western blot of HEK293ET cells with HECTD1 transiently depleted compared to non-targeting control. B) Quantification of pHistone H3 intensity normalised to beta actin, n=3, data plotted as mean with error bars that represent ±S.E.M., **p<0.01 by paired student's t-test. C) Representative western blot of HEK293T knockout cells compared to wild type control (n=2). Molecular weight markers are superimposed on the left-hand side of the immunoblot.

5.2.2. BUBR1 staining in HECTD1 knockout cells

A hypothesis based on Chapter 4 was that HECTD1 may regulate microtubules or mitotic spindle formation, and therefore the resultant phenotype might be caused by prolonged SAC activation. To try to elucidate whether the observed delayed mitotic phenotype associated with HECTD1 depletion is as a result of prolonged SAC activation, cells were scored based on the presence of the SAC component, BUBR1 (Sudakin, *et al.* 2001). BUBR1 is present at unattached kinetochores, and its localisation is required for recruitment of other checkpoint proteins (Chen. 2002). To this end, cells were synchronised using the CDK1 inhibitor, RO-3306, and fixed at 10, 30, 60, 90, and 120mins post-release to monitor SAC activation during mitosis (Figure 5.6). It can be seen at 10mins post-release from RO-3306 that BUBR1 stained cells at unattached kinetochores (Figure 5.6A), as suggested by Chen. (2002). The BUBR1 positive foci were seen to decorate the chromosomes (Hoechst), which are assumed to be unattached. However, due to time constraints it was not possible to characterise whether the SAC is persistent in HECTD1 knockout cells. Further work would be required to establish whether there is an enrichment of SAC markers upon HECTD1 depletion or knockout.

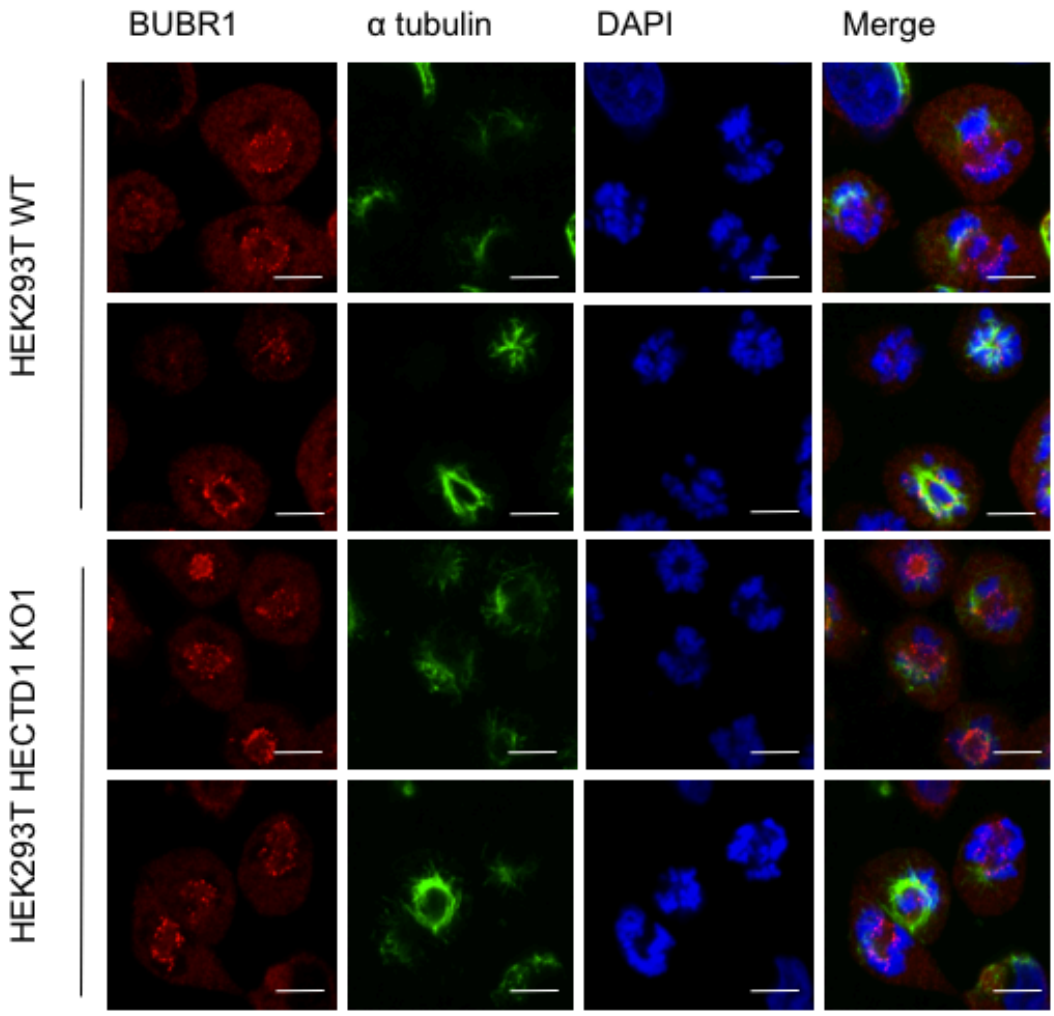

Figure 5.6. BUBR1 staining in HECTD1 knockout cells. Representative images of endogenous BUBR1 foci in HEK293T WT and HECTD1 KO1 cells. HEK293T cells were synchronised using 9μM RO-3306 for 20hrs, released, then fixed using 4% PFA at 10mins post-release. Cells were then stained using antibodies against BUBR1 (red) and α-tubulin (green), and DNA stained using DAPI (blue).

5.2.3. HECTD1 and mitotic spindle formation

Next, the possibility that HECTD1 may be involved in mitotic spindle regulation was explored. This could explain the phenotype seen in Chapter 4, which may be as a result prolonged SAC activation. For example, depletion of the mitotic spindle factor, NuMA, was associated with delayed microtubule regrowth, and reduced inter-kinetochore tension (Haren, *et al.* 2009). HECTD1 depletion and knockout display similar growth defects and enrichment of mitotic cells to NuMA depleted cells, which could suggest that HECTD1 depletion may result in similar microtubule defects.

To test whether HECTD1 was required for microtubule polymerisation, microtubule re-growth was studied in both HECTD1 siRNA depleted HEK293ET and knockout HEK293T cells. Cells were treated with 300ng/ml nocodazole for 1hr, followed by 30mins cold treatment to completely depolymerise the microtubules (Jordan, *et al*. 1992). Cells were then placed back at 37°C into fresh media to allow the microtubules to reform, permitting testing of the requirement of HECTD1 in spindle formation (Haren, *et al.* 2009). In HECTD1-depleted cells and knockout cells, there appeared to be no effect on mitotic spindle formation compared to control cells after 15mins recovery (Figure 5.7), however more work would be required to extensively image mitotic spindle formation. Therefore, it is not possible to determine whether HECTD1 is involved in mitotic spindle regulation. An additional consideration is that the phenotype may be subtle and may not be detected using the current assays.

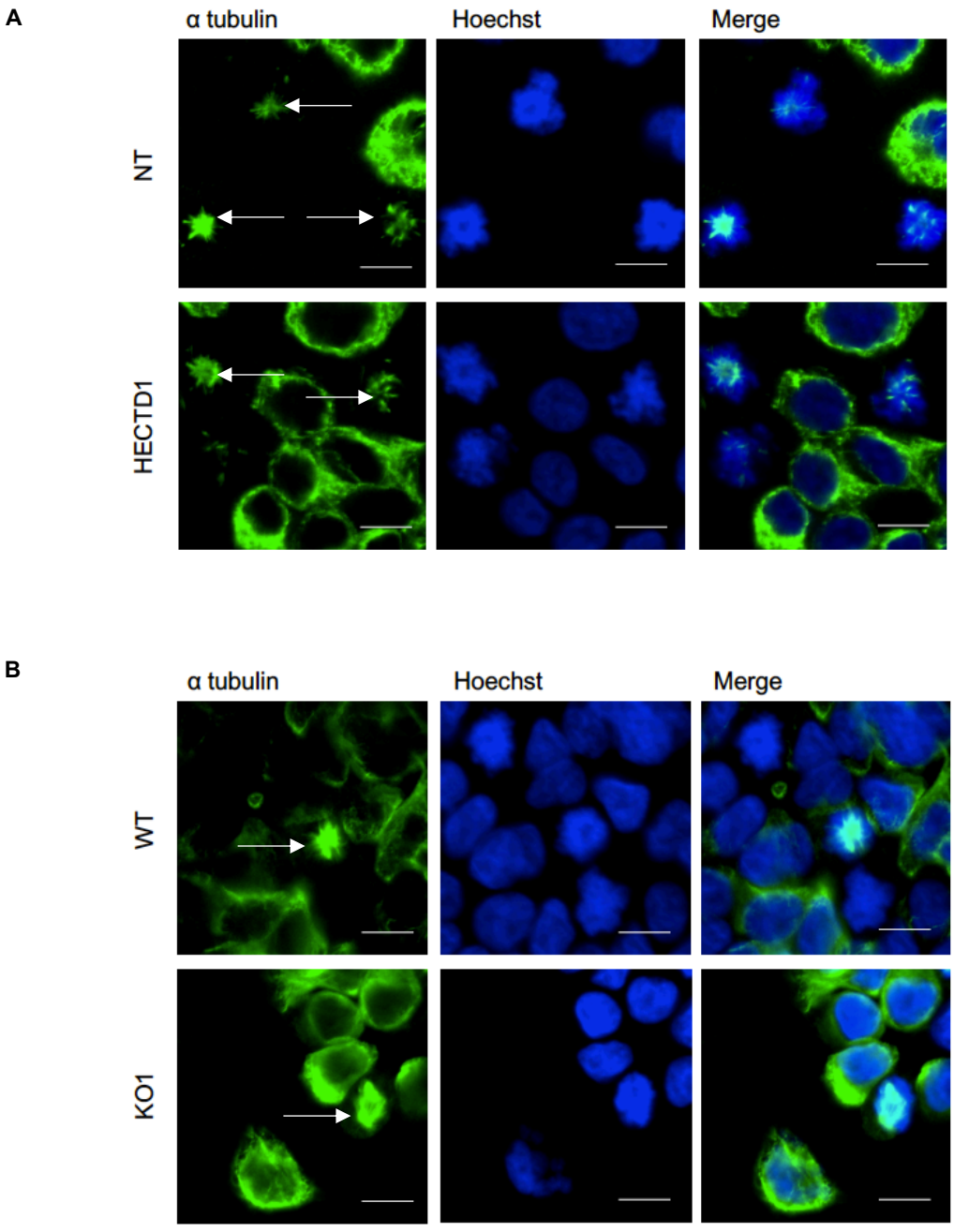

Figure 5.7. Mitotic spindle formation in HECTD1 depleted or knockout cells. A) Representative images of HEK293ET treated with 20pmol NT or HECTD1 SP siRNA, at 15mins post recovery from microtubule depolymerisation. B) Representative images of HEK293T WT and KO1 cells, at 15mins post recovery from microtubule depolymerisation. Cells were treated with 300ng/ml nocodazole for 1hr at 37ºC, followed by cold treatment on ice for 30mins, cells were released into DMEM at 37ºC before then fixing the cells in 4% PFA at 15mins post-release. Cells were stained for either α-tubulin (green) or Hoechst. Images are representative of two independent experiments. Images were taken using the LSM Meta 510 Confocal Microscope. Scale bar represents 10μm. White arrows indicate mitotic spindle.

5.2.4. TRABID$_{1-200}$ can be used to trap K29/K33 ubiquitin chains and HECTD1

As a parallel approach to identify a HECTD1 putative mitotic function, an alternative strategy, which aimed at developing an assay to enrich for HECTD1 substrates was used. To characterise the E3 ligase activity of HECTD1 in the cell cycle phenotype demonstrated in Chapter 4, GST-TRABID$_{1-200}$ was used to demonstrate the ability to trap K29/K33 ubiquitin chains in asynchronous and synchronised cell lysates. TRABID$_{1-200}$ is able to pull down K29 chains only, K33 chains only and mixed K29/K33 chains (Kristariyanto, *et al.* 2015a; Michel MA, *et al.* 2015). Here, both HEK293T WT and HECTD1 KO1 cell lysates were used in the GST-TRABID$_{1-200}$ pull down, to establish whether the amount of ubiquitin pulled down in the HECTD1 KO1 cell lysates was different to the WT cells, therefore indicating that the polyubiquitin captured was as a result of the activity of HECTD1. HECTD1 like UBE3C, is a E3 ubiquitin ligase that can synthesise atypical ubiquitin chains assembled via K29 and K48 (Figure 3.1). Recently, it has been shown that the NZF1 domains within TRABID enrich for branched K29/K48 ubiquitin chains (Crowe, *et al*. 2017). Therefore, in order to detect K29 in the cell cycle, bacterially expressed GST-TRABID$_{1-200}$ was used in pull down experiments using lysates from synchronised cells (Figure 5.1).

First to establish that the pull-down was specific to the binding domain, the TRABID$_{1-200\ TY/LV}$ mutant was used. This mutant comprises the 3 NZF binding domains that each have been mutated at the ubiquitin binding Thr and Tyr residues, which are responsible for interacting with the Ile44 patch on ubiquitin (Alam, *et al*. 2004). Mutation of each of the Thr and Tyr residues to Leu and Val, prevents ubiquitin binding in each of the NZF domains (Alam, *et al*. 2004). As seen in Figure 5.8, GST-TRABID$_{1-200}$ was able to pull down ubiquitin in the HEK293T WT cells, furthermore, HECTD1 was pulled down with ubiquitin. Importantly, neither the GST only nor the GST-TRABID$_{1-200\ TY/LV}$ mutant were able to pull down ubiquitin or HECTD1. Indicating that the association with HECTD1 is via K29/K33 polyubiquitin, and not through binding the TRABID$_{1-200}$ or GST-only. Therefore, this demonstrates that TRABID$_{1-200}$ can be used as a UBD to enrich for substrates modified with K29/ K33 chains in cell lysates. However, it is important to consider that the loading of the GST-TRABID$_{1-200\ TY/LV}$ mutant was less than GST-TRABID$_{1-200}$. This would reduce the HECTD1 and polyubiquitin signal seen in the western blot. A Coomassie gel with each protein loaded at 5µg, based on the protein concentration used for this assay, showed even loading of the protein (Appendix Figure A.4). Therefore, it is likely that this was an experimental issue that would be overcome by repeating the assay. HECTD1 KO1 cells were used as a control to determine the level of K29-containing polyubiquitin ubiquitin chains in cells without HECTD1. Interestingly, in the HEK293T HECTD1 KO1 cells, there were still K29 and K33 containing ubiquitin chains present, however as expected there were no HECTD1 in the pull-down or in the input. This suggests that these chain types are still synthesised without

the presence of HECTD1, this is expected given the activity of UBE3C in conjugating K29/K48 ubiquitin chains (Wang & Pickart. 2005). Additionally, the polyubiquitin smear appeared to be less intense than in the WT cells, suggesting that there may be fewer of these atypical polyubiquitin chains in HECTD1 KO1 cells and that HECTD1 activity contributes to the synthesis of these chains.

In addition, it also determined whether K29 and K33 chains were responsive to proteasomal inhibition using MG132 (Vinitsky, *et al*. 1992; Tsubuki, *et al*. 1993). This revealed that proteasome inhibition did indeed increase the amount of ubiquitin entities pulled down by $TRABID_{1-200}$ suggesting that K29 and or K33 are proteasomal signals (Figure 5.9). The GST only IP in both the DMSO and MG132 treated cells showed no ubiquitin signal, indicating that the increase in signal was specific to the $TRABID_{1-200}$. Based on this data and to increase the chance that the ubiquitin entities pull down by $TRABID_{1-200}$ are due to HECTD1 ligase activity, subsequent experiments were carried out in the absence of MG132. Interestingly, inhibition of the proteasome has been shown to result in increased activity of UBE3C, which would lead to enrichment of K29/K48 (Besche, *et al*. 2014, Wang & Pickart. 2005; Besche, *et al*. 2014).

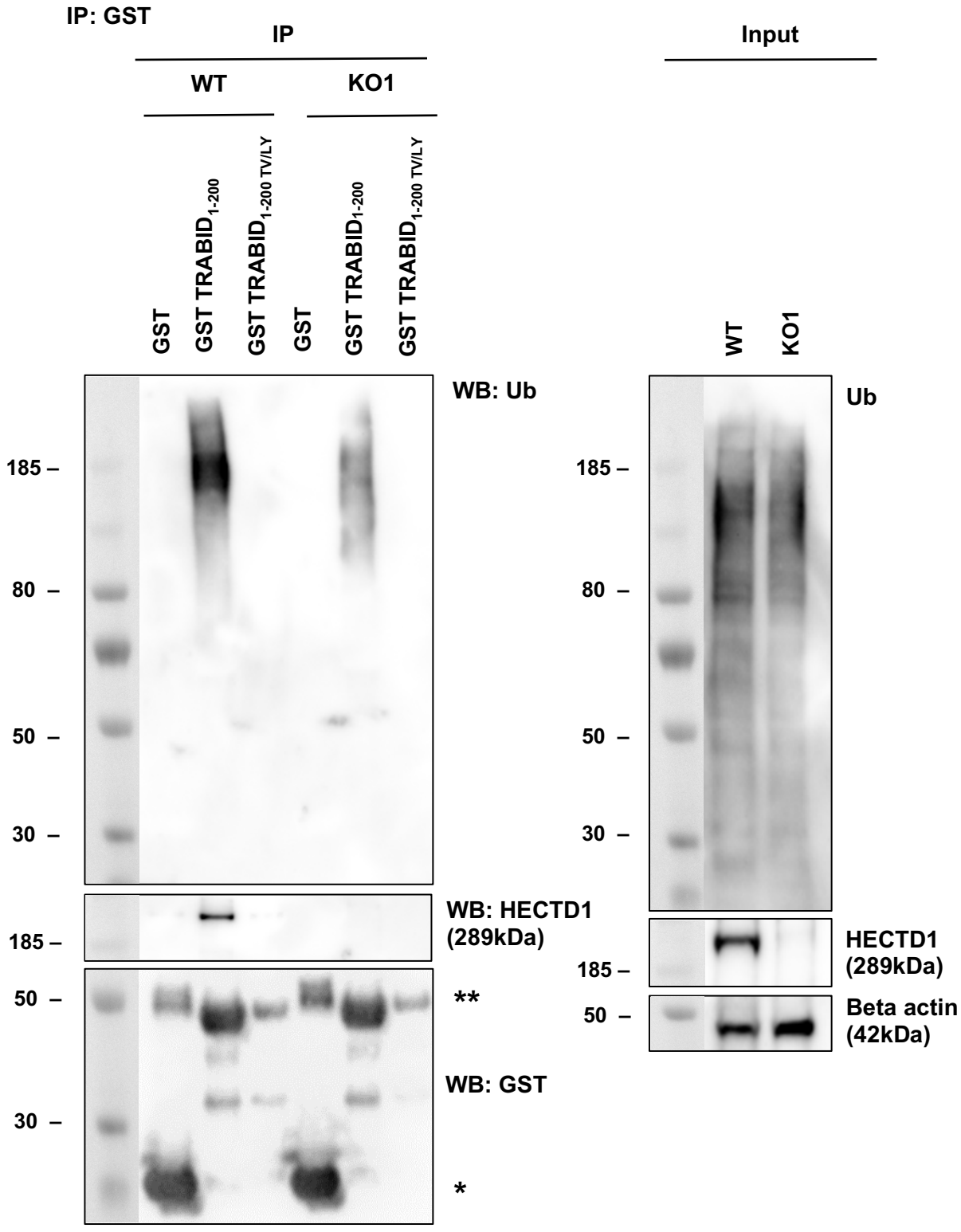
IP: GST
IP
Input
WT
KO1
GST
GST TRABID1-200
GST TRABID1-200 TV/LY
GST
GST TRABID1-200
GST TRABID1-200 TV/LY
WT
KO1
WB: Ub
Ub
185 –
80 –
50 –
30 –
WB: HECTD1 (289kDa)
HECTD1 (289kDa)
185 –
50 –
**
WB: GST
Beta actin (42kDa)
30 –
*

Figure 5.8. TRABID$_{1-200}$ but not the TRABID$_{1-200\ TV/LV}$ mutant is able to trap K29/ K33 ubiquitin chains in HEK293T cell lysates. Pull down assay to determine the ability of TRABID$_{1-200}$ to pull down endogenous ubiquitin from asynchronous HEK293T WT and KO1. For the IP GST fusions of bacterially expressed TRABID$_{1-200}$ and TRABID$_{1-200\ TY/LV}$ were used. Western blots of the immunoprecipitation (IP) and Input. Both HEK293T WT and KO1 cells were lysed in TRABID$_{1-200}$ IP lysis buffer and proteins levels were analysed on a 4-12% SDS PAGE. Following western blotting on PVDF, the membrane was blocked in 3%-BSA-PBST and incubated overnight with anti-Ub antibody (BML-PW0930) and anti-HECTD1 (ab101992) followed by detection with an appropriate secondary HRP antibody. The anti-Ub antibody was selected as per the optimisation seen in Appendix Figure A.5. Both anti-GST (27-4577-01) and anti-beta-actin (A5441) were used as loading controls. * = GST and ** = GST-TRABID$_{1-200}$ and GST-TRABID$_{1-200\ TY/LV}$. Of note is that there is a difference in loading between the TY/LV mutant and WT TRABID$_{1-200}$. A Coomassie gel showing even loading of 5µg of GST, GST-TRABID$_{1-200}$, and GST-TRABID$_{1-200\ TY/LV}$ (Appenix Figure A.4). Here, proteins were normalised to 5µg based on the concentration of protein, which was also used for this experiment. Molecular weight markers are superimposed on the left-hand side of the immunoblot.

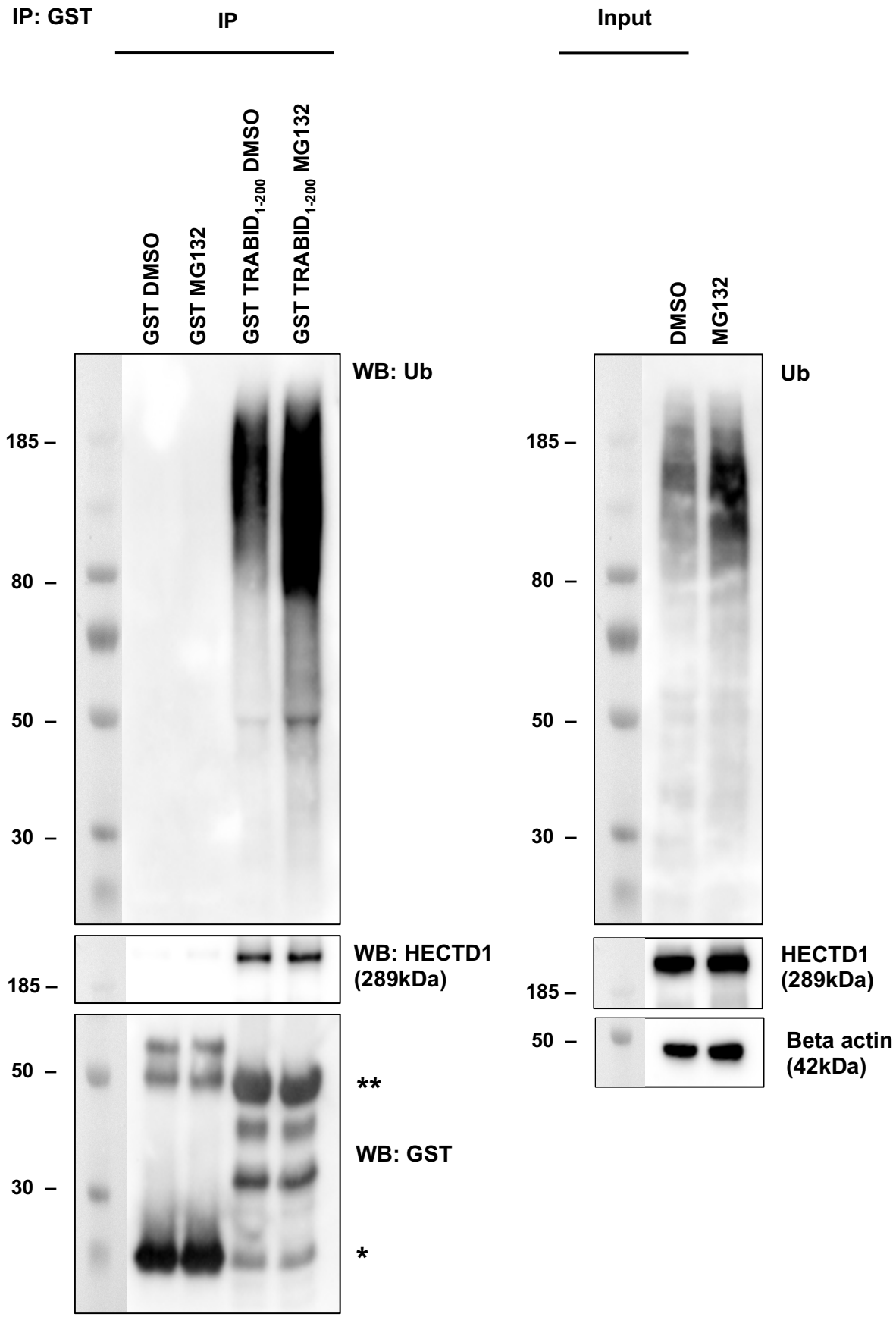
IP: GST
IP
Input
GST DMSO
GST MG132
GST TRABID1-200 DMSO
GST TRABID1-200 MG132
DMSO
MG132
WB: Ub
Ub
185 –
80 –
50 –
30 –
WB: HECTD1
(289kDa)
HECTD1
(289kDa)
Beta actin
(42kDa)
**
*
WB: GST

Figure 5.9. $TRABID_{1-200}$ can trap K29/ K33 ubiquitin chains in HEK293T cells treated with or without MG132. Pull down assay to determine the ability of $TRABID_{1-200}$ to pull down endogenous ubiquitin from asynchronous HEK293T WT. Samples were treated with DMSO or 10μM MG132 for 6hrs before lysis. For the IP GST fusions of bacterially expressed $TRABID_{1-200}$ and $TRABID_{1-200\ TY/LV}$ were used. HEK293T WT cells were lysed in $TRABID_{1-200}$ IP lysis buffer and proteins levels were analysed on a 4-12% SDS PAGE. Following western blotting on PVDF, the membrane was blocked in 3%-BSA-PBST and incubated overnight with anti-Ub antibody (BML-PW0930) and anti-HECTD1 (ab101992) followed by detection with an appropriate secondary HRP antibody. Both anti-GST (27-4577-01) and anti-beta-actin (A5441) were used as loading controls. * = GST and ** = GST-$TRABID_{1-200}$. Molecular weight markers are superimposed on the left-hand side of the immunoblot.

5.2.5. K29/K33 ubiquitin chains and HECTD1 are present throughout the cell cycle

Having optimised a protocol to enrich for K29 and K33 chains in HEK293T cell lysates in the absence of proteasomal inhibition, the next step was to determine whether these ubiquitin chain types might be enriched in specific stages of the cell cycle. Indeed, based on the data presented so far it is expected that the chains that are synthesised by HECTD1, and hypothesised to be K29 and K48 based on *in vitro* studies, might be present and even enriched during M phase of the cell cycle.

To establish the presence of K29 branched ubiquitin chains in the cell cycle, HEK293T WT cells were synchronised using three different cell synchronisers. As identified in the cell cycle synchroniser characterisation in Chapter 3, different synchronisers should be used to enrich for cells in particular phases of the cell cycle. Therefore, to enrich cells in G1, HEK293T WT cells were synchronised using Aphidicolin, and harvested at 0hr (no release). S phase cells were enriched by using a double thymidine block, and a 2hr release. Finally, G2 and M cells were enriched by using RO-3306 and harvested at 0hr and 20mins post-release respectively (Figure 5.10). Using GST-TRABID$_{1-200}$, ubiquitin chains containing most likely K29 and K33-linked ubiquitin were found to be present in all phases of the cell cycle. Interestingly, the levels of these chains appeared to be lower in M phase compared to G1, S, and G2 samples, and this is despite more ubiquitin being present in the input for the M phase. This suggests that there may be fewer K29-modified proteins during mitosis (Figure 5.10A). Despite no increase in the K29/K33 linked ubiquitin chains during mitosis, as hypothesised, this does not rule out the possibility that HECTD1 is active during mitosis. The reduction of K29/K33 linked polyubiquitin could be due to increased activity of the DUB TRABID during mitosis, to ensure the correct regulation of mitotic regulators. Additionally, given that the proteasome is not inhibited, the reduced chains in mitosis could be as a result of increased substrate turnover, therefore less modified species would be pulled down by GST-TRABID$_{1-200}$. HECTD1 was also found to immunoprecipitate along with ubiquitin using GST-TRABID$_{1-200}$ in all phases of the cell cycle, suggesting that it synthesises these chains throughout the whole of the cell cycle. However to confirm this, similar pulldown assays should be carried out in the knockout cells (HEK293T KO1) as a subtractive comparison.

The background staining of HECTD1 in the GST-only S phase sample may be a result of protein loading as seen in the beta actin of the S phase input. This demonstrates that there may some background interaction of HECTD1 and GST when high levels of protein are loaded in the sample. For the other samples where less protein had been loaded the background signal was much weaker. Finally, to ensure that the cell synchronisation was successful, and that cells were indeed in their expected cell cycle phase, flow cytometry with PI staining was carried out (Figure 5.10B). Samples were harvested from the cells used

for the IP, and taken to analyse their cell cycle profile. As expected, it can be seen that cells were successfully synchronised in G1, S, G2, and M phase.

Having fully shown for the first time the presence of K29 and/or K33-linked ubiquitin chains during all stages of the cell cycle, similar experiments were carried out to explore specifically the different phase of mitosis. Cells were synchronised using RO-3306 and harvested at 0h, 20mins, 2hrs, and 20hrs post-release (Figure 5.11). Here, K29 and/or K33 chains were present in G2 (0hr) and M phase (20mins and 2hr), and a time point when cells have exited mitosis (20hrs). This indicates that these chains are present from the G2/M transition, through mitosis, and after mitosis, and suggests that these K29/K33 chains may have a function in mitotic processes. However, the data does not suggest that during mitosis there are any drastic changes in the levels of K29/K33, indicating that their presence is relatively constant throughout mitosis.

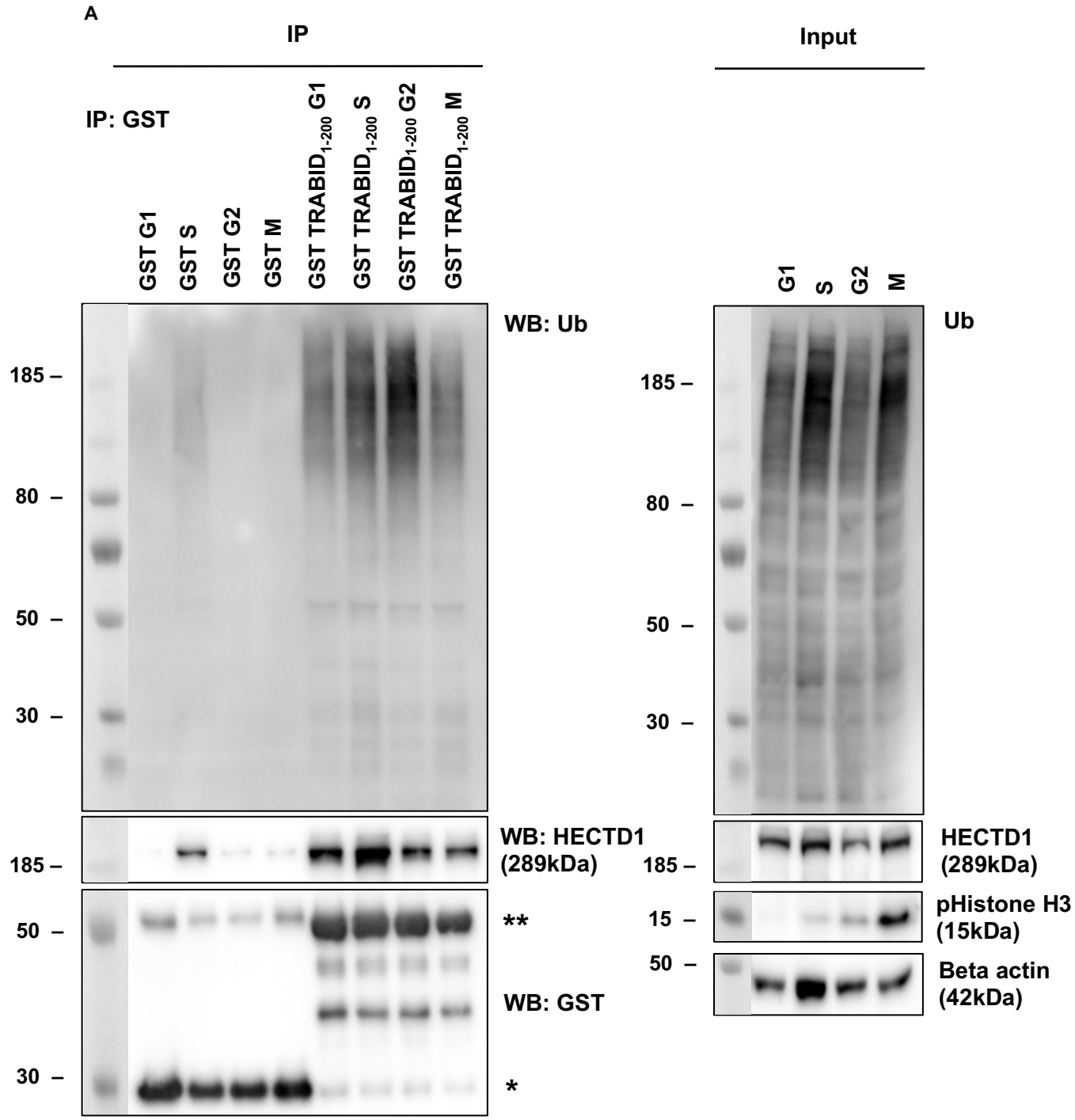
A
IP
Input
IP: GST
GST G1
GST S
GST G2
GST M
GST TRABID1-200 G1
GST TRABID1-200 S
GST TRABID1-200 G2
GST TRABID1-200 M
G1
S
G2
M
185 –
80 –
50 –
30 –
WB: Ub
Ub
WB: HECTD1 (289kDa)
HECTD1 (289kDa)
**
pHistone H3 (15kDa)
15 –
Beta actin (42kDa)
WB: GST
*

B

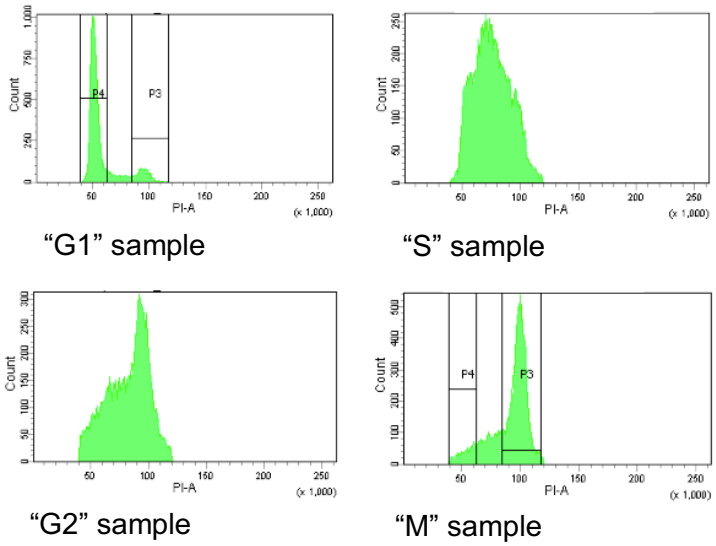

Figure 5.10. TRABID$_{1-200}$ captures K29/ K33 ubiquitin chains in all stages of the cell cycle. Pull down assay to determine the ability of TRABID$_{1-200}$ to pull down endogenous ubiquitin from synchronised HEK293T WT. HEK293T WT cells were synchronised using 4µg/ml Aphidicolin to enrich for G1 phase cells, 2mM Thymidine with a 2hr release (double thymidine block) to obtain S phase cells, and 9µM RO-3306 to obtain G2 and 20mins release from RO-3306 to obtain M phase cells. For the IP the GST fusion of bacterially expressed TRABID$_{1-200}$ was used. A) Western blots of the immunoprecipitation (IP) and Input. HEK293T WT cells were lysed in TRABID$_{1-200}$ IP lysis buffer and proteins levels were analysed on a 4-12% SDS PAGE. Following western blotting on PVDF, the membrane was blocked in 3%-BSA-PBST and incubated overnight with anti-Ub antibody (BML-PW0930), anti-HECTD1 (ab101992), and anti-pHistone H3 (ser28) (ab10543) followed by detection with an appropriate secondary HRP antibody. Both anti-GST (27-4577-01) and anti-beta-actin (A5441) were used as loading controls. B) Cell cycle profile of HEK293T WT cells. Cells were fixed using 70% ethanol, cells were stained using 2µg/ml PI, with 100µg/ml RNase A, for 30mins at room temperature. Stained samples were then analysed immediately by flow cytometry. Histograms for each cell cycle phase. PI-A of 50 is equivalent to 2N (G1 population), and PI-A of 100 is equivalent to 4N (G2/M population). Molecular weight markers are superimposed on the left-hand side of the immunoblot.

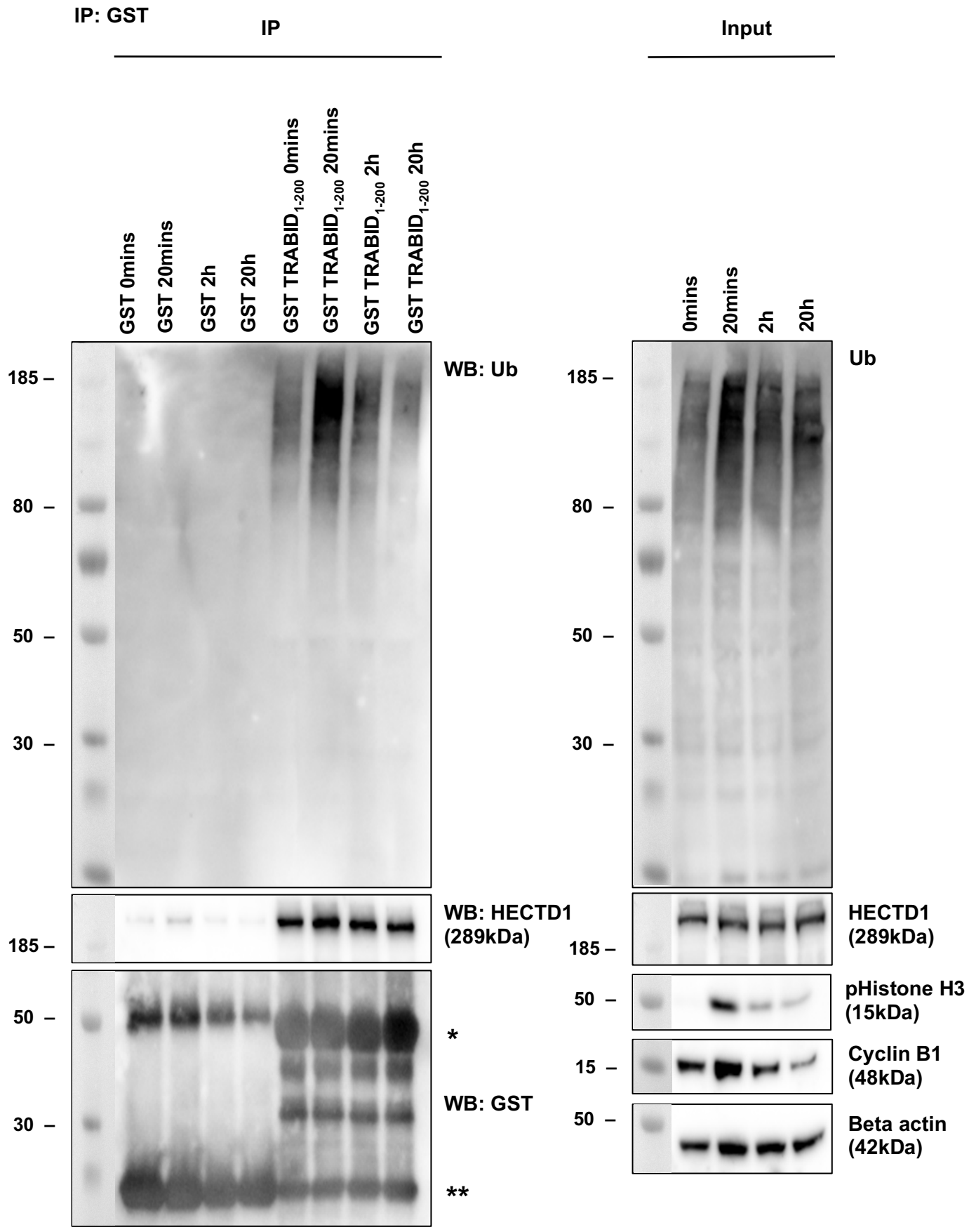
IP: GST
IP
Input
GST 0mins
GST 20mins
GST 2h
GST 20h
GST TRABID1-200 0mins
GST TRABID1-200 20mins
GST TRABID1-200 2h
GST TRABID1-200 20h
0mins
20mins
2h
20h
185 –
80 –
50 –
30 –
WB: Ub
Ub
WB: HECTD1 (289kDa)
HECTD1 (289kDa)
*
**
WB: GST
pHistone H3 (15kDa)
Cyclin B1 (48kDa)
Beta actin (42kDa)
15 –

Figure 5.11. TRABID$_{1-200}$ captures K29/ K33 ubiquitin chains throughout mitosis. Pull down assay to determine the ability of TRABID$_{1-200}$ to pull down endogenous ubiquitin from synchronised HEK293T WT. HEK293T WT cells were synchronised using 9μM RO-3306 for 20hrs. Cells were released and harvested at 0mins, 20mins, 2hrs, and 20hrs post-release. For the IP the GST fusion of bacterially expressed TRABID$_{1-200}$ was used. HEK293T WT and KO1 cells were lysed in TRABID$_{1-200}$ IP lysis buffer and proteins levels were analysed on a 4-12% SDS PAGE. Following western blotting on PVDF, the membrane was blocked in 3%-BSA-PBST and incubated overnight with anti-Ub antibody (BML-PW0930), anti-HECTD1 (ab101992), anti-pHistone H3 (ser28) (ab10543), and anti-cyclin B1 (sc-254) followed by detection with an appropriate secondary HRP antibody. Both anti-GST (27-4577-01) and anti-beta-actin (A5441) were used as loading controls. * = GST and ** = GST-TRABID$_{1-200}$. pHistone H3 (ser28) was used as a mitotic marker to show synchronisation, whilst Cyclin B1 was used as a G2/M marker. As seen in the input, cells were successfully synchronised, with Cyclin B1 appearing in the 0hr, 20mins, and 2hrs samples, and pHistone H3 present in the 20mins only. Molecular weight markers are superimposed on the left-hand side of the immunoblot.

5.3. Discussion:

The putative role of HECTD1 in mitotic regulation has been further demonstrated by the increase in the early mitotic marker pHistone H3 (ser28) in HECTD1 depleted or knockout cells using both cellular and molecular readouts. Due to time constraints it was not possible to establish whether HECTD1 depletion resulted in enrichment of the SAC marker BUBR1 or mitotic spindle defects. As a parallel approach to identify a HECTD1 putative mitotic function, the UBD $TRABID_{1-200}$ was used as a new tool to show that K29/K33 chains are readily detectable by IP and are a present during the cell cycle and mitosis. This was used because it is known that HECTD1 is able to synthesise K29/K48 chains (Figure 3.1). Therefore, K29 linkages synthesised by HECTD1 would be detected by $TRABID_{1-200}$ and may serve as a way to enrich for potential mitotic substrates modified with K29.

5.5.1. Increase in the early mitotic marker pHistone H3 (ser28)

Given previous data suggesting a delay in mitosis, pHistone H3 (ser28) was used as a mitotic marker. It was observed that upon depletion of HECTD1, pHistone H3 (ser28) increased by western blot and to a lesser extent by immunofluorescence. There appears to be no change in Cyclin B1 expression over two independent experiments, however given the broad expression of Cyclin B1 (Pines & Hunt. 1987; Murray & Kirschner. 1989), it is likely the increase of early mitotic cells is masked, unlike with pHistone H3 (Gurley, *et al*. 1978) (Figure 5.12). Cyclin B1 levels increase during G2, before peaking in early mitosis, which is followed by the degradation of the protein (Pines & Hunt. 1987; Murray & Kirschner. 1989). This degradation was found to be as a result of the ubiquitin proteasome pathway, where a D box was found at the N terminus of Cyclin B1 (Glotzer, *et al.* 1991). Cyclin B1 turnover is triggered at anaphase onset by the recognition of its N-terminal D-box degron (Glotzer, *et al.* 1991) by APC/C^{Cdc20} (Visintin, *et al.* 1997; Chang, *et al.* 2003). pHistone H3 (ser28), was found to be phosphorylated during mitosis during chromosomal condensation and dephosphorylated during exit from anaphase (Gurley, *et al*. 1978) (Figure 5.15). Aurora B kinase is responsible for the phosphorylation of Histone H3 at ser10 and ser28 (Goto, *et al*. 1999; Wei, *et al.*1999; Giet & Glover. 2001; Hauf, *et al.* 2003). Similarly, dephosphorylation of Histone H3 at both ser10 and ser28, was found to be as a result of the phosphatase PP1 (Murnion, *et al.* 2001; Goto, *et al.* 2002). In contrast to phosphorylation of ser10, which has been observed during interphase as well as mitosis, phosphorylation of ser28 is specific to mitosis suggesting that it is a more accurate readout for mitosis (Goto, *et al*. 1999).

Taken together the increase in metaphase cells and pHistone H3 indicates an enrichment of cells potentially caused by prolonged spindle assembly checkpoint activation. An

accumulation of early mitotic cells, as implicated by the enrichment of pHistone H3 (ser28) and the enrichment of metaphase cells (Chapter 4), has been associated with spindle regulation phenotypes in other studies. For example, depletion of the histone H3 lysine 36 dimethylation demethylase, JMJD5, is associated with an increase in metaphase cells, in addition to an increase in pHistone H3 (Ser10). JMJD5 was shown to colocalise with the mitotic spindle during mitosis, showing strongest staining at metaphase. When depleted, there was an associated decrease in α-tubulin acetylation, resulting in failure to generate enough inter-kinetochore tension to satisfy the SAC (He, *et al.* 2016). Furthermore, depletion of spindle regulatory proteins such as NuMA, and Tankyrase-1 result in increased mitotic index (Chang, *et al.* 2005; Haren, *et al.* 2009). In addition, NuMA depletion was associated with delayed microtubule regrowth, and reduced inter-kinetochore tension (Haren, *et al.* 2009). HECTD1 exhibited a similar phenotype to these spindle regulator proteins, which further suggest that HECTD1 might be involved in mitotic spindle regulation, which in turn could result in a lack of sufficient inter-kinetochore tension and a prolonged SAC activation.

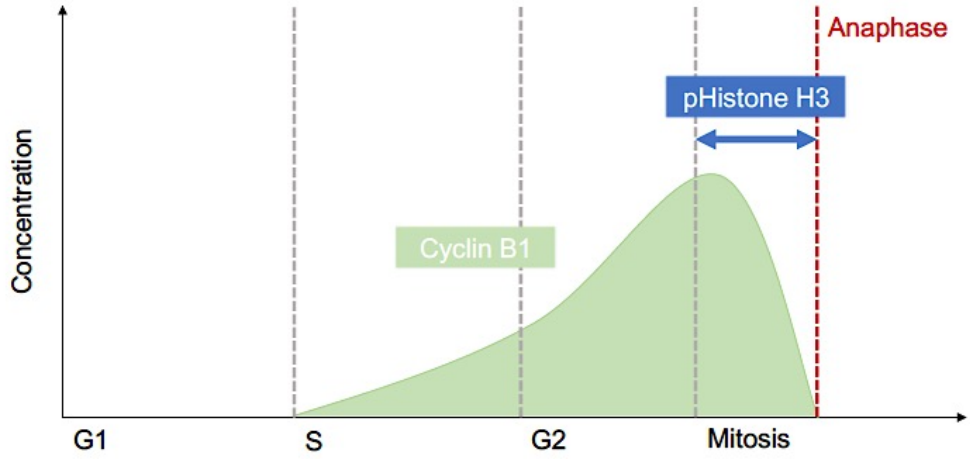

Figure 5.12. Diagram illustrating Cyclin B1 and pHistone H3 expression throughout the cell cycle. Expression of Cyclin B1 and pHistone H3 (ser10 and ser28) over the course of the cell cycle, red dashed line indicates anaphase onset.

5.3.2. BUBR1 staining as a marker for prolonged SAC activation

To address the hypothesis that in HECTD1-depleted or knockout cells the SAC is active for longer, synchronised cells were stained for the SAC marker BUBR1 and examined by immunofluorescence. BUBR1 is a SAC component, which together with CDC20, MAD2, and BUB3 forms the MCC (Sudakin, *et al.* 2001). Therefore, BUBR1 was used as a marker

to assess whether the SAC is active for longer in HECTD1 knockout cells. BUBR1 successfully stained unattached kinetochores, however due to time restraints it was not possible to quantify unattached kinetochores in HECTD1 knockout or depleted cells. To establish whether there is a prolonged SAC activation in HECTD1-depleted cells, the number of BUBR1 positive kinetochores in each cell, instead of BUBR1 positive cells can be scored as seen with JMJD5 depletion (He, *et al*. 2015). This would provide a less crude way of monitoring SAC activation. Furthermore, the use of another SAC marker, such as MAD2 would help to demonstrate persistent SAC activation, as seen in NuMA depleted cells (Haren, *et al.* 2009). Again, the number of MAD2 positive cells and kinetochores could be scored to demonstrate increased SAC activation in HECTD1 depleted cells.

It is hypothesised that there will be an increase in the number of BUBR1 positive cells in HECTD1 knockout cells compared to WT cells post-release from RO-3306. This would therefore suggest a prolonged SAC activation. For example, the mitotic spindle protein, JMJD5 was shown to regulate the mitotic spindle, by microtubule acetylation. The phenotype of increased metaphase cells, early mitotic markers, and prolonged NEBD to anaphase onset upon JMJD5 depletion is similar to that of the phenotype associated with HECTD1 depletion and knockout (He, *et al*. 2016). Interestingly, the authors reported an increase in the spindle assembly checkpoint marker BUBR1 when cells were depleted with JMJD5 indicating failure to satisfy the SAC (He, *et al*. 2016). However, further work with more SAC markers such as MAD2, and BUB3 would be required to establish whether the SAC is active for longer in HECTD1 depleted and knockout cells.

5.3.3. Mitotic spindle formation in HECTD1-depleted cells

To elucidate whether the phenotype observed in Chapter 4 is as a result of improper mitotic spindle regulation, microtubule dynamics in HECTD1 depleted cells were characterised by immunofluorescence. However, due to time constraints it was not possible to establish whether HECTD1 depletion or knockout resulted mitotic spindle formation defects. It is hypothesised, based on the phenotype seen in Chapter 4, that HECTD1 depletion or knockout may result in defects in mitotic spindle formation.

In cells depleted of the tumour suppressor DUB, CYLD (Cylindromatosis), involved in mitotic spindle regulation, nocodazole treatment to depolymerise the microtubules resulted in delayed microtubule regrowth (Gao, *et al.* 2008; Yang, *et al.* 2014). Depletion resulted in dramatically delayed microtubule regrowth, with only a few small microtubule asters detected after 5mins of regrowth, suggesting that CYLD regulates the dynamic property of microtubule assembly and enhances microtubule stability (Gao, *et al.* 2008). This regulation

of microtubules has been proposed to be mediated by the interaction of CYLD with EB1 (End-Binding 1) protein at the plus end of microtubules (Li, *et al.* 2014). Interestingly, CYLD has been reported to regulate spindle orientation by the stabilisation of astral microtubules. Where, it was shown mechanistically to deubiquitinate dishevelled and promote the formation of a dishevelled-NuMA-dynein/dynactin complex at the cell cortex, which is required for the generation of pulling forces on astral microtubules (Yang, *et al.* 2014).

The majority of mitotic cell cycle defects are not catastrophic and result in a subtle phenotype. For example, in NuMA depleted cells that have been cold treated, spindles were reported to have a lower density, lacking K fibre bundles, and were less compact compared to control cells, with no reported change to overall microtubules in the cell (Haren, *et al.* 2009), demonstrating the role that NuMA has in mitotic spindle formation. Similarly, the ubiquitin receptor protein, UBASH3B, was reported to facilitate mitotic recruitment of Aurora B to mitotic microtubules (Krupina, *et al.* 2016). Cold treatment of metaphase cells showed a decrease in the formation of stable kinetochore bundles upon UBASH3B depletion (Krupina, *et al.* 2016). This demonstrates the need for high-resolution microscopy, such as SIM, SMLM or STED microscopy (Alonso. 2013; Wegel, *et al*. 2016), to monitor spindle defects in HECTD1 depleted or knockout cells. As previously discussed, SIM or SMLM microscopy would be the most appropriate type of super resolution microscopy to study microtubule dynamics (Wegel, *et al*. 2016). Using super resolution microscopy would help to determine whether HECTD1-depleted cells exhibit spindles that, for example, lack K fibre bundles or other less obvious phenotypes that would not readily be identifiable from use of a regular confocal microscope.

Finally, in *C. elegans*, the HECTD1 orthologue, HECD-1, was found to be an activator of meiotic double strand break formation protein (MEI1) during meiosis but an inhibitor of the same protein during mitosis (Beard, *et al*. 2016). MEI1 together with MEI2 forms a katanin-like microtubule-severing complex essential for meiotic spindle formation, that has to be inactivated to allow for proper formation of the mitotic spindle (Srayko, *et al*. 2000). Failure to eliminate this severing complex during mitosis results in lethality due to excess microtubule cleavage (Mains, *et al*. 1990). It is hypothesised that HECTD1 does not regulate the protein levels of MEI1. Instead, ubiquitination of the substrate by HECTD1 leads to increased activation, however the exact mechanism remains unclear (Beard, *et al*. 2016). This suggests that in addition to the role that HECD-1 has in meiotic spindle formation in *C. elegans*, HECTD1 in mammalian cells may regulate mitotic spindle formation.

5.3.4. TRABID$_{1-200}$ can be used to trap K29 and K33 linked chains

In order to characterise the presence of K29 ubiquitin chains synthesised by HECTD1 in the cell cycle, GST-TRABID$_{1-200}$ was used to demonstrate the ability to trap K29/K33 ubiquitin chains in asynchronous and synchronised cell lysates. Importantly, GST-TRABID$_{1-200}$ was successfully used as a binding domain to trap ubiquitin in cell lysates. As demonstrated by Figure 3.1 (Chapter 3), HECTD1 is able to synthesise atypical ubiquitin chains, linked via K29/K48. Furthermore, recent work has used the NZF1 of TRABID to trap branched K29/K48 ubiquitin chains (Crowe, *et al.* 2017). Therefore, given that TRABID$_{1-200}$ can bind K29/K33 chains, it was hypothesised that this domain can be used as a ubiquitin binding domain (UBD) to pull down HECTD1 K29/K48 modified substrates by recognising the K29 linked ubiquitin modification. In resting mammalian cells, K33 (≤0.5%) is at a much lower abundance than K29 (8%) (Dammer, *et al*. 2011). Therefore, on this basis, in a pull down assay the majority of the ubiquitin captured is predicted to comprise more K29 linked ubiquitin than K33 linkages. Indeed, GST-TRABID$_{1-200}$ was able to pull down polyubiquitin chains in cell lysates, predicted to be polyubiquitin that contained K29/K33 linkages, given the specificity of NZF1 (Kristariyanto, *et al.* 2015a; Michel, *et al.* 2015). This is interesting, because it demonstrates the ability of this isolated domain to be used as a UBD to capture polyubiquitin from cell lysates. From this assay alone it is not possible to confirm that the captured K29 species are as a result of HECTD1-modification. A further consideration is that the use of proteasomal inhibitor MG132, has been shown to result in increased activity of UBE3C, which would lead to enrichment of K29/K48 (Besche, *et al*. 2014, Wang & Pickart. 2005; Besche, *et al*. 2014). Therefore, it was decided that use of MG132 would only function to mask any K29 linked chains synthesised by HECTD1, by the increased activity of UBE3C. Therefore, using TRABID$_{1-200}$ in combination with proteomics (as will be discussed in Section 5.4. Future Work), may identify whether some of the captured species are as a result of HECTD1 ubiquitination and not UBE3C (Wang & Pickart. 2005).

5.3.5. K29/ K33 linked chains are present throughout the cell cycle and mitosis

Using TRABID$_{1-200}$, it was demonstrated that HECTD1 is present in each stage of the cell cycle, where some K29 and K33-linked chains have been captured. This implies that HECTD1 activity in conjugating K29/K48 chains is present throughout the cell cycle. This is a novel and exciting observation because to date these chains have not been implicated in cell cycle function. Currently the main type of ubiquitin linkage driving mitosis is K11, which are conjugated onto substrates by the APC/C (Jin, *et al.* 2008). More compellingly branched K11/K48 synthesised by the APC/C and UBE2S, have been implicated in enhanced proteasomal degradation of cell cycle substrate such as NEK2A and p21 (Meyer & Rape. 2014). This demonstrates the potential scope of further mixed and branched linkages

involved in cell cycle regulation. Of the known HECT ligases with a cell cycle related function, only K48 has been implicated in the role of HERC2 and centrosome duplication most conclusively (Al-Hakim, *et al.* 2012). This highlights the lack of understanding of the type of ubiquitin chains synthesised by these HECT ligases in the cell cycle and the potential to implicate the activity of HECTD1 in synthesising K29/K48 linked ubiquitin chains in cell cycle regulation.

Interestingly, it has been reported that K29/K48 branched ubiquitin chains enriched by the NZF1 domain only, do not appear to target substrates to the proteasome (Crowe, *et al*. 2017). Therefore, since UBE3C activity is linked to the proteasome and degradation, it could suggest that UBE3C does not conjugate branched K29/K48 ubiquitin chains. This may suggest that only HECTD1 is able to conjugate K29/K48 branched chains in the cell. However, it has been suggested in *S. cerevisiae,* that branched K29/K48 ubiquitin chains promoted degradation of modified substrates (Liu, *et al*. 2017). Thus, demonstrating the infancy of our understanding of the role that branched ubiquitin chains have in cellular functions. As for HECTD1, it is not yet possible to know whether its cell cycle regulation is mediated by synthesis of K29/K48 onto its substrates either resulting in reduced or enhanced turnover by the proteasome.

The presence of K29/K33 ubiquitin chains and HECTD1 in the other phases of the cell cycle is expected and explained by the already known functions that HECTD1 in the cell, for example in Wnt signalling and cell migration (Tran, *et al.* 2013; Li, *et al.* 2013). Therefore, it is not surprising that there are K29 ubiquitinated species through the cell cycle because HECTD1 is active in different stages of the cell cycle. However, and against the previous hypothesis, there was no observed increase in K29/K33 ubiquitin chains pulled down by $TRABID_{1\text{-}200}$ during mitosis. This may not rule out a potential role for HECTD1 in mitosis, and as previously mentioned, the decrease in K29/K33 polyubiquitin could be due to increased activity of TRABID during mitosis. Here, the DUB would function to cleave the K29 and/or K33 chains from modified substrates. This would result in a reduction of substrates modified with K29/K33. An increase in DUB activity could be monitored using the ABPs that were previously discussed in Chapter 3. Here, the first generation of ABPs would be most appropriate because they are much more effective in labelling DUBs (Borodovsky, *et al.* 2002; Hemelaar, *et al.* 2004). The first generation of these probes Ub-ABP comprise a C-terminal modification of ubiquitin whereby the G76 is modified with a variety of thiol-reactive groups, known as warheads, which covalently modify the catalytic cysteine of the DUB (Love, *et al.* 2007). Thus, these ABPs would allow for the study of TRABID activity during mitosis to explore this hypothesis further. Additionally, as with Liu, *et al*. (2017), if branched K29/K48 result in increased turnover of potentially mitotic driven

HECTD1-modification of substrates that would be pulled down using $TRABID_{1-200,}$ then this would result in a reduction of these chains during mitosis. Additionally, MG132 was not used for these experiments, because of the effect in increasing the activity of UBE3C (Besche, *et al*. 2014), meaning that these chains would be readily degraded and not detected in the pull down assay. A final consideration is that through this study the overall ubiquitination status within the cell is being detected rather than protein-specific ubiquitination, which is likely to be quite different. However, a substrate will first need to be identified to be able to fully assess the role of these ubiquitin chains in the role of HECTD1 in mitosis,.

5.4. Future work:

To rule out HECTD1 as a regulator of all microtubules in cells, western blot analysis could be carried out to quantify the ratio of tubulin polymer (MTs) to soluble dimer in HECTD1-depleted or knockout cells. Here, HEK239T cells can be transfected with control or HECTD1 siRNAs. After performing a microtubule regrowth assay, samples can be collected and analysed by western blot to examine tubulin partitioning between the polymer and soluble dimer. This ratio can be measured by densitometric analysis of the western blot bands. This could therefore demonstrate the need for HECTD1 in MTs assembly as demonstrated with CYLD (Gao, *et al.* 2008). As previously mentioned, deletion of mitotic regulators such as NuMA and UBASH3B, showed a subtle phenotype during mitotic spindle regrowth, compromising K-fibre formation (Haren, *et al.* 2009; Krupina, *et al.* 2016). Therefore, HECTD1 may have a similar subtle mitotic spindle phenotype. In the NuMA study of mitotic spindle regulation, mitotic cells were scored based on the percentage of cells with regular compact spindles over time during the regrowth (Haren, *et al.* 2009). Time points for HECTD1 knock out or depleted cells were taken at 0, 5, 15, 30, 60, 90, and 120mins after nocodazole and cold treatment to depolymerise the spindle. However, as seen with NuMA, time points were taken at 2min intervals, between 0 and 15mins, with the full number of spindles restored after 15mins post-release (Haren, *et al.* 2009). Therefore, future work studying microtubule regrowth should be conducted over a smaller time frame from recovery from nocodazole and cold treatment.

Spindle regulation phenotypes have also been characterised by measuring the orientation of the mitotic spindle (Gallini, *et al.* 2016). Representative confocal z-sections of metaphase cells treated with DMSO or the Aurora A inhibitor, MLN8237, are scored based on the angle measured between the spindle axis and the plane of the coverslip. Here, it was found that phosphorylation of NuMA by Aurora A was required to ensure correct spindle orientation (Gallini, *et al.* 2016). Therefore, to understand the role HECTD1 has in spindle formation, further microscopy analysis would need to be conducted. In addition, another approach to identify whether HECTD1 is required for mitotic spindle formation, is to measure the inter-kinetochore distance. The DUB, BRISC, was shown to be required for the assembly of the mitotic spindle, where loss of BRISC resulted in unstable kinetochore-microtubule interactions, resulting in reduced inter-kinetochore tension contributing to increased time taken from NEBD to anaphase onset, increased cells with multipolar spindle, lagging chromosomes, and misaligned metaphase plate (Yan, *et al.* 2015). Furthermore, in NuMA depleted cells, there was an increase in inter-kinetochore distance due to the requirement of NuMA in spindle formation (Haren, *et al.* 2009). Therefore, further future work could include measuring the inter-kinetochore distance in HECTD1-depeleted cells to help identify if it is involved in mitotic spindle regulation.

The use of GST-TRABID$_{1-200}$ has been successful in trapping polyubiquitin in synchronised cell lysates. However, this would need to be confirmed to show that indeed K29/K33 are trapped by GST-TRABID$_{1-200}$. A method known as UbiCRest can be used to help determine ubiquitin chain linkages (Hospenthal, *et al.* 2015). UbiCRest helps to determine linkages by the treatment of polyubiquitin chains with a panel of linkage-specific DUBs in parallel reactions, followed by gel based analysis (Hospenthal, *et al.* 2015). For example, if the polyubiquitin chain was composed of K29 and K48 linkages, it is expected that TRABID (K29 specific) and Otubain 1 (K48 specific) would be able to partially cleave the smear (Licchesi, *et al.* 2012; Edelmann, *et al.* 2009). The DUBs USP21 or vOTU would be used as a control because they are able to cleave all linkages (Ye, *et al.* 2011; Hospenthal, *et al.* 2015). Therefore, this method would enable confirmation of the composition of the polyubiquitin captured by GST-TRABID$_{1-200}$. To confirm the topology of the polyubiquitin chains, proteomics can be used. As described in Meyer, *et al.* (2014), insertion of a Tobacco Etch Virus (TEV) protease cleavage sequence into the Glu-53 residue within ubiquitin can be used to demonstrated the presence of branched ubiquitin chains, the method of which is discussed in the final discussion (Chapter 7).

Ubiquitin linkage specific antibodies can be used to identify different chain linkages. For example, K48 and K63 specific antibodies have been used to study K48 and K63 linked ubiquitin in immune signalling (Newton, *et al.* 2008). Furthermore, K11/K48 bispecific antibodies have been generated to detect K11/K48 linked heterotypic chains (Yau, *et al.* 2017). This bispecific, K11/K48 antibody, was used to show the presence of those heterotypic chains within a mitotic cell by immunofluorescence (Yau, *et al.* 2017). Therefore, the generation of a K29/K48 antibody would facilitate detection of these heterotypic chains in the ubiquitin captured by GST-TRABID$_{1-200}$ and their localisation in the cell using immunofluorescence. However, a significant drawback is that linkage-specific antibodies are only available for 5 of the 8 different ubiquitin linkages, these include Met1, K11, K27, K48, and K63 (Michel, *et al.* 2017). Recently to overcome this limitation, K6 and K33 linkage specific “affimers” have been designed, which can be used in techniques such a western blot, immunofluorescence, and pull down assays to identify these linkages (Michel, *et al.* 2017). Affimers are 12kDa non-antibody scaffold that are based on the cystatin fold and importantly, provide an alternative specific high-affinity reagent (Tiede, *et al.* 2014; Tiede, *et al*. 2017). Therefore, using western blot the K33 linkage specific affimer could be used to confirm the specificity of GST-TRABID$_{1-200}$. Although, a current limitation is that no antibody or affimer is available that can detect K29 so more work is need in the field to expand this method of detection of ubiquitin linkages (Michel, *et al.* 2017). Furthermore, both antibodies and affimers present an alternative to the use of the TRABID$_{1-200}$, so would only be used to help confirm previous observations using this domain.

GST-TRABID$_{1-200}$ comprises NZF1, NZF2, and NZF3 domains, however only NZF1 has reported ubiquitin binding selectivity towards K29/K33 (Kristariyanto, *et al.* 2015a; Michel, *et al.* 2015). Recent work has used the NZF1 to trap branched K29/K48 ubiquitin chains (Crowe, *et al.* 2017). Here, Ubiquitin Chain Enrichment Middle-down Mass Spectrometry (UbiChEM-MS) was used to identify branched chains. Specifically, NZF1 TUBEs were used to enrich for chains from human cells. It was found that ~1% of chains isolated with TUBEs contain Ub branch points, with this value rising to ~4% after proteasome inhibition (Crowe, *et al.* 2017). This demonstrates a method for detecting and characterising the dynamics of branched conjugates under different cellular conditions, which could be used to study cell cycle K29 modified-substrates. Therefore, the NZF1 domain in isolation could be used to enrich for K29/K33 linked ubiquitin chains in future work as demonstrated in work carried out by Kristariyanto, *et al.* (2015a) and Michel, *et al.* (2015). TUBEs have been designed based on UBA domains to enhance that capture of polyubiquitinated proteins (Hjerpe, *et al.* 2009). They are designed with multiple UBAs to provide a higher affinity for polyubiquitin providing an increased capture of polyubiquitin within cell lysates (Hjerpe, *et al.* 2009). NZF1 TUBEs are now commercially available (UBPBio) and their use could improve detection of the K29/K33 linked polyubiquitin for use in future assays. An NZF1 TUBE could result in increased binding in comparison to TRABID$_{1-200}$ because the NZF1 domain is reported to be the K29/K33 ubiquitin binding domain (Michel, *et al.* 2015; Kristariyanto, *et al.* 2015a). Therefore, repeating units of NZF1 domains is likely to have a higher affinity towards K29/K33 than TRABID$_{1-200}$.

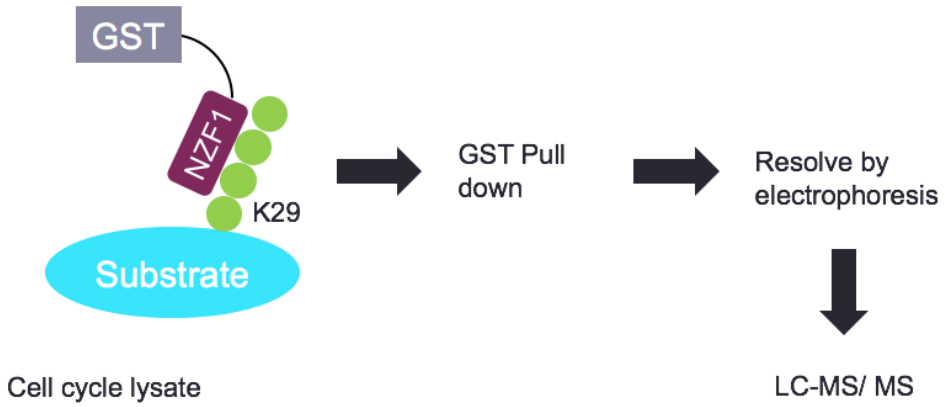

Figure 5.13. Schematic of downstream applications for the enrichment of polyubiquitin using ubiquitin associated domains. Example of a NZF1 domain trapping K29/K33 linked polyubiquitinated substrate in an immunoprecipitation assay for identification using mass spectrometry, such as Ubiquitin chain enrichment middle-down mass spectrometry (UbiChEM-MS) (Crowe, *et al*. 2017).

Identification of substrates can be carried out by a proteomics analysis of different cell cycle phases. Either an anti-HECTD1 antibody or GST-TRABID$_{1-200}$ can be used for a proteomics based analysis of interactors. Using an anti-HECTD1 antibody will help to identify HECTD1 interactors and potential substrates at different cell cycle phase, specifically the comparison of mitotic and non-mitotic cells. Whilst, an IP using GST-TRABID$_{1-200}$ should identify proteins modified with K29 or K33 linked ubiquitin at different cell cycle stages. This will confirm the association of HECTD1 with these ubiquitin chains during the cell cycle, but may also show that potential HECTD1 interactors identified using an anti-HECTD1 antibody are also modified with these ubiquitin chains. Additionally, proteomics can be carried out in HEK293T cells in comparison to HEK293T KO1 cells to see if HECTD1 depletion affects overall protein stability in a group of proteins.

There are two different techniques, which can be used to carry out quantitative mass spectrometry; stable isotopic labelling by amino acids in cell culture (SILAC) and tandem mass tag (TMT) labelling (Ong, *et al*. 2002; Thompson, *et al*. 2003). In SILAC two differently labelled samples can be studied by mass spectrometry to identify substrates. Where, mammalian cell lines are supplemented with a 'light' or 'heavy' form of an amino acid, which is incorporated into proteins, this allows for quantification of proteins and therefore comparison between the two samples (Ong, *et al*. 2002). In comparison, TMT labelling allows for the labelling of up to 10 different samples and are designed as such to allow identical proteins labelled with different TMTs to exactly comigrate in all separations. Each tag is chemically identical with the exception of different isotopes that have been substituted at various positions, allowing distinction between the samples (Thompson, *et al*. 2003). Both SILAC and TMT labelling have been used to identify cell cycle substrates (Singh, *et al.* 2014; Lafranchie, *et al.* 2014). SILAC was used to identify potential APC/C^{CDH1} samples by comparing cells that have been synchronised with nocodazole and lysed immediately (mitotic) and cells that were released for 2.5hrs before lysis (non-mitotic) (Lafranchie, *et al.* 2014). Using this approach alongside bioinformatics, CTLP was identified as an APC/C^{CDH1} target during the cell cycle and DNA damage response (Lafranchie, *et al.* 2014). TMT labelling has also been employed to identify APC/C targets (Singh, *et al.* 2014). Here, 6 samples were labelled with a TMT, cells were synchronised in S phase, G2/M phase, Metaphase/Anaphase, Anaphase/Cytokinesis, Telophase/ Cytokinesis, and late G1 phase, which led to the identification of kinesins as APC/C substrates (Singh, *et al.* 2014). However, a consideration is that with SILAC, samples are labelled before cell lysis, whereas with TMT labelling samples are labelled post lysis, therefore allowing for greater variability between samples when using TMT (Ong, *et al*. 2002; Thompson, *et al*. 2003; Singh, *et al.* 2014; Lafranchie, *et al.* 2014).

Chapter 6: Is HECTD1 dysregulated in cancer?

6.1. Introduction:

6.1.1. Cancer

Cancer is a disease that develops when normal cells begin to grow out of control unmonitored. Specifically, cancer arises due to the culmination of disruptions to the controls of cellular proliferation, immortality, angiogenesis, cell death, invasion, and metastasis (Hanahan & Weinberg. 2011; Shen & Laird. 2013). Previously, it was considered that cancer is a disease based primarily on genetics because genetic mechanisms such as mutation, copy number alteration, insertion, deletion, and recombination are all vehicles of persistent phenotypic change (Shen & Laird. 2013). However, more recently epigenetic mechanisms have been considered to also contribute to the development of cancer, providing a new "generation" of oncogenes and tumour suppressor genes (Esteller. 2006).

Two of the main types of genes that result in cancer formation are oncogenes and tumour suppressor genes (Lee & Muller. 2010). An oncogene is defined as a gene that has the potential to cause cancer and a proto-oncogene is defined as a normal gene that becomes an oncogene through mutation or overexpression (Lee & Muller. 2010). The first oncogene, *src,* was discovered in Rous Sarcoma Virus (RSV), a domestic foul virus, first discovered by Rous P. (1911) (Weiss & Vogt. 2011). Later, the first oncogenic human virus discovered was the Epstein-Barr virus (Epstein, *et al.* 1964). Finally, the first human oncogene, *ras,* was discovered in bladder carcinoma (Pulciani, *et al*. 1982; Parada, *et al*. 1982). In contrast, a tumour suppressor gene is a gene that protects a cell from one step on a pathway that will lead to cancer. A mutation that results in a loss or reduced function of the gene can result in cancer development (Lee & Muller. 2010). Tumour suppressor genes were first characterised using somatic cell hybridisation experiments, which involved fusion of normal cells with tumour cells. These experiments suggested that genes from normal non-cancerous cells functioned to inhibit tumour development (Harris, *et al*. 1969). The first tumour suppressor gene identified was *Rb*, discovered in retinoblastoma (Knudson. 1971; Fung, *et al.* 1987). The next tumour suppressor identified was *p53* (Lane & Crawford. 1979), which has been suggested to be mutated in almost every cancer with mutation rates of 38%-50% in ovarian, oesophageal, colorectal, head and neck, larynx, and lung cancers (Olivier, *et al.* 2010). These key discoveries of both oncogenes and tumour suppressor genes helped to understand cancer development at the genetic level.

6.1.2. Epigenetics and cancer

Epigenetic mechanisms are essential for normal development and maintenance of tissue specific gene expression patterns in animals (Sharma, *et al.* 2010). However, disruption of epigenetic processes can lead to altered gene function and malignant cellular

transformation (Sharma, *et al.* 2010). It is typically considered that global changes in an epigenetic landscape is a hallmark of cancer (Jones & Baylin. 2002; Hanahan & Weinberg. 2011). This results in the reprogramming of every component of the epigenetic machinery (Sharma, *et al.* 2010). Chromatin is composed of repeating units that consist of DNA that is wrapped around an octamer of four histone proteins: H3, H4, H2A, and H2B (Luger, *et al.* 1997). Epigenetic mechanisms that modify chromatin structure are subdivided into four main categories: DNA methylation, covalent histone modifications, nucleosome remodelling and non-coding RNAs (long non-coding RNAs). Together these modifications regulate the structural dynamics of the genome influencing its accessibility (Sharma, *et al.* 2010).

An example of epigenetic gene regulation is DNA methylation, which is a gene silencing mechanism required for maintaining genome stability (Kulis & Esteller. 2010). DNA methyltransferases (DNMTs), are responsible for the conversion of cytosine to 5-methylcytosine, by the transfer of a methyl group from the universal methyl donor, *S*-adenosyl-L-methionine (SAM) (Fienberg & Tycko. 2004; Kulis & Esteller. 2010). DNA methyltransferases, DNMT1, DNMT3A, and DNMT 3B, are responsible for DNA methylation whilst DNMT3L has no inherent enzymatic activity (Okano *et al.* 1998; Kareta, *et al*. 2006). DNMT3A and DNMT3B are *de novo* methyltransferases that act independent of replication showing a preference for both unmethylated and hemimethylated DNA, whereas DNMT1 acts during replication and preferentially methylates hemimethylated DNA (Okano, *et al*. 1999; Kim, *et al*. 2002). 5-methylcytosine is found at CpG islands, which comprise CpG dinucleotides, typically found overlapping or upstream of a gene promoter (Bird. 1980). Hypermethylation of a CpG island can result in gene silencing, and this was originally hypothesised to prevent transcription factor binding (Watt & Molloy. 1988).

Aberrant silencing of cell cycle regulators and hypermethylation of tumour suppressor genes can result in cancer (Robertson. 2005). For example, two cyclin dependent kinase inhibitor genes $p16^{INK4a}$ and $p15^{INK4a}$, that regulate G1 arrest, are silenced by DNA methylation in different types of cancer (Drexler. 1998; Kulis & Esteller. 2010). While, hypermethylation of the tumour suppressor gene, *death associated protein kinase 1* (*DAPK1*), results in cancer cell survival, by preventing interferon-γ-induced apoptosis (Michie, *et al*. 2010). 5-aza-2'-deoxycytidine, is a drug that is incorporated into DNA instead of cytosine during DNA replication. When a DNMT binds to the DNA, it binds irreversibly to 5-aza-2'-deoxycytidine and cannot disengage. As a result, DNMTs, are rendered inactive and therefore the DNA remains unmethylated. 5-aza-2'-deoxycytidine was first synthesised in 1964 and was first used as a chemotherapy for acute myeloid leukaemia, however its general toxicity meant that other nucleoside analogues were used as an alternative (Christman. 2002).

In addition to DNA methylation, covalent histone modifications are another level of epigenetic regulation. They occur in the unstructured N-terminal tail of histones, which can undergo methylation, acetylation, ubiquitination, sumoylation and phosphorylation (Luger, *et al.* 1997; Kouzarides. 2007). Histone modifications can lead to either transcriptional activation or repression depending upon the type of modification and the residue that has been modified (Shen & Laird. 2013). For example, lysine acetylation results in transcriptional activation (Hebbes, *et al*. 1988), whereas lysine methylation results in transcriptional activation or repression depending of the residue modified (Liang, *et al*. 2004; Kouzarides. 2007). Histone acetyltransferases (HATs) acetylate histones, and histone methyltransferases (HMTs) methylate histones, whereas histone deacetylases (HDACs) and histone demethylases (HDMs) remove the acetyl and methyl groups respectively (Shi. 2007; Haberland, *et al*. 2009).

Furthermore, non-covalent mechanisms also play a role in chromatin restructuring, such as nucleosome remodelling and replacement of canonical histone proteins with histone variants (Sharma, *et al.* 2010). Nucleosome remodelling occurs by the action of "nucleosome remodelling ATPases" altering histone-DNA interactions in target nucleosomes (Becker & Workman. 2013). While histone variants are deposited by distinct nucleosome assembly complexes after DNA replication (Henikoff & Smith. 2015). Finally, long non-coding RNAs are able to regulate chromatin remodelling to achieve transcriptional remodelling. For example, by regulating the transcriptional silencing of *potassium voltage-gated channel subfamily KT member 1 opposite strand/ antisense transcript 1* (*KCNQ1OT1*) (Fang & Fullwood. 2016).

6.1.3. Ubiquitin ligases and cancer

Ubiquitin E3 ligases are fundamental for the maintenance of protein homeostasis and dysregulation of their activity can result in cancer mediated by either oncogenic and tumour suppressive properties (Pickart. 2001; Satija, *et al*. 2013). For example, two F-box proteins that form the SCF E3 ligase, SKP2 and FBW7, have been shown to be involved in cancer formation (Nakayama & Nakayama. 2006). The F-box protein SKP2 acts as an oncogene where it is implicated in the degradation of the CDK inhibitor $p27^{Kip1}$ (Pagano, *et al*. 1995; Shirane, *et al.* 1999; Bloom & Pagano. 2003). $p27^{Kip1}$ is responsible for the cell cycle arrest at G1, preventing Cyclin E-CDK2 and Cyclin D-CDK4 activation (Shirane, *et al.* 1999; Besson, *et al.* 2008) (Figure 1.11). Decreased expression of $p27^{Kip2}$, was found in various human cancers, and has been associated with poor prognosis (Bloom & Pagano. 2003). In contrast, the F-box protein and tumour suppressor, FBW7, is responsible for the degradation of known oncoproteins including Cyclin E, MYC, NOTCH1, and NOTCH4

(Koepp, *et al.* 2001; Tsunematsu, *et al.* 2003; Yada, *et al*. 2004; Nakayama & Nakayama. 2006).

Currently, the only current ubiquitin-proteasome pathway targeting drugs are proteasome inhibitors such as Bortezomib (Cohen & Tcherpakov. 2010) and Cafilzomib (Stewart, *et al.* 2015). Inhibition of the proteasome has a large scope for side effects because it diminishes protein turnover in the whole cell, whereas targeting specific E3 ligases means that the scope of the side effects is reduced due to the specific nature of the enzyme (Bernassola, *et al.* 2008). Targeting of the ubiquitination pathway has the potential to yield many future therapeutics (Cohen & Tcherpakov. 2010). For example, drugs that target phosphorylation, a post translational modification that can be thought of as similar to ubiquitination, has resulted in many drugs for the treatments of different diseases (Cohen & Tcherpakov. 2010). An example is Gefitinib, which targets EGFR kinase and is used a cancer therapeutic for non-small cell lung cancers (Paez, *et al.* 2004). Similarly, cancer drugs have been designed that inhibit phosphatases, demonstrating that dephosphorylation can also be targeted for therapeutics (Scott, *et al*. 2010). The ubiquitin pathway comprises many components that are available to be targeted due to their enzymatic nature (Burger & Seth. 2004). For example, the enzymatic cascade components, E1 activating enzymes, E2 conjugating enzymes, and E3 ligases, in addition to DUBs and the proteasome. Therefore, demonstrating the impact that the targeting of ubiquitination could have on yielding more therapeutics (Burger & Seth. 2004; Cohen & Tcherpakov. 2010). An example of this is the inhibitor VLX1570, which targets USP14 to induce apoptosis in multiple myeloma cells (Wang, *et al.* 2016) and overcomes resistance to bortezomib (Tian, *et al*. 2014).

Interestingly, HECT ligases have been suggested as cancer targets with many different functions within the cell (Bernassola, *et al.* 2008) (Table 6.1). For example, HECT ligases such as E6-AP, HACE1, and HUWE1 have been implicated in p53 regulation that results in cancer formation (Scheffer, *et al.* 1990; Talis, *et al.* 1998; Yoon, *et al.* 2004; Zhang, *et al.* 2007; Sakata, *et al.* 2009; Sakata, *et al.* 2013). Whilst the HECT ligases NED4L and UBE3C, regulate the Wnt signalling pathway, a key signal transduction pathway regulating stem cell fate and tumorigenesis in epithelial tissues (Tanksley, *et al.* 2013; Wen, *et al.* 2015) (Table 6.1). Interestingly EDD, and HUWE1 have also been shown to regulate the Wnt signalling pathway, and may suggest that their role in cancer development also occurs via this pathway (Hay-Koren, *et al*. 2011; de Groot, *et al*. 2014; Gao, *et al.* 2014). Some HECT E3 ligases have been identified as tumour suppressors, whilst others have been shown to be oncogenic (Table 6.1). Interestingly, ligases such as HUWE1 and SMURF2 have been identified as both tumour suppressive and oncogenic, highlighting the complexity of HECT ligases in cancer formation (David, *et al.* 2014; Liu, *et al.* 2014; Vaughan, *et al.*

2015; Myant, *et al*. 2016). Finally, HECT E3 ligases offer ideal therapeutic targets because they harbour a catalytic cysteine (Huibregtse, *et al.* 1995), which can be targeted. For example, small molecule inhibitors have been designed that target ligases such as HUWE1 and ITCH, which appear to prevent ubiquitination of their target substrates (Peter, *et al.* 2014; Rossi, *et al.* 2014). This demonstrates the importance of characterising the function of these ligases, to yield future cancer therapeutics.

Table 6.1. HECT Ligase expression in cancer. HECT ligases and their implicated function, mechanism and alterations in cancer, where known.

HECT Ligase	Implicated function	Mechanism	Alterations in Cancer	References
AREL1	Unknown.	Unknown.	High expression in lung cancer.	Liu, *et al*. (2014).
EDD	Regulator of DNA Damage responses. Unknown.	Unknown. Unknown.	Overexpressed in breast, liver, and ovarian cancer. C terminal cluster of deleterious mutations, in mantle cell lymphoma.	Clancy, *et al*. (2003); O'Brien, *et al.* (2008). Meissner, *et al.* (2013).
E6-AP	Apoptosis.	Degradation of p53.	Overexpressed in cervical cancers.	Scheffer, *et al.* (1990); Talis, *et al.* (1998).
HACE1	HACE1 regulates cell cycle arrest. Depletion results in increased mobility and invasiveness.	Cooperates with p53 in cancer formation. Turnover of Cyclin D1 (no direct evidence). Degradation of RAC1.	Hypermethylation of CpG island upstream of the promoter. Found in Wilm's tumour, prostate, and gastric carcinoma. Hypermethylation in breast, and HER activation.	Zhang, *et al.* (2007); Sakata, *et al.* (2009); Sakata, *et al.* (2013). Goka & Lippman. (2015).
HECTD2	Unknown.	Overexpression of *microRNA 221* inhibits HECTD2.	Downregulation of HECTD1 in prostate cancer.	Sun, *et al.* (2014).
HECTD3	Facilitates cancer cell survival.	K63-linked ubiquitination of caspase-8.	Overexpressed in breast cancer.	Li, *et al*. (2013c).
HERC2	Overexpression results in reduced survival.	Unknown.	Increased expression in non-small lung cell cancer.	Bonanno, *et al.* (2016).

HERC4	Tumorigenesis.	Unknown.	Overexpressed in lung and breast cancer.	Zeng, *et al.* (2015); Zhou, *et al.* (2014).
HERC5	Unknown.	Unknown.	Promoter hypermethylation in non-small cell lung cancer.	Wrage, *et al*. (2015).
HUWE1	Cell adhesion, motility and invasion. Proliferation. Proliferation. MYC signalling, DNA damage accumulation and tumour initiation.	TIAM1 degradation. K63 ubiquitination of MYC. Degradation of p53. Loss of HUWE1 leads to increased Myc levels.	Overexpression in lung cancer. Over expression in breast, colon, prostate, liver, pancreas, and thyroid. Overexpression in colorectal cancer. Down regulated in colon cancer.	Vaughan, *et al.* (2015). Adhikary, *et al.* (2005); Confalonerieri, *et al.* (2009). Yoon, *et al.* (2004). Myant, *et al*. (2016).
NEDD4	Tumorigenesis.	p38 binds NEDD4 and controls PTEN ubiquitination.	Overexpressed in non-small cell lung carcinomas, colon, and gastric cancers.	Amodio, *et al.* (2010); Wang, *et al.* (2010); Hong, *et al.* (2014).
NEDD4L	Tumorigenesis.	Inhibits Canonical Wnt signalling.	Downregulated in colon cancer.	Tanksley, *et al.* (2013).
SMURF1	Invasiveness. Cell migration and invasiveness. Unknown. Cancer growth.	Unknown. EGF induction of SMURF1 results in RhoA downregulation. Unknown. Degradation of PIPKIγ.	Overexpressed in pancreatic cancer. Overexpressed in breast cancer. Overexpressed in clear cell renal cell carcinoma. Overexpressed in lung cancer.	Kwei, *et al.* (2011). Kwon, *et al.* (2013). Ke, *et al*. (2017). Li, *et al.* (2017).
SMURF2	Unknown. Proliferation and invasion.	Increased expression of microRNA inhibitors. CNKSR2 regulation and AKT signalling.	Downregulated in triple-negative breast cancer. Overexpressed in breast cancer.	Liu, *et al.* (2014). David, *et al.* (2014).

TRIP12	DNA damage response.	p16 overexpression leads to TRIP12 downregulation, which in turn results in radioresponsivenss.	Overexpression of TRIP12 leads to poor survival in Head and Neck cancers.	Wang, *et al.* (2017).
WWP1	Cell growth, anchorage independent colony formation, and apoptosis.	Potential suppression of caspases.	Overexpressed in breast and oral cancers.	Chen, *et al.* (2007); Nguyen Huu, *et al.* (2008); Lin, *et al.* (2013).
	Proliferation.	Degradation of LATS1 (Hippo signalling pathway).	Overexpressed in breast tumours.	Yeung, *et al.* (2013).
	Cell migration and invasion.	*microRNA 452* inhibits WWP1.	Overexpressed WWP1 and down regulated *microRNA 452* in prostate cancer.	Goto, *et al.* (2016).
WWP2	Apoptosis and tumourgenicitiy.	PTEN degradation and activation of the PI3K/AKT pathway.	Overexpressed in endometrial cancer and oral cancer.	Maddika, *et al.* (2011); Fukumoto, *et al.* (2014); Clements, *et al.* (2015).
	Migration and invasion.	Unknown.	Overexpressed in lung adenocarcinoma.	Yang, *et al.* (2016).
	Apoptosis and invasiveness.	HIF-1α regulation of WWP2.	Overexpressed in thyroid cancer.	Ding, *et al.* (2016).
UBE3C	Increased epithelial to mesenchymal transition (EMT).	EMT inducer possibly through degradation of E-cadherin.	Overexpression in melanoma cancer, and hepatocellular carcinoma (HCC).	Jiang, *et al.* (2014); Tang, *et al.* (2016).
	Cancer cell migration and invasiveness.	Ubiquitination and degradation of Annexin A7 (ANXA7).	Overexpressed in glioblastoma.	Pan, *et al.* (2015).
	Growth and metastasis.	Activation of the Wnt/ β-catenin pathway.	Overexpression in renal carcinoma.	Wen, *et al.* (2015).

6.1.4. Aims

Given the role that HECTD1 has in cell proliferation, it was hypothesised that this ligase may be dysregulated in cancer. Multiple HECT ligases function in cancer formation and have been identified as both tumour suppressive and oncogenic (Table 6.1). Therefore, to characterise the role of HECTD1 in cancer, both tumour suppressive and oncogenic functions were explored. The DNA methylation status of *HECTD1* was screened to determine if *HECTD1* is silenced in cancer, and acts as a tumour suppressor. Alternatively, overexpression studies were carried out to see whether HECTD1 is oncogenic and promotes cancer formation. To understand the regulation of *HECTD1* in cancer, the following objectives were addressed:

1. Determine whether HECTD1 is expressed or silenced by epigenetic mechanisms in lung cancer cell lines (NSCLC).

2. Examine whether *HECTD1* is mutated in different cancers, such as glioblastoma using the cancer genomics database, cBioPortal, and the cancer microarray database, Oncomine™.

3. Determine whether overexpression of HECTD1 increases cell proliferation in HEK293T and the glioblastoma cell line U87, using trypan blue cell counting.

4. Establish whether depletion of HECTD1 results in a reduction in cell proliferation in glioblastoma cell lines U87 and U251, using trypan blue cell counting.

5. Assess *HECTD1* mRNA expression in a small cohort of glioblastoma samples provided by Dr Kathreena Kurian (Bristol Southmead Hospital), using qRT-PCR.

6.2. Results:

6.2.1. HECTD1 expression does not appear to be affected by promoter methylation in lung cancer cell lines.

Given its suggested role in migration (Li, *et al.* 2013b), Wnt signalling (Tran, *et al.* 2013), and cell cycle regulation and cell proliferation (this thesis), it was hypothesised that HECTD1 expression could be altered in cancer cell lines and patient samples. Ubiquitin ligases have been shown to be both tumour suppressive and oncogenic in cancers, for example, FBW7 (tumour suppressor) and SKP2 (oncogenic) (Nakayama & Nakayama. 2006). Therefore, it was hypothesised that HECTD1 may be tumour suppressive and silenced in cancer. Interestingly, the expression of HECT ligases HACE1 and HERC5 was found to be downregulated due to DNA promoter hypermethylation in breast, gastric, and non-small cell lung cancer (Zhang, *et al.* 2007; Sakata, *et al.* 2009; Sakata, *et al.* 2013; Goka & Lippman. 2015; Wrage, *et al*. 2015). Therefore, the expression HECTD1, a close relative of HACE1, could also be under the regulation of epigenetic mechanisms such as DNA promoter methylation in cancer cell lines.

To test the hypothesis that *HECTD1* is silenced in cancer, mediated by DNA methylation, a potential methylation site was first characterised in the sequence of *HECTD1* using UCSC (University of California Santa Cruz) genome browser (https://genome-euro.ucsc.edu/cgi-bin/hgGateway?redirect=manual&source=genome.ucsc.edu (accessed 29.08.2017)) (Kent, *et al.* 2002). Interestingly, a CpG island was found within the promoter region of *HECTD1* (Figure 6.1). The CpG island was found to encompass the transcription start site of *HECTD1* and suggests that *HECTD1* could be regulated by DNA methylation. To further characterise the *HECTD1* promoter and transcription factors that may bind within the promoter, Sabiosciences DECODE (Decipherment of DNA Elements) (http://www.sabiosciences.com/chipqpcrsearch.php?app=TFBS (accessed 30.08.2017)) was used to identify known transcription factor binding sites. Five transcription factors were found to be located within the CpG island (Figure 6.1), including AHR, ARNT, C-MYC, MAX1 and PAX5. The transcription factors AHR, ARNT, C-MYC, and MAX1 all share the same DNA binding sequence, whilst PAX5 DNA binding sequence is downstream. Aryl hydrocarbon receptor (AHR) and aryl hydrocarbon receptor nuclear translocator (ARNT) form a heterodimeric transcription factor and can lead to the inhibition of cell proliferation (Puga, *et al.* 2002). Furthermore, both c-MYC and MAX1 form a heterodimeric transcription factor that promotes cell proliferation and growth (Blackwood & Eisenman. 1991). PAX5 is a transcription factor essential for commitment of lymphoid progenitors to the B cell lymphocyte lineage in addition to regulating cell adhesion and migration (Cobaleda, *et al*. 2007; Schebesta, *et al*. 2007).

Having used bioinformatic tools to identify a CpG island in the sequence of *HECTD1*, the next aim was to determine whether HECTD1 expression might be regulated by DNA promoter hypermethylation at CpG islands. To examine this, *HECTD1* mRNA expression was screened by RT-PCR using RNA from 8 non-small cell lung cancer (NSCLC) cell lines, which had been previously extracted from cell lines treated with DMSO or the demethylating agent 5-aza-2'-deoxycytidine (5-Aza) for 3-4 days (Figure 6.2) (Licchesi, *et al.* 2010). The DKO cell line was used as a negative control. The DKO cell line has two major DNMTs knocked out (DNMT1 and DNMT3b), therefore preventing gene silencing by methylation (Jacinto, *et al.* 2007). If *HECTD1* was regulated by methylation there would be a low signal for the amplification in the DMSO-treated samples compared to the 5-Aza treated samples. However, all samples screened showed a band in the DMSO control suggesting that, in these non-small cell lung cancer cell lines, HECTD1 is expressed and therefore is not repressed by DNA promoter methylation. A limitation is that screening eight different lung cancer cell lines is not definitive and *HECTD1* methylation may still occur in lung cancer and in other cancer and cell types. Furthermore, there is no 5-Aza positive control to demonstrate that the drug is working, which limits the interpretation of the data. A 5-Aza positive control would be to screen a known silenced gene, to see if 5-Aza treatment relieves silencing by preventing methylation.

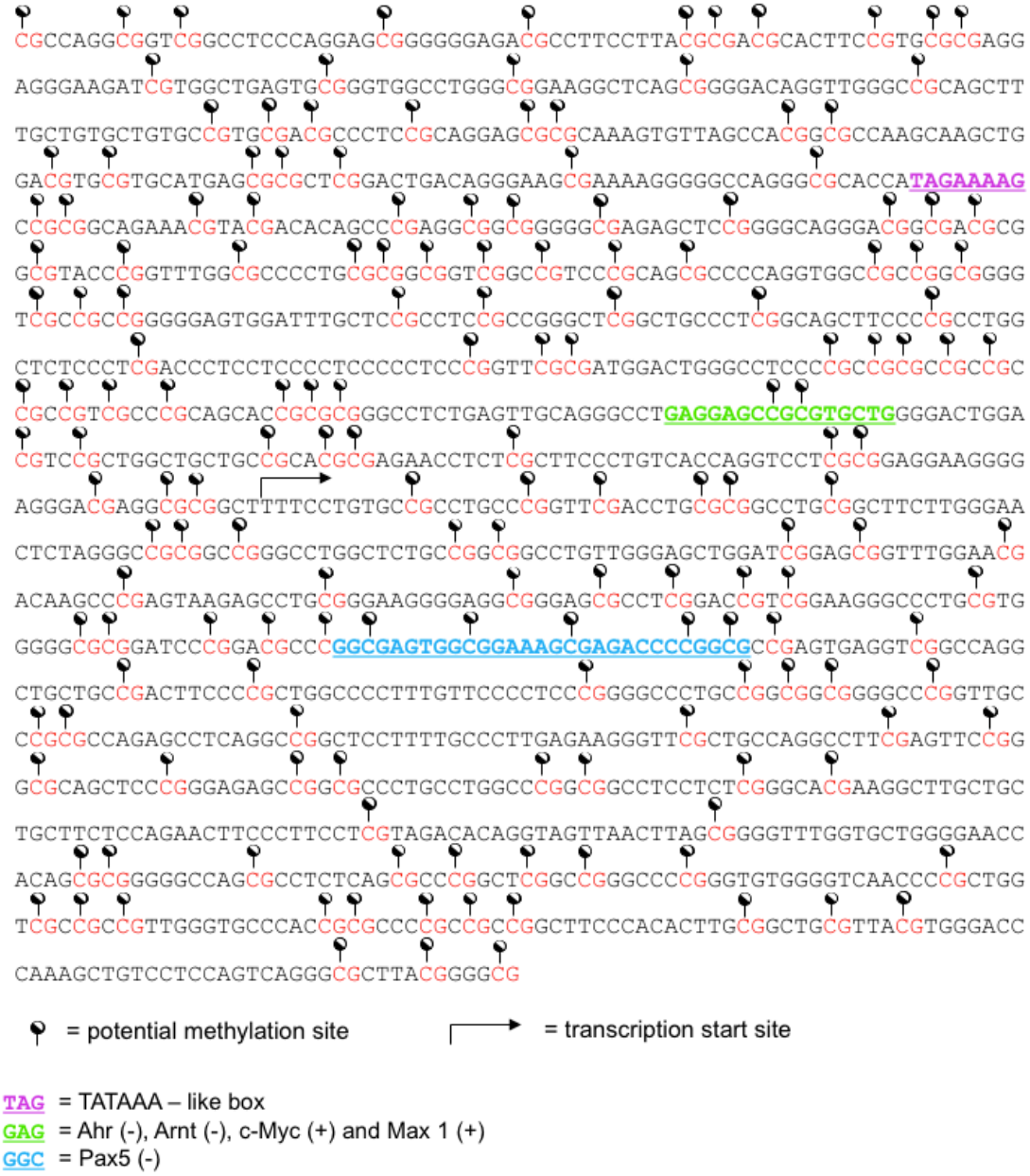

Figure 6.1. *HECTD1* has a CpG island extending upstream and downstream of its transcription start site (TSS). Schematic representation of CpG island, showing the density of CpG dinucleotides within the island annotated with transcription factor binding sites. The sequence was extracted from UCSC genome browser (https://genome-euro.ucsc.edu/cgi-bin/hgGateway?redirect=manual&source=genome.ucsc.edu (accessed 29.08.2017)) and annotated using two-tone "lollipops" to represent potential methylation sites and CpG dinucleotides highlighted in red. The CpG island contains 167 CG dinucleotides, which could all be potential methylation sites. The CpG island comprises a 71% CG content and 23.3% CpG content. Transcription factors that bind within the CpG island of *HECTD1* are highlighted in pink, blue and green. (+) = sense, and (-) = antisense. Transcription factor binding sites were identified using Sabiosciences DECODE (Decipherment of DNA Elements) (http://www.sabiosciences.com/chipqpcrsearch.php?app=TFBS (accessed 30.08.2017)).

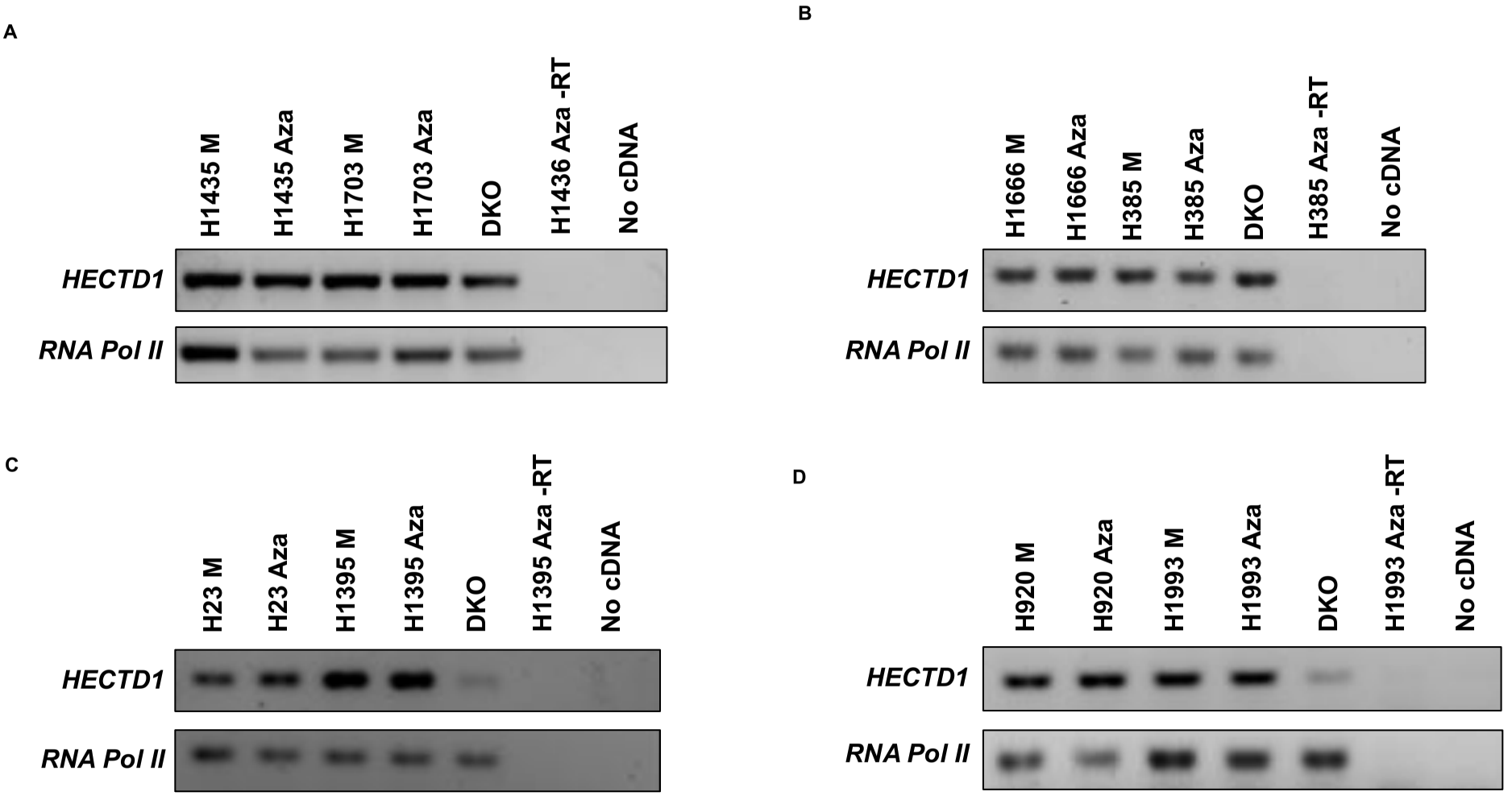

Figure 6.2. A semi-quantitative panel screen of lung cancer cell lines to assess the presence of *HECTD1* promoter methylation. 3% agarose gel of RT-PCR products, showing HECTD1 (JL7 + 8) expression in multiple cancer cell lines. A) H1435 and H1703, B) H1666 and H385, C) H23 and H1395, and D) H920 and H1993. Each cell line was treated with DMSO (M = Mock treated) or 5-aza-2'-deoxycytidine (2μM) (Aza = "5-Aza" treated). *HECTD1* was compared to *RNA Pol II* housekeeping gene. DKO cell line was used as a positive control, -RT and no cDNA were used as a negative control in the reaction. Full size gels (Appendix Figure A.6). *RNA Pol II* was used as a housekeeping reference gene, whilst DKO (HCT-116 DNMT1 and DNMT3b enzymes knock out cell line) was used as a positive control (Rhee, *et al.* 2002; Kozera B, & Rapacz M. 2013). Experiments performed with the help of Ruby Coates and Emma Thatcher.

6.2.2. *HECTD1* is mutated in cancer

Given that *HECTD1* does not appear to be regulated by methylation at least in the 8 NSCLC cell lines tested, it was next hypothesised that *HECTD1* may be mutated or amplified in cancer cells, indicating an oncogenic role. Specifically, this latter hypothesis makes more sense in view of the data presented in this thesis, which suggest that HECTD1 has a role in cell proliferation, by regulation of the cell cycle. Using the cancer genomics database cBioPortal (Cerami, *et al.* 2012), *HECTD1* was found to be mutated in multiple cancers, including prostate, bladder, lung, colorectal, and many others (Figure 6.3). The cBioPortal search result also suggests that *HECTD1* is also amplified and deleted in some cancers, suggesting that HECTD1 could be a novel cancer target. In the cBioPortal database mutations encompass missense, truncating and inframe mutations. Interestingly mutations found within HECTD1 (Figure 6.4) occur at multiple sites across the protein sequence and no mutation hotspot could be identified. The majority of the mutations that occur within *HECTD1* are missense mutations, which result in a nonsynonymous amino acid substitution, and could result in a gain of function or a loss of function resulting in cancer (Dittmer, *et al.* 1993; Sarraf, *et al*. 1999). Although, these databases provide general analysis of *HECTD1* in large and diverse cancer cDNA datasets, it does suggest that *HECTD1* may be altered in a variety of cancers. Further analysis would be needed to determine the exact role that HECTD1 has in individual cancers. Enhanced activity of oncogenes is often linked to specific mutations at functional sites. For example, there are multiple mutations present within the HECT domain of HECTD1, however none that occur at the position of the catalytic cysteine (2579). Some of these mutations that occur within the HECT domain could be characterised within cells to see whether they are associated with a change or increase in activity. Here, a crystal structure of the HECT domain would help to determine which particular mutations are likely to alter the architecture of the domain and therefore the activity of the ligase.

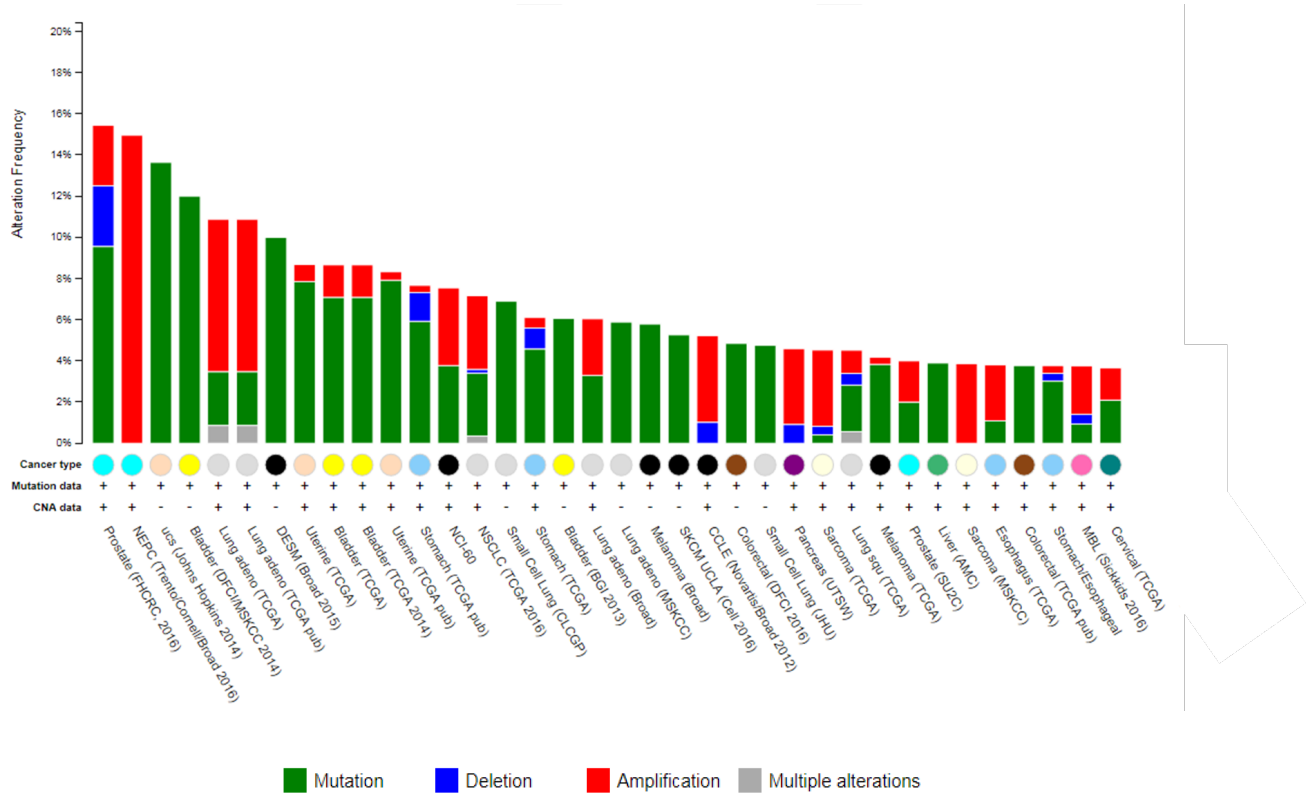

Figure 6.3. *HECTD1* alterations in human cancer samples, cBioPortal. The above figure displays the Cross-cancer alteration summary for *HECTD1* across 163 studies based on cDNA. Only 88 studies are shown, which have some form of *HECTD1* alteration present. Image obtained from cBioPortal, a database for Cancer Genomics (29/08/2017) (continued on page 180).

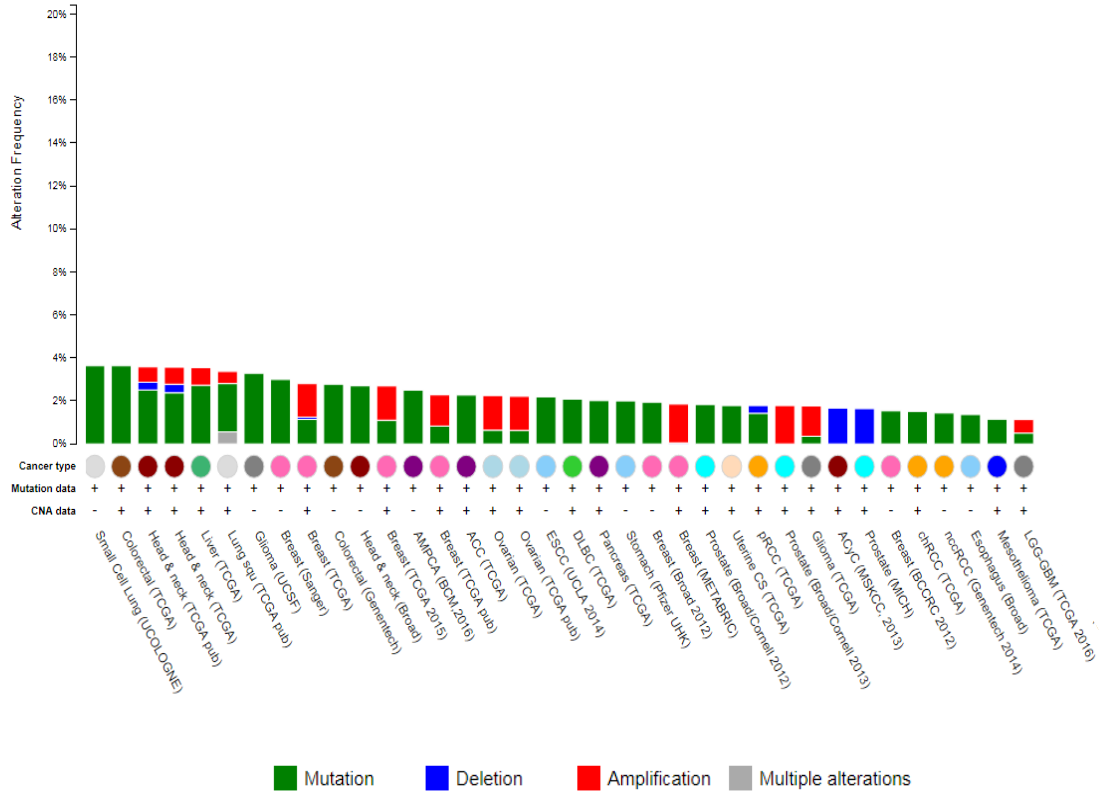

Figure 6.3 (continued). *HECTD1* alterations in human cancer samples, cBioPortal. The above figure displays the Cross-cancer alteration summary for *HECTD1* across 163 studies based on cDNA. Only 88 studies are shown, which have some form of *HECTD1* alteration present. Image obtained from cBioPortal, a database for Cancer Genomics (29/08/2017) (continued on page 181).

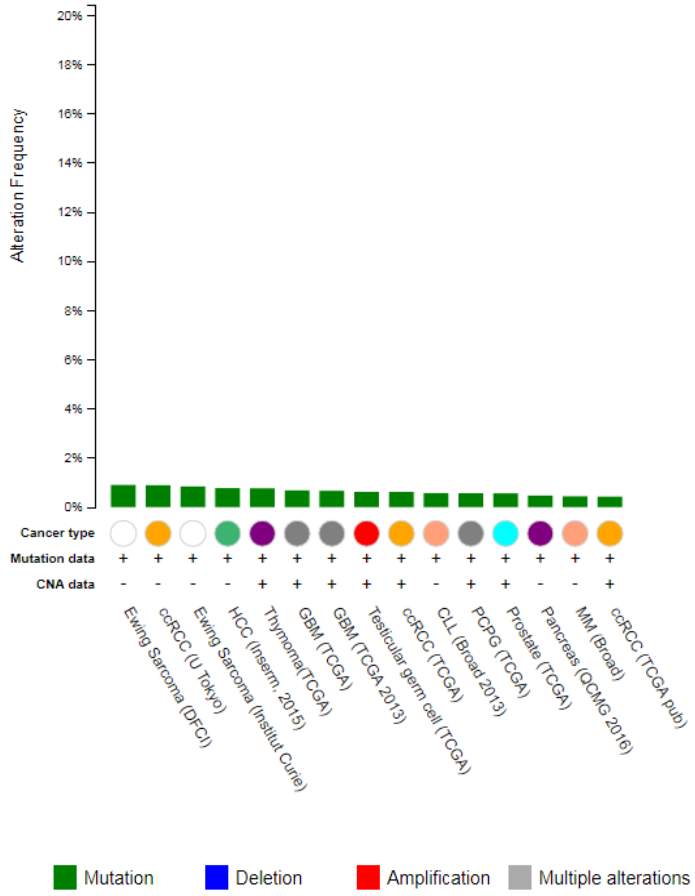

Figure 6.3 (continued). *HECTD1* alterations in human cancer samples, cBioPortal. The above figure displays the Cross-cancer alteration summary for *HECTD1* across 163 studies based on cDNA. Only 88 studies are shown, which have some form of *HECTD1* alteration present. Image obtained from cBioPortal, a database for Cancer Genomics (29/08/2017).

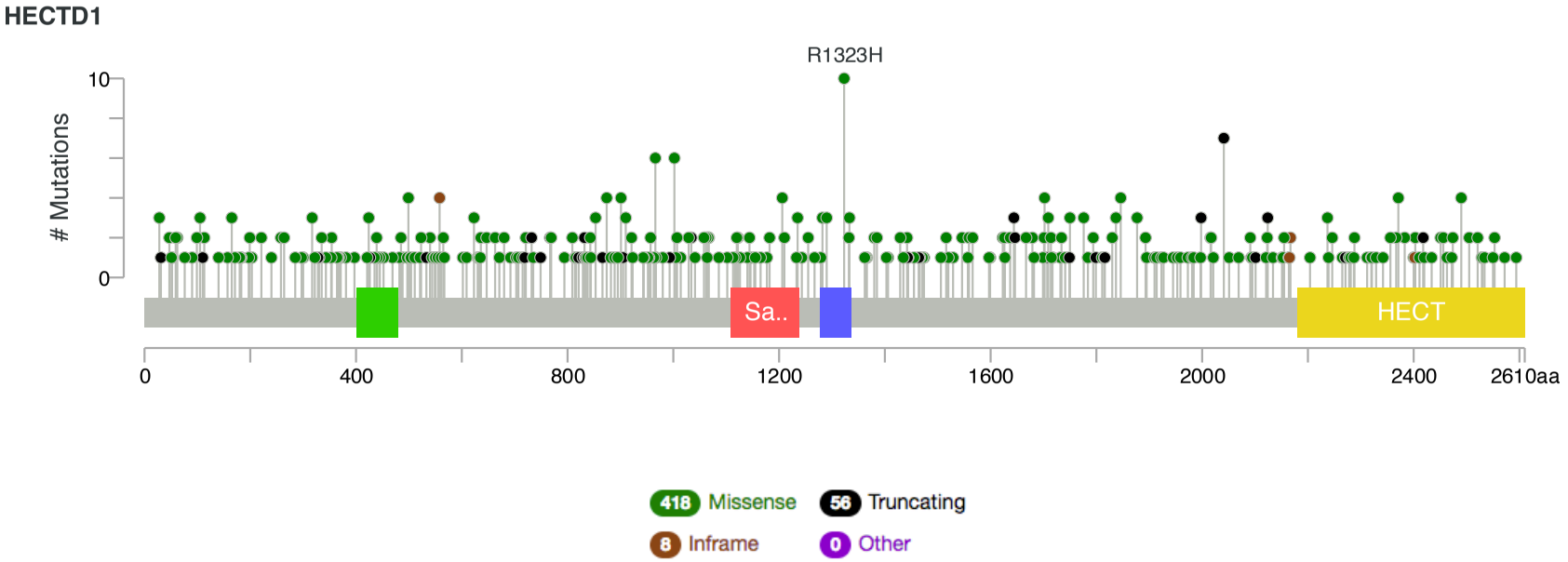

Figure 6.4. Mutations in *HECTD1*, cBioPortal. Image obtained from cBioPortal, a database for Cancer Genomics (29/08/2017). The mutation diagram circles are coloured with respect to the corresponding mutation types. The green dot denotes a missense mutation, black represents truncation mutations (that encompass nonsense, nonstop, frameshift deletion, frameshift insertion, and splice site mutations), brown are in-frame mutations (that encompass inframe deletion and inframe insertion mutations), and purple indicates "other mutations" (that encompass all other types of mutations). The ankyrin repeat domain is shown in green, Sad1/UNC in red, Mib2/HERC domain in blue and the HECT domain, containing the catalytic cysteine, in yellow.

6.2.3. HECTD1 is overexpressed in glioblastoma

In order to understand a potential oncogenic function of HECTD1 in cancer development, the effect of its overexpression was studied in glioblastoma. Unpublished data from Dr K Kurian at Bristol Southmead Hospital suggested that HECTD1 may be overexpressed in glioblastoma patients. In agreement with this finding, using Oncomine™ (Rhodes, *et al.* 2004), *HECTD1* mRNA appeared to be overexpressed in a glioblastoma cohort. Glioblastoma is the most common type of brain tumour in adults, representing 16% of all primary brain tumours (Davis, 2016). Glioblastoma is derived from neurological stem or progenitor cells, and accounts for 80% of malignant brain tumours (Weller, *et al*. 2015). It is therefore a very aggressive type of primary brain tumour in adults and is associated with a reported survival rate of 5% after 5 years (Haynes, *et al.* 2014; Delgado-López & Corrales-Gárcia. 2016).

To determine whether HECTD1 is overexpressed in glioblastoma, an analysis of cDNA microarray datasets was carried out using Oncomine™ (Rhodes, *et al.* 2004). The Oncomine™ cancer microarray database uses microarray data from different specific cancer study datasets, facilitating differential expression analysis. In the Bredel Brain 2 dataset composed of 24 glioblastoma (GBM) samples and 4 normal brain samples, HECTD1 appeared to be overexpressed compared to Normal Brain samples (Figure 6.5). This finding can also be seen in the Sun Brain data set (reporter: 1557100_s_at), which compares 81 glioblastoma samples to 23 normal brain samples (Sun *et al.* 2006). This is potentially a very exciting finding, which if confirmed, would suggest that HECTD1 overexpression could be used as a diagnostic marker. In addition this would also suggest that HECTD1 could be an attractive novel therapeutic target in glioblastoma.

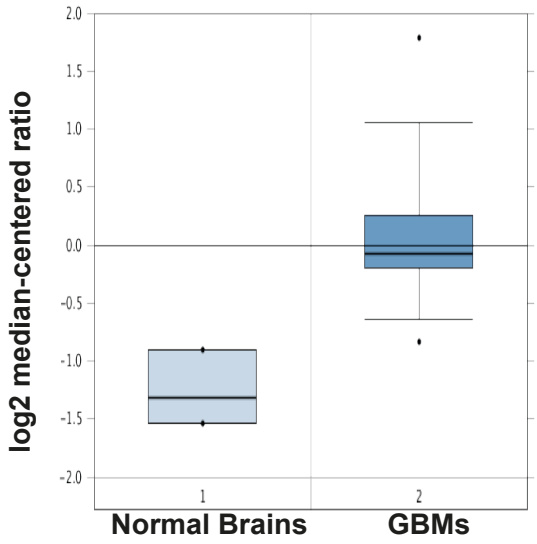

Figure 6.5. *HECTD1* mRNA expression in glioblastoma compared with Normal Brain, Oncomine™. Image obtained from Oncomine, a cancer microarray database. Oncomine™ compiles data from cancer transcriptome profiles allowing analysis of cancer gene expression in different cancer types. The median ratio for Normal Brain samples is negative, which suggests that they express HECTD1 at a lower level compared to GBMs. The median ratio at zero lies close to the median of the GBMs however the distribution of the data is larger than that of the normal brain data. Overall indicating increased *HECTD1* mRNA in GBMs compared to normal brains. 24 Glioblastoma samples and 4 normal brain samples were analysed on cDNA microarrays, from Bredel Brain 2 dataset, reporter: 1256904 (Bredel, *et al.* 2005).

6.2.4. HECTD1 overexpression in HEK293T and glioblastoma cell lines results in increased proliferation

Given that HECTD1 appears to be overexpressed in glioblastoma patient microarray data (Figure 6.5), the effect of overexpression of HECTD1 on cell proliferation was monitored (Figure 6.6). To determine an oncogenic role for *HECTD1*, initially, overexpression of HECTD1 was carried out in HEK293T cells due to their high transfection efficiency (Durocher, *et al.* 2002). Interestingly, using an ATP proliferation assay (Maehara, *et al.* 1987; Petty, *et al*. 1995), overexpression of HA-FL-mHectd1^{WT} in HEK293T WT cells resulted in a statistically significant increase in relative luminescence, indicating that overexpression of HECTD1 resulted in increased proliferation.

The above experiment was then repeated in the glioblastoma cell line U87, using a trypan blue cell counting assay. The glioblastoma cell line U87, has been frequently used as a model for glioblastoma because of its high transfectability, for example the cell line was used to demonstrate that RhoE inhibits glioblastoma cell line proliferation by inducing apoptosis (Poch, *et al*. 2007). U87 (also known as U87MG) was originally thought to have been derived from a stage 4 cancer patient, however a recent DNA profile revealed that whilst the cell line was indeed glioblastoma, it was from an unknown origin (Allen, *et al.* 2016). This means that U87 may not be the best glioblastoma model, however at this early stage using a glioblastoma cell line that was easy to use was deemed to be appropriate. To observe a change in proliferation when HECTD1 is overexpressed, U87 cells were transfected with empty vector (eV), wild type *HA-FL-mHectd1^{WT}* or the catalytically dead enzyme *HA-FL-mHectd1^{C2579G}* (Figure 6.7A). 48hrs post-transfection, U87 cells overexpressing wild-type mouse Hectd1 (HA-FL-mHectd1^{WT}) showed a significant 50% increase compared to the catalytic mutant and the empty vector control. This was also observed at 4 days post-transfection, which showed a 2-fold increase. However, at day 4, there was a significant increase in proliferation with the catalytic mutant compared to the eV control, however this is not to the same extent as the wild type protein. The viability of U87 transfected with either eV, wild type, or catalytic mutant constructs remained similar between the conditions throughout the 4 days, implying that there was no cell death (Figure 6.6B). Finally, a western blot confirmed the overexpression of HA-FL-Hectd1^{WT} and HA-FL-Hectd1^{C2579G} expressed at similar levels in U87 cells. This data suggests that overexpression of mHectd1 increases cell proliferation in both HEK293T and glioblastoma cell lines, and that this effect is dependent on the E3 ubiquitin ligase activity (Figure 6.8A).

Recently, it has been suggested that overexpression of HECTD1 in LN-299, a glioblastoma cell line, reduces colony formation in HECTD1 clones and negatively regulates Wnt signalling activity (Oikonomaki, *et al*. 2017). This suggests that in the LN-299 cell line,

HECTD1 overexpression may result in negative regulation of Wnt signaling. However, the evidence for this is limited because it is based on using HECTD1 overexpressing LN-299 clones, which may be affected by clonal selection. Furthermore, the western blot evidence provided to demonstrate that overexpression of HECTD1 does not convincingly show increased levels of HECTD1 protein. Therefore, this does not contribute to explain why in our hands overexpression of HECTD1 results in an increase in proliferation.

Finally, the localisation of HECTD1 in glioblastoma cell lines was identified, to elucidate whether HECTD1 would be likely to have a similar function in the cell cycle in glioblastoma cell lines as previously characterised in HEK293T, HEK293ET and HeLa cells. U87 cells were transfected with *HA-FL-mHectd1*^{WT}, and visualised using immunofluorescence to establish the localisation of HECTD1 in glioblastoma cells. As seen in Figure 4.5 in HEK293ET cells, HA-FL-mHectd1^{WT} localises to the mitotic spindle in U87 cells (Figure 6.8). This suggests that HECTD1 may serve a similar role in cell cycle regulation in glioblastoma cell lines.

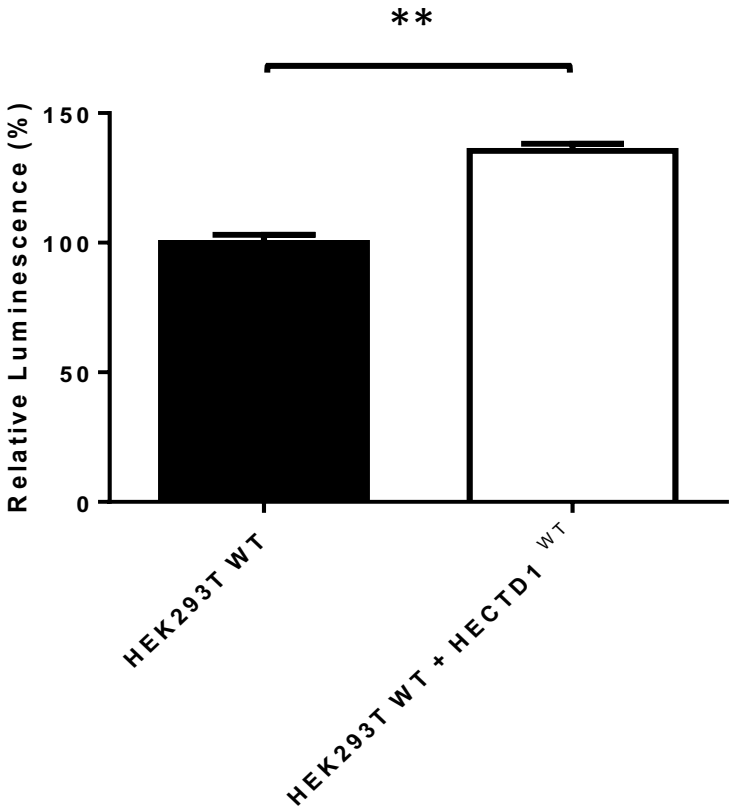

Figure 6.6. HA-FL-mHectd1^{WT} overexpression in HEK293T WT cell line. HEK293T WT cells were transfected with *HA-FL-mHectd1^{WT}*. Cells were transfected at 48hrs post-transfection with *HA-FL-mHectd1^{WT}* and an HA-tagged empty vector using PEI, in a 24 well format. Samples were harvested at 48h post-transfection. Cell proliferation count (relative luminescence) measured by CellTiter-Glo assay. Data plotted as mean with error bars that represent ±S.E.M, over three independent experiments (n=3), **p<0.01 by a paired student's t-test.

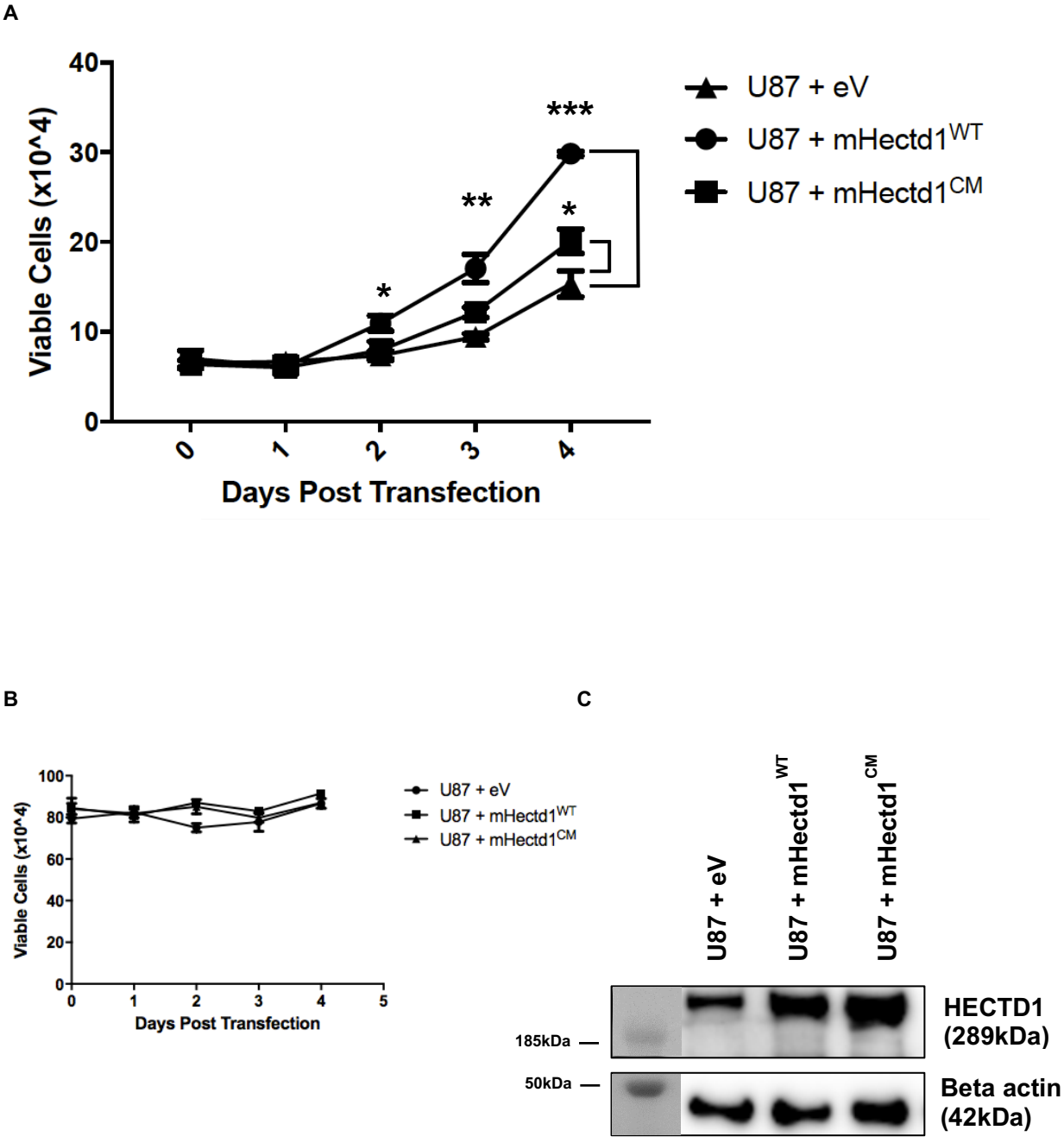

Figure 6.7. Increased cell proliferation upon overexpression of HA-FL-mHectd1^{WT} in U87 glioblastoma cell line. A) Viable cell count (x10^4), and B) showing cell viability for U87 cells transfected with 250ng either eV (empty vector), *HA-FL-mHectd1^{WT}* (mHectd1^{WT}), or *HA-FL-mHectd1^{C2579G}* (mHectd1^{CM}) and PEI. Samples were taken at intervals post-transfection. Harvested cells were counted using trypan blue to assess the viability of the cells. Data plotted as mean with error bars that represent ±S.E.M., over three independent experiments (n=3). ***p<0.001, **p<0.01, *p<0.05 by one-way ANOVA with a Dunnett's post-test. C) Western blot showing overexpression of HECTD1 in U87 cells. Molecular weight markers are superimposed on the left-hand side of the immunoblot.

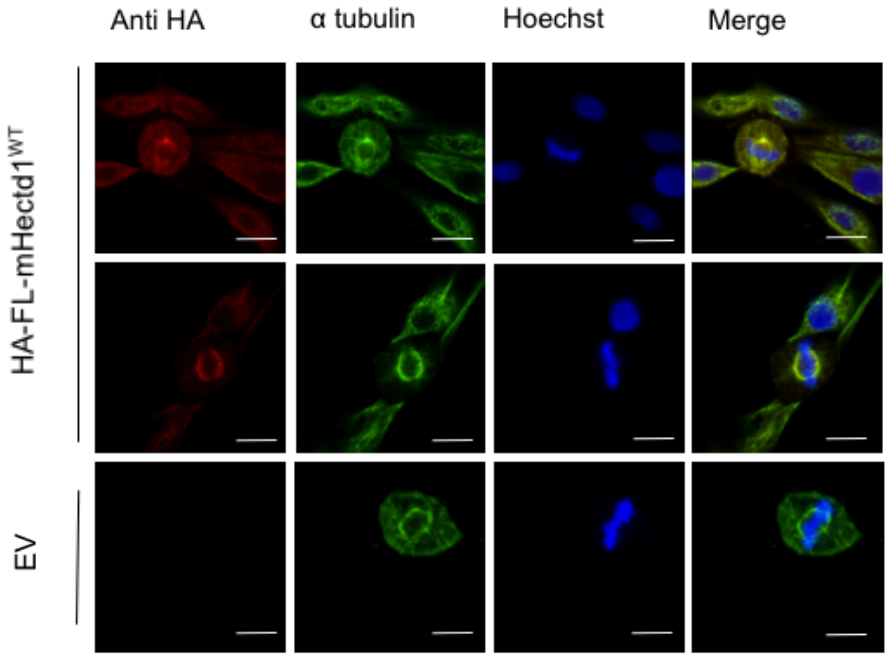

Figure 6.8. Localisation of HA-FL-mHectd1^{WT} in U87 glioblastoma cell line during mitosis. Representative images of HA-FL-mHectd1^{WT} in mitotic U87 cells. U87 cells were transfected with 500ng HA-mHectd1^{WT} and an HA-tagged empty vector using PEI, in a 12 well format. 24hrs post-transfection cells were fixed using 4% PFA, then stained with anti-HA, anti-α-tubulin and Hoechst. Images were taken using the LSM Meta 510 Confocal Microscope Scale bar represents 10μm.

6.2.5. HECTD1 depletion results in reduced glioblastoma cell line proliferation

This thesis has identified a cell cycle function for HECTD1, which appears to correlate with the increased proliferation seen in HEK293T and U87. It was therefore hypothesised that depletion of HECTD1 may result in decreased proliferation as seen in HEK283ET, HEK293T, and HeLa cells.

In order to further implicate HECTD1 as a therapeutic target in glioblastoma, loss-of-function experiments were carried out in both U87 and U251 (Figure 6.9). The U251 cell line is derived from human glioblastoma astrocytoma, and like U87, has been used for cancer studies such as the molecular profiling of MPS1 gene silencing in glioblastoma (Shankavaram, *et al.* 2015). Here, both cell lines were used to ensure that any observed change in proliferation as a result of HECTD1 knockdown was not cell line specific. Interestingly in both U87 and U251, the number of viable cells decreased in the cells treated with HECTD1 SMARTpool (SP) siRNA when compared to the non-targeting (NT) siRNA control (Figure 6.9A, C). Here, the reduced proliferation phenotype is similar to the reduction of proliferation seen in Figure 3.1 with HEK293ET and HeLa cells. In U87 cells, by day 3, there is a significant decrease in the number of viable cells in HECTD1 SMARTpool (SP) siRNA treated cells compared to the NT control (35% decrease in HECTD1 SMARTpool (SP) treated U87). (Figure 6.9A). However, by day 4 the decrease is no longer significant suggesting that the knockdown may not be as efficient at 96h post-transfection. Again, there was no change in viability across the 4 days between the cell lines (Figure 6.9B) suggesting that the cells are not undergoing cell death mechanisms. In U251 cells, there was a sustained significant decrease in the number of viable cells observed when comparing those treated with HECTD1 SMARTpool (SP) siRNA and NT siRNA from day 2 to day 4 (Figure 6.9C) (30% decrease in HECTD1 SMARTpool (SP) treated U251). Similarly, there was no change in viability between the NT and HECTD1 SMARTpool (SP) siRNA treated cells over the 4 days (Figure 6.9D), therefore indicating that the reduction in viable cell number is as a result of decreased proliferation, rather than increased cell death. Finally, western blots showed that in both U87 and U251, HECTD1 was efficiently knocked down at 48h post-transfection (Figure 6.9E,F). Taken together, this suggests that HECTD1 depletion could be a strategy to reduce cell proliferation in glioblastoma cells and potentially other cancer cell lines where it is found to be overexpressed. Hence, given that the increase in proliferation has been shown to be driven by the ubiquitin ligase activity of HECTD1 in HEK293T cells, it is therefore speculated that targeting this activity could phenocopy the observed decrease in cell proliferation obtained upon HECTD1 depletion.

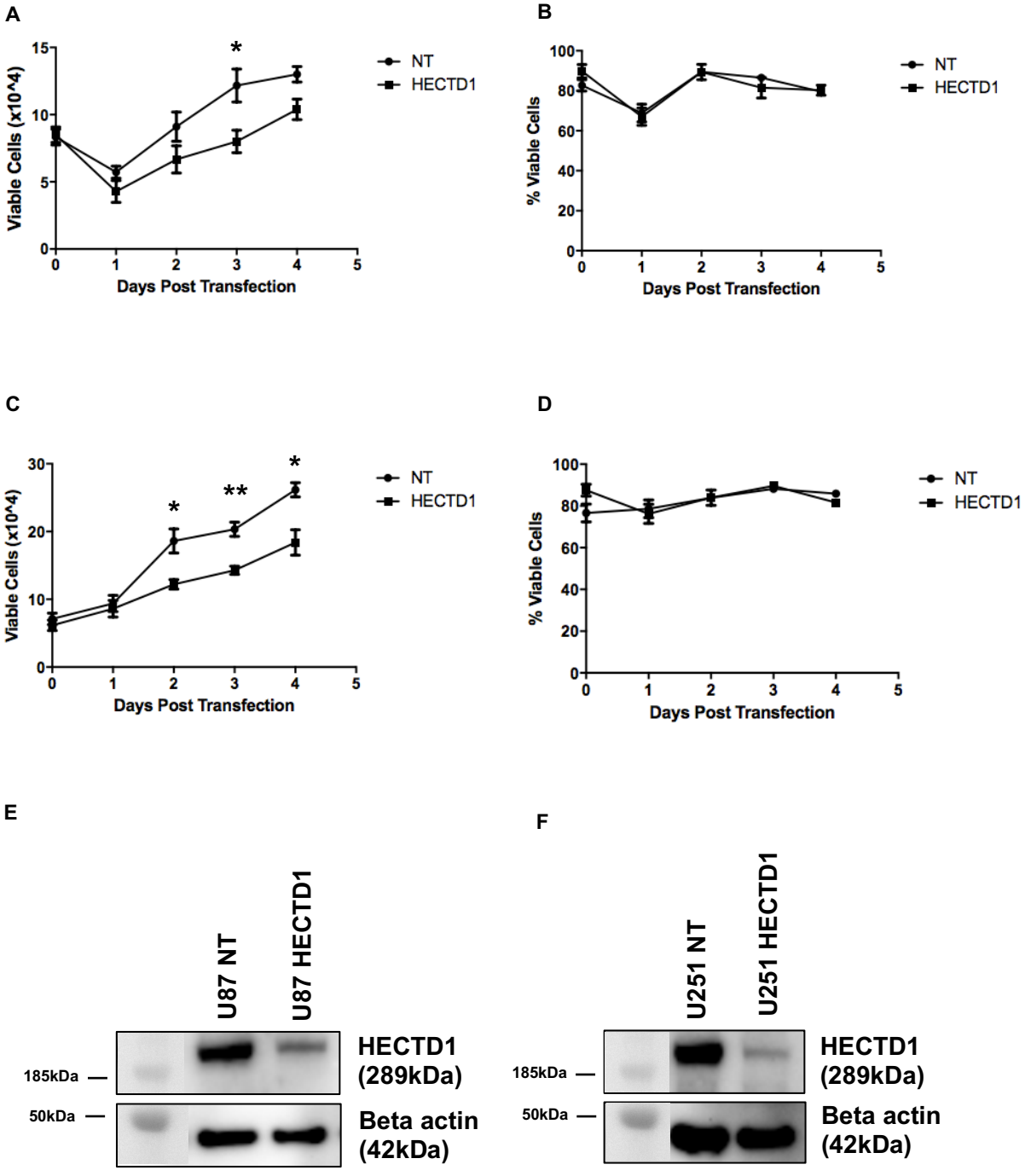

Figure 6.9. Reduced cell proliferation upon HECTD1 transient depletion but no effect in cell viability in glioblastoma cell lines. Viable cell count (x10^4) for U87 A) and U251 C) and cell viability (%) for U87 B) and U251 D) which had been treated with non-targeting siRNA and HECTD1 smart pool siRNA. Samples were taken at intervals post-transfection with 20pmol siRNA and Lipofectamine 2000®. Harvested cells were counted using trypan blue to assess the viability of the cells. Data plotted as mean with error bars that represent ±S.E.M., over three independent experiments (n=3). **p<0.01, *p<0.05 by paired student's t-test. Western blots indicating knockdown for U87 E) and U251 F) 48h post knockdown. Molecular weight markers are superimposed on the left-hand side of the immunoblot.

6.2.6. qRT-PCR in glioblastoma samples

To establish whether HECTD1 may be a novel biomarker or therapeutic target for glioblastoma, Dr K Kurian at Bristol Southmead Hospital provided the lab with cDNA from glioblastoma patients. Initially, 22 patients out of 50 cDNA samples provided by Dr K Kurian were analysed using qRT-PCR. The mRNA levels of *HECTD1* were compared to two housekeeping genes *RPS18* and *RNA Pol II*. These two housekeeping genes were selected because they are expressed at a relatively constant rate and at a high abundance (Kozera & Rapacz. 2013). *RPS18* has been shown to be a reliable housekeeping gene for head and neck squamous cell carcinoma gene expression studies and for tumour neovascularisation studies (Lallemant, *et al.* 2009; Rienzo, *et al.* 2013). Furthermore, *RNA pol II* has been demonstrated to have the most constant expression in different tissues and in human acute lymphoblastic leukaemia cells compared to other housekeeping genes, making it a suitable housekeeping gene for cancer (Radoníc, *et al.* 2004).

However, as seen in Figure 6.10, there were large variations between the normalisation to *RPS18* and *RNA Pol II*. The *HECTD1* mRNA relative expression was around 5-fold less when normalised with *RNA Pol II*, compared to *RPS18*. Furthermore, the trends of HECTD1 expression vary between the samples normalised to the two reference genes. For example, in sample 5 the relative *HECTD1* mRNA expression was the highest relative to the 6 samples screened when normalised to *RPS18* (Figure 6.10A), however this pattern was not seen when normalised to *RNA Pol II* (Figure 6.10B). This was seen in another sample set where, sample 8 showed the highest relative *HECTD1* mRNA, in samples 7-14, when normalised to *RPS18* (Figure 6.10C), which again was not reproduced when normalised to *RNA Pol II* (Figure 6.10D). Finally, sample 22 when normalised to *RNA Poll II,* showed the highest relative *HECTD1* mRNA expression, in samples 15 - 22 (Figure 6.10F), which was not seen when normalised to *RPS18* (Figure 6.10E).

Taken together this suggests that either or both *RNA Pol II* and *RPS18* are not the most appropriate reference genes to use for glioblastoma samples. Furthermore, the use of these two primer sets in combination result in data with a large degree of variance, potentially masking any observed changed in *HECTD1* mRNA expression between different patients. Therefore, other primer sets should be used to assess HECTD1 relative expression in glioblastoma patient cDNA. A further consideration is that in some samples C_T value of *HECTD1* was very low, compared to the no sample control. The low levels of *HECTD1* mRNA may be due to no or very low levels of HECTD1 or to poor quality of the samples and therefore the data for HECTD1 may be less reliable. The cDNA was extracted from paraffin embedded archived tissues, which is known to lead to fragmented RNA (Zeka, *et al*. 2016), therefore this could affect the readout for HECTD1 expression.

Given the issues with the differences in normalisation with both *RNA Pol II* and *RPS18* as housekeeping genes, a literature search was carried out to determine the most appropriate housekeeping genes for glioblastoma. Valente, *et al.* (2009) screened a panel of different primer sets for housekeeping genes for their suitability in human glioblastoma cDNA. This found that instead of the commonly used *beta actin, GAPDH, and RPS18,* the two most suitable reference genes were *TATA-Box binding protein* (*TBP*) and *Hypoxanthine guanine phosphoribosyl transferase 1* (*HPRT1*) used in combination (Valente, *et al.* 2009). Therefore, using RNA extracted from U87 and U251, the *TBP* and *HPRT1* primers were used alongside the original *RNA Pol II* and *RPS18* primers to test for their suitability as primers for qRT-PCR (Figure 6.11). It can be seen by gel based RT-PCR that all of the primers were suitable for U251, giving a strong clear signal for each primer set (Figure 6.11B). None of the primer sets showed contamination, with the exception of *RPS18* primers, which in both cell lines showed some level of background in the negative controls as a result of either contamination (Figure 6.11A) or primer dimers (Figure 6.11B). Furthermore, *RPS18* primers in U87 yielded a weaker cDNA band in comparison to the other housekeeping primer sets (Figure 6.11A). Therefore, this suggests that *RPS18* may not be a suitable housekeeping gene for qRT-PCR using glioblastoma patient cDNA and given the screen carried out by Valente, *et al.* (2009), *TBP* and *HPRT1* should be used as reference genes in the future.

Given that this study is still in progress, correlations between HECTD1 expression and the type of samples and the corresponding meta data were not carried out at this stage.

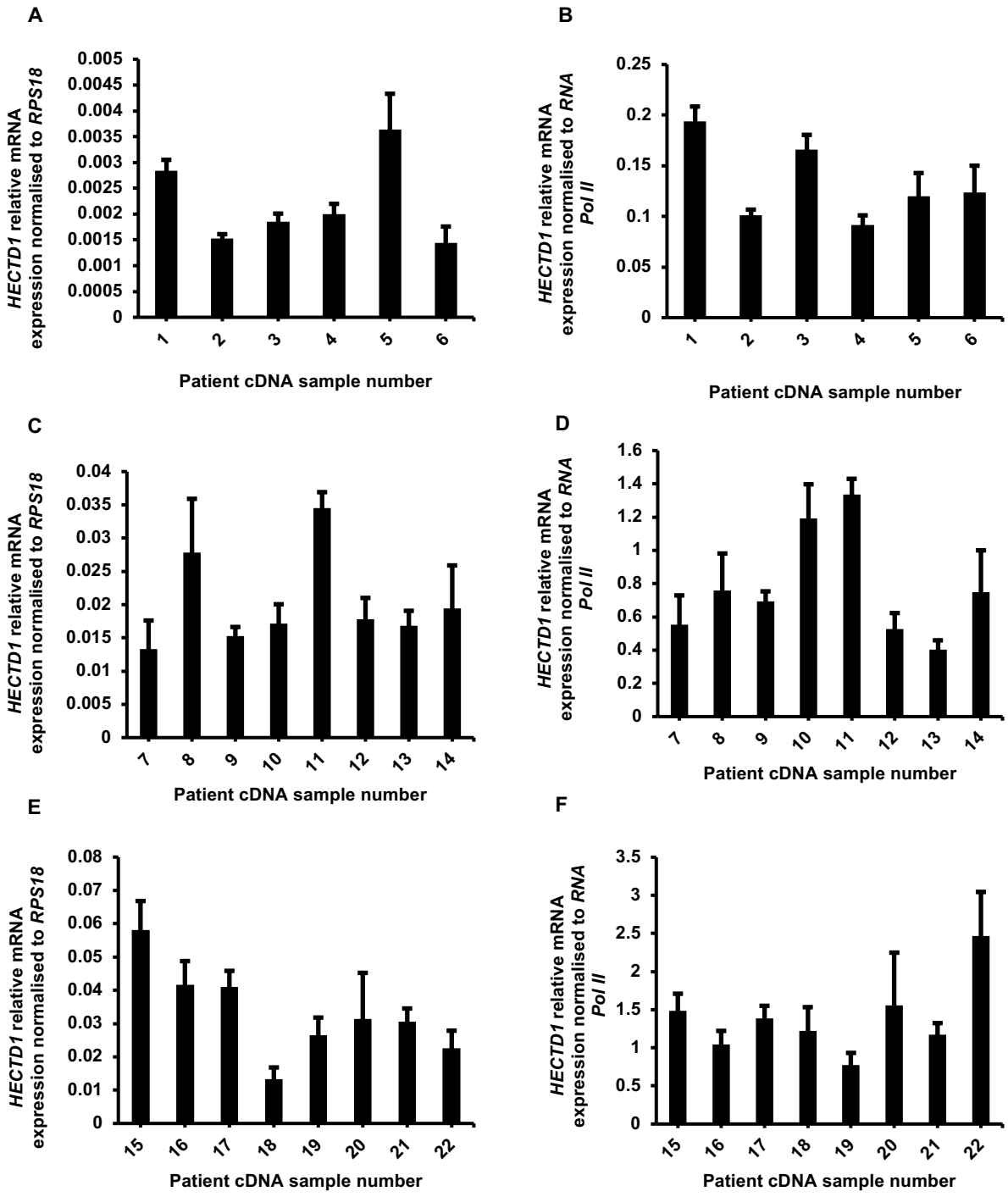

Figure 6.10. *HECTD1* mRNA expression in glioblastoma patient cDNA samples relative to *RPS18* and *RNA Pol II*. Glioblastoma patient cDNA was provided by Dr K Kurian (Bristol Southmead Hospital). Relative *HECTD1* mRNA levels were determined by qRT-PCR and normalised to two reference genes, *RPS18* and *RNA Pol II*. Samples 1-6 normalised to A) *RPS18* and B) *RNA Poll II*. Samples 7-14 normalised to C) *RPS18* and D) *RNA Poll II*. Samples 15-22 normalised to E) *RPS18* and F) *RNA Pol II.* Data are present as mean relative expression ± S.E.M.

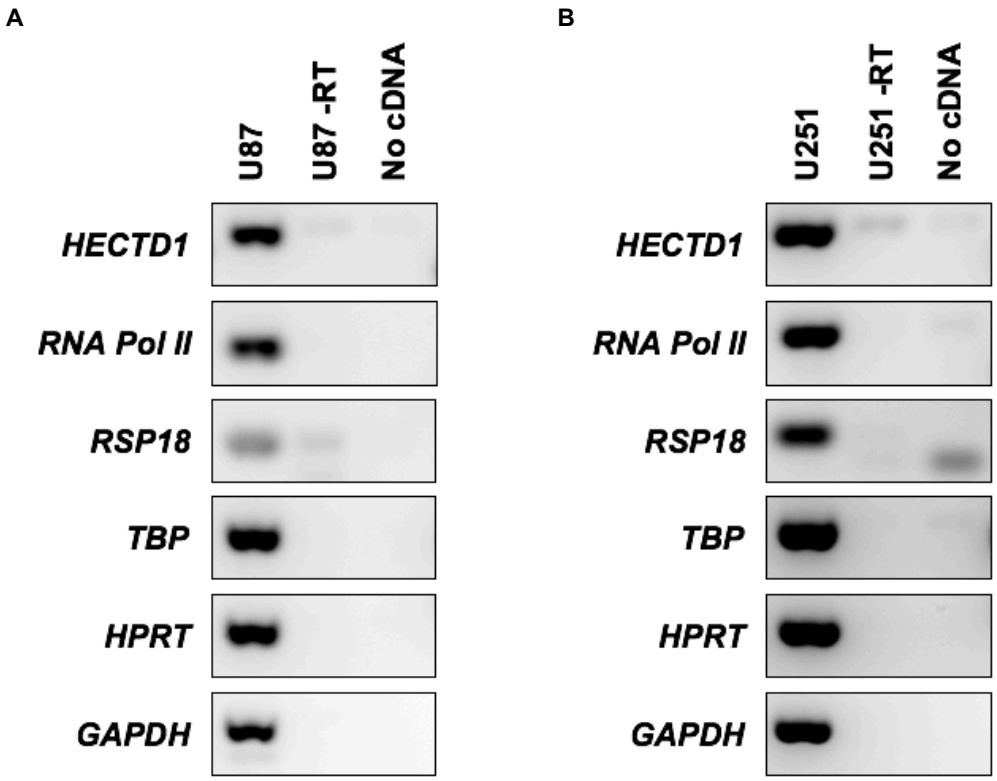

Figure 6.11. A panel screen of glioblastoma cancer cell lines to assess primers for qRT-PCR. 3% agarose gel stained with GelStar™ showing the resolution of RT-PCR products, including *HECTD1* and housekeeping gene expression in A) U87 and B) U251 glioblastoma cancer cell lines. Primers for *HECTD1*, *RNA Pol II*, *RPS18*, *TBP*, *HPRT*, and *GAPDH* were used on both cell lines. -RT and no cDNA were used as negative controls.

6.3. Discussion:

In order to implicate HECTD1 in cancer development, both tumour suppressive and oncogenic functions were explored. Initially to explore the role of *HECTD1* as a tumour suppressor, the epigenetic regulation of *HECTD1* was characterised in lung cancer cell lines (NSCLC). A CpG island was identified in the promoter of *HECTD1* using the UCSC genome browser, which suggested a possible site of DNA methylation within the sequence of *HECTD1*. Therefore, the DNA methylation status of *HECTD1* in NSCLC cell lines was screened to see if *HECTD1* functioned as a tumour suppressor in this type of cancer. However, it was revealed that HECTD1 expression does not appear to be regulated by DNA methylation in NSCLC, and therefore is likely to not have a tumour suppressor role in this cancer. To explore the role of *HECTD1* as an oncogene, using cBioPortal, it was identified that *HECTD1* is mutated and amplified in numerous cancers. To test, this predicted oncogenic role in a specific cancer model, a collaboration was established with Dr K Kurian. Unpublished data has previously reported that HECTD1 is overexpressed in glioblastoma patient samples. In agreement with this finding, the cancer database Oncomine^{TM} showed that *HECTD1* mRNA was increased in glioblastoma patient samples in comparison to normal brain samples. HECTD1 overexpression in a glioblastoma cell line, U87, showed an increase in cell proliferation. Furthermore, HECTD1 depletion was associated with reduced proliferation in glioblastoma cell lines. This therefore suggests an oncogenic role of *HECTD1* in glioblastoma. The final work carried out involved screening of 50 cDNA patient samples to confirm the overexpression of HECTD1 in patient samples, however this experiment required further optimisation.

6.3.1. *HECTD1* does not appear to be regulated by methylation in NSCLC cell lines

To establish whether *HECTD1* functioned as a tumour suppressor, the epigenetic regulation of *HECTD1* was characterised. It was found that within the *HECTD1* sequence, there is a CpG island that spans the first exon, suggesting that *HECTD1* may be regulated by DNA methylation. However, a screen of lung cancer cell line cDNA revealed that HECTD1 is expressed in both the untreated DMSO samples and the Aza treated samples. Indicating that in NSCLC cell lines, HECTD1 expression does not appear to be regulated by DNA methylation. It is not possible to completely rule out the role of DNA methylation in the regulation of *HECTD1* in NSCLC due to the lack of a positive control, however there are only two known examples of HECT ligases that are regulated by hypermethylation in cancer out of the 18 ligases that have been published in cancer formation (Zhang, *et al.* 2007; Sakata, *et al.* 2009; Sakata, *et al.* 2013; Goka & Lippman. 2015; Wrage, *et al*. 2015).

Screening of other cell lines may reveal that DNA methylation occurs in other cancers that result in downregulation of *HECTD1*. The database Oncomine, could be used to help identify cancers which show *HECTD1* silencing, for example, in mixed gastric adenocarcinoma *HECTD1* mRNA expression shows a negative 2.5-fold change compared to noncancerous cells (Oncomine, accessed 30/09/17). If DNA methylation is shown to be important for *HECTD1* regulation in cancers such as gastric adenocarcinomas, the methylation status of the CpG island could be studied using bisulphite genome sequencing (Li & Tollefsbol. 2011). Bisulphite genome sequencing involves bisulphite treatment of DNA, converting exposed cytosine bases into uracil bases, whilst methylated cytosine bases are protected from conversion. Following this treatment, samples are sequenced to reveal the extent of the cytosine methylation (Li & Tollefsbol. 2011). However, DNA methylation is only one form of epigenetic regulation, and it is possible that other forms of epigenetic regulation are involved in *HECTD1* regulation in other cancers. In addition to DNA methylation, histones can be modified by acetylation, methylation, ubiquitination, and phosphorylation affecting gene expression and result in cancer (Baxter, *et al*. 2014). For example, H3K27 acetylation is associated with active enhancers which lead to promoting of gene expression (Creyghton, *et al.* 2010). The UCSC genome browser highlighted high H3K27 acetylation in the promoter region of *HECTD1*, indicating that this enhancer may be active potentially leading to increased gene expression. Furthermore, in colorectal cancer patient samples it was found that H3K27 acetylation of histones was increased, suggesting its role in regulating genes involved in the development of colorectal cancer (Karczmarski, *et al.* 2014). As future work a Chromatin Immunoprecipitation Pulldown (ChIP) assay could be used to assess the histone modification status to understand *HECTD1* regulation within different cancer samples (O'Geen, *et al.* 2011).

6.3.2. *HECTD1* is mutated and amplified in multiple cancers

Since HECTD1 was expressed in the lung cancer cells screened, it appeared that it might not behave as a tumour suppressor in cancer. In this thesis, HECTD1 has been shown to control cell cycle progression, regulating the timely progression through mitosis. Furthermore, HECTD1 has been previously reported to have a role in Wnt signalling, transcriptional regulation, cell adhesion and migration (Sarkar, *et al.* 2012; Li, *et al.* 2013b; Tran, *et al.* 2013; Li, *et al*. 2015; Shen, *et al*. 2017). In cancer, mechanisms that regulate cell cycle progression and cell migration are often exploited. For example, UBE3C is overexpressed in renal carcinoma and results in over-activation of the Wnt signalling pathway (Wen, *et al*. 2015). Whilst HUWE1 overexpression promotes cell migration by increased TIAM1 degradation in lung cancer (Vaughan, *et al.* 2015). Therefore, a hypothesis may be that *HECTD1* is amplified in cancer.

Using cBioPortal it was found that in many different cancer types *HECTD1* was amplified, furthermore it showed that *HECTD1* was also mutated. Interestingly, both amplification and mutations of genes are oncogene activation mechanisms (Niedercher, *et al*. 1999), supporting the hypothesis that *HECTD1* behaves as an oncogene. In the two lung cancer studies (Figure 6.3), it was found that the majority of *HECTD1* alterations were amplifications, however in most other cancers the *HECTD1* alterations were as a result of mutations. In addition, the mutations that occur within *HECTD1* were found to occur throughout its sequence and not located at one loci, indicating that there was no mutation hotspot in the sequence of *HECTD1*. Mutations are regarded as a hallmark of cancer and facilitate the evolution of the cancer (Loeb & Loeb. 2000). A number of cancer candidate (CAN) genes have seen identified by somatic screens of mutations to search for cancer therapeutics. In glioblastoma, melanoma, and pancreatic cancers, 19 CAN genes were identified because they displayed a mutation frequency above 10% in these cancers. In addition, some of these genes were found to encode protein kinases, opening the possibility for drug discovery (Balakrishnan, *et al*. 2007). Therefore, a high mutation frequency in *HECTD1* could suggest that its function needs to be modified in order to provide cancer cells with a growth advantage. Mutations can result in a gain of function, for example expression of mutant p53 resulted in enhanced tumorigenic potential (Dittmer, *et al*. 1993), which may result in a cancer promoting mutant of HECTD1. Mutations in *HECTD1* could occur within a localisation domain, changing the functional localisation or within the HECT domain of HECTD1 resulting in an increase in ligase activity. This may lead to oncogenic mutations that result in a new activity for HECTD1 or increased activity that leads to cancer development. However, without functional characterisation of the effect on these mutations, the mechanism by which these mutations can cause cancer is only speculative.

6.3.3. HECTD1 as a novel biomarker or therapeutic target for glioblastoma

Finally, to test an oncogenic role for *HECTD1* in a cancer model, a collaboration was established with Dr K Kurian at Bristol Southmead Hospital, to elucidate the role of HECTD1 in glioblastoma. Taking into account the data in Chapters 3, 4, and 5 showing that HECTD1 regulates cell cycle progression, it was next hypothesised that this mechanism could be at play and contribute to an increase in cell proliferation upon overexpression of wild-type, but not the catalytic dead HECTD1.

Currently, there are 4 commonly used biomarkers used to detect and grade glioblastoma allowing for personalised treatment. These are *isocitrate dehydrogenase 1* (*IDH1*) mutations, 1p/19q codeletion, TERT promoter methylation, and O-6-methylguanine-DNA methyltransferase promoter methylation (Haynes, *et al.* 2014; Weller, *et al.* 2015). For

example, *IDH1* mutations are more common in lower grade gliomas in younger patients. These patients with *IDH1* mutations are further subdivided into those with either 1p/19q codeletion or TERT promoter methylation. Finally, O-6-methylguanine-DNA methyltransferase (MGMT), is a DNA repair protein, and interestingly, patients with MGMT promoter methylation had a higher survival rate when treated with temozolomide (TMZ) than those without MGMT promoter methylation (Weller, *et al*. 2015). TMZ, one of the only chemotherapies for glioblastoma, works by alkylating or methylating DNA, often occurring at the N-7 or O-6 positions on guanine residues and results in DNA damage and cell death of tumour cells (Newlands, *et al.* 1997; Jacinto & Esteller. 2007). However, in patients without O-6-methylguanine-DNA methyltransferase promoter methylation, MGMT is able to repair this DNA damage and prevent cell death, reducing the efficacy of TMZ (Jacinto & Esteller. 2007). Highlighting that despite the research into glioblastoma, the cancer is still related with a poor prognosis, and presents limited treatment options for the patients. Furthermore, there is only one main chemotherapy available to patients limiting the treatment options.

Interestingly, the HECT ligase UBE3C has been shown to be overexpressed in glioblastoma and correlated with high grade tumours, poor survival and early tumour recurrence (Pan, *et al.* 2015). Here, UBE3C ubiquitinates and degrades the calcium-dependent phospholipid binding protein, Annexin A7, facilitating migration and invasion of glioblastoma (Pan, *et al.* 2015). This provided the first example that the ubiquitin system might be an attractive target for cancer therapies, specifically in GBM. Therefore, targeting of the ubiquitin system, specifically HECT ligases, may provide further treatment options for patients with glioblastoma. Given that TMZ is one of the only chemotherapies for glioblastoma, and this is ineffective in patients without O-6-methylguanine-DNA methyltransferase promoter methylation, there is great demand for a new therapeutic. The potential of HECTD1 as a novel therapeutic holds large promise, given that it can be enzymatically targeted, and the ubiquitin proteasome system has the potential to furnish many cancer therapeutics (Weathington & Mallampalli. 2014). Compellingly, knockdown of HECTD1 resulted in decreased proliferation in glioblastoma cell lines, and this suggests that the inhibition of the catalytic activity of HECTD1 could result in reduced proliferation, potentially providing a novel glioblastoma therapeutic target. There is already evidence to suggest that targeting the ubiquitin proteasome system is an attractive therapeutic. For example, VLX1570 has been shown to inhibit proteasome associated DUB, USP14, and induce apoptosis in multiple myeloma cells (Wang, *et al.* 2016). When USP14 was transiently knocked down this mimicked the effect caused by VLX1570, reducing proliferation and viability of multiple myeloma cells (Wang, *et al.* 2016).

6.4. Future work:

To further establish a clinical relevance for HECTD1 in glioblastoma, in addition to the qRT-PCR screen of glioblastoma patient samples, immunohistochemistry (IHC) on glioblastoma tissue sections could be performed to look for HECTD1 protein expression in these tissues. Here, HECTD1 could be validated as a diagnostic marker, by screening different cohorts of glioblastoma patients. HECTD1 expression could be correlated with patients of different age or with different grades of glioblastoma. For example, *IDH1* mutations are more common in lower grade gliomas in younger patients. HECTD1 and IDH1 expression by IHC can be used to see whether HECTD1 expression correlated with IDH1 in young patients with a lower grade of glioblastoma.

To validate the hypothesis that HECTD1 depletion results in a decrease in cell proliferation, HECTD1 depletion mouse models can be carried out. Here, shRNA can be transfected into a glioblastoma cell line, such as U87, that is luciferase-expressing (Seibler, *et al*. 2007). These cells can then be injected into the tail vein of a mouse, for example a T-cell deficient nude mouse (Ikehara, *et al*. 1984). The bioluminescence of HECTD1 depleted cells compared to control cells will reveal the extent of tumour formation. The aim here would be to demonstrate that HECTD1 depletion decreases glioblastoma cell proliferation *in vivo*, and would implicate it as a potential new drug target.

Finally, using a retroviral virus containing a selectable marker (such as neomycin) for longer-term overexpression (Deregowski & Canalis. 2008) of full length human HECTD1 in U87 and U251, a colony formation assay could be performed to demonstrate how the increase in the proliferation could result in tumour formation. To establish whether HECTD1 plays an oncogenic role in the pathogenesis of glioblastoma, HECTD1 should be overexpressed *in vivo*, such as in transgenic mice, in a xenograft cancer model. For example, as demonstrated with the transcription factor, PDX1, transgenic mice models can be generated that express the gene of interest using the Tetracycline inducible system. The Tetracycline transactivator (tTA) can be targeted to specific cell populations using Bacterial Artificial Chromosomes (BAC) transgenic mice to produce, in this case, pancreatic progenitor cells that overexpress the gene of interest (Blondeau, *et al*. 2012). For use in this project, this system could be used to induce overexpression of HECTD1 in astrocytes, for example, to monitor for tumour formation and to demonstrate that HECTD1 overexpression results in glioblastoma *in vivo*. However, an important consideration is that for this experiment to be successful, HECTD1 would have to first be identified as a key driver of glioblastoma.

Chapter 7: Final discussion

7.1. The role of HECTD1 in cell cycle regulation

In this thesis HECTD1 has been identified as a novel cell cycle regulator. Transient depletion and knockout of HECTD1 resulted in a delayed mitotic phenotype. Interestingly, whilst the mechanism behind the regulation of HECTD1 in the cell cycle was not fully characterised, the cell cycle phenotype identified was similar to those cell cycle phenotypes associated with delayed SAC satisfaction. For example, as seen with the mitotic spindle regulator, JMJD5 (He, *et al*. 2015). The delay in NEBD to Anaphase onset associated with HECTD1-depletion suggests that cells are unable to progress through mitosis as quickly as cells that express HECTD1 (Figure 7.1). This was further evidenced by the enrichment of cells in metaphase observed in HECTD1-depleted and knockout cells. This enrichment of cells in metaphase suggests that cells are prolonged at this phase, where the SAC is active. Eventual satisfaction of the SAC results in cells that can progress from metaphase to anaphase and go on to complete mitosis (Murray. 1994; Stern & Murray. 2001). Satisfaction of the SAC depends on microtubule attachment resulting in sufficient inter-kinetochore tension (Stern & Murray. 2001; Uchida, *et al.* 2009; Mansfeld, *et al.* 2011). This then results in the activation of the APC/C, resulting in proteasomal degradation of Cyclin B1 and securin, triggering sister chromatid separation and exit from mitosis (Glotzer, *et al*. 1991; Holloway, *et al.* 1993; Cohen-Fix & Koshlan. 1999). Furthermore, it was shown that the E3 ligase activity of HECTD1 is required to rescue the mitotic phenotype, so therefore, the K29/K48 ubiquitin chains synthesized by HECTD1 may be involved in its function in the cell cycle.

A possible explanation for the hypothesised delay in SAC satisfaction, is that HECTD1 has a role in regulating mitotic spindle formation. Mitotic spindle regulators such as NuMA and JMJD5 show similar phenotypes to HECTD1 depletion (Haren, *et al*. 2009; He, *et al*. 2015). Despite the lack of a clear mechanism for the regulation of the mitotic spindle by HECTD1 (Chapter 5), there is evidence to suggest that this may be an area worth further investigation in the future. For example, Tran, *et al.* (2013) found that HECTD1 depletion resulted in cells that had reduced microtubule stability. Here, it is hypothesised that the negative regulation of the APC conferred by HECTD1 results in destabilisation of microtubules (Tran, *et al*. 2013). The APC is a tumour suppressor protein that is also a conventional microtubule associated protein, which functions to bind to microtubules to stabilise them (Mimori-Kiyosue & Tsukita. 2003). The APC has been implicated in the regulation of the mitotic spindle, together with its binding partner, EB1, a tubulin binding protein (Berrueta, *et al.* 1998; Mimori-Kiyosue & Tsukita. 2003; Green, *et al.* 2005). Furthermore, EB1 has been shown to be associated with familial and sporadic forms of colorectal cancer (Berrueta, *et al.* 1998). Interestingly, Cyclin A/CDK2-dependent phosphorylation of APC in late G2, is required for mitotic spindle localisation to the central position in cells (Beamish, *et al.* 2009).

The APC has been identified as a substrate for HECTD1 (Tran, *et al*. 2013). Therefore, HECTD1 may be recruited to the mitotic spindle during mitosis to function in its regulation of the cell cycle. This is possibly mediated through APC or its binding partner, EB1, which has been shown to colocalise with the mitotic spindle (Berrueta, *et al.* 1998; Green, *et al.* 2005), showing similar staining to HECTD1 in mitosis. Here, HECTD1 may facilitate the regulation of the mitotic spindle.

Additionally, another previously identified HECTD1 substrate, HSP90, was shown to be required for the localisation of Cyclin B1 and Msps/ch-TOG to the mitotic spindle in both *Drosophila. M* and Humans (Basto, *et al*. 2007). Msps/ch-TOG is required for microtubule dynamics and mitotic spindle formation (Byrnes & Slep. 2017). Therefore, a hypothesis is that HECTD1 regulates HSP90 localisation as seen in Sarkar, *et al*. (2012), which in turn regulates localisation of the mitotic spindle regulator Msps (Byrnes, & Slep. 2017). Therefore, in HECTD1-depleted cells, a potential hypothesis is that the localisation of HSP90 is perturbed resulting in aberrant MSPS localisation, preventing correct formation of the mitotic spindle, and so resulting in prolonged SAC activation. Alternatively, another explanation for the phenotype observed in HECTD1-depleted and knockout cells is that HECTD1 regulates the inter-kinetochore distance directly. It has been shown that HECTD1 is associated with condensins I and II, which function to recruit HECTD1 to active gene enhancers (Li, *et al*. 2015). Codensins have been previously implicated in facilitating kinetochore tension at the centromeres, to ensure correct segregation of sister chromatids (Yong-Gonzalez, *et al.* 2009). In cells depleted of condensin I, the inter-kinetochore stretching is not sufficient to inactivate the spindle assembly checkpoint. The associated phenotype results in cells with an increased NEBD to Anaphase onset, similar to the observed phenotype upon HECTD1 depletion or knockout (Uchida, *et al.* 2009). Therefore, HECTD1 could be recruited by condensin I to the kinetochores to mediate sufficient inter-kinetochore tension. Whilst, conversely, a loss of HECTD1 may result in loss of inter-kinetochore tension. A final consideration is that future experiments may identify a novel HECTD1 substrate, which is cell cycle specific. From the experiments outlined in Chapter 5, it would be possible to probe for novel HECTD1 substrates, which may begin to elucidate the mechanism by which HECTD1 regulates the cell cycle.

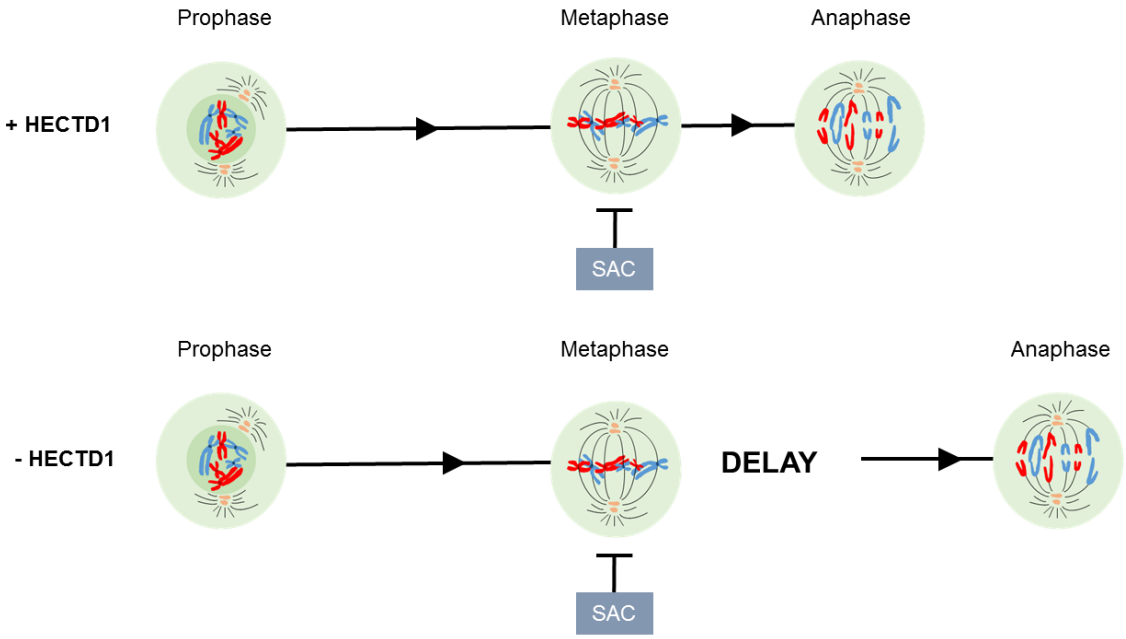

Figure 7.1. Schematic of the hypothesised role of HECTD1 in mitotic progression. HECTD1-depleted cells and control cells are able to enter mitosis at the same time, where they progress until metaphase. Here, at metaphase the SAC acts as a checkpoint to prevent mitotic progression until each kinetochore is attached to the mitotic spindle. It is hypothesised that in HECTD1-depleted cells, the observed delay in NEBD to anaphase onset is as a result of prolonged SAC activation. This delay in the satisfaction of the checkpoint results in a delay until anaphase onset, where cells are then able to progress to complete mitosis.

7.2. K29/K48 ubiquitin chains in cell cycle regulation?

The E3 ligase activity of HECTD1 was shown to be required to rescue the mitotic phenotype associated with HECTD1-depletion. In addition, K29-linked ubiquitin chains were found to be present during the cell cycle and mitosis. Therefore, a hypothesis is that the K29/K48 atypical activity of HECTD1 is involved in its cell cycle function. Atypical ubiquitin chains have been demonstrated to function in the cell cycle. For example, it has been shown that K11/K48 chains synthesised by the APC/C together with UBE2S and UBE2C result in the degradation of cell cycle substrates such as Cyclin A, CDC20, p21, and NEK2A (Meyer & Rape. 2014; Yau, *et al.* 2017).

The role that mixed and branched ubiquitin chains have in different cellular functions is still largely unknown. This is in part due to the difficulty in discerning the chain topology in heterotypic chains. Each unique ubiquitin chain topology confers different functions within the cell (Komander. 2009). Therefore, a consideration is that whilst HECTD1 has been shown to synthesise K29/K48-linked ubiquitin chains, the topology of these chains and the

signal they confer is unknown. A combination of linkage selective UBDs and DUBs has been used to investigate the different composition of heterotypic chains (Emmerich & Cohen. 2015; Heap, *et al*. 2017). Heterotypic ubiquitin chains come in two forms: mixed and branched. Mixed ubiquitin chains are defined by comprising different linkages but each ubiquitin is modified with only one other ubiquitin molecule. Whilst branched ubiquitin chains are composed of single ubiquitin subunits that have been modified with two or more ubiquitin molecules (Yau & Rape. 2016) (Figure 1.8). Interestingly, biophysical studies have implied that mixed and branched ubiquitin chains confer distinct signals (Nakasone, *et al*. 2013). Linkage-selective receptors from hHR23A and RAP80 were found to bind preferentially to K48 or K63 linkages that were in a branched trimer, furthermore the 26S proteasome recognised and processed these branched chains (Nakasone, *et al*. 2013).

Interestingly, Meyer, *et al.* (2014) demonstrated that heterotypic ubiquitin chains of K11/K48 synthesised by the APC/C were branched and not mixed linkages. This was achieved by the insertion of a Tobacco Etch Virus (TEV) protease cleavage sequence into the Glu-53 residue within ubiquitin. This enabled protease cleavage at this site, which generated a TEV sequence-containing signature peptide upon cleavage of the polyubiquitin chains using TEV. The proteins were then analysed by western blot to show a change in molecular weight in accordance with the number of TEV cleavage peptides as evidence for branched ubiquitin chains (Meyer, *et al.* 2014) (Figure 7.2). Furthermore, the generation of a bi-specific antibody against K11/K48 permitted the recognition and characterisation of branched K11/K48 chains synthesised by the APC/C in cells (Yau, *et al*. 2017). Here, branched ubiquitin chains are suggested to serve a role in substrate degradation (Meyer, *et al.* 2014; Yau, *et al*. 2017).

Interestingly, it has been recently found that branched chains containing K29-linked ubiquitin are more likely to be involved in non-degradative signalling (Crowe, *et al*. 2017). UbiChEM-MS has been demonstrated to characterise branching in polyubiquitin chains (Xu, & Peng. 2008; Valkevich, *et al.* 2014; Lee, *et al*. 2014). Recently, it was shown that minimal trypsinolysis and limited acid cleavage retains information of the connectivity of Ub chains, especially branched chains (Crowe, *et al*. 2017). If a branch point was found to be present within the ubiquitin chain, the ubiquitin moiety that harbours the branch point is modified with two Gly-Gly modifications; left behind from the two branching ubiquitin moieties. Interestingly, the NZF1 domain was used to enrich the pool of branched ubiquitin chains for the UbiChEM-MS. Here, they confirmed that the NZF1 domain of TRABID enriches for K29/K48 branched ubiquitin chains. Strikingly, using this technique, Crowe, *et al*. 2017 concluded that while chain branching does target substrates for the proteasome, branched chains containing K29 linkages are likely to serve non-degradative roles. A hypothesis for

this, is that the K29-linkage “caps” the K48 linkage, resulting in a non-degradative signal. However, work conducted in *S. cerevisiae,* suggests that K29-linked ubiquitin chains, that have been modified with K48-linked ubiquitin resulting in branched chains, promoted the degradation of modified substrates (Liu, *et al*. 2017). More compellingly, this modification is mediated by Ufd2 and Ufd4, the latter of which is a HECTD1 orthologue. Here, the K48 branching modifies the K29-linkage transforming the ubiquitin chain into a degradative signal (Liu, *et al*. 2017). Therefore, the exact composition of the K29/K48-linked ubiquitin chains synthesised by HECTD1 needs to be elucidated to understand whether they serve as a degradative or a non-degradative signal. Therefore, the above techniques used in combination could be used in the future to confirm the topology of the ubiquitin chains synthesised by HECTD1.

In the context of the proposed mechanism that HECTD1 has in regulating the cell cycle, it is important to understand whether the K29/K48 linkage targets cell cycle substrates to the proteasome. For example, if these atypical ubiquitin chains are indeed shown to serve as a degradative signal, then this would rule out the hypotheses regarding the previously known substrates and interactors of HECTD1. This would include the substrates where HECTD1 has been demonstrated to ubiquitinate substrates leading to a change in localisation (APC and HSP90) (Sarkar, *et al*. 2012; Tran, *et al*. 2013). The exception is condensin I where, HECTD1 is required for the degradation of RIP40, however this does not tie in with a role in mitosis (Li, *et al*. 2015). Therefore, this opens up the avenue that there is another unidentified substrate of HECTD1, required for the cell cycle function. This substrate is hypothesised to be modified with K29/K48 leading to its degradation by the proteasome. However, if these chains are non-degradative then they may facilitate the localisation of cell cycle substrates, which in turn facilitates mitotic progression. However, this is only speculative, and more work would be required in the future to confirm the function of K29/K48 linked ubiquitin chains in the context of cell cycle regulation. Finally, a further consideration is the role that these K29/K48 linked chains have in the UFD pathway. Interestingly, Ufd4, is a HECTD1 ortholog in *S. cerevisiae*, that has been demonstrated to be a UFD pathway ligase and conjugates K29/K48 branched ubiquitin chains together with Ufd2 (Liu, *et al*. 2017). This may suggest that the role that HECTD1 has in mitosis may be mediate through the UFD pathway, however further work would be required to demonstrate a direct link.

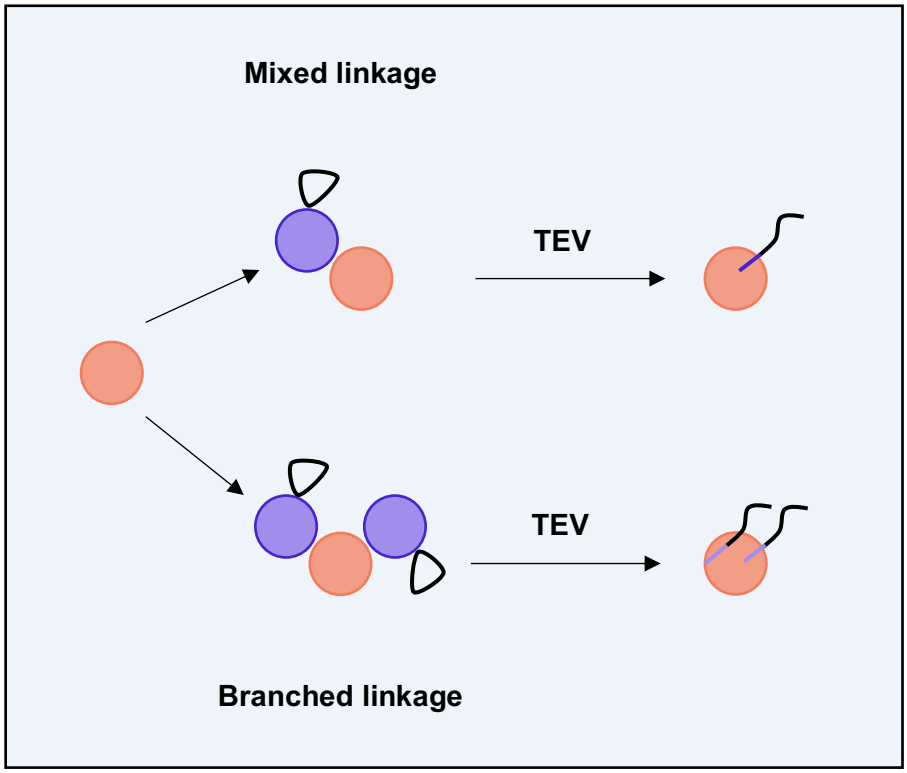

Figure 7.2. Schematic of how to determine ubiquitin chain topology using the Tobacco Etch Virus (TEV). The TEV protease cleavage sequence is inserted into the Glu-53 residue of ubiquitin. Upon cleavage of this protease cleavage site, TEV sequence-containing peptides are left on each ubiquitin. Here, where linkages are mixed, ubiquitin will only be modified with one signature peptide, whilst branched ubiquitin will be modified with two signature peptides. This modification can be visualised by western blot (Meyer, *et al.* 2014).

7.3. HECTD1 as a novel therapeutic target

Interestingly, overexpression of wild-type mHectd1 in glioblastoma cell lines was shown to lead to an increase in cell proliferation, demonstrating a possible oncogenic function. Speculatively, this increase in proliferation could be due to the reported role that HECTD1 has in Wnt signalling (Tran, *et al.* 2013) and in regulation of mitochondrial metabolism (Segref, *et al.* 2014) as discussed in Chapter 6. However, given the reported role that HECTD1 has as a negative regulator in Wnt signaling (Tran, *et al*. 2013), it is unlikely that its overexpression would result in increased proliferation. Furthermore, HECTD1 is reported to regulate mitochondrial protein turnover, and its depletion resulted in increased ROS production in *C. elegans* (Segref, *et al.* 2014). This again does not easily align with the increased in proliferation observed. Therefore, this led to the hypothesis that the increased cell proliferation observed in glioblastoma cell lines may be caused by the role that HECTD1

has in cell cycle regulation. Strikingly, immunofluorescent staining of HA-FL-mHectd1^{WT} was observed at the mitotic spindle during metaphase, aligning with previous observations in HEK293ET cells in Chapter 4. Therefore, based on the assumption that HECTD1 regulates the mitotic spindle as hypothesised from Chapters 3-5, it is conceivable that when overexpressed, HECTD1 may lead to aberrant regulation of the mitotic spindle. Here, an increase in proliferation could be seen as a result of a decrease in the time taken from NEBD to anaphase onset. Interestingly, depletion of the E3 ligases TRAIP and SMURF22 have been shown to lead to a decrease in the time taken from NEBD to anaphase onset (Osmundson, *et al*. 2008; Chapard, *et al.* 2014). Both ligases are reported to regulate the stability and localisation of MAD2 at unattached kinetochores (Osmundson, *et al*. 2008; Chapard, *et al.* 2014). Therefore, a speculative model for how HECTD1 overexpression leads to increased cell proliferation in glioblastoma cell lines, it that it causes the SAC to be compromised. A compromised SAC leads to a decrease in the time taken from NEBD to anaphase onset (Pines. 2006). This may result by aberrant regulation of a SAC component, for example MAD2. Based on the assumption that K29/K48-linked ubiquitin chains have a degradative role (Liu, *et al*. 2017), overexpression of HECTD1 could result in the degradation of MAD2, and therefore a compromised SAC (Figure 7.3). Therefore, implicating HECTD1 in the fine tuning of MAD2 levels. This would result in a decrease in the length of time taken to progress through mitosis leading to an increase in cell proliferation. Additionally, a compromised SAC will result in an unchecked mitosis, potentially causing chromosomal aberrations and aneuploidy (Osmundson, *et al*. 2008). Both chromosomal aberrations and aneuploidy are known to result in cancer formation (Sen. 2000).

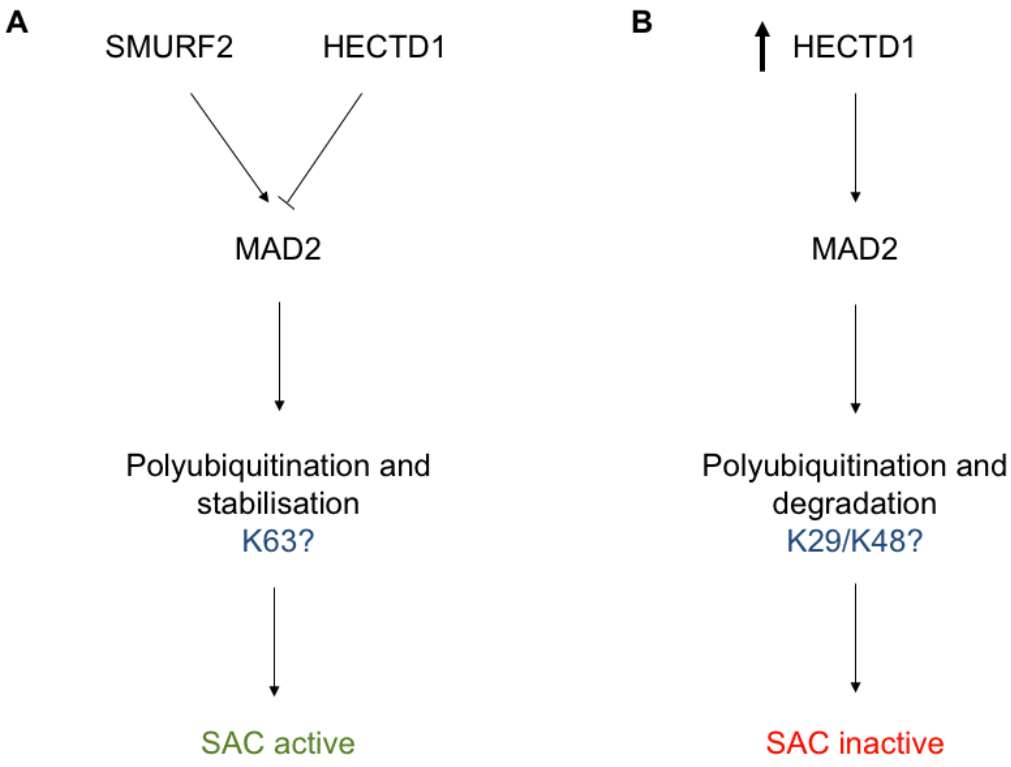

Figure. 7.3. Hypothesis for HECTD1 overexpression in cancer. As shown in Osmundson, *et al*. (2008), SMURF2 regulates the SAC by stabilising MAD2, ensuring the integrity of the checkpoint. In this proposed model, overexpression of HECTD1 could lead to the polyubiquitination and degradation of MAD2, resulting in a compromised checkpoint, and therefore a reduction in the time taken to progress from NEBD to anaphase onset.

Strikingly, overexpression of the catalytically active version and not the mutant of *mHectd1* in a glioblastoma cell line, resulted in increased proliferation. Furthermore, depletion of HECTD1 resulted in a decrease in cell proliferation in glioblastoma cells. This therefore strongly suggests that depletion of HECTD1 in glioblastoma could be a strategy to reduce cell proliferation. Given that the increase in proliferation has been shown to be driven by the E3 ligase activity of HECTD1, targeting of this activity could lead to a reduction in cell proliferation. Targeting of the catalytic activity of HECTD1 could provide a novel cancer therapeutic for glioblastoma and other cancers where HECTD1 is found to be overexpressed. This inhibition would phenocopy the depletion of HECTD1 in glioblastoma cell lines leading to a reduction in proliferation, potentially by restoration of the SAC. Therefore, targeting HECTD1 may provide another potential UPS based cancer therapy, in addition to the currently used proteasome inhibitors; Bortezomib (Cohen & Tcherpakov. 2010) and Cafilzomib (Stewart, *et al.* 2015). Inhibiting proteasomes have a large scope for side effects, whereas targeting specific E3 ligases reduces these side effects because of

the high substrate specific nature of the enzymes (Bernassola, *et al.* 2008). Furthermore, given that TMZ is one of the only chemotherapies for glioblastoma, and this is ineffective in patients without O-6-methylguanine-DNA methyltransferase promoter methylation, there is great demand for a new therapeutic (Weller, *et al*. 2015).

Small molecule and peptide inhibitors have been made to target RING E3s with the example of MDM2, which targets p53 (Chang, *et al.* 2013; Yang, *et al.* 2005). More recently small molecule and peptide inhibitors of HECT E3 ligases have been produced. Using phage display bicyclic peptide inhibitors of HECT domains of SMURF2, NEDD4, WWP1, and HUWE1 were isolated, which targeted the E2 binding site and prevented binding. The small molecule Heclin was found to inhibit several HECT ligases in tissue culture cells and led to cell death in HEK293. In this case it does not prevent binding of the E2, instead it induces a conformational change leading to the oxidation of the active site cysteine. Heclin was found not to lead to oxidation of other cysteine containing enzymes such as E1 or E2 enzymes, suggesting that it has a specific binding site in HECT ligases (Mund, *et al.* 2014). However, Heclin targets all HECT E3 ligases, and for a viable cancer therapeutic it would be desirable for the targeting to be to a specific ligase. For example, specific small molecule inhibitors of HUWE1 (B18622 and B18626) were identified via high throughput screening. HUWE1 associates with MYC and MIZ1, and upon inhibition of HUWE1, transcriptional activation by MYC is reduced in colon cancer cells, because MIZ1 is not degraded by HUWE1 and therefore is able to bind and repress MYC-activated genes (Peter, *et al.* 2014). In addition, a small molecule inhibitor, clomipramine an antidepressant, was found to prevent ITCH autoubiquitylation, as well as p73 ubiquitylation. A panel of breast, prostate, and bladder cancer cell lines were treated with clomipramine, or its homologs, which led to reduced cancer cell growth (Rossi, *et al.* 2014). Taken together, this therefore shows promise for the future of designing small molecule or peptide cancer therapeutics, which target HECT E3 ligases. Furthermore, with more research a small molecule inhibitor could be designed to target HECTD1 in the context of glioblastoma. For example, small molecule inhibitors of HECTD1 can be designed based on the structure of the active site of the ligase. This can be achieved by using X-ray crystallography to determine the structure of the HECT domain of HECTD1 to model compounds in the catalytic site, as achieved with the active site of the metalloprotease Neproilysin (Voisin, *et al.* 2004). From this, small molecules can be screened from a compound library such as the NCI/DTP Open Chemical Repository. Using molecular docking, these compounds can be modelled into the active site to limit the number of candidate compounds. Finally, once a limited number of compounds have been screened, a high throughput cell proliferation assay could be conducted to assess for reduction in proliferation in glioblastoma cell lines. This reduction would phenocopy the observed reduction in proliferation as observed in Chapter 6. This rationale for designing

small molecule inhibitors of enzymes is well characterised and has been used for the design of an inhibitor of the Ras GEF, SOS1 (Evelyn, *et al.* 2014). Thus, demonstrating how an inhibitor of HECTD1 could be obtained.

7.4. New tools in studying HECT ligase activity

Recently with the expansion of the Ub toolbox, there are increasingly more ways to study HECT ligase activity. Activity based probes have been designed, which are able to assess the activity of HECT ligases. Activity based protein profiling (ABPP) utilises chemical probes that target the active site of enzymes, to profile their activity within complex mixtures of proteins (Love, *et al.* 2007). Development of these probes has led to increased understanding of deubiquitinases, whereby new members of DUB families have been identified (Borodovsky, *et al.* 2002; Hemelaar, *et al.* 2004). The first generation of these probes Ub-ABP comprise a C-terminal modification of ubiquitin whereby the G76 is modified with a variety of thiol-reactive groups, known as warheads, which covalently modify the catalytic cysteine of the enzyme (Love KR, *et al.* 2007). These C-terminal warheads include aldehyde, vinyl sulfone, vinylmethylester (VME), and propargylamide (PA) (Hershko, & Rose. 1987; Palmer, *et al*. 1995; Borodovsky, *et al.* 2001; Borodovsky, *et al.* 2002; Ekkebus, *et al.* 2013). Both Ub-VME-ABP and Ub-PA-ABP have been used to covalently modify HUWE1 (Love, *et al.* 2009; Ekkebus, *et al.* 2013). Ub-VME-ABP was used to covalently modify the recombinant HECT domain of HUWE1, and interestingly, when characterising the interaction between Ub-VME-ABP and the HECT domain of HUWE1, it was revealed that the probe labelled multiple cysteines within the domain (Love, *et al.* 2009). Mutation of the catalytic cysteine of HUWE1 resulted in reduced but not a total loss of ligase activity, suggesting that the other cysteine residues may contribute to the activity of HUWE1. Finally, Ub-VME-ABP was shown to label HUWE1, E6AP, and TRIP12 ligases in mouse and human cell lysates (Love, *et al.* 2009). Therefore, demonstrating the ability of these first-generation probes to label HECT ligases and facilitate the understanding of the catalytic residues involved in their activity.

However, the next generation of ABPs are much more suited to probing the activity of HECT ligases and specifically HECTD1. The first generation Ub-ABPs are much more effective in labelling DUBs and less physiologically relevant when labelling E3 ligases. Therefore, the next generation of activity based probes were based on the substrate of E3 ligases, Ub-E2. These probes known as E2-based ABPs, mimic a ubiquitin-charged E2 that contains a C-terminal electrophilic warhead, that is able to label RBR and HECT E3 ubiquitin ligases. This allows for specific labelling of RBR and HECT ligases, as only active sites with an E2

binding site will result in covalent modification of the cysteine, thus excluding labelling of deubiquitinases (Pao, *et al.* 2016). Use of this novel probe enabled direct and quantitative labelling of endogenous activity of the RBR ligase, Parkin (Pao, *et al.* 2016). Since, Byrne, *et al.* (2017) have used this E2-Ub-ABP to label recombinant HECT domains of NEDD4, UBE3C, and HECTD1. Only UBE3C was successfully labelled by the E2-Ub-ABP in human cell-line lysates under basal conditions (Byrne, *et al*. 2017). These novel reagents, with further optimisation provide the future for assessing the activity of HECT ligases *in cellulo*. For example, these E2-Ub-ABP could be used to probe the activity of HECTD1 throughout the cell cycle, and understand the physiological conditions that result in its activation.

Interestingly, in addition to modifying E3 ligases only, a cascading activity-based probe can be used to sequentially target the E1-, E2-, and E3- ubiquitin enzymes (Mulder, *et al.* 2016). The cascading activity based-probe, was developed to comprise a C-terminal dehydroalanine (Dha) residue, which upon E1 activation by ATP can travel downstream labelling E2 enzymes and E3 enzymes. At each step, the probe can irreversibly label the active site cysteine of the enzyme, thus enabling its detection, without transfer to subsequent substrates. The probe was able to successfully label NEDD4 family members, NEDD4, SMURF2, WWP1 and WWP2, in addition to HECTD1, UBE3A, UBE3C, and TRIP12 (Mulder, *et al.* 2016). Therefore, presenting another reagent to probe HECT ligase activity. Finally, ubiquitin variants (UbVs) have been employed to inhibit or activate HECT ligases (Zhang, *et al.* 2016). These UbVs were previously used as inhibitors to block active sites in DUBs, however it was also found that a UbV bound weakly to the HECT domain of NEDD4 leading to the activation of the enzyme instead of inhibition (Ernst, *et al.* 2013). In a later screen of these UbVs to study HECT ligase activation, structural analysis of six HECT-UbV complexes showed that they can behave as inhibitors, hijacking the E2-binding exosite, and activators, occupying a ubiquitin-binding exosite. Thus, providing a tool for understanding functions of HECT ligases and providing modulators of enzymatic activity (Zhang, *et al.* 2016). Interestingly, this reagent may be used in future studies to inhibit or modulate HECTD1 activity in the cell cycle to probe predicted function in the cell cycle.

Therefore, the expansion of the ubiquitin tool kit is providing new methods to probe HECT ligases and enable deeper understanding of mechanisms underlying ubiquitination in cellular functions. The use of this toolkit could help with the understanding and manipulation of HECTD1 to elucidate the mechanism by which HECTD1 regulates the cell cycle.

7.5. Conclusion

In conclusion, targeting the ubiquitin proteasome system is a promising avenue for the future of cancer therapeutics. HECTD1 has been identified to function in the cell cycle and cell proliferation, and therefore could provide a novel target for the treatment of cancer. The short term aim would be to characterise the molecular mechanisms by which HECTD1 regulates the cell cycle through proteomics and ABPs. The mid-term aim, would be to study specifically the role that HECTD1 has in cancer, such as glioblastoma, by using mouse genetics and orthotopic models of brain cancer. Additionally, to evaluate the potential that HECTD1 has as a diagnostic and prognostic marker of glioblastoma. Finally, the long term aim would be to develop an inhibitor of HECTD1 and screen for small molecule inhibition.

References

Abdul Rehman, S.A., Kristariyanto, Y.A., Choi, S.-Y., Nkosi, P.J., Weidlich, S., Labib, K., Hofmann, K., & Kulathu, Y. (2016). MINDY-1 is a Member of an Evolutionarily Conserved and Structurally Distinct New Family of Deubiquitinating Enzymes. *Molecular Cell, 63*(1), 146-155.

Acharya, U., Jacobs, R., Peters, J.M., Watson, N., Farquhar, M. G., & Malhotra, V. (1995). The formation of Golgi stacks from vesiculated Golgi membranes requires two distinct fusion events. *Cell*, *82*(6), 895–904.

Ackermann, L., Schell, M., Pokrzywa, W., Kevei, E., Gartner, A., Schumacher, B., & Hoppe, T. (2016). E4 Ligase Specific Ubiquitylation Hubs Coordinate DNA Double Strand Break Repair and Apoptosis. *Nature Structural & Molecular Biology, 23*(11), 995-1002.

Acquaviva, C., & Pines, J. (2006). The anaphase-promoting complex/cyclosome: APC/C. *Journal of Cell Science*, *119*(12), 2401–2404.

Adhikary, S., Marinoni, F., Hock, A., Hulleman, E., Popov, N., Beier, R., Bernard, S., Quarto, M., Capra, M., Goettig, S., Kogel, U., Scheffner, M., Helin, K., & Eilers, M. (2005). The ubiquitin ligase HectH9 regulates transcriptional activation by Myc and is essential for tumor cell proliferation. *Cell*, *123*(3), 409–421.

Alam, S.L., Sun, J, Payne, M., Welch, B.D., Blake, B.K., Davis, D.R., Meyer, H.H., Emr, S. D., & Sundquist, W.I. (2004). Ubiquitin interaction of NZF zinc fingers. *EMBO Journal, 23*(7), 1411-1421.

Al-Hakim, A.K., Zagorska, A., Chapman, L., Deak, M., Peggie, M., & Alessi, D.R. (2008). Control of AMPK-related kinases by USP9X and atypical Lys(29)/Lys(33)- linked polyubiquitin chains. *The Biochemical Journal, 411*(2), 249-260.

Al-Hakim, A.K., Bashkurov, M., Gingras, A. -C., Durocher, D., & Pelletier, L. (2012). Interaction proteomics identify NEURL4 and the HECT E3 ligase HERC2 as novel modulators of centrosome architecture. *Molecular & Cellular Proteomics: MCP*, *11*(6), M111.014233–M111.014233. http://doi.org/10.1074/mcp.M111.014233.

Allen, M., Bjerke, M., Edlund, H., Nelander, S., & Westermark, B. (2016). Origin of the U87MG glioma cell line: Good news and bad news. *Science Translational Medicine, 8*(354): 354re3. DOI: 10.1126/scitranslmed.aaf6853.

Alonso, C. (2013). An Overview of Stimulated Emission Depletion (STED) Microscopy and Applications. *Journal of Biomolecular Techniques, 24*(Supplementary): S4.

Amodio, N., Scrima, M., Palaia, L., Salman, A.N., Quintiero, A., Franco, R., Botti, G., Pirozzi, P., Rocco, G., De Rosa, N., & Viglietto, G. (2010). Oncogenic Role of the E3 Ubiquitin Ligase NEDD4-1, a PTEN Negative Regulator, in Non-Small-Cell Lung Carcinomas. *American Journal of Pathology, 177*(5), 2622-2634.

Archibald, J.M., The, E.M., & Keeling, P.J. (2003). Novel Ubiquitin Fusion Proteins: Ribosomal Protein P1 and Actin. *Journal of Molecular Biology, 328*(4), 771-778.

Ardley, H.C., & Robinson, P.A. (2005). E3 ubiquitin ligases. *Essays in Biochemistry, 41*, 15-30.

Attali, I., Tobelaim, S. W., Persaud, A., Motamedchaboki, K., Simpson-Lavy, K.J., Mashahreh, B., Levin-Kravets, O., Keren-Kaplan, T., Pilzer, I., Kupiec, M., Wiener, R., Wolf, D. A., Rotin, D., & Prag, G. (2017). Ubiquitylation-dependent oligomerization regulates activity of Nedd4 ligases. *The EMBO Journal, 36*(4), 425-440.

Aubin, J.E., Osborn, M., & Weber, K. (1980). Variations in the distribution and migration of centriole duplexes in mitotic PtK2 cells studied by immunofluorescence microscopy. *Journal of Cell Science, 43*, 177-194.

Bachmair, A., Finley, D., & Varshavsky, A. (1986). In vivo half-life of a protein is a function of its amino-terminal residue. *Science*, *234*(4773), 179–186.

Balakrishana, A., Bleeker, F.E., Lamba, S., Rodolfo, M., Daniotti, M., Scarpa, A., van Tilborg, A.A., Leenstra, S., Zanon, C., & Bardelli, A. (2007). Novel Somatic and Germline Mutations in Cancer Candidate Genes in Glioblastoma, Melanoma, and Pancreatic Carcinoma. *Cancer Research, 67*(8), 3545-3550.

Baskin, T.I., & Cande, W.Z. (1990). Kinetic analysis of mitotic spindle elongation in vitro. *Journal of Cell Science, 97*(1), 79-89.

Basto, R., Gergely, F., Draviam, V.M., Ohkura, H., Liley, K., & Raff, J.W. (2007). Hsp90 is required to localise cyclin B and Msps/ch-TOG to the mitotic spindle in Drosophila and humans. *Journal of Cell Science, 120*(7), 1278-1287.

Barr, F.A., & Gruneberg, U. (2007). Cytokinesis: placing and making the final cut. *Cell, 131*(5), 847-860.

Baxter, E., Windloch, K., Gannon, F., & Lee, J.S. (2014). Epigenetic regulation in cancer progression. *Cell & Bioscience, 4*, 45. DOI: 10.1186/2045-3701-4-45.

Beach, D., Durkacz, B., & Nurse, P. (1982). Functionally homologous cell cycle control genes in budding and fission yeast. *Nature, 300*. 706–709.

Beamish, H., de Boer, L., Giles, N., Stevens, F., Oakes, V., & Gabrielli, B. (2009). Cyclin A/cdk2 regulates adenomatous polyposis coli-dependent mitotic spindle anchoring. *Journal of Biological Chemistry*, *284*(42), 29015–29023.

Beard, S.M., Smit, R.B., Chan, B.G., & Mains, P.E. (2016). Regulation of the MEI-1/MEI-2 Microtubule-Severing Katanin Complex in Early *Caenorhabditis elegans* Development. *G3: Genes, Genomes, Genetics, 6*(10), 3257-3268.

Beaudouin, J., Gerlich, D., Daigle, N., Elis, R., & Ellenburg, J. (2002). Nuclear Envelope Breakdown Proceeds by Microtubule-Induced Tearing of the Lamina. *Cell, 108*(1), 83-96.

Becker, P.B., & Workman, J.L. (2013). Nucleosome remodelling and epigenetics. *Cold Spring Harbour Perspectives in Biology, 5*(9): a017905. DOI: 10.1101/cshperspect.a017905.

Bekker-Jensen, S., Rendtlew Danielsen, J., Fugger, K., Gromova, I., Nerstedt, A., Lukas, C., Bartek, J., Lukas, J., & Mailand, N. (2010). HERC2 coordinates ubiquitin-dependent assembly of DNA repair factors on damaged chromosomes. *Nature Cell Biology*, *12*(1), 80-86.

Bellomaria, A., Barbato, G., Melino, G., Paci, M., & Melino, S. (2012). Recognition mechanism of p63 by the E3 ligase Itch: novel strategy in the study and inhibition of this interaction. *Cell Cycle, 11*(19), 3638–3648.

Benavides, M., Chow-Tsang, L.-F., Zhang, J., & Zhong, H. (2013). The novel interaction between microspherule protein Msp58 and ubiquitin E3 ligase EDD regulates cell cycle progression. *Biochimica Et Biophysica Acta-Molecular Cell Research*, *1833*(1), 21–32.

Bennett, E.J., Shaler, T.A., Woodman, B., Ryu, K.-Y., Zaitseva, T.S., Becker, C.H., Bates, G.P., Schulman, H., & Kopito, R.R. (2007). Global changes to the ubiquitin system in Huntington's disease. *Nature, 448*, 704-708.

Bergink, S., Salomons, F.A., Hoogstraten, D., Groothuis, T., de Waard, H., Wu, J., Yuan, L., Citterio, E., Houtsmuller, A.B., Neefjes, J., Hoeijmakes, J.H.J., Vermeulen, W., & Dantuma, N.P. (2006). DNA damage triggers nucleotide excision repair-dependent monoubiquitylation of histone H2A. *Genes & Development*, *20*(10), 1343–1352.

Bernassola, F., Karin, M., Ciechanover, A., & Melino, G. (2008). The HECT Family of E3 Ubiquitin Ligases: Multiple Players in Cancer Development. *Cancer Cell*, *14*(1), 10–21.

Berndsen, C.E., & Wolberger, C. (2014). New insights into ubiquitin E3 ligase mechanism. *Nature Structural & Molecular Biology*, *21*(4), 301–307.

Berrueta, L., Kraeft, S.K., Tirnauer, J.S., Schuyler, S.C., Chen, L.B., Hill, D.E., Pellman, D., & Bierer, B.E. (1998). The adenomatous polyposis coli-binding protein EB1 is associated with cytoplasmic and spindle microtubules. *Proceedings of the National Academy of Sciences of the United States of America*, *95*(18), 10596–10601.

Besche, H.C., Sha, Z., Kukushkin, N.V., Peth, A., Hock, E.M., Kim, W., Gygi, S., Gutierrez, J.A., Liao, H., Dick, L., & Goldberg, A. L. (2014). Autoubiquitination of the 26S proteasome on Rpn13 regulates breakdown of ubiquitin conjugates. *EMBO Journal, 33*(10), 1159-1176.

Besson, A., Dowdy, S.F., & Roberts, J.M. (2008). CDK inhibitors: cell cycle regulators and beyond. *Developmental Cell, 14*(2), 159-169.

Bhalla, V., Daidié, D., Li, H., Pao, A. C., LaGrange, L.P., Wang, J., Vandewalle, A., Stockand, J.D., Staub, O., & Pearce, D. (2005). Serum- and glucocorticoid-regulated kinase 1 regulates ubiquitin ligase neural precursor cell-expressed, developmentally down-regulated protein 4-2 by inducing interaction with 14-3-3. *Molecular Endocrinology (Baltimore, Md.)*, *19*(12), 3073–3084.

Bird, A.P. (1980). DNA methylation and the frequency of CpG in animal DNA. *Nucleic Acids Research, 8*(7), 1499-1504.

Birsa, N., Norkett, R., Wauer, T., Mevissen, T.E.T., Wu, H.C., Foltynie, T., Bhatla, K., Hirst, W.D., Komander, D., Plun-Favreau, H., & Kittler, J.T. (2014). Lysine 27 Ubiquitination of the Mitochondrial Transport Protein Miro Is Dependent on Serine 65 of the Parkin Ubiquitin Ligase, *289*(21), 14569–14582.

Blackwood, E.M., & Eisenman, R.N. (1991). Max: a helix-loop-helix zipper protein that forms a sequence-specific DNA-binding complex with Myc. *Science, 251*(4997), 1211-1217.

Blondeau, B., Sahly, I., Massouridès, E., Singh-Estivalet, A., Valtat, B., Dorchene, D., Jaisser, F., Bréant, B., & Tronche, F. (2012). Novel Transgenic Mice for Inducible Gene Overexpression in Pancreatic Cells Define Glucocorticoid Receptor-Mediated Regulations of Beta Cells. *PLOS One*, DOI: 10.1371/journal.pone.0030210.

Bloom, J., & Pagano, M. (2003). Deregulated degradation of the cdk inhibitor p27 and malignant transformation. *Seminars in Cancer Biology, 13*(1), 41-47.

Boname, J., Thomas, M., Stagg, H.R., Xu, P., Peng, J., & Lehner, P.J. (2010). Efficient Internalization of MHC I Requires Lysine-11 and Lysine-63 Mixed Linkage Polyubiquitin Chains. *Traffic, 11*(2), 210–220.

Bonanno, L., Costa, C., Majem, M., Sanchez, J.J., Rodriguez, I., Gimenez-Capitan, A., Molina-Vila, M.A., Vergnenegre, A., Massuti, B., Favaretto, A., Rugge, M., Pallares, C., Taron, M., & Rosell, R. (2016). Combinatory effect of BRCA1 and HERC2 expression on outcome in advanced non-small-cell lung cancer. *BMC Cancer, 16*, 312. DOI: 10.1186/s12885-016-2339-5.

Bootsma, D., Budke, L., & Vos, O. (1964). Studies on synchronous division of HeLa cells initiated by excess thymidine. *Experimental Cell Research, 33,* 301-309.

Borden, K.L.B. (2000). RING domains: Master builders of molecular scaffolds? *Journal of Molecular Biology*, *295*(5), 1103–1112.

Borodovsky, A., Kessler, B.M., Casagrande, R., Overkleeft, H.S., Wilkinson, K.D., & Ploegh, H. L. (2001). A novel active site-direct probes specific for deubiquitylating enzymes reveals proteasome association of USP14. *The EMBO Journal, 20*(18), 5187-5196.

Borodovsky, A., Ovaa, H., Kolli, N., Gan-Erdene, T., Wilkinson, K.D., Ploegh, H.L., & Kessler, B.M. (2002). Chemistry-Based Functional Proteomics Reveals Novel Members of the Deubiquitinating Enzyme Family. *Chemistry & Biology, 9*(10), 1149-1159.

Bredel, M., Bredel, C., Juric, D., Harsh, G.R., Vogel, H., Recht, L.D., Sikic, B.I. (2005). Functional network analysis reveals extended gliomagenesis pathway maps and three novel MYC-interacting genes in human gliomas. *Cancer Research, 65*(19), 8679-8689.

Brinkley, B.R., & Stubblefield, E. (1966). The fine structure of the kinetochore of a mammalian cell in vitro. *Chromosoma, 19*(1), 28-43.

Brooks, W.S., Banerjee, S., & Crawford, D.F. (2006). G2E3 is a nucleo-cytoplasmic shuttling protein with DNA damage responsive localization. *Experimental Cell Research*, *313*(4), 665–676.

Brooks, W.S., Helton, E.S., Banerjee, S., Venable, M., Johnson, L., Schoeb, T.R., Kesterson, R.A., & Crawford, D.F. (2008). G2E3 is a dual function ubiquitin ligase required for early embryonic development. *The Journal of Biological Chemistry*, *283*(32), 22304–22315.

Brzovic, P.S., Rajagopal, P., Hoyt, D.W., King, M.C., Klevit, R.E. (2001). Structure of a BRCA1-BARD1 heterodimer RING-RING complex. *Nature Structural Biology, 8*(10), 833-837.

Buetow, L., & Huang, D.T. (2016). Structural insights into the catalysis and regulation of E3 ubiquitin ligases. *Nature Reviews Molecular Cell Biology, 17*, 626-642.

Burger, A.M., & Seth, A.K. (2004). The ubiquitin-mediated protein degradation pathway in cancer: therapeutic implications. *European Journal of Cancer, 40*(15), 2217-2229.

Burridge, K., & Chrzanowska-Wodnicka, M. (1996). Focal adhesions, contractility, and signaling. *Annual Review of Cell and Developmental Biology, 12*, 463-519.

Byrne, R., Mund, T., Licchesi, J.D.F. (2017). Activity-Based Probes for HECT E3 Ubiquitin Ligases. *ChemBioChem, 18*(14), 1415-1427.

Byrnes, A.E., & Slep, K.C. (2017). TOG-tubulin binding specificity promotes microtubule dynamics and mitotic spindle formation. *Journal of Cell Biology, 216*(6), 1641-1657.

Cardozo, T., & Pagano, M. (2004). The SCF ubiquitin ligase: insights into a molecular machine. *Nature Reviews Molecular Cell Biology*, *5*(9), 739–751.

Carmena, M., Wheelock, M., Funabiki, H., & Earnshaw, W.C. (2012). The chromosomal passenger complex (CPC): from easy rider to the godfather of mitosis. *Nature Reviews, Molecular Cell Biology, 13*(12), 789-803.

Castiel, A., Danieli, M.M., David, A., Moshkovitz, S., Aplan, P.D., Kirsch, I.R., Brandeis, M., Krämer, A., & Izraeli, S. (2011). The Stil protein regulates centrosome integrity and mitosis through suppression of Chfr. *Journal of Cell Science, 124*(4), 532-539.

Cerami, E., Gao, J., Dogrusoz, U., Gross, B.E., Sumer, S.O., Aksoy, B.A., Jacobsen, A., Byrne, C.J., Heuer, M.L., Larsson, E., Antipin, Y., Reva, B., Goldberg, A.P., Sander, C., & Schultz, N. (2012). The cBio Cancer Genomics Portal: An Open Platform for Exploring Multidimensional Cancer Genomics Data. *Cancer Discovery, 2*(5), 401-404.

Chan, N.C., Besten den, W., Sweredoski, M.J., Hess, S., Deshaies, R.J., & Chan, D.C. (2014). Degradation of the deubiquitinating enzyme USP33 is mediated by p97 and the ubiquitin ligase HERC2. *Journal of Biological Chemistry*, *289*(28), 19789–19798.

Chang, D.C., Xu, N., Luo, K.Q. (2003). Degradation of Cyclin B1 is Required for the Onset of Anaphase in Mammalian Cells. *Journal of Biological Chemistry, 278*(39), 37865-37873.

Chang, P., Coughlin, M., & Mitchinson, T.J. (2005). Tankyrase-1 polymerisation of poly(ADP-ribose) is required for spindle structure and function. *Nature Cell Biology, 7*(11), 1133-1139.

Chang, Y.S., Graves, B., Guerlavais, V., Tovar, C., Packman, K., To, K.-H., Olsen, K.A., Kesavan, K., Gangurde, P., Mukherjee, A., Baker, T., Darlak, K., Elkin, C., Filipovic, Z., Qureshi, F.Z., Cai, H., Berry, P., Feyfant, E., Shi, X.E., Horstick, J., Annis, D.A., Manning, A.M., Fotouhi, N., Nash, H., Vassilev, L.T., & Sawyer, T.K. (2013). Stapled alpha-helical peptide drug development: A potent dual inhibitor of MDM2 and MDMX for p53-dependent cancer therapy. *PNAS*, *110*(36), E3445–E3454.

Chapard, C., Meraldi, P., Gleich, T., Bachmann, D., Hohl, D., & Huber, M. (2014). TRAIP is a regulator of the spindle assembly checkpoint. *Journal of Cell Science, 127*, 5149-5156.

Chastagner, P., Israël, A., & Brou, C. (2006). Itch/AIP4 mediates Deltex degradation through the formation of K29-linked polyubiquitin chains, *EMBO Reports 7*(11), 1147–1153.

Chau, V., Tobias, J.W., Bachmair, A., Marriott, D., Ecker, D.J., Gonda, D.K., & Varshavsky, A. (1989). A multiubiquitin chain is confined to specific lysine in a targeted short-lived protein. *Science*, *243*(4898), 1576–1583.

Chaudhary, N., & Courvalin, J.C. (1993). Stepwise reassembly of the nuclear envelope at the end of mitosis. *Journal of Cell Biology, 122*(2), 295-306.

Chen, C., Zhou, Z., Ross, J.S., Zhou, W., Dong, J.T. (2007). The amplified WWP1 gene is a potential molecular target in breast cancer. *International Journal of Cancer, 121*(1), 80-87.

Chen, D., Kon, N., Li, M., Zhang, W., Qin, J., & Gu, W. (2005). ARF-BP1/Mule is a critical mediator of the ARF tumor suppressor. *Cell*, *121*(7), 1071–1083.

Chen, H.I., & Sudol, M. (1995). The WW domain of Yes-associated protein binds a proline-rich ligand that differs from the consensus established for Src homology 3-binding modules. *Proceedings of the National Academy of Sciences of the United States of America*, *92*, 7819–7823.

Chen, R.-H. (2002). BubR1 is essential for kinetochore localization of other spindle checkpoint proteins and its phosphorylation requires Mad1. *Journal of Cell Biology, 158*(3), 487-496.

Chen, Z., Jiang, H., Xu, W., Li, X., Dempsey, D.R., Zhang, X., Devreotes, P., Wolberger, C., Amzel, L.M., Gabelli, S.B., & Cole, P.A. (2017). A Tunable Brake for HECT Ubiquitin Ligases. *Molecular Cell, 66*(3), 345-357.

Christman, J.K. (2002). 5-Azacytidine and 5-aza-2'-deoxycytidie as inhibitors of DNA methylation: mechanistic studies and their implications for cancer therapy. *Oncogene, 21*(35), 5483-5495.

Ciechanover, A., Hod, Y., & Hershko, A. (1978). A heat-stable polypeptide component of an ATP-dependent proteolytic system from reticulocytes. *Biochemical and biophysical research communications, 425*, 565–570.

Ciechanover, A., Heller, H., Katz-Etzion, R., & Hershko, A. (1981). Activation of the heat-stable polypeptide of the ATP-dependent proteolytic system. *Proceedings of the National Academy of Sciences of the United States of America*, *78*(2), 761–765.

Ciechanover, A., Elias, S., Heller, H., & Hershko, A. (1982). “Covalent affinity” purification of ubiquitin-activating enzyme. *The Journal of Biological Chemistry*, *257*(5), 2537–2542.

Clague, M.J., Barsukov, I., Coulson, J.M., Liu, H., Rigden, D.J., & Urbé, S. (2013). Deubiquitylases From Genes to Organism. *Physiological Reviews, 93*(3), 1289-1315.

Clancy, J.L., Henderson, M.J., Russell, A.J., Anderson, D.W., Bova, R.J., Campbell, I.G., Choong, D.Y., Macdonald, G.A., Mann, G.J., Nolan, T., Brady, G., Olopade, O.I., Woollatt, E., Davies, M.J., Segara, D., Hacker, N.F., Henshall, S.M., Sutherland, R.L., & Watts, C.K. (2003). EDD, the human orthologue of the hyperplastic discs tumour suppressor gene, is amplified and expressed in cancer. *Oncogene, 22*(32), 5070-5081.

Clements, A.E., Bravo, V., Koivisto, C., Cohn, D.E., & Leone, G. (2015). WWP2 and its association with PTEN in endometrial cancer. *Gynecologic Oncology Reports, 3*(12), 26-29.

Cobaleda, C., Schebesta, A., Delogu, A., & Busslinger, M. (2007). Pax5: the guardian of B cell identity and function. *Nature Immunology, 8*, 463-470.

Cohen-Fix, O., & Koshland, D. (1999). Pds1p of budding yeast has dual roles: inhibition of anaphase initiation and regulation of mitotic exit. *Genes and Development. 13*(15), 1950-1959.

Cohen, P., & Tcherpakov, M. (2010). Will the Ubiquitin System Furnish as Many Drug Targets as Protein Kinases? *Cell*, *143*(5), 686–693.

Confalonieri, S., Quarto, M., Goisis, G., Nuciforo, P., Donzelli, M., Jodice, G., Pelosi, G., Viale, G., Pece, S., & Di Fiore, P.P. (2009). Alterations of ubiquitin ligases in human cancer and their association with the natural history of the tumor. *Oncogene, 28*(33), 2959-2968.

Cong, L., Ran, F.A., Cox, D., Lin, S., Barretto, R., Habib, N., Hsu, P.D., Wu, X., Jiang, W., Marraffini, L.A., & Zhang, F. (2013). Multiplex genome engineering using CRISPR/Cas systems. *Science, 339*(6121), 819-823.

Creyghton, M.P., Cheng, A.W., Welstead, G.G., Kooistra, T., Carey, B.W., Steine, E.J., Hanna, J., Lodato, M.A., Frampton, G.M., Sharp, P.A., Boyer, L.A., Young, R.A., & Jaenisch, R. (2010). Histone H3K27a separates active from poised enhances and predicts developmental state. *PNAS, 107*(50), 21931-21936.

Crowe, S.O., Rana, A.S.J.B., Deol, K.K, Ge, Y., & Strieter, E.R. (2017). Ubiquitin Chain Enrichment Middle-Down Mass Spectrometry Enables Characterization of Branched Ubiquitin Chains *in Cellulo*. *Analytical Chemistry, 89*(8), 4428-4434.

Cubillos-Rojas, M., Amair-Pinedo, F., Peiró-Jordán, R., Bartrons, R., Ventura, F., & Rosa, J.L. (2014). The E3 ubiquitin protein ligase HERC2 modulates the activity of tumor protein p53 by regulating its oligomerization. *Journal of Biological Chemistry*, *289*(21), 14782–14795.

Cunningham, C.N., Baughman, J.M., Phu, L., Tea, J.S., Yu, C., Coons, M., Kirkpatrick, D.S., Bingol, B., & Corn, J.E. (2015). USP30 and parkin homeostatically regulate atypical ubiquitin chains on mitochondria. *Nature Cell Biology*, *17*(2), 160–169.

Dahlmann, B., Kopp, F., Kuehn, L., Niedel, B., Pfeifer, G., Hegerl, R., & Baumeister, W. (1989). The multicatalytic proteinase (prosome) is ubiquitous from eukaryotes to archaebacteria. *FEBS Letters, 251*(1-2), 125–131.

Dammer, E.B., Na, C.H., Xu, P., Seyfried, N.T., Duong, D.M., Cheng, D., Gearing, M., Rees, H., Lah, J.J., Levey, A.I., Rush, J., & Peng, J. (2011). Polyubiquitin linkage profiles in three models of proteolytic stress suggest the etiology of Alzheimer disease. *Journal of Biological Chemistry*, *286*(12), 10457–10465.

Darling, S., Fielding, A.B., Sabat-Pośpiech, D., Prior, I.A., & Coulson, J.M. (2017). Regulation of the cell cycle and centrosome biology by deubiquitylases. *Biochemical Society Transactions, 45*(5), 1125-1136.

David, D., Jagadeeshan, S., Hariharan, R., Nair, A.S., Pillai, R.M. (2014). Smurf2 E3 ubiquitin ligase modulates proliferation and invasiveness of breast cancer cells in a CNKSR2 dependent manner. *Cell Division, 9*(2). DOI: 10.1186/1747-1028-9-2.

Davis, M.E. (2016). Glioblastoma: Overview of Disease and Treatment. *Clinical Journal of Oncology Nursing, 20*(5); S2-S8.

de Groot, R.E., Ganji, R.S., Bernatik, O., Lloyd-Lewis, B., Seipel, K., Šedová, K., Zdráhal, Z., Dhople, V.M., Dale, T.C., Korswagen, H.C., Bryia, V. (2014). Huwe1-mediated ubiquitylation of dishevelled defines a negative feedback loop in the Wnt signaling pathway. *Science Signalling, 7*(317): ra26. DOI: 10.1126/scisignal.2004985.

Debonneville, C., Flores, S.Y., Kamynina, E., Plant, P.J., Tauxe, C., Thomas, M.A., Münster, C., Chraïbi, A., Pratt, J.H., Horisberger, J.-D., Pearce, D., Loffing, J., & Staub, O. (2001). Phosphorylation of Nedd4-2 by Sgk1 regulates epithelial Na(+) channel cell surface expression. *The EMBO Journal*, *20*(24), 7052–7059.

Decarreau, J., Driver, J., Asbury, C., & Wordeman, L. (2014). Rapid measurement of mitotic spindle orientation in cultured mammalian cells. *Methods in Molecular Biology, 1136*, 31-40.

Delgado-López, P.D., & Corrales-Gárcia, E.M. (2016). Survival in glioblastoma: a review on the impact of treatment modalities. *Clinical and Translational Oncology, 18*(11), 1062-1071.

Deng, C.-X. (2006). BRCA1: cell cycle checkpoint, genetic instability, DNA damage response and cancer evolution. *Nucleic Acids Research*, *34*(5), 1416–1426.

Deng, L., Wang, C., Spencer, E., Yang, L., Braun, A., You, J., Slaughter, C., Pickart, C., & Chen, Z.J. (2000). Activation of the IκB Kinase Complex by TRAF6 Requires a Dimeric Ubiquitin-Conjugating Enzyme Complex and a Unique Polyubiquitin Chain. *Cell*, *103*, 351–361.

Deregowski, V., & Canalis, E. (2008). Gene delivery by retroviruses. *Methods in Molecular Biology, 455*, 157-162.

Deshaies, R.J., & Joazeiro, C.A.P. (2009). RING Domain E3 Ubiquitin Ligases. *Annual Review of Biochemistry, 82*, *78*(1), 399–434.

Di Fiore, P.P., Polo, S., & Hofman, K. (2003). When ubiquitin meets ubiquitin receptors: a signalling connection. *Nature Reviews Molecular Cell Biology, 4*, 491-497.

Di Lisa, F., & Bernardi, P. (1998). Mitochondrial function as a determinant of recovery or death in cell response to injury. *Molecular and Cellular Biochemistry, 184*(1-2), 379-391.

Ding, Z.-Y., Huang, Y.-J., Tang, J.-D., Li, G., Jiang, P.-Q., & Wu, H.-T. (2016). Silencing of hypoxia-inducible factor-1α promotes thyroid cancer cell apotosis and inhibits invasion by down regulating WWP2, WWP9, VEGF and VEGFR2. *Experimental and Therapeutic Medicine, 12*(6), 3735-3741.

Dittmer, D., Pati, S., Zambetti, G., Chu, S., Teresky, A.K., Moore, M., Finlay, C., & Levine, A.J. (1993). Gain of function mutations in p53. *Nature Genetics, 4*, 42-46.

Draetta, G., & Beach, D. (1988). Activation of cdc2 protein kinase during mitosis in human cells: cell cycle-dependent phosphorylation and subunit rearrangement. *Cell, 54*(1), 17-26.

Drexler, H.G. (1998). Review of alterations of the cyclin-dependent kinase inhibitor INK4 family in p15, p16, p18 and p19 in human leukemia-lymphoma cells. *Leukemia, 12*, 845-859.

Drury, L.S., Perkins, G., & Diffley, J.F. (1997). The Cdc4/34/53 pathway targets Cdc6p for proteolysis in budding yeast. *The EMBO Journal*, *16*(19), 5966–5976.

Dumont, S., & Mitchison, T.J. (2009). Force and Length in the Mitotic Spindle. *Current Biology, 19*(17), R749-R761.

Durocher, Y., Perret, S., & Kamen, A. (2002). High-level and high-throughput recombinant protein production by transient transfection of suspension-growing human 293-EBNA1 cells. *Nucleic Acids Research, 30*(2), e9.

Duronio, R.J., & Xiong, Y. (2013). Signaling Pathways that Control Cell Proliferation. *Cold Spring Harbour Perspectives in Biology, 5*(3), a008904. DOI: 10.1101/cshperspect.a008904.

Edelmann, M.J., Iphöfer, A., Akutsu, M., Altun, M., di Gleria, K., Kramer, H.B., Fiebiger, E., Dhe-Paganon, S., & Kessler, B.M. (2009). *The Biochemical Journal, 418*(2), 379-390.

Edelstein, A.D., Tsuchida, M.A., Amodaj, N., Pinkard, H., Vale, R.D., & Stuurman, N. (2014). Advanced methods of microscope control using μManager software. *Journal Biological Methods, 1(2):* e10. doi: 10.14440/jbm.2014.36

Ekkebus, R., van Kasteren, S.I., Kulathu, Y., Scholten, A., Berlin, I., Geurink, P.P., de Jong, A., Goerdayal, S., Neefjes, J., Heck, A.J., Komander, D., & Ovaa, H. (2013). On terminal alkynes that can react with active-site cysteine nucleophiles in proteases. *Journal of the American Chemical Society, 135*(8), 2867-2870.

Elvin, P., & Evans, C.W. (1984). Cell adhesiveness and the cell cycle: correlation in synchronized Balb/c 3T3 cells. *Biology of the Cell, 48*(1), 1-9.

Emmerich, C.H., & Cohen, P. (2015). Optimising methods for the preservation, capture and identification of ubiquitin chains and ubiquitylated proteins by immunoblotting. *Biochemical and Biophysical Research Communications, 466*(1), 1-14.

Engler, C., Kandzia, R., & Marillonnet, S. (2008). A One Pot, One Step, Precision Cloning Method with High Throughput Capability. *PLOS One.* DOI: 10.1371/journal.pone.0003647.

Epstein, M.A., Achong, B.G., & Barr, Y.M. (1964). Virus particles in cultured lymphoblasts from Burkitt's lymphoma. *Lancet, 1*(7335), 702-703.

Ernst, A., Avvakumov, G., Tong, J., Fan, Y., Zhao, Y., Alberts, P., Persaud, A., Walker, J.R., Neculai, A.M., Neculai, D., Vorobyov, A., Garg, P., Beatty, L., Chan, P.K., Juang, Y.C., Landry, M.C., Yeh, C., Zeqiraj, E., Karamboulas, K., Allali-Hassani, A., Vedadi, M., Tyers, M., Moffat, J., Sicheri, F., Pelletier, L., Durocher, D., Raught, B., Rotin, D., Yang, J., Moran, M.F., Dhe-Paganon, S., & Sidhu, S.S. (2013). A strategy for modulation of enzymes in the ubiquitin system. *Science, 339*(6119), 590-590.

Escobedo, A., Gomes, T., Aragón, E., Martín-Malpartida, P., Ruiz, L., & Macias, M.J. (2014). Structural basis of the activation and degradation mechanisms of the E3 ubiquitin ligase Nedd4L. *Structure*, *22*(10), 1446–1457.

Esteban, V., Sacristán, M., Andrés, S., & Bueno, A. (2008). The Flp1/Clp1 phosphatase cooperates with HECT-type Pub1/2 protein-ubiquitin ligases in *Schizosaccharomyces pombe*. *Cell Cycle*, *7*(9), 1269–1276.

Esteller, M. (2006). Epigenetics provides a new generation of oncogenes and tumour-suppressor genes. *British Journal of Cancer, 94*(2), 179-183

Evans, T., Rosenthal, E.T., Youngblom, J., Distel, D., & Hunt, T. (1983). Cyclin: A Protein Specified by Maternal mRNA in Sea Urchin Eggs That is Destroyed at Each Cleavage Division. *Cell*, *33*, 389-396.

Evans, P.C., Smith, T.S., Lai, M.J., Williams, M.G., Burke, D.F., Heyninck, K., Kreike, M.M., Beyaert, R., Blundell, T.L., & Kilshaw, P.J. (2003). A novel type of deubiquitinating enzyme. *Journal of Biological Chemistry, 278*, 23180-23186.

Evelyn, C.R., Duan, X., Biesiada, J., Siebel, W.L., Meller, J., & Zheng, Y. (2014). Rational Design of Small Molecule Inhibitors Targeting the Ras GEF, SOS1. *Chemistry & Biology, 21*(12), 1618-1628.

Fang, G., Yu, H., & Kirschner, M.W. (1998). Direct binding of CDC20 protein family members activates the anaphase-promoting complex in mitosis and G1. *Molecular Cell, 2*(2), 163-171.

Fang, Y., & Fullwood, M.J. (2016). Role, Functions, and Mechanisms of Long Non-coding RNAs in Cancer. *Genetics, Proteomics & Bioinformatics, 14*(1), 42-54.

Faronato, M., Patel, V., Darling, S., Dearden, L., Clague, M.J., Urbé, S., & Coulson, J.M. (2013). The deubiquitylase USP15 stabilizes newly synthesized REST and rescues its expression at mitotic exit. *Cell Cycle, 12*(12), 1964-1977.

Feinberg, A.P., & Tycko, B. (2004). The history of cancer epigenetics. *Nature Reviews Cancer 4*(2), 143-153.

Fernando, M.D.A., Kounatidis, I., & Ligoxygakis, P. (2014). Loss of Trabid, a New Negative Regulator of the *Drosophila* Immune-Deficiency Pathway at the Level of TAK1, Reduces Life Span. *PLOS One*. DOI: 10.1371/journal.pgen.1004117.

Ferreira, J.V., Soares, A.R., Ramalho, J.S., Pereira, P., & Girao, H. (2015). K63 linked ubiquitin chain formation is a signal for HIF1A degradation by Chaperone-Mediated Autophagy. *Scientific Reports, 5*, 10210. DOI: 10.1038/srep10210.

Finley, D., Sadis, S., Monia, B.P., Boucher, P., Ecker, D.J., Crooke, S.T., & Chau, V. (1994). Inhibition of proteolysis and cell cycle progression in a multiubiquitination-deficient yeast mutant. *Molecular and Cellular Biology*, *14*(8), 5501–5509.

Fire, A., Xu, S., Montgomery, M.K., Kostas, S.A., Driver, S.E., & Mello, C.C. (1998) Potent and specific genetic interference by double-stranded RNA in *Caenorhabditis elegans*. *Nature, 391*, 806–811.

Flack, J.E., Mieszczanek, J., Novcic, N., & Bienz, M. (2017). Wnt-Dependent Inactivation of the Groucho/TLE Co-repressor by the HECT E3 Ubiquitin Ligase Hyd/UBR5. *Cell, 67*(2), 181-193.

Floyd, S., Pines, J., & Lindon, C. (2008). APC/C Cdh1 targets aurora kinase to control reorganization of the mitotic spindle at anaphase. *Current Biology: CB*, *18*(21), 1649–1658.

Fortungo, P., Wall, N.R., Giodinin, A., O'Connor, D.S., Plescia, J., Padgett, K.M., Tognin, S., Marchisio, P.C., & Altieri, D.C. (2002). Survinin exists in immunochemically distinct subcellular pools and is involved in spindle microtubule function. *Journal of Cell Science, 115*, 575-585.

French, M.E., Klosowiak, J.L., Aslanian, A., Reed, S.I., Yates, III. J.R., & Hunter, T. (2017). Mechanism of ubiquitin chain synthesis employed by a HECT ubiquitin ligase. *Journal of Biological Chemistry, 292,* 10398-10413.

Fukumoto, C., Nakashima, D., Kasamatsu, A., Unozawa, M., Shida-Sakazume, T., Higo, M., Ogawara, K., Yokoe, H., Shiiba, M., Tanzawa, H., & Uzawa, K. (2014). WWP2 is overexpressed in human oral cancer, determining tumor size and poor prognosis in patients: downregulation of WWP2 inhibits the AKT signalling and tumor growth in mice. *Oncoscience, 1*(12), 807-820.

Fung, Y.K., Murphree, A.L., T'Ang, A., Qian, J., Hinrichs, S.H., Benedict, W.F. (1987). Structural evidence for the authenticity of the human retinoblastoma gene. *Science, 236*(4809), 1657-1661.

Gaglio, T., Saredi, A., Bingham, J.B., Hasbani, M.J., Gill, S.R., Schroer, T.A., & Compton, D.A. (1996). Opposing motor activities are required for the organization of the mammalian mitotic spindle pole. *Journal Cell Biology, 135*(2), 399-414.

Gallagher, E., Gao, M., Liu, Y.-C., & Karin, M. (2006). Activation of the E3 ubiquitin ligase Itch through a phosphorylation-induced conformational change. *Proceedings of the National Academy of Sciences of the United States of America*, *103*(6), 1717-1722.

Gallini, S., Carminati, M., De Mattia, F., Pirovano, L., Martini, E., Oldani, A., Asreriti, I.A., Guarguaglini, G., & Mapelli, M. (2016). NuMA Phosphorylation by Aurora-A Orchestrates Spindle Orientation. *Current Biology, 26*(4), 458-469.

Gao, C., Xiao, G., & Hu, J. (2014). Regulation of Wnt/β-catenin signaling by posttranslational modifications. *Cell & Bioscience, 4*(13). DOI: 10.1186/2045-3701-4-13.

Gao, J., Huo, L., Sun, X., Liu, M., Li, D., Dong, J.T., & Zhou, J. (2008). The tumor suppressor CYLD regulates microtubule dynamics and plays a role in cell migration. *Journal of Biological Chemistry, 283*(14), 8802-8809.

Geisler, S., Holmstroem, K.M., Skujat, D., Fiesel, F.C., Rothfuss, O.C., Kahle, P.J., & Springer, W. (2010). PINK1/Parkin-mediated mitophagy is dependent on VDAC1 and p62/SQSTM1. *Nature Cell Biology*, *12*(2), 119-131.

Geley, S., Kramer, E., Gieffers, C., Gannon, J., Peters, J.M., & Hunt, T. (2001). Anaphase-promoting complex/cyclosome-dependent proteolysis of human cyclin A starts at the beginning of mitosis and is not subject to the spindle assembly checkpoint. *Journal of Cell Biology, 153*(1), 137-148.

Ghoshal, K., Datta, J., Majumder, S., Bai, S., Kutay, H., Motiwala, T., & Jacob, S.T. (2005). 5-Aza-deoxycytidine induces selective degradation of DNA methyltransferase 1 by a proteasomal pathway that requires the KEN box, bromo-adjacent homology domains, and nuclear localisation signal. *Molecular and Cellular Biology, 25*(11), 4727-4741.

Giet, R., & Glover, D.M. (2001). *Drosophila* Aurora B Kinase is Required for Histone H3 Phosphorylation and Condesin Recruitment during Chromosome Condensation and to Organize the Central Spindle during Cytokinesis. *Journal of Cell Biology, 152*(4), 669-681.

Giono, L.E., & Manfredi, J.J. (2006). The p53 tumour suppressor participates in multiple cell cycle checkpoints. *Journal of Cell Physiology, 209*(1), 13-20.

Glotzer, M., Murray, A.W., & Kirschner, M.W. (1991). Cyclin is degraded by the ubiquitin pathway. *Nature, 349*, 132-137.

Goka, E.T., & Lippman, M.E. (2015). Loss of the E3 ubiquitin ligase *HACE1* results in enhanced Rac1 signaling contributing to breast cancer progression. *Oncogene, 34,* 5395-5405.

Goldstein, G., Scheid, M., Hammerling, U., Schlesinger, D.H., Niall, H.D., & Boyse, E.A. (1975). Isolation of a polypeptide that has lymphocyte-differentiating properties and is probably represented universally in living cells. *Proceedings of the National Academy of Sciences of the United States of America*, *72*(1), 11–15.

Gong, W., Zhang, X., Zhang, W., Li, J., & Li, Z. (2015). Structure of the HECT domain of human WWP2. *Acta Crystallographica. Section F, Structural Biology Communications*, *71*(Pt 10), 1251–1257.

Goshima, G., Mayer, M., Zhang, N., Stuurman, N., & Vale, R.D. (2008). Augmin: a protein complex required for centrosome-independent microtubule generation within the spindle. *Journal of Cell Biology, 181*(3), 421-429.

Goto, H., Tomono, Y., Ajiro, K., Kosako, H., Fujita, M., Sakurai, M., Okawa, K., Iwamatsu, A., Okigaki, T., Takahashi, T., & Inagaki, M. (1999). Identification of a novel phosphorylation site on histone H3 coupled with mitotic chromosome condensation. *Journal Biological Chemistry, 274*(36), 25543-25549.

Goto, H., Yasui, Y., Nigg, E.A., & Inagaki, M. (2002). Aurora-B phosphorylates Histone H3 at serine28 with regard to the mitotic chromosome condenstation. *Genes to Cells, 7*(1), 11-17.

Goto, Y., Kojima, S., Kurozumi, A., Kato, M., Okato, A., Matsushita, R., Ichikawa, T., & Seki, N. (2016). Regulation of E3 ubiquitin ligase-1 (WWP1) by *microRNA-452* inhibits cancer cell migration and invasion in prostate cancer. *British Journal of Cancer, 114*, 1135-1144.

Graham, D.B., & and Root, D.E. (2015). Resources for the design of CRISPR gene editing experiments. *Genome Biology, 16*(260). DOI: 10.1186/s13059-015-0823-x.

Gratzner, H.G. (1982). Monoclonal antibody to 5-bromo- and 5-iododeoxyuridine: A new reagent for detection of DNA replication. *Science, 281*(4571), 474-475.

Grau-Bove, X., Sebe-Pedros, A., & Ruiz-Trillo, I. (2013). A Genomic Survey of HECT Ubiquitin Ligases in Eukaryotes Reveals Independent Expansions of the HECT System in Several Lineages. *Genome Biology and Evolution*, *5*(5), 833–847.

Green, L.C., Kalitsis, P., Chang, T.M., Cipetic, M., Kim, J.H., Marshall, O., Turnbull, L., Whitchurch, C.B., Vagnarelli, P., Samejima, K., Earnshaw, W.C., Choo, K.H.A., & Hudson, D.F. (2012). Contrasting roles of condensin I and condensin II in mitotic chromosome formation. *Journal of Cell Science*, *125*(Pt 6), 1591–1604.

Grice, G.L., Lobb, I.T., Weekes, M.P., Gygi, S.P., Antrobus, R., & Nathan, J.A. (2015). The Proteasome Distinguishes between Heterotypic and Homotypic Lysine-11-Linked Polyubiquitin Chains. *Cell Reports, 12*(4), 545-553.

Grill, S.W., & Hyman, A.A. (2005). Spindle positioning by cortical pulling forces. *Developmental Cell, 8*(4), 461-465.

Gurley, L.R., D'Anna, J.A., Barham, S.S., Deaven, L.L., & Tobey, R.A. (1978). Histone phosphorylation and chromatin structure during mitosis in Chinese hamster cells. *European Journal of Biochemistry, 84*(1), 1-15.

Haas, A.L., Warms, J.V., Hershko, A., & Rose, I.A. (1982). Ubiquitin-activating enzyme. Mechanism and role in protein-ubiquitin conjugation. *The Journal of Biological Chemistry*, *257*(5), 2543–2548.

Haberland, M., Montgomery, R.L., & Olson, E.N. (2009). The many roles of histone deacetylases in development and physiology: implications for disease and therapy. *Nature Reviews Genetics, 10*(1), 32-42.

Haglund, K., Sigismund, S., Polo, S., Szymkiewicz, I., Di Fiore, P.P., & Dikic, I. (2003). Multiple monoubiquitination of RTKs is sufficient for their endocytosis and degradation. *Nature Cell Biology*, *5*(5), 461–466.

Hagting, A., Elzen Den, N., Vodermaier, H.C., Waizenegger, I.C., Peters, J.M., & Pines, J. (2002). Human securin proteolysis is controlled by the spindle checkpoint and reveals when the APC/C switches from activation by Cdc20 to Cdh1. *The Journal of Cell Biology*, *157*(7), 1125–1137.

Hall, J.R., Kow, E., Nevis, K.R., Lu, C.K., Luce, K.S., Zhong, Q., & Cook, J.G. (2007). Cdc6 stability is regulated by the Huwe1 ubiquitin ligase after DNA damage. *Molecular Biology of the Cell*, *18*(9), 3340–3350.

Haloom, R., Orlowski, C., Georgiadis, G.T., Ververis, K., El-Osta, A., & Karagiannis, T.C. (2011). Clonogenic Assay: Adherent Cells. *Journal of Visualized Experiments,* 49, 2573. DOI: 10.3791/2573.

Han, S.-O., Kommaddi, R.P., & Shenoy, S.K. (2013). Distinct roles for β-arrestin2 and arrestin-domain-containing proteins in β2 adrenergic receptor trafficking. *EMBO Reports*, *14*(2), 164–171.

Hanahan, D., & Weinberg, R.A. (2011). Hallmarks of Cancer: The Next Generation. *Cell, 144*(5), 646-674.

Haren, L., Gnadt, N., Wright, M., & Merdes, A. (2009). NuMA is required for proper spindle assembly and chromosome alignment in prometaphase. *BMC Research Notes, 2*(64). DOI: 10.1186/1756-0500-2-64.

Harris, H., Miller, O.J., Klein, G., Worst, P., & Tachibana, T. (1969). Suppression of Malignancy by Cell Fusion. *Nature, 223*, 363-368.

Harvey, K.F., Shearwin-Whyatt, L.M., Fotia, A., Parton, R.G., & Kumar, S. (2002). N4WBP5, a potential target for ubiquitination by the Nedd4 family of proteins, is a novel Golgi-associated protein. *The Journal of Biological Chemistry*, *277*(11), 9307–9317.

Hatakeyama, S., Yada, M., Matsumoto, M., Ishida, N., & Nakayama, K.I. (2001). U box proteins as a new family of ubiquitin-protein ligases. *Journal of Biological Chemistry, 276*(35), 33111-33120.

Hauf, S., Cole, R.W., LaTerra, S., Zimmer, C., Schnapp, G., Walter, R., Heckel, A., van Meel, J., Rieder, C.L., & Peters, J.M. (2003). The small molecule Hesperadin reveals a role for Aurora B in correcting kinetochore-microtubule attachment and in maintaining the spindle assembly checkpoint. *Journal of Cell Biology, 161*(2), 281- 294.

Hay, W.W. Jr. (1994). Placental transport of nutrients to the fetus. *Hormone Research, 42*(4-5), 215-222.

Hay-Koren, A., Caspi, M., Zilberberg, A., & Rosin-Arbesfeld, R. (2011). The EDD E3 ubiquitin ligase ubiquitinates and up-regulates β-catenin. *Molecular Biology of the Cell, 22*(3), 399-411.

Hayden, J.H., Bowser, S.S., & Rieder, C.L. (1990). Kinetochores capture astral microtubules during chromosome attachment to the mitotic spindle: direct visualization in live newt lung cells. *Journal of Cell Biology, 111*(3), 1039-45.

Haynes, H.R., Camelo-Piragua, S., & Kurian, K.M. (2014). Prognostic and predictive biomarkers in adult and pediatric gliomas: toward personalized treatment. *Frontiers in Oncology, 4*, 47. DOI: 10.3389/fonc.2014.00047.

He, Z., Wu, J., Su, X., Zhang, Y., Pan, L., Wei, H., Fang, Q., Li, H., Wang, L.-D., & Sun, F.-L. (2015). JMJD5 (Jumonji Domain-containing 5) Associates with Spindle Microtubules and Is Required for Proper Mitosis. *Journal of Biological Chemistry, 291*(9), 4684-4694.

Heald, R., Tournebize, R., Blank, T., Sandaltzopoulous, R., Becker, P., Hyman, A., Karsenti, E. (1996). Self-organization of microtubules into bipolar spindles around artificial chromosomes in *Xenopus* egg extracts. *Nature, 382*, 420-425.

Heald, R., & Khodjakov, A. (2015). Thirty years of search and capture: The complex simplicity of mitotic spindle assembly. *Journal of Cell Biology, 211*(6), 1103-1111.

Heap, R.E., Gant, M.S., Lamoliatte, F., Peltier, J., & Trost, M. (2017). Mass spectrometry techniques for studying the ubiquitin system. *Biochemical Society Transactions, 45*, 1137–1148.

Hebbes, T.R., Thorne, A.W., & Crane-Robinson, C. (1988). A direct link between core histone acetylation and transcriptionally active chromatin. *EMBO Journal, 7*(5), 1395-1402.

Hein, J., Hertz, E.P.T., Garvanska, D.H., Kruse, T., & Nilsson, J. (2017). Distinct kinetics of serine and threonine dephosphorylation are essential for mitosis. *Nature Cell Biology*. DOI: 10.1038/ncb3634.

Hemelaar, J., Galardy, P.J., Borodovsky, A., Kessler, B.M., Ploegh, H.L., & Ovaa, H. (2004). Chemistry-Based Functional Proteomics: Mechanism-Based Activity-Profiling Tools for Ubiquitin and Ubiquitin-like Specific Proteases. *Journal of Proteome Research, 3*(2), 268-276.

Henderson, M.J., Munoz, M.A., Saunders, D.N., Clancy, J.L., Russell, A.J., Williams, B., Pappin, D., Khanna, K.K., Jackson, S.P., Sutherland, R.L., & Watts, C.K.W. (2006). EDD mediates DNA damage-induced activation of CHK2. *The Journal of Biological Chemistry*, *281*(52), 39990–40000.

Hengstschläger, M., Braun, K., Soucek, T., Miloloza, A., Hengstschläger-Ottnad, E. (1999). Cyclin-dependent kinases at the G1-S transition of the mammalian cell cycle. *Mutation Research, 436*(1), 1-9.

Henikoff, S., & Smith, M.M. (2015). Histone variants and Epigenetics. *Cold Spring Harbour Perspectives in Biology, 7*(1): a019364. DOI: 10.1101/cshperspect.a019364.

Herold, S., Hock, A., Herkert, B., Berns, K., Mullenders, J., Beijersbergen, R., Bernards, R., & Eilers, M. (2008). Miz1 and HectH9 regulate the stability of the checkpoint protein, TopBP1. *The EMBO Journal*, *27*(21), 2851–2861.

Hershko, A., Ciechanover, A., Heller, H., Haas, A.L., & Rose, I.A. (1980). Proposed role of ATP in protein breakdown: conjugation of protein with multiple chains of the polypeptide of ATP-dependent proteolysis. *Proceedings of the National Academy of Sciences of the United States of America*, *77*(4), 1783–1786.

Hershko, A., Heller, H., Elias, S., & Ciechanover, A. (1983). Components of ubiquitin-protein ligase system. Resolution, affinity purification, and role in protein breakdown. *The Journal of Biological Chemistry*, *258*(13), 8206–8214.

Hershko, A., Leshinsky, E., Ganoth, D., & Heller, H. (1984). ATP-dependent degradation of ubiquitin-protein conjugates. *Proceedings of the National Academy of Sciences of the United States of America*, *81*(6), 1619–1623.

Hershko, A., & Rose, I.A. (1987). Ubiquitin-aldehyde: a general inhibitor of ubiquitin-recycling processes. *PNAS, 84*(7), 1829-1833.

Hershko, A. (1997). Roles of ubiquitin-mediated proteolysis in cell cycle control. *Current Opinion in Cell Biology, 9*(6), 788-799.

Hershko, A., & Ciechanover, A. (1998). The Ubiquitin System. *Annual Review of Biochemistry, Vol 82*, *67*, 425–479.

Hjerpe, R., Aillet, F., Lopitz-Otsoa, F., Lang, V., England, P., & Rodriguez, M.S. (2009). Efficient protection and isolation of ubiquitylated proteins using tandem ubiquitin-binding entities. *EMBO Reports, 10*(11), 1250-1258.

Hoebeke, J., Van Nijen, G., & De Brabander, M. (1976). Interaction of Nocodazole (R 17934), A New Anti-tumoral Drug, with Rat Brain Tubulin. *Biochemical and Biophysical Research Communications*, *69*(2), 319–324.

Hofmann, R.M., & Pickart, C.M. (1999). Noncanonical *MMS2*-Encoded Ubiquitin-Conjugating Enzyme Functions in Assembly of Novel Polyubiquitin Chains for DNA Repair. *Cell*, *96*, 645–653.

Holloway, S.L., Glotzer, M., King, R.W., & Murray, A.W. (1993). Anaphase is initiated by proteolysis rather than by the inactivation of maturation-promoting factor. *Cell, 73*(7), 1393-1402.

Holy, T.E., & Leibler, S. (1994). Dynamic instability of microtubules as an efficient way to search in space. *PNAS*, *Cell Biology, 91,* 5682-5685.

Honda, Y., Tojo, M., Matsuzaki, K., Anan, T., Matsumoto, M., Ando, M., Saya, H., & Nakao, M. (2002). Cooperation of HECT-domain ubiquitin ligase hHYD and DNA topoisomerase II-binding protein for DNA damage response. *The Journal of Biological Chemistry*, *277*(5), 3599–3605.

Hong, S.-W., Moon, J.-H., Kim, J.-S., Shin, J.-S., Jung, K.-A., Lee, W.-K., Jeong, S.-Y., Hwang, J.J., Lee, S.-J., Suh, Y.-A., Kim, I., Nam, K.-Y., Han, S., Kim, J.E., Kim, K.-P., Hong, Y.S., Lee, J.-L., Lee, W.-J., Choi, E.K., Lee, J.S., Jin, D.-H., & Kim, T.W. (2014). P34 is a novel regulator of the oncogenic behaviour of NEDD4-1 and PTEN. *Cell Death and Differentiation, 21*, 146-160.

Hospenthal, M.K., Mevissen, T.E.T., & Komander, D. (2015). Deubiquitinase-based analysis of ubiquitin chain architecture using Ubiquitin Chain Restriction (UbiCRest). *Nature Protocols, 10*(2), 349-361.

Hoyt, M.A., Totis, L., & Roberts, B.T. (1991). S. cerevisiae genes required for cell cycle arrest in response to loss of microtubule function. *Cell, 66*(3), 507-517.

Huang, L., Kinnucan, E., Wang, G., Beaudenon, S., Howley, P.M., Huibregtse, J.M., & Pavletich, N.P. (1999). Structure of an E6AP-UbcH7 complex: insights into ubiquitination by the E2-E3 enzyme cascade. *Science*, *286*(5443), 1321–1326.

Huang, Q., & Szebenyi, D.M.E. (2010). Structural basis for the interaction between the growth factor-binding protein GRB10 and the E3 ubiquitin ligase NEDD4. *Journal of Biological Chemistry*, *285*(53), 42130–42139.

Huang, X., Poy, F., Zhang, R., Joachimiak, A., Sudol, M., & Eck, M.J. (2000). Structure of a WW domain containing fragment of dystrophin in complex with β-dystroglycan. *Nature Structural Biology, 8,* 634-638.

Huibregtse, J.M., Scheffner, M., Beaudenon, S., & Howley, P.M. (1995). A Family of Proteins Structurally and Functionally Related to the E6-AP Ubiquitin Protein Ligase. *Proceedings of the National Academy of Sciences of the United States of America*, *92*(7), 2563–2567.

Hussain, S., Benavente, S.B., Mascimento, E., Dragoni, I., Kurowski, A., Gilich, A., Humphreys, P., & Frye, M. (2009). The nucleolar RNA methyltransferase Misu (NSun2) is required for mitotic spindle stability. *Journal of Cell Biology, 186*(1), 27-40.

Hwang, L.H., Lau, L.F., Smith, D.L., Mistrot, C.A., Hardwick, K.G., Hwang, E.S., Amon, A., & Murray, A.W. (1998). Budding yeast Cdc20: a target of the spindle checkpoint. *Science, 279*(5353), 1041-1044.

Ichimura, T., Yamamura, H., Sasamoto, K., Tominaga, Y., Taoka, M., Kakiuchi, K., Shinkawa, T., Takahashi, N., Shimada, S., & Isobe, T. (2005). 14-3-3 proteins modulate the expression of epithelial Na+ channels by phosphorylation-dependent interaction with Nedd4-2 ubiquitin ligase. *The Journal of Biological Chemistry*, *280*(13), 13187–13194.

Ikehara, S., Pahwa, R.N., Fernandes, G., Hansen, C.T., & Good, R.A. (1984). Functional T cells in thymic nude mice. *PNAS, 81*(3), 886-888.

Inoué, S., & Salmon, E.D. (1995). Force Generation by Microtubule Assembly/Disassembly in Mitosis and Related Movements. *Molecular Biology of the Cell, 6*(12), 1619-1640.

Ionov, Y., Nowak, N., Perucho, M., Markowitz, S., & Cowell, J.K. (2004). Manipulation of nonsense mediated decay identified gene mutations in colon cancer Cells with microsatellite instability. *Oncogene, 23*, 639-645.

Izawa, N., Wu, W., Sato, K., Nishikawa, H., Kato, A., Boku, N., Itoh, F., & Ohta, T. (2011). HERC2 Interacts with Claspin and regulates DNA origin firing and replication fork progression. *Cancer Research*, *71*(17), 5621–5625.

Jacinto, F.V., & Esteller, M. (2007). MGMT hypermethylation: a prognostic foe, a predictive friend. *DNA Repair, 6*(8), 1155-1160.

Jacinto, F.V., Ballestar, E., Ropero, S., & Esteller, M. (2007). Discovery of epigenetically silenced genes by methylated DNA immunoprecipitation in colon cancer cells. *Cancer Research, 67*(24), 11481-11486.

Jevtić, P., Edens, L.J., Vuković, L.D., & Levy, D.L. (2015). Sizing and shaping the nucleus: mechanisms and significance. *Current Opinion in Cell Biology, 28*, 16-27.

Jiang, J., Ballinger, C.A., Wu, Y., Dai, Q., Cyr, D.M., Höfeld, J., & Patterson, C. (2001). CHIP is a U-box-dependent E3 ubiquitin ligase: identification of Hsc70 as a target for ubiquitylation. *Journal of Biological Chemistry, 276*(46), 42938-42944.

Jiang, J.H., Liu, Y.F., Ke, A.W., Gu, F.M., Yu, Y., Dai, Z., Gao, Q., Shi, G.M., Liao, B.Y., Xie, Y.H., Fan, J., Huang, X.W., & Zhou, J. (2014). Clinical significance of the ubiquitin ligase UBE3C in hepatocellular carcinoma revealed by exome sequencing. *Hepatology, 59*(6), 2216-2227.

Jin, L., Williamson, A., Banerjee, S., Philipp, I., & Rape, M. (2008). Mechanism of Ubiquitin-Chain Formation by the Human Anaphase-Promoting Complex. *Cell*, *133*(4), 653–665.

Johnson, E.S., Philip, C.M.M., Ota, I.M., & Varshavsky, A. (1995). A Proteolytic Pathway That Recognizes Ubiquitin as a Degradation Signal. *The Journal of Biological Chemistry*, *270*(29), 17442–17456.

Johnson, A., & Skotheim, J.M. (2013). Start and the restriction point. *Current Opinion in Cell Biology, 25*(6), 717-723.

Jones, P.A., & Baylin, S.B. (2002). The fundamental role of epigenetic events in cancer. *Nature Reviews Genetics, 3*(6), 415-428.

Jordan, M.A., Thrower, D., & Wilson, L. (1992). Effects of vinblastine, podophyllotoxin and nocodazole on mitotic spindles. Implications for the role of microtubule dynamics in mitotis. *Journal of Cell Science, 102*(3), 401-416.

Kalab, P., Weis, K., Heald, R. (2002). Visualisation of a Ran-GTP gradient in interphase and mitotic Xenopus egg extracts. *Science, 295*(5564), 2452-2456.

Kamadurai, H.B., Souphron, J., Scott, D.C., Duda, D.M., Miller, D.J., Stringer, D., Piper, R.C., & Schulman, B.A. (2009). Insights into ubiquitin transfer cascades from a structure of a UbcH5B approximately ubiquitin-HECT^{NEDD4L} complex. *Molecular Cell*, *36*(6), 1095–1102.

Kamadurai, H.B., Qiu, Y., Deng, A., Harrison, J.S., MacDonald, C., Actis, M., Rodrigues, P., Miller, D.J., Souphron, J., Lewsi, S.M., Kurinov, I., Fujii, N., Hammel, M., Piper, R., Kuhlman, B., & Schulman, B.A. (2013). Mechanism of ubiquitin ligation and lysine prioritization by a HECT E3. *eLife*, *2*, 10–26. http://doi.org/10.7554/eLife.00828

Kannan, M., Lee, S.-J., Schwedhelm-Domeyer, N., & Stegmüller, J. (2012). The E3 ligase Cdh1-anaphase promoting complex operates upstream of the E3 ligase Smurf1 in the control of axon growth. *Development, 139*, 3600-3612.

Karczmarski, J., Rubel, T., Paziewska, A., Mikula, M., Bujko, M., Kober, P., Dadlez, M., & Ostrowski, J. (2014). Histone H3 lysine 27 acetylation is altered in colon cancer. *Clinical Proteomics, 11*(1), 24. DOI: 10.1186/1559-0275-11-24.

Kareta, M.S., Botello, Z.M., Ennis, J.J., Chou, C., & Chédin, F. (2006). Reconstitution and mechanism of the stimulation of de novo methylation by human DNMT3L. *Journal of Biological Chemistry, 281*(36), 25893-25902.

Kauffman, M.G., Noga, S.J., Kelly, T.J., & Donnenberg, A.D. (1990). Isolation of cell cycle fractions by counterflow centrifugal elutriation. *Analytical Biochemistry, 191*(1), 41-46.

Ke, M., Mo, L., Li, W., Zhang, X., Li, F., & Yu, H. (2017). Ubiquitin ligase SMURF1 functions as a prognostic marker and promotes growth and metastasis of clear cell renal cell carcinoma. *FEBS Open Bio, 7*(4), 577-586.

Kent, W.J., Sugnet, C.W., Furey, T.S., Roskin, K.M., Pringle, T.H., Zahler, A.M., & Haussler, D. (2002). The human genome browser at UCSC. *Genome Research, 12*(6), 996-1006.

Kettenbach, A.N., Rush, J., & Gerber, S.A. (2011). Absolute quantification of protein and post-translational modification abundance with stable isotope-labeled synthetic peptides. *Nature Protocols, 6,* 175-186.

Keusekotten, K., Elliott, P.R., Glockner, L., Fiil, B.K., Damgaard, R.B., Kulathu, Y., Wauer, T., Hospenthal, M.K., Gyrd-Hansen, M., Krappmann, D., Hofmann, K., & Komander, D. (2013). OTULIN antagonizes LUBAC signaling by specifically hydrolyzing Met1-linked polyubiquitin. *Cell*, *153*(6), 1312–1326.

Kim, D.-H., & Koepp, D.M. (2012a). Hect E3 ubiquitin ligase Tom1 controls Dia2 degradation during the cell cycle. *Molecular Biology of the Cell*, *23*(21), 4203–4211.

Kim, D.-H., Zhang, W., & Koepp, D.M. (2012b). The Hect domain E3 ligase Tom1 and the F-box protein Dia2 control Cdc6 degradation in G1 phase. *Journal of Biological Chemistry*, *287*(53), 44212–44220.

Kim, E.M., & Burke, D.J. (2008). DNA damage activates the SAC in an ATM/ATR-dependent manner, independently of the kinetochore. *Plos Genetics*, *4*(2), e1000015. http://doi.org/10.1371/journal.pgen.1000015

Kim, G.D., Ni, J., Kelesoglu, N., Roberts, R.J., & Pradhan, S. (2002). Co-operation and communication between the human maintenance and de novo DNA (cytosine-5) mehtyltransferases. *EMBO Journal, 21*(15), 4183-4195.

Kim, H.C., & Huibregtse, J.M. (2009). Polyubiquitination by HECT E3s and the Determinants of Chain Type Specificity. *Molecular and Cellular Biology*, *29*(12), 3307–3318.

Kim, H.C., Steffen, A.M., Oldham, M.L., Chen, J., & Huibregtse, J. (2011). Structure and function of a HECT domain ubiquitin-binding site. *EMBO Reports*, *12*(4), 334–341.

Kim, H.T., Kim, K.P., Lledias, F., Kisselev, A.F., Scaglione, K.M., Skowyra, D., Gygi, S.P., & Goldberg, A.L. (2007). Certain pairs of ubiquitin-conjugating enzymes (E2s) and ubiquitin-protein ligases (E3s) synthesize nondegradable forked ubiquitin chain containing all possible isopeptide linkages. *Journal of Biological Chemistry, 282*(24), 17375-17386.

Kim, H.T., Kim, K.P., Uchiki, T., Gygi, S.P., & Goldberg, A.L. (2009). S5a promotes protein degradation by blocking synthesis of nondegradable forked ubiquitin chains. *EMBO Journal, 26*(13), 1867-1877.

Kipreos, E.T., Lander, L.E., Wing, J.P., He, W.W., & Hedgecock, E.M. (1996). cul-1 is required for cell cycle exit in C. elegans and identifies a novel gene family. *Cell*, *85*(6), 829–839.

Kirisako, T., Kamei, K., Murata, S., Kato, M., Fukumoto, H., Kanie, M., Sano, S., Tokunaga, F., Tanaka, K., & Iwai, K. (2006). A ubiquitin ligase complex assembles linear polyubiquitin chains. *The EMBO Journal*, *25*(20), 4877–4887.

Kline-Smith, S.L., & Walczak, C.E. (2004). Mitotic spindle assembly and chromosome segregation: refocusing on microtubule dynamics. *Molecular Cell*, *15*(3), 317–327.

Knudson, A.G. Jr. (1971). Mutation and cancer: statistical study of retinoblastoma. *PNAS, 68*(4), 820-823.

Koepp, D.M., Schaefer, L.K., Ye, X., Keyomarsi, K., Chu, C., Wade Harper, J., & Elledge, S.J. (2001). Phosphorylation-Dependent Ubiquitination of Cyclin E by the SCF^{Fbw7} Ubiquitin Ligase. *Science, 294*(5540), 173-177.

Komander, D., Clague, M.J., & Urbé, S. (2009). Breaking the chains: structure and function of the deubiquitinases. *Nature Reviews. Molecular Biology, 10*(8), 550-563.

Komander, D. (2009). The emerging complexity of protein ubiquitination. *Biochemical Society Transactions*, *37*(Pt 5), 937–953.

Komander, D., Reyes-Turcu, F., Licchesi, J.D.F., Odenwaelder, P., Wilkinson, K.D., & Barford, D. (2009). Molecular discrimination of structurally equivalent Lys 63-linked and linear polyubiquitin chains. *EMBO Reports, 10*(5), 466-473.

Komander, D., & Rape, M. (2012). The ubiquitin code. *Annual Review of Biochemistry*, *81*(1), 203–229.

Kouzarides, T. (2007). Chromatin modifications and their function. *Cell, 128*(4), 693-705.

Kovalenko, A., Chable-Bessia, C., Cantarella, G., Israël, A., Wallach, D., & Courtois, G. (2003). The tumour suppressor CYLD negatively regulates NF-kappaB singalling by deubiquitination. *Nature, 424*(6950). 801-805.

Kozera, B., & Rapacz, M. (2013). Reference genes in real-time PCR. *Journal of Applied Genetics, 54*(4), 391-406.

Kraft, C., Herzog, F., Gieffers, C., Mechtler, K., Hagting, A., Pines, J., & Peters, J.M. (2003). Mitotic regulation of the human anaphase-promoting complex by phosphorylation. *The EMBO Journal*, *22*(24), 6598–6609.

Kramer, E.R., Gieffers, C., Hölzl, G., Hengstschläger, M., & Peters, J.M. (1998). Activation of the human anaphase-promoting complex by proteins of the CDC20/Fizzy family. *Currently Biology, 8*(22), 1207-1210.

Kramer, E.R., Scheuringer, N., Podtelejnikov, A.V., Mann, M., & Peters, J.M. (2000). Mitotic Regulation of the APC Activator Proteins CDC20 and CDH1. *Molecular Biology of the Cell, 11*(5), 1555-1569.

Kristariyanto, Y.A., Rehman, S.A.A., Campbell, D.G., Morrice, N.A., Johnson, C., Toth, R., & Kulathu, Y. (2015a). K29-Selective Ubiquitin Binding Domain Reveals Structural Basis of Specificity and Heterotypic Nature of K29 Polyubiquitin. *Molecular Cell, 58*(1), 83-94

Kristariyanto, Y.A., Choi, S.-Y., Rehman, S.A.A., Ritorto, M.S., Campbell, D.G., Morrice, N.A., Toth, R., & Kulathu, Y. (2015b). Assembly and structure of Lys33-linked polyubiquitin reveals distinct conformations. *The Biochemical Journal*, *467*(2), 345–352.

Krokan, H., Wist, E., & Krokan, R.H. (1981). Aphidicolin inhibits DNA synthesis by DNA polymerase alpha and isolated nuclei by a similar mechanism. *Nuclei Acids Research*, *9(18)*, 4709-4719.

Krupina, K., Kleiss, C., Metzger, T., Fournane, S., Schmucker, S., Hofmann, K., Fischer, B., Paul, N., Porter, I.M., Raffelsberger, W., Poch, O., Swedlow, J.R., Brino, L., & Sumara, I. (2016). Ubiquitin Receptor Protein UBASH3B Drives Aurora B Recruitment to Mitotic Microtubules. *Developmental Cell, 36*(1), 63-78.

Kuhn, J., & Dumont, S. (2017). Spindle assembly checkpoint satisfaction occurs via end-on but not lateral attachments under tension. *Journal of Cell Biology, 216*(6), 1533-1542.

Kulathu, Y., & Komander, D. (2012). Atypical ubiquitylation — the unexplored world of polyubiquitin beyond Lys48 and Lys63 linkages. *Nature Reviews Molecular Cell Biology*, *13*(8), 508–523.

Kulis, M., & Esteller, M. (2010). DNA Methylation and Cancer. *Advances in Genetics, 70*, 27-56.

Kumar, S., Tomooka, Y., & Noda, M. (1992). Identification of a set of genes with developmentally down-regulated expression in the mouse brain. *Biochemical and Biophysical Research Communications*, *185*(3), 1155–1161.

Kwei, K.A., Hunter Shain, A., Bair, R., Montogomery, K., Karikari, C.A., van de Rijn, M., Hidalgo, M., Maitra, A., Bashyam, M.D., & Pollack, J.R. (2011). *SMURF1* Amplification Promotes Invasiveness in Pancreatic Cancer. *PLOS One.* DOI: 10.1371/journal.pone.0023924.

Kwon, A., Lee, H.L., Woo, K.M., Ryoo, H.M., & Baek, J.H. (2013). SMURF1 plays a role in EGF-induced breast cancer cell migration of invasion. *Molecules and Cells, 36*(6), 548-555.

Lackner, D.H., Carré, A., Guzzardo, P.M., Banning, C., Mangena, R., Henley, T., Oberndorfer, S., Gapp, B.V., Nijman, S.M.B., Brummelkamp, T.R., & Bürckstümmer, T. (2015). A generic strategy for CRISPR-Cas9-mediated gene tagging. *Nature Communications, 6*(10237). DOI: 10.1038/ncomms10237.

Lafranchi, L., de Boer, H.R., de Vries, E.G.E., Ong, S.-E., Sartori, A.A., & van Vugt, M.A.T.M. (2014). APC/C^{Cdh1} controls CtIP stability during the cell cycle and in responsible to DNA damage. *EMBO Journal, 33*(23), 2860-2879.

Lallemant, B., Evrard, A., Combescure, C., Chapuis, H., Chambon, G., Raynal, C., Reynaud, C., Sabra, O., Joubert, D., Hollande, F., Lallemant, J.-G., Lumbroso, S., & Brouillet, J.-P. (2009). Reference gene selection for head and neck squamous cell carcinoma gene expression studies. *BMC Molecular Biology, 10*:78. DOI: 10.1186/1471-2199-10-78.

Lan, W., Zhang, X., Kline-Smith, S.L., Rosasco, S.E., Barrett-Wilt, G.A., Shabanowitz, J., Hunt, D.F., Walczak, C.E., & Stukenberg, P.T. (2004). Aurora B phosphorylates centromeric MCAK and regulates its localisation and microtubule depolymerization activity. *Current Biology, 14*(4), 273-286.

Lane, D.P., & Crawford, L.V. (1979). T antigen is bound to a host protein in SY40-transformed cells. *Nature, 278*, 261-263.

Lawrence, K.C., Chau, T., & Engebrecht, J. (2015). DNA Damage Response and Spindle Assembly Checkpoint Function throughout the Cell Cycle to Ensure Genomic Integrity. *PLOS One.* DOI:10.1371/journal.pgen.1005150.

Lee, A.E., Castañeda, C.A., Wang, Y., Fushman, D., & Fenselau, C. (2014). Preparing to read the ubiquitin code: a middle-out strategy for characterization of all lysine-linked diubiquitins. *Journal of Mass Spectrometry, 49*(12), 1272-1278.

Lee, E.Y.H.P., & Muller, W.J. (2010). Oncogenes and Tumour Suppressor Genes. *Cold Spring Harbour Perspectives in Biology, 2*(10): a003236. DOI: 10.1101/cshperspect.a003236.

Lee, I.-H., Dinudom, A., Sanchez-Perez, A., Kumar, S., & Cook, D.I. (2007). Akt mediates the effect of insulin on epithelial sodium channels by inhibiting Nedd4-2. *The Journal of Biological Chemistry*, *282*(41), 29866–29873.

Lee, M.J., Lee, B.-H., Hanna, J., King, R.W., & Finley, D. (2011). Trimming of Ubiquitin Chains by Proteasome-associated Deubiquitinating Enzymes. *Molecular & Cellular Proteomics, 10*(5): R110.003871.

Lens, S.M., Voest, E.E., & Medema, R.H. (2010). Shared and separated functions of polo-like kinases and aurora kinases in cancer. *Nature Reviews Cancer, 10*(12), 825-841.

Li, D., Gao, J., Yang, Y., Sun, L., Suo, S., Luo, Y., Shui, W., Zhou, J., & Liu, M. (2014). CYLD coordinates with EB1 to regulate microtubule dynamics and cell migration. *Cell Cycle, 13*(6), 974-983.

Li, H., Xiao, N., Wang, Y., Wang, R., Chen, Y., Pan, W., Liu, D., Li, S., Sun, J., Zhang, K., Sun, Y., & Ge, X. (2017). Smurf1 regulates lung cancer cell growth and migration through interaction with and ubiquitination of PIPKIγ. *Oncogene, 36,* 5668-5680.

Li, J., D'Angiolella, V., Seeley, E.S., Kim, S., Kobayashi, T., Fu, W., Campos, E.I., Pagano, M., & Dynlacht, B.D. (2013a). USP33 regulates centrosome biogenesis via deubiquitination of the centriolar protein CP110. *Nature*, *495*(7440), 255–259.

Li, R., & Murray, A.W. (1991). Feedback on mitosis in budding yeast. *Cell, 66(*3), 519-531.

Li, W., Bengtson, M.H., Ulbrich, A., Matsuda, A., Reddy, V.A., Orth, A., Chanda, S.K., Batalov, S., & Joazeiro, C.A. (2008). Genome-wide and functional annotation of human E3 ubiquitin ligases identifies MULAN, a mitochondrial E3 that regulates the organelle's dynamics and signaling. *Plos One*, *3*(1), e1487. http://doi.org/10.1371/journal.pone.0001487

Li, W., Hu, Y., Oh, S., Ma, Q., Merkurjev, D., Song, X., Zhou, X., Liu, Z., Tanasa, B., He, X., Chen, A.Y., Ohgi, K., Zhang, J., Liu, W., & Rosenfeld, M.G. (2015). Condensin I and II Complexes License Full Estrogen Receptor α-Dependent Enhancer Activation. *Molecular Cell*, *59*(2), 188–202.

Li, X., Zhao, Q., Liao, R., Sun, P., & Wu, X. (2003). The SCF^{Skp2} Ubiquitin Ligase Complex Interacts with the Human Replication Licensing Factor Cdt1 and Regulated Cdt1 Degradation. *Journal of Biological Chemistry, 278,* 30854-30858.

Li, X., Zhou, Q., Sunkara, M., Kutys, M.L., Wu, Z., Rychahou, P., Morris, A.J., Zhu, H., Evers, B.M., & Huang, C. (2013b). Ubiquitylation of phosphatidylinositol 4-phosphate 5-kinase type I gamma by HECTD1 regulates focal adhesion dynamics and cell migration. *Journal of Cell Science*, *126*(12), 2617–2628.

Li, Y., & Tollefsbol, T.O. (2011). DNA methylation detection: Bisulfite genomic sequencing analysis. *Methods in Molecular Biology, 791,* 11-21.

Li, Y., Kong, Y., Zhou, Z., Chen, H., Wang, Z., Hsieh, Y.-C., Zhao, D., Zhi, X., Huang, J., Zhang, J., & Chen, C. (2013c). The HECTD3 E3 ubiquitin ligase facilitates cancer cell survival by promoting K63-linked polyubiquitination of caspase-8. *Cell Death & Disease*, *4*(11), e935. http://doi.org/10.1038/cddis.2013.464.

Liang, G., Lin, J.C., Wei, V., Yoo, C., Cheng, J.C., Nguyen, C.T., Weisenberger, D.J., Egger, G., Takai, D., Gonzales, F.A., & Jones, P.A. (2004). Distinct localisation of histone H3 acetylation and H3-K4 methylation to the transcription start sites in the human genome. *PNAS, 101*(19), 7357-7362.

Liang, J.R., Martinez, A., Lane, J.D., Mayor, U., Clague, M.J., & Urbé, S. (2015). USP30 deubiquitylates mitochrondrial Parkin substrates and restricts apoptotic cell death. *EMBO Reports, 16*(5), 618-627.

Liberali, P., Snijder, B., & Pelkmans, L. (2014). A Hierarchical Map of Regulatory Generics in Membrane Trafficking. *Cell, 157*(6), 1473-1487.

Licchesi, J.D.F., Van Neste, L., Tiwari, V.K., Cope, L., Lin, X., Baylin, S.B., & Herman, J.G. (2010). Transcriptional regulation of Wnt inhibitory factor-1 by Miz-1/c-Myc. *Oncogene, 29*, 5923-5934.

Licchesi, J.D.F., Mieszczanek, J., Mevissen, T.E.T., Rutherford, T.J., Akutsu, M., Virdee, S., El Oualid, F., Chin, J.W., Ovaa, H., Bienz, M., & Komander, D. (2012). An ankyrin-repeat ubiquitin-binding domain determines TRABID's specificity for atypical ubiquitin chains. *Nature Structural and Molecular Biology, 19*, 62-71.

Lim, S., & Kaldis, P. (2013). Cdks, cyclins and CKIs: roles beyond cell cycle regulation. *Development*, *140*(15), 3079–3093.

Lin, J.H., Hsieh, S.C., Chen, J.N., Tsai, M.H., & Chang, C.C. (2013). WWP1 gene is a potential molecular target of human oral cancer. *Oral Surgery, Oral Medicine, Oral Pathology, Oral Radiology, 116*(2), 221-231.

Lindahl, P.E. (1948). Principle of a counter-streaming centrifuge for the separation of particles of different sizes. *Nature, 161*, 648.

Lineberry, N., Su, L., Soares, L., & Fathman, C.G. (2008). The single subunit transmembrane E3 ligase gene related to anergy in lymphocytes (GRAIL) captures and then ubiquitinates transmembrane proteins across the cell membrane, *283*(42), 28497–28505.

Ling, S., & Lin, W.-C. (2011). EDD inhibits ATM-mediated phosphorylation of p53. *Journal of Biological Chemistry*, *286*(17), 14972–14982.

Liu, C., Liu, W., Ye, Y., & Li, W. (2017). Ufd2p synthesizes branched ubiquitin chains to promote the degradation of substrates modified with atypical chains. *Nature Communications, 8*, 14274. DOI: 10.1038/ncomms14274.

Liu, X., Gu, X., Sun, L., Flowers, A.B., Rademaker, A.W., Zhou, Y., & Kiyokawa, H. (2014). Downregulation of Smurf2, a tumor-suppressive ubiquitin ligase, in triple-negative breast cancers: involvement of the RB-microRNA axis. *BMC Cancer*, *14*(1), 57.

Liu, Y.-Z., Jiang, Y.-Y., Wang, B.-S., Hao, J.-J., Li, S., Zhang, T.-T., Cao, J., Xu, X., Zhan, Q.-M., Wang, M.-R,. (2014). A panel of protein markers for the early detection of lung cancer with bronchial brushing specimens. *Cancer Cytopathology, 122*(11), 833-841.

Livak, K.J., & Schmittgen, T.D. (2001). Analysis of relative gene expression data using real-time quantitative PCR and the $2^{-\Delta\Delta C(T)}$ Method. *Methods, 25(4).* 402-406.

Löbrich, M., & Jeggo, P.A. (2007). The impact of a negligent G2/M checkpoint on genomic instability and cancer induction. *Nature Reviews Cancer, 7*, 861-869.

Loeb, K.R., & Loeb, L.A. (2000). Significance of multiple mutations in cancer. *Carcinogenesis, 21*(3), 379-385.

Love, K.R., Catic, A., Schlieker, C., & Ploegh, H.L. (2007). Mechanisms, biology and inhibitors of deubiquitinating enzymes. *Nature Chemical Biology, 3*, 697-705.

Love, K.R., Pandya, R.K., Spooner, E., & Ploegh, H.L. (2009). Ubiquitin C-terminal electrophiles are activity-based probes for identification and mechanistic study of ubiquitin conjugating machinery. *ACS Chemical Biology, 4*(4), 275-287.

Lu, L., Hu, S., Wei, R., Qiu, X., Lu, K., Fu, Y., Li, H., Xing, G., Li, D., Peng, R., He, F., & Zhang, L. (2013). The HECT type ubiquitin ligase NEDL2 is degraded by anaphase-promoting complex/cyclosome (APC/C)-Cdh1, and its tight regulation maintains the metaphase to anaphase transition. *Journal of Biological Chemistry*, *288*(50), 35637-35650.

Lüders, J., Patel, U.K., & Stearns, T. (2005). GCP-WD is a γ-tubulin targeting factor required for centrosomal and chromatin-mediated microtubule nucleation. *Nature Cell Biology, 8*, 137-147.

Luger, K., Mäder, A.W., Richmond, R.K., Sargent, D.F., & Richmond, T.J. (1997). Crystal structure of the nucleosome core particle at 2.8A resolution. *Nature, 389*(6648), 251-260.

Maddika, S., & Chen, J. (2009). Protein kinase DYRK2 is a scaffold that facilitates assembly of an E3 ligase. *Nature Cell Biology*, *11*(4), 409–419.

Maddika, S., Kavela, S., Rani, N., Palicharla, V.R., Pokorny, J.L., Sarkaria, J.N., & Chen, J. (2011). WWP2 is an E3 ubiquitin ligase for PTEN. *Nature Cell Biology, 13*, 728-733.

Maehara, Y., Anai, H., Tamamda, R., & Sugimachi, K. (1987). The ATP assay is more sensitive than the succinate dehydrogenase inhibition test for predicting cell viability. *European Journal of Cancer and Clinical Oncology, 23*(3), 273-276.

Maiato, H., Rieder, C.L., & Khodjakov, A. (2004). Kinetochore-driven formation of kinetochore fibres contributes to spindle assembly during animal mitosis. *Journal of Cell Biology, 167*(5), 831-840.

Mains, P.E., Kemphues, K.J., Sprunger, S.A., Sulston, I.A., & Wood, W.B. (1990). Mutations affecting the meiotic and mitotic divisions of the early *Caenorhabditis elegans* embryo. *Genetics, 126*(3), 593-605.

Mali, P., Yang, L., Esvelt, K.M., Aach, J., Guell, M., DiCarlo, J.E., Norville, J.E., & Church, G.M. (2013). RNA-guided human genome engineering via Cas9. *Science, 339*(6121), 823-826.

Mandelkow, E., & Mandelkow, E.M. (1989). Microtubular structure and tubulin polymerization. *Current Opinion in Cell Biology*, *2*(1), 5–9.

Mansfeld, J., Collin, P., Collins, M.O., Choudhary, J.S., & Pines, J. (2011). APC15 drives the turnover of MCC-Cdc20 to make the Spindle Assembly Checkpoint responsive to kinetochore attachment. *Nature Cell Biology, 13*(10), 1234-1243.

Marcus, J.M., Burke, R.T., DeSisto, J.A., Landesman, Y., & Orth, J.D. (2015). Longitudinal tracking of single live cancer cells to understand cell cycle effects of the nuclear export inhibitor, selinexor. *Scientific Reports, 5,* 14391. DOI: 10.1038/srep14391.

Marín, I., Lucas, J.I., Gradilla, A.C., & Ferrús, A. (2004). Parkin and relatives: the RBR family of ubiquitin ligases. *Physiological Genomics, 17*(3), 253-263.

Marín, I. (2010). Animal HECT ubiquitin ligases: evolution and functional implications. *BMC Evolutionary Biology*, *10*(1), 56. http://doi.org/10.1186/1471-2148-10-56

Maspero, E., Mari, S., Valentini, E., Musacchio, A., Fish, A., Pasqualato, S., & Polo, S. (2011). Structure of the HECT:ubiquitin complex and its role in ubiquitin chain elongation. *EMBO Reports*, *12*(4), 342–349.

Maspero, E., Valentini, E., Mari, S., Cecatiello, V., Soffientini, P., Pasqualato, S., & Polo, S. (2013). Structure of a ubiquitin-loaded HECT ligase reveals the molecular basis for catalytic priming. *Nature Structural & Molecular Biology*, *20*(6), 696-701.

Massey, A. (2015). Multiparametric Cell Cycle Analysis Using the Operatte High-Content Imager and Harmony Software with PhenoLOGIC. *PLOS One.* DOI: 10.1371/journal.pone.0134306.

Mastrandrea, L.D., You, J., Niles, E.G., & Pickart, C.M. (1999). E2/E3-mediated Assembly of Lysine 29-linked Polyubiquitin Chains. *Journal of Biological Chemistry*, *274*(38), 27299–27306.

Mastronarde, D.N., McDonald, K.L., Ding, R., & McIntosh, J.R. (1993). Interpolar spindle microtubules in PTK cells. *Journal of Cell Biology, 123*(6), 1475-1489.

Matsusaka, T., Enquist-Newman, M., Morgan, D.O., & Pines, J. (2014). Co-activator independent differences in how the metaphase and anaphase APC/C recognise the same substrate. *Biology Open*, *3*(10), 904–912.

McCullough, J., Clague, M.J., & Urbé, S. (2004). AMSH is an endosome-associated ubiquitin isopeptidase. *Journal of Cell Biology*, *166*(4), 487–492.

McDonald, K.L., O'Toole, E.T., Mastronarde, D.N., & McIntosh, J.R. (1992). Kinetochore microtubules in PTK cells. *Journal of Cell Biology, 118*(2), 369-383.

McGarry, T.J., & Kirschner, M.W. (1998). Geminin, an Inhibitor of DNA Replication, is Degraded during Mitosis. *Cell, 93*(6), 1043-1053.

McNally, F.J. (2013). Mechanisms of spindle positioning. *Journal of Cell Biology, 200*(2), 131-140.

Meissner, B., Kridel, R., Lim, R.S., Rogic, S., Tse, K., Scott, D.W., Moore, R., Mungall, A.J., Marra, M.A., Connors, J.M., Steidl, C., & Gascoyne, R.D. (2013). The E3 ubiquitin ligase UBR5 is recurrently mutated in mantle cell lymphoma. *Blood, 121*(16), 3161-3164.

Merdes, A., & De May, J. (1990). The mechanism of kinetochore-spindle attachment and polewards movement analyzed in PtK2 cells at the prophase-prometaphase transition. *European Journal of Cell Biology, 53*(2), 313-325.

Meunier, S., & Vernos, I. (2011). K-fibre minus ends are stabilised by a RanGTP-dependent mechanism essential for functional spindle assembly. *Nature Cell Biology, 13*, 1406-1414.

Meyer, H.J., & Rape, M. (2014). Enhanced protein degradation by branched ubiquitin chains. *Cell, 157*(4), 910-921.

Michel, M.A., Elliot, P.R., Swatek, K.N., Simicek, M., Pruneda, J.N., Wagstaff, J.L., Freund, S.M.V., & Komander, D. (2015). Assembly and Specific Recognition of K29- and K33-Linked Polyubiquitin. *Molecular Cell, 58*(1), 95-109.

Michel, M.A., Swatek, K.N., Hospenthal, M.K., & Komander, D. (2017). Ubiquitin Linkage-Specific Affimers Reveal Insights into K6-Linked Ubiquitin Signaling. *Molecular Cell, 68*(1), 233-246.

Michie, A.M., McCaig, A.M., Nakagawa, R., & Vukovic, M. (2010). Death-associated protein kinase (DAPK) and signal transduction: regulation in cancer. *FEBS Journal, 277*(1), 74-80.

Mimori-Kiyosue, Y., & Tsukita, S. (2003). “Search-and-capture” of microtubules through plus-end-binding proteins (+TIPs). *Journal of Biochemistry*, *134*(3), 321–326.

Mitchison, T., & Kirschner, M. (1984). Dynamic instability of microtubule growth. *Nature, 312*(5991), 237-242.

Miyazaki, K., Ozaki, T., Kato, C.,, Hanamoto, T., Fujita, T., Irino, S., Watanabe, K.-I., Nakagawa, T., & Nakagawara, A. (2003). A novel HECT-type E3 ubiquitin ligase, NEDL2, stabilizes p73 and enhances its transcriptional activity. *Biochemical and Biophysical Research Communications*, *308*(1), 106–113.

Mizuno-Yamasaki, E., Rivera-Molina, F., & Novick, P. (2012). GTPase networks in membrane traffic. *Annual Review of Biochemistry*, *81*(1), 637–659.

Morgan, D.O. (2013). The D Box Meets Its Match. *Molecular Cell, 50*(5), 609-610.

Mosavi, L.K., Cammett, T.J., Desrosiers, D.C., & Peng, Z.Y. (2004). The ankyrin repeat as molecular architecture for protein recognition. *Protein Science*, *13*(6), 1435–1448.

Mulder, M.P.C., Witting, K., Berlin, I., Pruneda, J.N., Wu, K.-P., Chang, J.-G., Merkx, R., Bialas, J., Groettrup, M., Vertegaal, A.C.O., Schulman, B.A., Komander, D., Neefjes, J., El Oualid, F., & Ovaa, H. (2016). A cascading activity-based probe sequentially targets E1-E2-E3 ubiquitin enzymes. *Nature Chemical Biology, 12,* 523-530.

Mund, T., & Pelham, H.R.B. (2009). ,42*EMBO Reports*, *10*(5), 501–507.

Mund, T., Lewis, M.J., Maslen, S., & Pelham, H.R. (2014). Peptide and small molecule inhibitors of HECT-type ubiquitin ligases. *Proceedings of the National Academy of Sciences of the United States of America*, *111*(47), 16736–16741.

Mund, T., Graeb, M., Mieszczanek, J., Gammons, M., Pelham, H.R.B., & Bienz, M. (2015). Disinhibition of the HECT E3 ubiquitin ligase WWP2 by polymerized Dishevelled. *Open Biology*, *5*(12), 150185. http://doi.org/10.1098/rsob.150185

Munoz, M.A., Saunders, D.N., Henderson, M.J., Clancy, J.L., Russell, A.J., Lehrbach, G., Musgrove, E.A., Watts, C.K., & Sutherland, R.K. (2007). The E3 ubiquitin ligase EDD regulates S-phase and G(2)/M DNA damage checkpoints. *Cell Cycle*, *6*(24), 3070–3077.

Muralikrishna, B., Chaturvedi, P., Sinha, K., & Parnaik, V.K. (2012). Lamin misexpression upregulates three distinct ubiquitin ligase systems that degrade ATR kinase in HeLa cells. *Molecular and Cellular Biochemistry*, *365*(1-2), 323–332.

Murnion, M.E., Adams, R.R., Callister, D.M., Allis, C.D., Earnshaw, W.C., & Swedlow, J.R. (2001). Chromatin-associated protein phosphatase 1 regulates aurora-B and histone H3 phosphorylation. *Journal of Biological Chemistry, 276*(28), 26656-26665.

Murray, A.W., & Kirschner, M.W. (1989). Cyclin synthesis drives the early embryonic cell cycle. *Nature, 339*(6222), 275-280.

Murray, A.W. (1994). Cell cycle checkpoints. *Current Opinion in Cell Biology, 6*(6), 872-876.

Murray, A.W. (2004). Recycling the Cell Cycle: Cyclins Revisited. *Cell, 116*(2), 221-234.

Musacchio, A., & Salmon, E.D. (2007). The spindle-assembly checkpoint in space and time. *Nature Reviews in Molecular Cell Biology, 8,* 379-393.

Myant, K.B., Cammareri, P., Hodder, M.C., Wills, J., Von Kriegsheim, A.V., Györrfy, B., Rashid, M., Polo, S., Maspero, E., Vaughan, L., Gurung, B., Barry, E., Malliri, A., Camargo, F., Adams, D.J., Iavarone, A., Lasorella, A., & Sansom, O.J. (2016). *HUWE1* is a critical tumour suppressor gene that prevents MYC signalling, DNA damage accumulation and tumour initiation. *EMBO Molecular Medicine, 9*(2), 181-197.

Nagaki, K., Yamamura, H., Shimada, S., Saito, T., Hisanaga, S., Taoka, M., Isobe, T., & Ichimura, T. (2006). 14-3-3 Mediates phosphorylation-dependent inhibition of the interaction between the ubiquitin E3 ligase Nedd4-2 and epithelial Na+ channels. *Biochemistry, 45*(21), 6733-6740.

Nakamura, T., Hamada, F., Ishidate, T., Anai, K., Kawahara, K., Toyoshima, K., & Akiyama T. (1998). Axin, an inhibitor of the Wnt signaling pathway, interacts with beta-catenin, GSK-3beta and APC and reduces the beta-catenin level. *Genes to Cells, 3*(6), 395-403.

Nakamura, M., Zhou, X.Z., Kishi, S., & Lu, K.P. (2002). Involvement of the telomeric protein Pin2/TRF1 in the regulation of the mitotic spindle. *FEBS Letters*, *514*(2-3), 193–198.

Nakasone, M.A., Livant-Levanon, N., Glickman, M.H., Cohen, R.E., & Fushman, D. (2013). Mixed-Linkage Ubiquitin Chains Send Mixed Messages. *Structure, 21*(5), 727-740.

Nakayama, K.I., & Nakayama, K. (2006). Ubiquitin ligases: cell-cycle control and cancer. *Nature Reviews Cancer, 6,* 369-381.

Nalefski, E.A., & Falke, J.J. (1996). The C2 domain calcium-binding motif: structural and functional diversity. *Protein Science*, *5*(12), 2375–2390.

Nam, E.A., & Cortez, D. (2011). ATR signalling: more than meeting at the fork. *The Biochemical Journal, 436*(3), 527-536.

Nathan, J.A., Kim, H.T., Ting, L., Gygi, S.P., & Goldberg, A.L. (2013). Why do cellular proteins linked to K63- polyubiquitin chains not associate with proteasomes? *EMBO Journal, 32*(4), 552-565.

Navarro, F.J., & Nurse, P. (2012). A systematic screen reveals new elements acting at the G2/M cell cycle control. *Genome Biology, 13*(5), R36. DOI: 10.1186/gb-2012-13-5-r36.

Nefsky, B., & Beach, D. (1996). Pub1 acts as an E6-AP-like protein ubiquitin ligase in the degradation of cdc25. *The EMBO Journal*, *15*(6), 1301–1312.

Neganova, I., Zhang, X., Atkinson, S., & Lako, M. (2009). Expression and functional analysis of G1 to S regulatory components reveal an important role for CDK2 in cell cycle regulation in human embryonic stem cells. *Oncogene, 28,* 20-30.

Neumann, B., Walter, T., Hériché, J.K., Bulkescher, J., Erfle, H., Conrad, C., Rogers, P., Poser, I., Held, M., Liebel, U., Cetin, C., Sieckmann, F., Pau, G., Kabbe, R., Wünsche, A., Satagopam, V., Schmitz, M.H., Chapuis, C., Gerlich, D.W., Schnieder, R., Eils, R., Huber, W., Peters, J.M., Hyman, A.A., Durbin, R., Pepperkok, R., & Ellenberg, J. (2010). Phenotypic profiling of the human genome by time-lapse microscopy reveals cell division genes. *Nature, 464*(7289), 721-727.

Newlands, E.S., Stevens, M.F.G., Wedge, S.R., Wheelhouse, R.T., & Brock, C. (2007). Temozolomide: a review of its discovery, chemical properties, pre-clinical development and clinical trials. *Cancer Treatment Reviews, 23*(1), 35-61.

Newton, K., Matsumoto, M.L., Wertz, I.E., Kirkpatrick, D.S., Lill, J.R., Tan, J., Dugger, D., Gordon, N., Sidhu, S.S., Fellouse, F.A., Komuves, L., French, D.M., Ferrando, R.E., Lam, C., Compaan, D., Yu, C., Bosanac, I., Hymowitz, S.G., Kelly, R.F., & Dixit, V.M. (2008). Ubiquitin Chains Editing Revealed by Polyubiquitin Linkage-Specific Antibodies. *Cell, 134*(4), 668-678.

Nguyen Huu, N.S., Ryder, W.D., Zeps, N., Flasza, M., Chiu, M., Hanby, A.M., Poulsom, R., Clarke, R.B., & Baron, M. (2008). Tumour-promoting activity of altered WWP1 expression in breast cancer and its utility as a prognostic indicator. *Journal of Pathology, 16*(1), 93-102.

Niederacher, D., An, H.X., Cho, Y.J., Hantschmann, P., Bender, H.G., & Beckmann, M.W. (1999). Mutations and amplification of oncogenes in endometrial cancer. *Oncology, 56*(1), 59-65.

Nijman, S.M.B., Luna-Vargas, M.P.A., Velds, A., Brummelkamp, T.R., Dirac, A.M.G., Sixma, T.K., & Bernards, R. (2005). A genomic and functional inventory of deubiquitinating enzymes. *Cell*, *123*(5), 773–786.

Nilsson, J., Yekezare, M., Minshull, J., & Pines, J. (2008). The APC/C maintains the spindle assembly checkpoint by targeting Cdc20 for destruction. *Nature Cell Biology*, *10*(12), 1411–1420.

Norbury, C., & Nurse, P. (1992). Animal-Cell Cycles and Their Control. *Annual Review of Biochemistry, Vol 82*, *61*, 441–470.

Nurse, P., Thuriaux, P., & Nasmyth, K. (1976). Genetic control of the cell division cycle in the fission yeast *Schizosaccharomyces pombe*. *Molecular Genetics and Genome, 146*. 167–178.

Nurse, P., & Thuriaux, P. (1980). Regulatory genes controlling mitosis in the fission yeast *Schizosaccharomyces pombe. Genetics, 96*. 627–637.

Oberst, A., Malatesta, M., Aqeilan, R.I., Rossi, M., Salomoni, P., Murillas, R., Sharma, P., Kuehn, M.R., Oren, M., Croce, C.M., Bernassola, F., & Melino, G. (2007). The Nedd4-binding partner 1 (N4BP1) protein is an inhibitor of the E3 ligase Itch. *Proceedings of the National Academy of Sciences of the United States of America*, *104*(27), 11280–11285.

O'Brien, P.M., Davies, M.J., Scurry, J.P., Smith, A.N., Barton, C.A., Henderson, M.J., Saumders, D.N., Gloss, B.S., Patterson, K.I., Clancy, J.L., Heinzelmann-Schwarz, V.A., Murali, R., Scolyer, R.A., Zeng, Y., Williams, E.D., Scurr, L., Defazio, A., Quinn, D.I., Watts, C.K., Hacker, N.F., Henshall, S.M., & Sutherland, R.L. (2008). The E3 ubiquitin ligase EDD is an adverse prognostic factor for serous epithelial ovarian cancer and modulates cisplatin resistance in vitro. *British Journal of Cancer, 98*(6), 1085-1093.

O'Geen, H., Echipare, L., & Farnham, P.J. (2011). Using ChIP-Seq Technology to Generate High-Resolution Profiles of Histone Modifications. *Methods in Molecular Biology, 791*, 265-286.

Ogunjimi, A.A., Briant, D.J., Pece-Barbara, N., Le Roy, C., Di Guglielmo, G.M., Kavsak, P., Rasmussen, R.K., Seet, B.T., Sicheri, F., & Wrana, J.L. (2005). Regulation of Smurf2 ubiquitin ligase activity by anchoring the E2 to the HECT domain. *Molecular Cell*, *19*(3), 297–308.

Ohtsubo, M., Kai, R., Furuno, N., Sekiguchi, T., Sekiguchi, M., Hayashida, H., Kuma, K.-I., Miyata, T., Fukushige, S., Murotsu, T., Matsubara, K., & Nishimoto, T. (1987). Isolation and characterization of the active cDNA of the human cell cycle gene (RCC1) involved in the regulation of onset of chromosome condensation. *Genes & Development*, *1*(6), 585–593.

Oikonomaki, M., Bady, P., & Hegi, M.E. (2017). Ubiquitin Specific Peptidase 15 (USP15) suppresses glioblastoma cell growth via stabilisation of HECTD1 E3 ligase attenuating WNT pathway activity. *Oncotarget, 8*, 110490-110502.

Okano, M., Xie, S., & Li, E. (1998). Cloning and characterisation of a family of novel mammalian DNA (cytosine-5) methyltransferases. *Nature Genetics, 19*(3), 219-220.

Okano, M., Bell, D.W., Haber, D.A., & Li, E. (1999). DNA methyltransferases Dnmt3a and Dnmt3b are essential for de novo methylation and mammalian development. *Cell, 99*(3), 247-257.

Olivier, M., Hollstein, M., & Hainaut, P. (2010). TP53 Mutations in Human Cancers: Origins, Consequences, and Clinical Use. *Cold Spring Harbour Perspectives in Biology, 2*(1): a001008.

Ong, S.E., Blagoev, B., Kratchmarova, I., Kristensen, D.B., Steen, H., Pandey, A., & Mann, M. (2002). Stable isotope labeling by amino acids in cell culture, SILAC, as a simple and accurate approach to expression proteomics. *Molecular & Cellular Proteomics, 1*(5), 376-386.

Ormerod, M.G., & Kubbies, M. (1992). Cell cycle analysis of asynchronous cell populations by flow cytometry using bromodeoxyuridine label and Hoechst-propidium iodide stain. *Cytometry, 13*(7), 678-685.

Osmundson, E.C., Ray, D., Moore, F.E., Gao, Q., Thomsen, G.H., & Kiyokawa, H. (2008). The HECT E3 ligase Smurf2 is required for Mad2-dependent spindle assembly checkpoint. *The Journal of Cell Biology*, *183*(2), 267–277.

Ozkaynak, E., Finley, D., Solomon, M.J., & Varshavsky, A. (1987). The yeast ubiquitin genes: a family of natural gene fusions. *EMBO Journal, 6,* 1429-1439.

Paez, J.G., Jänne, P.A., Lee, J.C., Tracy, S., Greulich, H., Gabriel, S., Herman, P., Kaye, F.J., Lindeman, N., Boggon, T.J., Naoki, K., Sasaki, H., Fujii, Y., Eck, M.J., Sellers, W.R., Johnson, B.E., & Meyerson, M. (2004). *EGFR* Mutations in Lung Cancer: Correlation with Clinical Response to Gefitinib Therapy. *Science, 304*(5676), 1497-1500.

Pagano, M., Tam, S.W., Theodoras, A.M., Beer-Romero, P., Del Sal, G., Chau, V., Yew, P.R., Draetta, G.F., & Rolfe, M. (1995). Role of the ubiquitin-proteasome pathway in regulating abundance of the cyclin-dependent kinase inhibitor p27. *Science, 269*(5224), 682-685.

Palmer, J.T., Rasnick, D., Klaus, J.L., & Bromme, D. (1995). Vinyl Sulfones as Mechanism-Based Cysteine Protease Inhibitors. *Journal of Medicinal Chemistry, 38*(17), 3193-3196.

Pan, S.J., Zhan, S.K., Ji, W.Z., Pan, Y.X., Liu, W., Li, D.Y., Huang, P., Zhang, X.X., Cao, C.Y., Zhang, J., Bian, L.G., Sun, B., Sun, Q.F. (2015). Ubiquitin-protein ligase E3C promotes glioma progression by mediating the ubiquitination and degrading of Annexin A7. *Scientific Reports, 5*, 11066. DOI: 10.1038/srep11066.

Pandya, R.K., Partridge, J.R., Love, K.R., Schwartz, T.U., & Ploegh, H.L. (2010). A structural element within the HUWE1 HECT domain modulates self-ubiquitination and substrate ubiquitination activities. *Journal of Biological Chemistry*, *285*(8), 5664–5673.

Pao, K.-C., Stanley, M., Han, C., Lai, Y.-C., Murphy, P., Balk, K., Wood, N.T., Corti, O., Corvol, J.-C., Muqit, M.M.K., & Virdee, S. (2016). Probes of Ubiquitin E3 ligases distinguish different stages of Parkin activation. *Nature Chemical Biology, 12*(5), 324-331.

Parada, L.F., Tabin, C.J., Shih, C., & Weinberg, R.A. (1982). Human EJ bladder carcinoma oncogene is homologue of Harvey sarcoma virus ras gene. *Nature, 297*(5866), 474-478.

Park, S., Ntai, I., Thomas, P., Konishcheva, E., Kelleher, N.L., & Statsuk, A.V. (2012). Mechanism-Based Small Molecule Cross-Linkers of HECT E3 Ubiquitin Ligase-Substrate Pairs. *Biochemistry*, *51*(42), 8327–8329.

Park, Y., Yoon, S.K., & Yoon, J.B. (2009). The HECT Domain of TRIP12 Ubiquitinates Substrates of the Ubiquitin Fusion Degradation Pathway, *284*(3), 1540–1549.

Pedrali-Noy, G., Spadari, S., Miller-Faurès, A., Miller, A., Kruppa, J., & Koch, G. (1980). Synchronization of Hela-Cell Cultures by Inhibition of DNA Polymerase-Alpha with Aphidicolin. *Nucleic Acids Research*, *8*(2), 377–387.

Peng, Y., Dai, H., Wang, E., Lin, C.C.-J., Mo, W., Peng, G., & Lin, S.-Y. (2015). TUSC4 functions as a tumor suppressor by regulating BRCA1 stability. *Cancer Research*, *75*(2), 378–386.

Persaud, A., Alberts, P., Mari, S., Tong, J., Murchie, R., Maspero, E., Safi, F., Moran, M.F., Polo, S., & Rotin, D. (2014). Tyrosine phosphorylation of NEDD4 activates its ubiquitin ligase activity. *Science Signaling*, *7*(346), –ra95. http://doi.org/10.1126/scisignal.2005290

Peter, S., Bultinck, J., Myant, K., Jaenicke, L.A., Walz, S., Muller, J., Gmachl, M., Treu, M., Boehmelt, G., Ade, C.P., Schmitz, W., Wiegering, A., Otto, C., Popov, N., Sansom, O., Kraut, N., & Eilers, M. (2014). H Tumor cell-specific inhibition of MYC function using small molecule inhibitors of the HUWE1 ubiquitin ligase. *EMBO Molecular Medicine*, *6*(12), 1525–1541.

Peters, J.M. (1998). SCF and APC: the Yin and Yang of cell cycle regulated proteolysis. *Current Opinion in Cell Biology*, *10*(6), 759–768.

Petroski, M.D., & Deshaies, R. (2005). Mechanism of Lysine 48-Linked Ubiquitin-Chain Synthesis by the Cullin-RING Ubiquitin-Ligase Complex SCF-Cdc34. *Cell, 123*(6), 1107-1120.

Petty, R.B., Sutherland, L.A., Hunter, E.M., & Cree, I.A. (1995). Comparison of MTT and ATP-based assays for the measurement of viable cell number. *Journal of Bioluminescence and Chemiluminescence, 10*(1), 29-34.

Pfleger, C.M., Lee, E., & Kirschner, M.W. (2001). Substrate recognition by the Cdc20 and Cdh1 components of the anaphase-promoting complex. *Genes & Development, 15*(18), 2396-2407.

Pickart, C.M. (1997). Targeting of substrates to the 26S proteasome. *FASEB Journal: Official Publication of the Federation of American Societies for Experimental Biology*, *11*(13), 1055–1066.

Pickart, C.M. (2001). Mechanisms underlying ubiquitination. *Annual Review of Biochemistry, Vol 82*, *70*(1), 503–533.

Pines, J., & Hunt, T. (1987). Molecular cloning and characterization of the mRNA for cyclin from sea urchin eggs. *EMBO Journal, 6*(10), 2987-2995.

Pines, J. (2006). Mitosis: a matter of getting rid of the right protein at the right time. *Trends in Cell Biology*, *16*(1), 55–63.

Pines, J. (2011). Cubism and the cell cycle: the many faces of the APC/C. *Nature Reviews Molecular Cell Biology*, *12*(8), 427-533.

Plant, P.J., Lafont, F., Lecat, S., Verkade, P., Simons, K., & Rotin, D. (2000). Apical membrane targeting of Nedd4 is mediated by an association of its C2 domain with annexin XIIIb. *Journal of Cell Biology*, *149*(7), 1473–1484.

Plechanovová, A., Jaffray, E.G., McMahon, S.A., Johnson, K.A., Navrátilová, I., Naismith, J.H., & Hay, R.T. (2011). Mechanism of ubiquitylation by dimeric RING ligase RNF4. *Nature Structural and Molecular Biology, 18*, 1052-1059.

Poch, E., Mińambres, R., Mocholí, E., Ivorra, C., Pérez-Aragó, A., Guerri, C., Pérez-Roger, I., & Guasch, R.M. (2007). RhoE interferes with Rb inactivation and regulates the proliferation and survival of the U87 human glioblastoma cell line. *Experimental Research, 313*(4), 719-731.

Pollack, A., & Ciancio, G. (1990). Cell cycle phase-specific analysis of cell viability using Hoechst 33342 and propidium iodide after ethanol preservation. *Methods in Cell Biology, 33*, 19-24.

Poulsen, E.G., Steinhauer, C., Lees, M., Lauridsen, A.-M., Ellgaard, L., & Hartmann-Petersen, R. (2012). HUWE1 and TRIP12 Collaborate in Degradation of Ubiquitin-Fusion Proteins and Misframed Ubiquitin. *PLOS One.* DOI: 10.1371/journal.pone.0050548.

Prins, K.W., Humston, J.L., Mehta, A., Tate, V., Ralston, E., & Ervastil, J.M. (2009). Dystrophin is a microtubule-associated protein. *Journal of Cell Biology, 186*(3), 363-369.

Prosser, S.L., & Pelletier, L. (2017). Mitotic spindle assembly in animal cells: a fine balancing act. *Nature Reviews Molecular Cell Biology, 18*, 187-201.

Puck, T.T. (1964). Phasing, Mitotic Delay, and Chromosomal Aberrations in Mammalian Cells. *Science*, *144*, 565–566.

Pulciani, S., Santos, E., Lauver, A.V., Long, L.K., Robbins, K.C., & Barbacid, M. (1982). Oncogenes in human tumor cell lines: molecular cloning of a transforming gene from human bladder carcinoma cells. *PNAS, 79*(9), 2845-2849.

Puga, A., Xia, Y., & Elferink, C. (2002). Role of the aryl hydrocarbon receptor in cell cycle regulation. *Chemico-Biological Interactions, 141*(1-2), 117-130.

Rabouille, C., Kondo, H., Newman, R., Hui, N., Freemont, P., & Warren, G. (1998). Syntaxin 5 is a common component of the NSF- and p97-mediated reassembly pathways of Golgi cisternae from mitotic Golgi fragments in vitro. *Cell*, *92*(5), 603–610.

Radoníc, A., Thulke, S., Mackay, I.M., Landt, O., Siegert, W., & Nitsche, A. (2004). Guideline to reference gene selection for quantitative real-time PCR. *Biochemical and Biophysical Research Communications, 313*(4), 856-862.

Rape, M., & Kirschner, M.W. (2004). Autonomous regulation of the anaphase-promoting complex couples mitosis to S-phase entry. *Nature*, *432*(7017), 588–595.

Ratz, M., Testa, I., Hell, S.W., & Jakobs, S. (2015). CRISPR/Cas9-mediated endogenous protein tagging for RESOLFT super-resolution microscopy of living human cells. *Scientific Reports, 5*, 9592. DOI: 10.1038/srep09592.

Redman, K.L., & Rechsteiner, M. (1989). Identification of the long ubiquitin extension as ribosomal protein S27a. *Nature, 338*, 438-440.

Reed, S.I., Ferguson, J., & Groppe, J.C. (1982). Preliminary characterization of the transcriptional and translational products of the *Saccharomyces cerevisiae* cell division cycle gene CDC28. *Molecular and Cellular Biology, 2*. 412–425.

Reinhardt, H.C., & Yaffe, M.B. (2009), Kinases that control the cell cycle in response to DNA damage: Chk1, Chk2, and MK2. *Current Opinion in Cell Biology, 21*(2), 245-255.

Renault, L., Nassar, N., Vetter, I., Becker, J., Klebe, C., Roth, M., & Wittinghofer, A. (1998). The 1.7 A crystal structure of the regulator of chromosome condensation (RCC1) reveals a seven-bladed propeller. *Nature*, *392*(6671), 97–101.

Renault, L., Kuhlmann, J., Henkel, A., & Wittinghofer, A. (2001). Structural basis for guanine nucleotide exchange on Ran by the regulator of chromosome condensation (RCC1). *Cell*, *105*(2), 245–255.

Rhee, I., Bachman, K.E., Park, B.H., Jair, K.-W., Yen, R.-W.C., Schuebel, K., Cui, H., Feinburg, A.P., Lengauer, C., Kinzler, K.W., Baylin, S.B., & Vogelstein, B. (2002). DNMT1 and DNMT3b cooperate to silence genes in human cancer cells. *Nature*, *416*, 52–56.

Rhodes, D.R., Yu, J., Shanker, K., Deshpande, N., Varambally, R., Ghosh, D., Barrette, T., Pandey, A., & Chinnaiyan, A.M. (2004). ONCOMINE: A Cancer Microarray Database and Integrated Data-Mining Platform. *Neoplasia, 6*(1), 1-6.

Rieder, C.L., & Alexander, S.P. (1990). Kinetochores are transported poleward along a single astral microtubule during chromosome attachment to the spindle in newt lung cells. *Journal of Cell Biology, 110*(1), 81-95.

Rieder, C.L., Schultz, A., Cole, R., & Sluder, G. (1994). Anaphase onset in vertebrate somatic cells is controlled by a checkpoint that monitors sister kinetochore attachment to the spindle. *Journal of Cell Biology, 127*(5), 1301-1310.

Rieder, C.L., Cole, R.W., Khodjakov, A., Sluder, G. (1995). The checkpoint delaying anaphase in response to chromosome monoorientation is mediated by an inhibitory signal produced by unattached kinetochores. *Journal of Cell Biology, 130*(4), 941-948.

Rieder, C.L., & Salmon, E.D. (1998). The vertebrate cell kinetochore and its roles during mitosis. *Trends in Cell Biology, 8*(8), 310-318.

Rienzo, M., Schiano, C., Casamassimi, A., Grimaldi, V., Infante, T., & Napoli, C. (2013). Identification of valid reference housekeeping genes for gene expression analysis in tumor neovascularization studies. *Clinical and Translational Oncology, 15*(3), 211-218.

Riss, T.L., Moravec, R.A., Niles, A.L., Duellman, S., Benink, H.A., Worzella, T.J., & Minor, L. (2004). Cell Viability Assays. *Assay Guidance Manual*.

Robertson, K.D. (2005). DNA methylation and human disease. *Nature Reviews Genetics, 6,* 597-610.

Rodrgio-Brenni, M.C., & Morgan, D.O. (2007). Sequential E2s drive polyubiquitin chain assembly on APC targets. *Cell, 130*(1), 127-139.

Rohaim, A., Kawasaki, M., Kato, R., Dikic, I., & Wakatsuki, S. (2012). Structure of a compact conformation of linear diubiquitin. *Acta Crystallographica. Section D, Biological Crystallography*, *68*(Pt 2), 102–108.

Rosner, M., Schipany, K., & Hengstschläger, M. (2013). Merging high-quality biochemical fractionation with a refined flow cytometry approach to monitor nucleocytoplasmic protein expression throughout the unperturbed mammalian cell cycle. *Nature Protocols*, *8*(3), 602–626.

Rossi, M., De Laurenzi, V., Munarriz, E., Green, D.R., Liu, Y.-C., Vousden, K.H., Cesareni, G., & Melino, G. (2005). The ubiquitin-protein ligase Itch regulates p73 stability. *The EMBO Journal*, *24*(4), 836–848.

Rossi, M., Aqeilan, R.I., Neale, M., Candi, E., Salomoni, P., Knight, R.A., Croce, C.M., & Melino, G. (2006). The E3 ubiquitin ligase Itch controls the protein stability of p63. *Proceedings of the National Academy of Sciences of the United States of America*, *103*(34), 12753–12758.

Rossi, M., Rotblat, B., Ansell, K., Amelio, I., Caraglia, M., Misso, G., Bernassola, F., Cavasotto, C.N., Knight, R.A., Ciechanover, A., & Melino, G. (2014). High throughput screening for inhibitors of the HECT ubiquitin E3 ligase ITCH identifies antidepressant drugs as regulators of autophagy. *Cell Death & Disease*, *5*(5), e1203. http://doi.org/10.1038/cddis.2014.113

Rotin, D., & Kumar, S. (2009). Physiological functions of the HECT family of ubiquitin ligases. *Nature Reviews Molecular Cell Biology*, *10*(6), 398–409.

Roukos, V., Pegoraro, G., Voss, T.C., & Misteli, T. (2015). Cell cycle staging of individual cells by fluorescence microscopy. *Nature Protocols, 10*, 334-348.

Rous, P. (1911). A Sarcoma of the Fowl transmissible by an agent separable from the tumour cells. *Journal of Experimental Medicine, 13*(4), 397-411.

Rusan, N.M., Fagerstrom, C.J., Yvon, A.M.C., & Wadworth, P. (2001). Cell Cycle-Dependent Changes in Microtubule Dynamics in Living Cells Expressing Green Fluorescent Protein-α Tubulin. *Molecular Biology of the Cell, 12*(4), 971-980.

Sager, P.R., Rothfield, N.L., Oliver, J.M., & Berlin, R.D. (1986). A novel mitotic spindle pole component that originates from the cytoplasm during prophase. *Journal of Cell Biology, 103*(5), 1863-1872.

Sakata, M., Kitamura, Y.H., Sakuraba, K., Goto, T., Mizukami, H., Saito, M., Ishibashi, K., Kigawa, G., Nemoto, H., Sanada, Y., & Hibi, K. (2009). Methylation of HACE1 in gastric carcinoma. *Anticancer Research, 29*(6), 2231-2233.

Sakata, M., Yokomizo, K., Kitamura, Y., Sakuraba, K., Shirahata, A., Goto, T., Mizukami, H., Saito, M., Ishibashi, K., Kigawa, G., Nemoto, H., & Hibi, K. (2013). Methylation of the HACE1 gene is frequently detected in hepatocellular carcinoma. *Hepatogastroenterology, 60*(124), 781-783.

Sakaue-Sawano, A., Kurokawa, H., Morimura, T., Hanyu, A., Hama, H., Osawa, H., Kashiwagi, S., Fukami, K., Miyata, T., Miyoshi, H., & Imamura, T. (2008). Visualizing Spatiotemporal Dynamics of Multicellular Cell-Cycle Progression. *Cell, 132*(3), 487-498.

Sampath, S.C., Ohi, R., Leismann, O., Salic, A., Pozniakovski, A., & Funabiki, H. (2004). The chromosomal passenger complex is required for chromatin-induced microtubule stabilisation and spindle assembly. *Cell, 118*(2), 187-202.

Sánchez-Tena, S., Cubillos-Rojas, M., Schneider, T., & Rosa, J.L. (2016). Functional and pathological relevance of HERC family proteins: a decade later. *Cellular and Molecular Life Sciences: CMLS*, 1–14. http://doi.org/10.1007/s00018-016-2139-8

Sander, B., Xu, W., Eilers, M., Popov, N., Lorenz, S. (2017). A conformational switch regulates the ubiquitin ligase HUWE1. *eLife*. DOI: 10.7554/eLife.21036.

Sarkar, A.A., & Zohn, I.E. (2012). Hectd1 regulates intracellular localization and secretion of Hsp90 to control cellular behavior of the cranial mesenchyme. *The Journal of Cell Biology*, *196*(6), 789–800.

Sarkar, A.A., Nuwayhid, S.J., Maynard, T., Ghandchi, F., Hill, J.T., Lamantia, A.S., & Zohn, I.E. (2014). Hectd1 is required for development of the junctional zone of the placenta. *Developmental Biology*, *392*(2), 368–380.

Sarker, A.A., Sabatino, J.A., Sugrue, K.F., & Zohn, I.E. Abnormal Labyrinthine Zone in the *Hectd1*-null Placenta. *Placenta*, *38*, 16-23.

Sarraf, P., Muller, E., Smith, W.M., Wright, H.W., Kum, J.B., Aaltonen, L.A., de la Chapelle, A., Spiegelman, B.H., & Eng, C. (1999). Loss-of-Function Mutations in PPARγ Associated with Human Colon Cancer. *Molecular Cell, 3*(6), 799-804.

Satija, Y.K., Bhardwaj, A., & Das, S. (2013). A portrayal of E3 ubiquitin ligases and deubiquitylases in cancer. *International Journal of Cancer. Journal International Du Cancer*, *133*(12), 2759–2768.

Sato, Y., Yoshikawa, A., Yamagata, A., Mimura, H., Yamashita, M., Ookata, K., Nureki, O., Iwai, K., Komada, M., & Fukai, S. (2008). Structural basis for specific cleavage of Lys 63-linked polyubiquitin chains. *Nature, 455,* 358-362.

Schebesta, A., McManus, S., Salvagiotto, G., Delogu, A., Busslinger, G.A., & Busslinger, M. (2007). Transcription Factor Pax5 Activates the Chromatin of Key Genes Involved in B Cell Signaling, Adhesion, Migration, and Immune Function. *Immunity, 27*(1), 49-63.

Scheffner, M., Huibregtse, J.M., Vieestra, R.D., & Howley, P.M. (1993). The Hpv-16 E6 and E6-Ap Complex Functions as a Ubiquitin-Protein Ligase in the Ubiquitination of P53. *Cell*, *75*(3), 495–505.

Scheffner, M., & Kumar, S. (2014). Mammalian HECT ubiquitin-protein ligases: biological and pathophysiological aspects. *Biochimica Et Biophysica Acta-Molecular Cell Research*, *1843*(1), 61–74.

Schlesinger, D.H., Goldstein, G., & Niall, H.D. (1975). The complete amino acid sequence of ubiquitin, an adenylate cyclase stimulating polypeptide probably universal in living cells. *Biochemistry*, *14*(10), 2214–2218

Schwalm, F.E. (1969). Changes in the formation of nuclear membranes and the ultrastructure of chromosomes during the early development of locust eggs (*Locusta migratoria*). *Wilhelm Roux' Archiv Fur Entwicklungsmechanik Der Organismen, 162*(1), 41-55.

Scialpi, F., Malatesta, M., Peschiaroli, A., Rossi, M., Melino, G., & Bernassola, F. (2008). Itch self-polyubiquitylation occurs through lysine-63 linkages. *Biochemical Pharmacology*, *76*(11), 1515–1521.

Scialpi, F., Mellis, D., & Ditzel, M. (2015). EDD, a Ubiquitin-Protein Ligase of the N-end Rule Pathway, Associates with Spindle Assembly Checkpoint Components and Regulates the Mitotic Response to Nocodazole. *The Journal of Biological Chemistry*, *290*(20), 12585–12594. http://doi.org/10.1074/jbc.M114.625673

Scott, L.M., Lawrence, H.R., Sebti, S.M., Lawrence, N.J., & Wu, J. (2010). Targeting protein tyrosine phosphatases for anticancer drug discovery. *Current Pharmaceutical Design, 16*(16), 1843-1862.

Scott, D., Oldham, N.J., Strachan, J., Searle, M.S., & Layfield, R. (2015). Ubiquitin-binding domains: mechanisms of ubiquitin recognition and use as tools to investigate ubiquitin-modified proteomes. *Proteomics, 15*(5-6), 844-861.

Segref, A., Kevei, É., Pokrzywa, W., Schmeisser, K., Mansfeld, J., Livnat-Levanon, N., Ensenauer, R., Glickman, M.H., Ristow, M., & Hoppe, T. (2014). Pathogenesis of Human Mitochondrial Diseases Is Modulated by Reduced Activity of the Ubiquitin/Proteasome System. *Cell Metabolism*, *19*(4), 642–652.

Seibler, J., Kleinridders, A., Küter-Luks, B., Niehaves, S., Brüning, J.C., & Schwenk, F. (2007). Reversible gene knockdown in mice using a tight, inducible shRNA expression system. *Nucleic Acids Research, 35*(7): e54.

Seipel, K., Medley, Q.G., Kedersha, N.L., Zhang, X.A., O'Brien, S.P., Serra-Pages, C., Helmer, M.E., Streuli, M. (1999). Trio amino-terminal guanine nucleotide exchange factor domain expression promotes actin cytoskeleton reorganization, cell migration and anchorage-independent cell growth. *Journal of Cell Science*, *112(12)*, 1825–1834.

Seipel, K., O'Brien, S.P., Iannotti, E., Medley, Q.G., & Streuli, M. (2001). Tara, a novel F-actin binding protein, associates with the Trio guanine nucleotide exchange factor and regulates actin cytoskeletal organization. *Journal of Cell Science*, *114*(2), 389–399.

Sen, S. (2000). Aneuploidy and cancer. Current Opinion in Oncology, 12(1), 82–88.

Shaik, S., Liu, P., Fukushima, H., Wang, Z., & Wei, W. (2012). Protein Degradation in Cell Cycle. eLS. DOI: 10.1002/9780470015902.a0023158

Shankavaram, U., Maachani, U.B., Zhao, S., Camphausen, K., & Tandle, A. (2015). Molecular profiling of MPS1 gene silencing in U251 glioma cell line. *Genomics Data, 6*, 36-39.

Sharma, S., Kelly, T.K., & Jones, P.A. (2010). Epigenetics and cancer. *Carcinogenesis, 31*(1), 27-36.

Shea, F.F., Rowell, J.L., Li, Y., Chang, T.-H., & Alvarez, C.E. (2012). Mammalian α arrestins link activated seven transmembrane receptors to Nedd4 family e3 ubiquitin ligases and interact with β arrestins. *Plos One*, *7*(12), e50557. http://doi.org/10.1371/journal.pone.0050557

Shearwin-Whyatt, L.M., Brown, D.L., Wylie, F.G., Stow, J.L., & Kumar, S. (2004). N4WBP5A (Ndfip2), a Nedd4-interacting protein, localizes to multivesicular bodies and the Golgi, and has a potential role in protein trafficking. *Journal of Cell Science*, *117*(16), 3679–3689.

Shearwin-Whyatt, L.M., Dalton, H.E., Foot, N., & Kumar, S. (2006). Regulation of functional diversity within the Nedd4 family by accessory and adaptor proteins. *BioEssays: News and Reviews in Molecular, Cellular and Developmental Biology*, *28*(6), 617–628.

Shen, H., & Laird, P.W. (2013). Interplay between the Cancer Genome and Epigenome. *Cell, 153*(1), 38-55.

Shen, X., Jia, Z., D'Alonzo, D., Wang, E., Bruder, E., Emch, F.H., De Geyter, C., & Zhang, H. (2017). HECTD1 controls the protein level of IQGAP1 to regulate the dynamics of adhesive structures. *Cell Communication and Signaling, 15*(2). DOI: 10.1186/s12964-016-0156-8.

Sherr, C.J., & Roberts, J.M. (2004). Living with or without cyclins and cyclin-dependent kinases. *Genes & Development*, *18*(22), 2699–2711.

Shi, Y. (2007). Histone lysine demethylases: emerging roles in development, physiology and disease. *Nature Reviews Genetics, 8*(11), 829-833.

Shimura, H., Hattori, N., Kubo, S., Mizuno, Y., Asakawa, S., Minoshima, S., Shimizu, K., Chiba, T., Tanaka, K., & Suzuki, T. (2000). Familial Parkinson disease gene product, parkin, is a ubiquitin-protein ligase. *Nature Genetics, 25*, 302-305.

Shirane, M., Harumiya, Y., Ishida, N., Hirai, A., Miyamoto, C., Hatakeyama, S., Nakayama, K., & Kitagawa, M. (1999). Down-regulation of p27(Kip1) by two mechanisms, ubiquitin-mediated degradation and proteolytic processing. *Journal of Biological Chemistry, 274*(20), 13886-13893.

Singh, S.A., Winter, D., Kirchner, M., Chauhan, R., Ahmed, S., Ozlu, N., Tzur, A., Steen, J.A., & Steen, H. (2014). Co-regulation proteomics reveals substrates and mechanisms of APC/C-dependent degradation. *EMBO Journal, 33*(4), 385-399.

Sivakumar, S., & Gorbsky, G.J. (2015). Spatiotemporal regulation of the anaphase-promoting complex in mitosis. *Nature Reviews Molecular Cell Biology*, *16*(2), 82–94.

Smits, V.A.J. (2012). EDD induces cell cycle arrest by increasing p53 levels. *Cell Cycle*, *11*(4), 715–720.

Sokolova, V., Li, F., Polovin, G., & Park, S. (2015). Proteasome Activation is Mediated via a Functional Switch of the Rpt6 C-terminal Tail Following Chaperone-dependent Assembly. *Scientific Reports, 5,* 14909. DOI: 10.1038/srep14909

Spratt, D.E., Walden, H., & Shaw, G.S. (2014). RBR E3 ubiquitin ligases, new insights, new questions. *Biochemical Journal, 458*(3), 421-437.

Spence, J, Sadis S, Haas AL, & Finley D. (1995). A Ubiquitin Mutant with Specific Defects in DNA Repair and Multiubiquitination. *Molecular and Cellular Biology, 15(3)*, 1265–1273.

Srayko, M., Buster, D.W., Bazirgan, O.A., McNally, F.J., Mains, P.E. (2000). MEI-1/MEI-2 katanin-like microtubule severing activity is required for the *Caenorhabditis elegans* meiosis. *Genes & Development, 14*(9), 1072-1084.

Stefansson, B., Ohama, T., Daugherty, A.E., & Brautigan, D.L. (2008). Protein phosphatase 6 regulatory subunits composed of ankyrin repeat domains. *Biochemistry*, *47*(5), 1442–1451.

Stempin, C.C., Chi, L., Giraldo-Vela, J.P., High, A.A., Häcker, H., & Redecke, V. (2011). The E3 ubiquitin ligase mind bomb-2 (MIB2) protein controls B-cell CLL/lymphoma 10 (BCL10)-dependent NF-κB activation. *Journal of Biological Chemistry, 286*(43), 37147–37157.

Stern, B.M., & Murray, A.W. (2001). Lack of tension at kinetochores activates the spindle assembly checkpoint in budding yeast. *Current Biology, 11*, 1462-1467.

Stewart, K., Rajkumar, V., Dimopoulos, M.A., Masszi, R., Špička, I., Oriol, A., Hájek, R., Rosiñol, L., Siegel, D.S., Mihaylov, G.G., Goranova-Marinova, V., Rajnics, P., Suvorov, A., Niesvizky, R., Jakubowiak, A.J., San-Miguel, J.F., Ludwig, H., Wang, M., Maisnar, V., Minarik, J., Bensinger, W.I., Mateos, M.V., Ben-Yehuda, D., Kukreit, V., Zojwalla, N., Tonda, M.E., Yang, X., Xing, B., Moreau, P., & Palumbo, A. (2015). Carfizomib, Lenlidomide, and Dexamethasone for Relapsed Multiple Myeloma. *The New England Journal of Medicine, 372*, 142-152.

Strunnikov, A.V. (2003). Condensin and biological role of chromosome condensation. *Progress in Cell Cycle Research, 5*, 361-367.

Su, H., Meng, S., Lu, Y., Trombly, M.I., Chen, J., Lin, C., Turk, A., & Wang, X. (2011). Mammalian hyperplastic discs homolog EDD regulates miRNA-mediated gene silencing. *Molecular Cell*, *43*(1), 97–109. http://doi.org/10.1016/j.molcel.2011.06.013

Sudakin, V., Chan, G.K.T., & Yen, T.J. (2001). Checkpoint inhibition of the APC/C in HeLa cells is mediated by a complex of BUBR1, BUB3, CDC20, and MAD2. *Cell, 154*(5), 925-936.

Sun, L., Hui, A.M., Su, Q., Vortmeyer, A., Kotilarov, Y., Pastorino, S., Passanti, A., Menon, J., Walling, J., Bailey, R., Rosenblum, M., Mikkelsen, T., & Fine, H.A. (2006). Neuronal and glioma-derived stem cell factor induces angiogenesis within the brain. *Cancer Cell, 9*(4), 287-300.

Sun, T., Wang, X., He, H.H., Sweeney, C.J., Liu, S.X., Brown, M., Balk, S., Lee, G.S., Kantoff, P.W. (2014). MiR-221 promotes the development of androgen independence in prostate cancer cells via downregulation of HECTD2 and RAB1A. *Oncogene, 33*(21), 2790-2800.

Suryaraja, R., Anitha, M., Anbarasu, K., Kumari, G., & Mahalingam, S. (2013). The E3 ubiquitin ligase Itch regulates tumor suppressor protein RASSF5/NORE1 stability in an acetylation-dependent manner. *Cell Death & Disease*, *4*(3). http://doi.org/10.1038/cddis.2013.91

Takizawa, C.G., & Morgan, D.O. (2000). Control of mitosis by changes in the subcellular location of cyclin-B1-Cdk1 and Cdc25C. *Current Opinion in Cell Biology, 12*(6), 658-665.

Talis, A.L., Huibregtse, J.M., & Howley, P.M. (1998). The Role of E6AP in the Regulation of p53 Protein Levels in Human Papillomavirus (HPV)-positive and HPV-negative Cells. *The Journal of Biological Chemistry*, *273*(11), 639–6445.

Tamai, K.K, & Shimoda, C. (2002). The novel HECT-type ubiquitin-protein ligase Pub2p shares partially overlapping function with Pub1p in Schizosaccharomyces pombe. *Journal of Cell Science*, *115*(9), 1847–1857.

Tang, D., Xiang, Y., De Renzis, S., Rink, J., Zheng, G., Zerial, M., & Wang, Y. (2011). s *Nature Communications*, *2*, 501. http://doi.org/10.1038/ncomms1509

Tang, L., Yi, X.-M., Chen, J., Chen, F.-J., Lou, W., Gao, Y.-L., Zhou, J., Su, L.-N., Xu, X., Lu, J.-Q., Ma, J., Yu, N., & Ding, Y.-F. (2016). Ubiquitin ligase UBE3C promotes melanoma progression by increasing epithelial-mesenchymal transition in melanoma cells. *Oncotarget, 7*(13), 15738-15746.

Tanksley, J.P., Chen, X., & Coffey, R.J. (2013). NEDD4L Is Downregulated in Colorectal Cancer and Inhibits Canonical WNT Signaling. *PLOS One.* DOI: 10.1371/journal.pone.0081514.

Tauchman, E.C., Boehm, F.J., & DeLuca, J.G. (2015). Stable kinetochore-microtubules attachment is sufficient to silence the spindle assembly checkpoint in human cells. *Nature Communications, 6,* 10036. DOI: 10.1038/ncomms10036.

Taylor, W.R., & Stark, G.R. (2001). Regulation of the G2/M transition by p53. *Oncogene, 20*(15), 1803-1815.

Teixeira, L.K., & Reed, S.I. (2013). Ubiquitin ligases and cell cycle control. *Annual Review of Biochemistry, 82*, 387-414.

Tenno, T., Fujiwara, K., Tochio, H., Iwai, K., Morita, E.H., Hayashi, H., Murata, S., Hiroaki, H., Sato, M., Tanaka, K., & Shirakawa, M. (2004). Structural basis for distinct roles of Lys63- and Lys48-linked polyubiquitin chains. *Genes to Cells, 9*(10), 865-875.

Thomas, D.B., & Lingwood, C.A. (1975). A Model of Cell Cycle Control: Effects of Thymidine on Synchronous Cell Cultures. *Cell*, *5*, 37–42.

Thompson, A., Schäfer, J., Kuhn, K., Kienle, S., Schwarz, J., Schmidt, G., Neumann, T., & Hamon, C. (2003). Tandem Mass Tags: A Novel Quantification Strategy for Comparative Analysis of Complex Protein Mixtures by MS/MS. *Analytical Chemistry, 75*(8), 1895-1904.

Thrower, J.S., Hoffman, L., Rechsteiner, M., & Pickart, C.M. Recognition of the polyubiquitin proteolytic signal. (2000). *EMBO, 19*(1), 94–102.

Tian, Z., D'Arcy, P., Wang, X., Ray, A., Tai, Y.T., Hu, Y., Carrasco, R.D., Richardson, P., Linder, S., Chauhan, D., & Anderson, K.C. (2014). A novel small molecule inhibitor of deubiquitylating enzyme USP14 and UCHL5 induces apoptosis in multiple myeloma and overcomes bortezomib resistance. *Blood, 123*(5), 706-716.

Tiede, C., Tang, A.A., Deacon, S.E., Mandal, U., Nettleship, J.E., Owen, R.L., George, S.E., Harrison, D.J., Owens, R.J., Tomlinson, D.C., & McPherson, M.J. (2014). Adhiron: a stable and versatile peptide display scaffold for molecular recognition applications. *Protein Engineering, Design & Selection, 27*(5), 145-155.

Tiede, C., Bedford, R., Heseltine, S.J., Smith, G., Wijetunga, I., Ross, R., AlQallaf, D., Roberts, A.P., Balls, A., Curd, A., Hughes, R.E., Martin, H., Needham, S.R., Zanetti-Domingues, L.C., Sadigh, Y., Peacock, T.P., Tang, A.A., Gibson, N., Kyle, H., Platt, G.W., Ingram, N., Taylor, T., Coletta, L.P., Manfield, I., Knowles, M., Bell, S., Esteves, F., Maqbool, A., Prasad, R.K., Drinkhill, M., Bon, R.S., Patel, V., Goodchild, S.A., Martin-Fernandez, M., Owens, R.J., Nettleship, J.E., Webb, M.E., Harrison, M., Lippiat, J.D., Ponnambalam, S., Peckham, M., Smith, A., Ferrigno, P.K., Johnson, M., McPherson, M.J., & Tomlinson, D.C. (2017). Affimer proteins are versatile and renewable affinity reagents. *Elife, 6,* e24903. DOI: 10.7554/eLife.24903.

Tokunaga, F., Sakata, S.I., Saeki, Y., Satomi, Y., Kirisako, T., Kamei, K., Nakagawa, T., Kato, M., Murata, S., Yamaoka, S., Yamamoto, M., Akira, S., Takao, T., Tanaka, K., & Iwai, K. (2009). Involvement of linear polyubiquitylation of NEMO in NF-kappaB activation. *Nature Cell Biology*, *11*(2), 123–132.

Tran, H., Hamada, F., Schwarz-Romond, T., & Bienz, M. (2008). Trabid, a new positive regulator of Wnt-induced transcription with preference for binding and cleaving K63-linked ubiquitin chains. *Genes & Development*, *22*(4), 528–542.

Tran, H., Bustos, D., Yeh, R., Rubinfeld, B., Lam, C., Shriver, S., Zilberleyb, I., Lee, M.W., Phu, L., Sarkar, A.A., Zohn, I.E., Wertz, I.E., Kirkpatrick, D.S., & Polakis, P. (2013). HectD1 E3 Ligase Modifies Adenomatous Polyposis Coli (APC) with Polyubiquitin to Promote the APC-Axin Interaction. *The Journal of Biological Chemistry*, *288*(6), 3753–3767.

Tsubuki, S., Hiroshi, K., Saito, Y., Miyashita, N., Inomata, M., & Kawashima, S. (1993). Purification and characterization of a ZLeuLeuLeupMCA degrading protease expected to regulate neurite formation: a novel catalytic activity in proteasome. *Biochemical and Biophysical Research Communications, 196*, 1195-1201.

Tsunematsu, R., Nakayama, K., Oike, Y., Nishiyama, M., Ishida, N., Hatakeyama, S., Bessho, Y., Kageyama, R., Suda, T., & Nakayama, K.I. (2004). Mouse Fbw7/Sel-10/Cdc4 is required for notch degradation during vascular development. *Journal of Biological Chemistry, 279*(10), 9417-9423.

Tsutsumi, S., & Neckers, L. (2007). Extracellular heat shock protein 90: a role for a molecular chaperone in cell motility and cancer metastasis. *Cancer Science*, *98*(10), 1536–1539.

Uchida, K.S.K., Takagaki, K., Kumada, K., Hirayama, Y., Noda, T., & Hirota, T. (2009). Kinetochore stretching inactivates the spindle assembly checkpoint. *Journal of Cell Biology, 184*(3), 383-390.

Uetake, Y., & Sluder, G. (2010). Prolonged Prometaphase Blocks Daughter Cell Proliferation Despite Normal Completion of Mitosis. *Current Biology, 20*(18), 1666-1671.

Utsugi, T., Hirata, A., Sekiguchi, Y., Sasaki, T., Toh-e, A., & Kikuchi, Y. (1999). Yeast tom1 mutant exhibits pleiotropic defects in nuclear division, maintenance of nuclear structure and nucleocytoplasmic transport at high temperatures. *Gene*, *234*(2), 285–295.

Uzunova, K., Dye, B.T., Schutz, H., Ladurner, R., Petzold, G., Toyoda, Y., Jarvis, M.A., Brown, N.G., Poser, I., Novatchkova, M., Mechtler, K., Hyman, A.A., Stark, H., Schulman, B.A., & Peters, J.-M. (2012). APC15 mediates CDC20 auto-ubiquitination by APC/C^{MCC} and MCC disassembly. *Nature Structural & Molecular Biology, 19*(11), 1116-1123.

Valente, V., Teixeira, S.A., Neder, L., Okamoto, O.K., Oba-Shinjo, S.M., Marie, S.N.K., Scrideli, C.A., Paçó-Larson, M.L., & Carlotti, Jr. C.G. (2009). Selection of suitable housekeeping genes for expression analysis in glioblastoma using quantitative RT-PCR. *BMC Molecular Biology, 10*(17). DOI: 10.1186/1471-2199-10-17.

Valkevich, E.M., Sanchez, N.A., Ge, Y., & Strieter, E.R. (2014). Middle-Down Mass Spectrometry Enables Characterisation of Branched Ubiquitin Chains. *Biochemistry, 53*(30), 4979-4989.

Van Hooser, A.A., & Heald, R. (2001). Kinetochore function: The complications of becoming attached. *Current Biology, 11*(21), 855-857.

van Leeuwen, F.W., de Kleijn, D.P., van den Hurk, H.H., Neubauer, A., Sonnemans, M.A., Sluijs, J.A., Köycü, S., Ramdjielal, R.D., Salehi, A., Martens, G.J., Grosveld, F.G., Peter, J., Burbach, H., & Hol, E.M. (1998). Frameshift mutants of beta amyloid precursor proteins and ubiquitin-B in Alzheimer's and Down patients. *Science, 279*(5348), 242-247.

Vassilev, L.T., Tovar, C., Chen, S., Knezevic, D., Zhao, X., Sun, H., Heimbrook, D.C., & Chen, L. (2006). Selective small-molecule inhibitor reveals critical mitotic functions of human CDK1. *PNAS, 103*(28), 10660-10665.

Vaughan, L., Tan, C.-T., Chapman, A., Nonaka, D., Mack, N.A., Smith, D., Booton, R., Hurlstone, A.F.L., & Malliri, A. (2015). HUWE1 Ubiquitylates and Degrades the RAC Activator TIAM1 Promoting Cell-Cell Adhesion Disassembly, Migration, and Invasion. *Cell Reports, 10*(1), 88-102.

Verdecia, M.A., Bowmann, M.E., Lu, K.P., Hunter, T., & Noel, J.P. (2000). Structural basis for phosphoserine-proline recognition by group IV WW domains. *Nature Structural Biology, 7*, 639-643.

Verdecia, M.A., Joazeiro, C., Wells, N.J., Ferrer, J.L., Bowman, M.E., Hunter, T., & Noel, J.P. (2003). Conformational flexibility underlies ubiquitin ligation mediated by the WWP1 HECT domain E3 ligase. *Molecular Cell*, *11*(1), 249–259.

Vermeulen, K., Van Bockstaele, D.R., & Berneman, Z.N. (2003). The cell cycle: a review of regulation, deregulation and therapeutic targets in cancer. *Cell Proliferation, 36*(3), 131-149.

Viniksy, A., Michaud, C., Powers, J., & Orlowski, M. (1992). Inhibition of the chymotrypsin-like activity of the pituitary multicatalytic proteinase complex. *Biochemistry, 31*, 9421-9428.

Virdee, S., Ye, Y., Nguyen, D.P., Komander, D., & Chin, J.W. (2010). Engineered diubiquitin synthesis reveals Lys29- isopeptide specificity of an OUT deubiquitinase. *Nature Chemical Biology,* 6(10), 750-757.

Visintin, R., Prinz, S., & Amon, A. (1997). CDC20 and CDH1: a family of substrate-specific activators of APC-dependent proteolysis. *Science, 278*(5337), 460-463.

Voisin, S., Rognan, D., Gros, C., & Ouimet, T. (2004). A Three-dimensional Model of the Neprilysin 2 Active Site Based on the X-ray Structure of Neprilysin. *Journal of Biological Chemistry, 279*, 46172-46181.

Vordermaier, H.C. (2004). APC/C and SCF: controlling each other and the cell cycle. *Current Biology, 14*(18), 787-796.

Wainman, A., Buster, D.W., Duncan, T., Metz, J., Ma, A., Sharp, D., & Wakefield, J.G. (2009). A new Augmin subunit, Msd1, demonstrates the importance of mitotic spindle-templated microtubule nucleation in the absence of functioning centrosomes. *Genes & Development, 23*(16), 1876-1881.

Walczak, C.E., Vernos, I., Mitchison, T.J., Karsenti, E., & Heald, R. (1998). A model for the proposed roles of different microtubule-based motor proteins in establishing spindle bipolarity. *Current Biology, 8*(16), 903-913.

Walczak, C.E., & Heald, R. (2008). Chapter Three – Mechanisms of Mitotic Spindle Assembly and Function. *International Review of Cytology, 265*, 111-158.

Wang, J., Peng, Q., Lin, Q., Childress, C., Carey, D., Yang, W. (2010). Calcium activates Nedd4 E3 ubiquitin ligases by releasing the C2 domain-mediated auto-inhibition. *Journal of Biological Chemistry, 16;285*(16), 12279-12288.

Wang, L., Zhang, P., Molkentine, D.P., Chen, C., Molkentine, J.M., Piao, H., Raju, U., Zhang, J., Valdecanas, D.R., Tailor, R.C., Thames, H.D., Bucholz, T.A., Chen, J., Ma, L., Mason, K.A., Ang, K.-K., Meyn, R.E., & Skinner, H.D. (2017). TRIP12 as a mediator of human papillomavirus/ p16-related radiation enhancement effects. *Oncogene, 36*, 820-828.

Wang, M., & Pickart, C.M. (2005). Different HECT domain ubiquitin ligases employ distinct mechanisms of polyubiquitin chain synthesis. *The EMBO Journal*, *24*(24), 4324–4333.

Wang M, Cheng D, Peng J, & Pickart CM. (2006). Molecular determinants of polyubiquitin linkage selection by an HECT ubiquitin ligase. *The EMBO Journal*, *25*(8), 1710–1719.

Wang, X., Lu, G., Li, L., Yi, J., Yan, K., Wang, Y., Zhu, B., Kuang, J., Lin, M., Zhang, S., & Shao, G. (2014). HUWE1 interacts with BRCA1 and promotes its degradation in the ubiquitin-proteasome pathway. *Biochemical and Biophysical Research Communications*, *444*(4), 549–554.

Wang, X., Mazurkiewicz, M., Hillert, E.-K., Olofsson, M.H., Pierrou, S., Hillerstz, P., Gullbo, J., Selvaraji, K., Paulus, A., Akhtar, S., Bossler, F., Khan, A.C., Linder, S., & D'Arcy, P. (2016). The proteasome deubiquitinase inhibitor VLX1570 shows selectivity for ubiquitin-specific protease-14 and induces apoptosis of multiple myeloma cells. *Scientific Reports, 6*, 26979. DOI: 10.1038/srep26979.

Wang, Y.Y., Ye, Z.Y., Zhao, Z.S., Tao, H.Q., & Li, S.G. (2010). Systems biology approach to identification of biomarker for metastatic progression in gastric cancer. *Journal of Cancer Research and Clinical Oncology, 136*(1), 135-141.

Watt, F., & Molloy, P.L. (1988). Cytosine methylation prevents binding to DNA of a HeLa cell transcription factor required for optimal expression of the adenovirus major late promoter. *Genes & Development, 2,* 1136-1143.

Watts, C.K., & Saunders, D.N. (2011). Effects of EDD on p53 function are context-specific. *Journal of Biological Chemistry*, *286*(28), le13–author reply le14. http://doi.org/10.1074/jbc.L110.182527

Weathington, N.M., & Mallampalli, R.K. (2014). Emerging therapies targeting the ubiquitin proteasome system in cancer. *The Journal of Clinical Investigation, 124*(1), 6-12.

Weeks, S.D., Grastly, K.C., Hernandez-Cuebas, L., & Loll, P.J. (2009). Crystal structures of Lys-63-linked tri- and di- ubiquitin reveal a highly extended chain architecture. *Proteins, 77*(4), 753-759.

Wegel, E., Göhler, A., Christoffer Lagerholm, B., Wainman, A., Uphoff, S., Kaufmann, R., & Dobbie, I.M. (2016). Imaging cellular structures in super-resolution with SIM, STED and Localisation Microscopy: A practical comparison. *Scientific Reports, 6*, a27290.

Wei, R., Guo, J., Li, M., Yang, X., Zhu, R., Huang, H., Li, K., Zhang, L., & Gao, R. (2017). Smurf1 controls S phase progression and tumorigenesis through Wee1 degradation. *FEBS Letters, 591*(8), 1150-1158.

Wei, W., Ayad, N.G., Wan, Y., Zhang, G.J., Kirschner, M.W., Kaelin, W.G. Jr. (2004). Degradation of the SCF component Skp2 in cell-cycle phase G1 by the anaphase-promoting complex. *Nature, 428*(6979), 194-198.

Wei, W., Ayad, N.G., Wan, Y., Zhang, G.J., Kirschner, M.W., Kaelin, W.G. Jr. (2004). Degradation of the SCF component Skp2 in cell-cycle phase G1 by the anaphase-promoting complex. *Nature, 428*(6979), 194-198.

Wei, Y., Yu, L., Bowen, J., Gorovsky, M.A., & Allis, D.C. (1999). Phosphorylation of Histone H3 is Required for Proper Chromosome Condensation and Segregation. *Cell, 97*(2), 99-109.

Weinberg, F., Hamanaka, R., Wheaton, W.W., Weinberg, S.E., Joesph, J., Lopez. M., Kalyanaraman, B., Mutlu, G.M., Budinger, G.R., Chandel, N.S. (2010). Mitochondrial metabolism and ROS generation are essential for Kras-mediated tumorigenicity. *PNAS, 107*(19), 8788-8793.

Weinberg, S.E., & Chandel, N.S. (2015). Targeting mitochondria metabolism for cancer therapy. *Nature Chemical Biology, 11*, 9-15.

Weiss, E., & Wilney, M. (1996). The Saccharomyces cerevisiae spindle pole body duplication gene MPS1 is part of a mitotic checkpoint. *Journal of Cell Biology, 132*(1-2), 111-123.

Weiss, R.A., & Vogt, P.K. (2011). 100 years of Rous sarcoma virus. *Journal of Experimental Medicine, 208*(12), 2351-2355.

Weller, M., Wick, W., Aldape, K., Brada, M., Berger, M., Pfister, S.M., Nishikawa, R., Rosenthal, M., Wen, P.Y., Stupp, R., & Reifenberger, G. (2015). Glioma. *Nature Reviews Disease Primers, 1*, 15017. DOI: 10.1038/nrdp.2015.17

Wen, J.L., Wen, X.F., Li, R.B., Jin, Y.C., Wang, X.L., Zhou, L., & Chen, H.X. (2015). UBE3C Promotes Growth and Metastasis of Renal Cell Carcinoma via Activating Wnt/β-Catenin Pathway. *PLOS One*. DOI: 10.1371/journal.pone.0115622.

Wiesner, S., Ogunjimi, A.A., Wang, H.-R., Rotin, D., Sicheri, F., Wrana, J.L., & Forman-Kay, J.D. (2007). Autoinhibition of the HECT-type ubiquitin ligase Smurf2 through its C2 domain. *Cell*, *130*(4), 651–662.

Wollman, R., Cytrynbaum, E.N., Jones, J.T., Meyer, T., Scholey, J.M., & Mogilner, A. (2005). Efficient chromosome capture requires a bias in the 'search-and-capture' process during mitotic spindle assembly. *Current Biology, 15*(9), 828-832.

Wong, R.W., Blobel, G., & Coutavas, E. (2006). Rae1 interaction with NuMA is required for bipolar spindle formations. *PNAS, 103*(52), 19783-19787.

Wrage, M., Hagmann, W., Kemming, D., Uzunoglu, F.G., Riethdorf, S., Effenberger, K., Westphal, M., Lamszus, K., Kim, S.Z., Becker, N., Izbicki, J.R., Sandoval, J., Esteller, M., Pantel, K., Risch, A., & Wikman, H. (2015). Identification of HERC5 and its potential role in NSCLC progression. *International Journal of Cancer, 136*(10), 2264-2272.

Wu, W., Sato, K., Koike, A., Nishikawa, H., Koizumi, H., Venkitaraman, A.R., & Ohta, T. (2010). HERC2 is an E3 ligase that targets BRCA1 for degradation. *Cancer Research*, *70*(15), 6384–6392.

Xeros, N. (1962). Deoxyribose Control and Synchronisation of Mitosis. *Nature*, *194*, 682–683.

Xu, P., & Peng, J. (2008). Characterization of polyubiquitin chain structure by middle-down mass spectrometry. *Analytical Chemistry, 80*(9), 3438-3444.

Xu, P., Duong, D.M., Seyfried, N.T., Cheng, D., Xie, Y., Robert, J., Rush, J., Hochstrasser, M., Finely, D., & Peng, J. (2009). Quantitative Proteomics Reveals the Function of Unconventional Ubiquitin Chains in Proteasomal Degradation. *Cell*, *137*(1), 133–145.

Xu, Z., Ogawa, H., Vagnarelli, P., Bergmann, J.H., Hudson, D.F., Ruchaud, S., Fukagawa, T., Earnshaw, W.C., & Samejima, K. (2009). INCENP-aurora B interactions modulate kinase activity and chromosome passenger complex localisation. *Journal of Cell Biology, 187*(5), 637-653.

Yada, M., Hatakeyama, S., Kamura, T., Nishiyama, M., Tsunematsu, R., Imaki, H., Okumura, F., Nakayama, K., & Nakayama, K.I. (2004). Phosphorylation-dependent degradation of c-Myc is mediated by the F-box protein Fbw7. *EMBO Journal, 23*, 2116-2125.

Yan, K., Li, L., Wang, X., Hong, R., Zhang, Y., Yang, H., Lin, M., Zhang, S., He, Q., Zheng, D., Tang, J., Yin, Y., and Shao, G. (2015). The deubiquitinating enzyme complex BRISC is required for proper mitotic spindle assembly in mammalian cells. *Journal of Cell Biology, 210*(2), 209-224.

Yang, R., He, Y., Chen, S., Lu, X., Huang, C., & Zhang, G. (2016). Elevated expression of WWP2 in human lung adenocarcinoma and its effect on migration and invasion. *Biochemical and Biophysical Research Communications, 479*(2). 146-151.

Yang, Y., Liu, M., Li, D., Ran, J., Gao, J., Suo, S., Sun, S.-C., & Zhou, J. (2014). CYLD regulates spindle orientation by stabilizing astral microtubules and promoting dishevelled-NuMA-dynein/dynactin complex formation. *PNAS, 111*(6), 2158-2163.

Yang, Y.L., Ludwig, R.L., Jensen, J.P., Pierre, S.A., Medaglia, M.V., Davydov, I.V., Safiran, Y.J., Oberoi, P., Kenten, J.H., Philips, A.C., Weissman, A.M., & Vousden, K.H. (2005). Small molecule inhibitors of HDM2 ubiquitin ligase activity stabilize and activate p53 in cells. *Cancer Cell*, *7*(6), 547–559.

Yau, R.G., & Rape, M. (2016). The increasing complexity of the ubiquitin code. *Nature Cell Biology, 18*, 579-586.

Yau, R.G., Doerner, K., Castellanos, E.R., Haakonsen, D.L., Werner, A., Wang, N., Yang, X.W., Martinez-Martin, N., Matsumoto, M.L., Dixit, V.M., & Rape, M. (2017). Assembly and Function of Heterotypic Ubiquitin Chains in Cell-Cycle and Protein Quality Control. *Cell, 171*(4), 918-933.

Ye, Y., Akutsu, M., Reyes-Turcu, F., Ehchev, R.I., Wilkinson, K.D., & Komander, D. (2011). Polyubiquitin binding and cross-reactivity in the USP domain deubiquitinase USP21. *EMBO Reports, 12*(4), 350-357.

Ye, Y., Blaser, G., Horrocks, M.H., Ruedas-Rama, M.J., Ibrahim, S., Zhukov, A.A., Orte, A., Klenerman, D., Jackson, S.E., & Komander, D. (2012). Ubiquitin chain conformation regulates recognition and activity of interacting proteins. *Nature, 492*, 266-270.

Yeung, B., Ho, K.-C., & Yang, X. (2013). WWP1 E3 Ligase Targets LATS1 for Ubiquitin-Mediated Degradation in Breast Cancer Cells. *PLOS One.* DOI: 10.1371/journal.pone.0061027.

Yong-Gonzalez, V., Wang, B.-D,, Butylin, P., Ouspenski, I., & Strunnikov, A. (2009). Condensin function at centromere chromatin facilitates proper kinetochore tension and ensures correct mitotic segregation of sister chromatids. *Genes to Cells, 12*(9), 1075-1090.

Yoon, S.Y., Lee, Y., Kim, J.H., Chung, A.-S., Joo, J.H., Kim, C.-N., Kim, N.-S., Choe, I.S., & Kim, J.W. (2005). Over-expression of human UREB1 in colorectal cancer: HECT domain of human UREB1 inhibits the activity of tumor suppressor p53 protein. *Biochemical and Biophysical Research Communications*, *326*(1), 7–17.

You, J., & Pickart, C.M. (2001). A HECT domain E3 enzyme assembles novel polyubiquitin chains. *Journal of Biological Chemistry, 276*(23), 19871-19878.

Yu, J., Lan, J., Zhu, Y., Li, X., Lai, X., Xue, Y., Changjiang, J., & Huang, H. (2008). The E3 ubiquitin ligase HECTD3 regulates ubiquitination and degradation of Tara. *Biochemical and Biophysical Research Communications*, *367*(4), 805–812.

Yuan, J., Luo, K., Deng, M., Li, Y., Yin, P., Gao, B., Fang, Y., Wu, P., Liu, T., & Lou, Z. (2014). HERC2-USP20 axis regulates DNA damage checkpoint through Claspin. *Nucleic Acids Research*, *42*(21), 13110–13121.

Zachos, G., Black, E.J., Walker, M., Scott, M.T., Vagnarelli, P., Earnshaw, W.C., & Gillespie, D.A.F. (2007). Chk1 is Required for Spindle Checkpoint Function. *Cell, 12*(2), 247-260.

Zeka, F., Vanderheyden, K., De Smet, E., Cuvelier, C.A., Mestdagh, P., & Vadesompele, J. (2016). Straightforward and sensitive RT-qPCR based gene expression analysis of FFPE samples. *Scientific Reports, 6*, a21418. DOI: 10.1038/srep21418.

Zeng, K., Bastos, R.N., Barr, F.A., & Gruneberg, U. (2010). Protein phosphatase 6 regulates mitotic spindle formation by controlling the T-loop phosphorylation state of Aurora A bound to its activator TPX2. *Journal of Cell Biology, 191*(7), 1315-1332.

Zeng, W.L., Chen, Y.W., Zhou, H., Zhou, J.Y., Wei, M., & Shi, R. (2015). Expression of HERC4 in lung cancer and its correlation with clinicopathlogical parameters. *Asian Pacific Journal of Cancer Prevention (APJCP), 16*(2), 513-517.

Zetterberg, A., Larsson, O., Wiman, K.G. (1995). What is the restriction point? *Current Opinion in Cell Biology, 7*(6), 835-842.

Zhang, L., Anglesio, M.S., O'Sullivan, M., Zhang, F., Yang, G., Sarao, R., Mai, P.N., Cronin, S., Hara, H., Melnyk, N., Li, L., Wada, T., Liu, P.P., Farrar, J., Arceci, R.J., Sorensen, P.H., & Penninger, J.M. (2007). The E3 ligase HACE1 is a critical chromosome 6q21 tumor suppressor involved in multiple cancers. *Nature Medicine, 13*(9), 1060-1069.

Zhang, M., Windheim, M., Roe, S.M., Peggie, M., Cohen, P., Prodromou, C., & Pearl, L.H. (2005). Chaperoned ubiquitylation-crystal structures of the CHIP U box E3 ubiquitin ligase and a CHIP-Ubc13-Uev1a complex. *Molecular Cell, 20*(4), 525-538.

Zhang, W., Wu, K., Sartori, N., Kamadurai, H.B., Ordureau, A., Jiang, C., Mercredi, P.Y., Murchie, R., Hu, J., Persaud, A., Mukherjee, M., Li, N., Doye, A., Walker, J.R., Sheng, Y., Hao, Z., Li, Y., Brown, K.R., Lemichez, E., Chen, J., Tong, Y., Harper, J.W., Moffat, J., Rotein, D., Schulman, B.A., & Sidhu, S.S. (2016). System-Wide Modulation of HECT E3 ligases with Selective Ubiquitin Variant Probes. *Molecular Cell. 62*(1), 121-136.

Zhou, H., Shi, R., Chen, Y., Zeng, W., Liang, S., Zheng, W., & Ma, W. (2014). Expression of E3 ligase HERC4 in breast cancer and its clinical implications. *Nan Fang Yi Ke Da Xue Xue Bao, 34*(8), 1110-1114.

Zhou, X., Li, T.-T., Feng, X., Hsiang, E., Xiong, Y., Guan, K.-L., & Lei, Q.-Y. (2012). Targeted polyubiquitylation of RASSF1C by the Mule and SCFβ-TrCP ligases in response to DNA damage. *The Biochemical Journal*, *441*(1), 227–236.

Zhou, Z., Du, X., Cai, Z., Song, X., Zhang, H., Mizuno, T., Suzuki, E., Yee, M.R., Berezov, A., Murali, R., Wu, S.L., Karger, B.L., Greene, M.I., & Wang, Q. (2012). Structure of Sad1-UNC84 homology (SUN) domain defines features of molecular bridge in nuclear envelope. *Journal of Biological Chemistry*, *287(8),* 5317–5326.

Zickert, P., Wejde, J., Skog, S., Zetterberg, A., & Larsson, O. (1993). Growth-regulatory properties of G1 cells synchronized by centrifugal elutriation. *Experimental Cell Research, 207*(1), 115-121.

Zieve, G.W., Turnbull, D., Mullins, J.M., & McIntosh, J.R. (1980). Production of Large Numbers of Mitotic Mammalian Cells by Use of the Reversible Microtubule Inhibitor Nocodazole. *Experimental Cell Research*, *126*, 1–9.

Zohn, I.E., Anderson, K.V., & Niswander, L. (2007). The Hectd1 ubiquitin ligase is required for development of the head mesenchyme and neural tube closure. *Developmental Biology*, *306*(1), 208–221.

Appendix

HECTD1 WT cDNA (codant)

ATGGCAGATGTGGACCCAGATACATTGCTGGAATGGCTACAGATGGGACAGGGAGATGAAAGGGAC
ATGCAACTAATAGCCCTTGAACAGCTATGCATGCTGCTTTTGATGTCTGACAACGTGGATCGTTGT
TTTGAAACATGTCCTCCTCGCACTTTCTTACCAGCCCTTTGCAAAATTTTTCTTGATGAAAGTGCT
CCAGACAATGTATTAGAGGTGACAGCCCGTGCCATAACATACTACCTGGATGTATCTGCGGAATGT
ACC.CGAAGGATTGTTGGGGTAGATGGAGCTATAAAAGCACTTTGTAATCGTTTGGTTGTAGTTGA
ACTTAACA20ACAGGACTAGCAGAGACTTAGCCGAACAGTGTGTAAAGGTATTAGAACTGATATGT
ACTCGTGAGTCAGGAGCAGTCTTTGAGGCTGGTGGTTTGAATTGTGTGCTTACCTTCATTCGTGAC
AGTGGACATCTAGTTCATAAAGACACCTTGCACTCTGCTATGGCTGTGGTATCAAGACTCTGTGGC
AAAATGGAGCCTCAAGATTCTTCTTTAGAAATTTGTGTAGAATCTCTGTCTAGTTTATTAAAGCAT
GAAGATCATCAGGTTTCAGATGGAGCTCTGCGATGCTTTGCATCACTGGCTGACCGATTTACCCGT
CGTGGTGTTGACCCAGCTCCATTAGCCAAGCATGGATTAACTGAGGAGCTGTTATCTCGAATGGCT
GCTGCTGGTGGTACTGTTTCAGGACCATCATCAGCATGCAAACCAGGTCGCAGCACCACAGGAGCT
CCATCCACCACTGCAGATTCCAAATTGAGTAATCAGGTGTCAACAATTGTAAGTCTGCTCTCAACA
CTTTGCAGAGGCTCTCCGGTAGTAACAC

*HEK293T HECTD1 KO #2

Add 1

ATGGCAGATGTGGACCCAGATACATTGCTGGAATGGCTACAGATGGGACAGGGAGATGAAAGGGAC
ATGCAACTAATAGCCCTTGAACAGCTATGCATGCTGCTTTTGATGTCTGACAACGTGGATCGTTGT
TTTGAAACATGTCCTCCTCGCACTTTCTTACCAGCCCTTTGCAAAATTTTTCTTGATGAAAGTGCT
CCAGACAATGTATTAGAGGTGACAGCCCGTGCCATAACATACTACCTGGATGTATCTGCGGAATGT
ACC.CCG.AAG.GAT.TGT.TGG.GGT.AGA.TGG

MADVDPDTLLEWLQMGQGDERDMQLIALEQLCMLLLMSDNVDRCFETCPPRTFLPALCKIFLDESA
PDNVLEVTARAITYYLDVSAECTPKDCWGRWSYKSTL*

Del 10

ATGGCAGATGTGGACCCAGATACATTGCTGGAATGGCTACAGATGGGACAGGGAGATGAAAGGGAC
ATGCAACTAATAGCCCTTGAACAGCTATGCATGCTGCTTTTGATGTCTGACAACGTGGATCGTTGT
TTTGAAACATGTCCTCCTCGCACTTTCTTACCAGCCCTTTGCAAAATTTTTCTTGATGAAAGTGCT
CCAGACAATGTATTAGAGGTGACAGCCCGTGCCATAACATACTACCTGGATGTATCTGCGGAATGT
ACC.TTG.GGG.TAG

MADVDPDTLLEWLQMGQGDERDMQLIALEQLCMLLLMSDNVDRCFETCPPRTFLPALCKIFLDESA
PDNVLEVTARAITYYLDVSAECTLG*

Del 11

ATGGCAGATGTGGACCCAGATACATTGCTGGAATGGCTACAGATGGGACAGGGAGATGAAAGGGAC
ATGCAACTAATAGCCCTTGAACAGCTATGCATGCTGCTTTTGATGTCTGACAACGTGGATCGTTGT
TTTGAAACATGTCCTCCTCGCACTTTCTTACCAGCCCTTTGCAAAATTTTTCTTGATGAAAGTGCT
CCAGACAATGTATTAGAGGTGACAGCCCGTGCCATAACATACTACCTGGATGTATCTGCGGAATGT
ACC.TGG.GGT.AGA.TGG.AGC.TAT

MADVDPDTLLEWLQMGQGDERDMQLIALEQLCMLLLMSDNVDRCFETCPPRTFLPALCKIFLDESA
PDNVLEVTARAITYYLDVSAECTWGRWSYKSTL*

Figure A.1. Sequencing of HEK293T HECTD1 KO2. Sequencing carried out to confirm that the mutation induced by CRISPR/Cas9 causes a frame shift and premature stop codon leading to nonsense mediated decay. Provided by Dr Bienz lab.

Table A.1. siRNA specificity to each HECTD1 isoform. Each siRNA was compared to each variant of HECTD1 nucleotide sequence, below is a table to show, which siRNA can target, which isoform of HECTD1.

	HECTD1-201	HECTD1-001	HECTD1-202	HECTD1-005	HECTD1-006	HECTD1-003	HECTD1-010	HECTD1-012
#06	✓	✓	✓	✓	✗	✗	✗	✗
#07	✓	✓	✓	✓	✓	✗	✗	✗
#08	✓	✓	✓	✗	✓	✗	✗	✗
#09	✓	✓	✓	✗	✗	✓	✗	✗

```
mHECTD1      MADVDPDTLLEWLQMGQGDERDMQLIALEQLCMLLLMSDNVDRCFETCPPRTFLPALCKI   60
hHECTD1      MADVDPDTLLEWLQMGQGDERDMQLIALEQLCMLLLMSDNVDRCFETCPPRTFLPALCKI   60
             ************************************************************

mHECTD1      FLDESAPDNVLEVTARAITYYLDVSAECTRRIVGVDGAIKALCNRLVVVELNNRTSRDLA   120
hHECTD1      FLDESAPDNVLEVTARAITYYLDVSAECTRRIVGVDGAIKALCNRLVVVELNNRTSRDLA   120
             ************************************************************

mHECTD1      EQCVKVLELICTRESGAVFEAGGLNCVLTFIRDSGHLVHKDTLHSAMAVVSRLCGKMEPQ   180
hHECTD1      EQCVKVLELICTRESGAVFEAGGLNCVLTFIRDSGHLVHKDTLHSAMAVVSRLCGKMEPQ   180
             ************************************************************

mHECTD1      DSSLEICVESLSSLLKHEDHQVSDGALRCFASLADRFTRRGVDPAPLAKHGLTEELLSRM   240
hHECTD1      DSSLEICVESLSSLLKHEDHQVSDGALRCFASLADRFTRRGVDPAPLAKHGLTEELLSRM   240
             ************************************************************

mHECTD1      AAAGGTVSGPSSACKPGRSTTGAPSAAADSKLSNQVSTIVSLLSTLCRGSPLVTHDLLRS   300
hHECTD1      AAAGGTVSGPSSACKPGRSTTGAPSTTADSKLSNQVSTIVSLLSTLCRGSPVVTHDLLRS   300
             ************************::************************:********

mHECTD1      ELPDSIESALQGDERCVLDTMRLVDLLLVLLFEGRKALPKSSAGSTGRIPGLRRLDSSGE   360
hHECTD1      ELPDSIESALQGDERCVLDTMRLVDLLLVLLFEGRKALPKSSAGSTGRIPGLRRLDSSGE   360
             ************************************************************

mHECTD1      RSHRQLIDCIRSKDTDALIDAIDTGAFEVNFMDDVGQTLLNWASAFGTQEMVEFLCERGA   420
hHECTD1      RSHRQLIDCIRSKDTDALIDAIDTGAFEVNFMDDVGQTLLNWASAFGTQEMVEFLCERGA   420
             ************************************************************

mHECTD1      DVNRGQRSSSLHYAACFGRPQVAKTLLRHGANPDLRDEDGKTPLDKARERGHSEVVAILQ   480
hHECTD1      DVNRGQRSSSLHYAACFGRPQVAKTLLRHGANPDLRDEDGKTPLDKARERGHSEVVAILQ   480
             ************************************************************

mHECTD1      SPGDWMCPVNKGDDKKKKDTNKDEEECNEPRGDPEMAPLYLKRLLPVFAQTFQHTMLPSI   540
hHECTD1      SPGDWMCPVNKGDDKKKKDTNKDEEECNEPKGDPEMAPIYLKRLLPVFAQTFQQTMLPSI   540
             ******************************:********:**************:******

mHECTD1      RKASLALIRKMIHFCSEALLKEVCDSDVGHNLPTTLVEITATVLDQEDDDDGHLLALQII   600
hHECTD1      RKASLALIRKMIHFCSEALLKEVCDSDVGHNLPTILVEITATVLDQEDDDDGHLLALQII   600
             ********************************* ************************

mHECTD1      RDLVDKGGDIFLDQLARLGVISKVSALAGPSSDDENEEESKPEKEDEPQEDAKELQQGKP   660
hHECTD1      RDLVDKGGDIFLDQLARLGVISKVSTLAGPSSDDENEEESKPEKEDEPQEDAKELQQGKP   660
             ************************:***********************************

mHECTD1      YHWRDWSIIRGRDCLYIWSDAAALELSNGSNGWFRFILDGKLATMYSSGSPEGGSDSSES   720
hHECTD1      YHWRDWSIIRGRDCLYIWSDAAALELSNGSNGWFRFILDGKLATMYSSGSPEGGSDSSES   720
             ************************************************************

mHECTD1      RSEFLEKLQRARGQVKPSTSSQPILSAPGPTKLTVGNWSLTCLKEGEIAIHNSDGQQATI   780
hHECTD1      RSEFLEKLQRARGQVKPSTSSQPILSAPGPTKLTVGNWSLTCLKEGEIAIHNSDGQQATI   780
             ************************************************************

mHECTD1      LKEDLPGFVFESNRGTKHSFTAETSLGSEFVTGWTGKRGRKLKSKLEKTKQKVRTMARDL   840
hHECTD1      LKEDLPGFVFESNRGTKHSFTAETSLGSEFVTGWTGKRGRKLKSKLEKTKQKVRTMARDL   840
             ************************************************************

mHECTD1      YDDHFKAVESMPRGVVVTLRNIATQLESSWELHTNRQCIEGENTWRDLMKTALENLIVLL   900
hHECTD1      YDDHFKAVESMPRGVVVTLRNIATQLESSWELHTNRQCIESENTWRDLMKTALENLIVLL   900
             ****************************************.*******************

mHECTD1      KDENTISPYEMCSSGLVQALLTVLNNSIDLDMKQDCSQLVERINVFKTAFSESEDDESRP   960
hHECTD1      KDENTISPYEMCSSGLVQALLTVLNNSMDLDMKQDCSQLVERINVFKTAFSENEDDESRP   960
             ***************************:************************.*******

mHECTD1      AVALIRKLIAVLESIERLPLHLYDTPGSTYNLQILTRRLRFRLERAPGETSLIDRTGRML   1020
hHECTD1      AVALIRKLIAVLESIERLPLHLYDTPGSTYNLQILTRRLRFRLERAPGETALIDRTGRML   1020
             ************************************************:*********

mHECTD1      KMEPLATVESLEQYLLKMVAKQWYDFDRSSFVFVRKLREGQNFIFRHQHDFDENGIIYWI   1080
hHECTD1      KMEPLATVESLEQYLLKMVAKQWYDFDRSSFVFVRKLREGQNFIFRHQHDFDENGIIYWI   1080
             ************************************************************
```

```
mHECTD1      GTNAKTAYEWVNPAAYGLVVVTSSEGRNLPYGRLEDILSRDNSALNCHSNDDKNAWFAID   1140
hECTD1       GTNAKTAYEWVNPAAYGLVVVTSSEGRNLPYGRLEDILSRDNSALNCHSNDDKNAWFAID   1140
             ************************************************************

mHECTD1      LGVWVIPSAYTLRHARGYGRSALRNWVFQVSKDGQNWTSLYTHVDDCSLNEPGSTATWPL   1200
hECTD1       LGLWVIPSAYTLRHARGYGRSALRNWVFQVSKDGQNWTSLYTHVDDCSLNEPGSTATWPL   1200
             **:********************************************************

mHECTD1      DPAKDEKQGWRHVRLKQMGKNASGQTHYLSLSGFELYGTVNGVCEDQLGKAAKEAEANLR   1260
hECTD1       DPPKDEKQGWRHVRIKQMGKNASGQTHYLSLSGFELYGTVNGVCEDQLGKAAKEAEANLR   1260
             ** ***********:********************************************

mHECTD1      RQRRLVRSQVLKYMVPGARVIRGLDWKWRDQDGSPQGEGTVTGELHNGWIDVTWDAGGSN   1320
hECTD1       RQRRLVRSQVLKYMVPGARVIRGLDWKWRDQDGSPQGEGTVTGELHNGWIDVTWDAGGSN   1320
             ************************************************************

mHECTD1      SYRMGAEGKFDLKLAPGYDPDTVASPKPVSSTVSGTTQSWSSLVKNNCPDKTSAAAGSSS   1380
hECTD1       SYRMGAEGKFDLKLAPGYDPDTVASPKPVSSTVSGTTQSWSSLVKNNCPDKTSAAAGSSS   1380
             ************************************************************

mHECTD1      RKGSSSSVCSVASSSDISLASTKTERRSEIVMEHSIVSGADVHEPIVVLSSAENVPQTEV   1440
hECTD1       RKGSSSSVCSVASSSDISLGSTKTERRSEIVMEHSIVSGADVHEPIVVLSSAENVPQTEV   1440
             ******************.*****************************************

mHECTD1      GSSSSASTSTLTAETGSENAERKLGPDSSVRAPGESSAISMGIVSVSSPDVSSVSELTNK   1500
hECTD1       GSSSSASTSTLTAETGSENAERKLGPDSSVRTPGESSAISMGIVSVSSPDVSSVSELTNK   1500
             ********************************:***************************

mHECTD1      EAASQRPLSSSASNRLSVSSLLAAGAPMSSSASVPNLSSRETSSLESFVRRVANIARTNA   1560
hECTD1       EAASQRPLSSSASNRLSVSSLLAAGAPMSSSASVPNLSSRETSSLESFVRRVANIARTNA   1560
             ************************************************************

mHECTD1      TNNMNLSRSSSDNNTNTLGRNVMSTATSPLMGAQSFPNLTTPGTTSTVTMSTSSVTSSSN   1620
hECTD1       TNNMNLSRSSSDNNTNTLGRNVMSTATSPLMGAQSFPNLTTPGTTSTVTMSTSSVTSSSN   1620
             ************************************************************

mHECTD1      VATATTVLSVGQSLSNTLTTSLTSTSSESDTGQEAEYSLYDFLDSCRASTLLAELDDDED   1680
hECTD1       VATATTVLSVGQSLSNTLTTSLTSTSSESDTGQEAEYSLYDFLDSCRASTLLAELDDDED   1680
             ************************************************************

mHECTD1      LPEPDEEDDENEDDNQEDQEYEEVMILRRPSLQRRAGSRSDVTHHVVTSQLPQVPSGAGS   1740
hECTD1       LPEPDEEDDENEDDNQEDQEYEEVMILRRPSLQRRAGSRSDVTHHAVTSQLPQVPAGAGS   1740
             *******************************************.*********:****

mHECTD1      RPVGEQEEEEYETKGGRRRAWDDDYVLKRQFSALVPAFDPRPGRTNVQQTTDLEIPPPGT   1800
hECTD1       RPIGEQEEEEYETKGGRRRTWDDDYVLKRQFSALVPAFDPRPGRTNVQQTTDLEIPPPGT   1800
             **:****************:*******************************************

mHECTD1      PHSELLEEVECTPSPRLALTLKVTGLGTTREVELPLTNFRSTIFYYVQKLLQLSCNGNVK   1860
hECTD1       PHSELLEEVECTPSPRLALTLKVTGLGTTREVELPLTNFRSTIFYYVQKLLQLSCNGNVK   1860
             ************************************************************

mHECTD1      SDKLRRIWEPTYTIMYREMKDSDKEKENGKMGCWSIEHVEQYLGTDELPKNDLITYLQKN   1920
hECTD1       SDKLRRIWEPTYTIMYREMKDSDKEKENGKMGCWSIEHVEQYLGTDELPKNDLITYLQKN   1920
             ************************************************************

mHECTD1      ADAAFLRHWKLTGTNKSIRKNRNCSQLIAAYKDFCEHGTKSGLNQGAISSLQSSDILNLT   1980
hECTD1       ADAAFLRHWKLTGTNKSIRKNRNCSQLIAAYKDFCEHGTKSGLNQGAISTLQSSDILNLT   1980
             ************************************************:***********

mHECTD1      KEQPQAKAGNGQSPCGVEDVLQLLRILYIVASDPYSRISQEDGDEQPQFTFPPDEFTSKK   2040
hECTD1       KEQPQAKAGNGQNSCGVEDVLQLLRILYIVASDPYSRISQEDGDEQPQFTFPPDEFTSKK   2040
             ************. ********************************************

mHECTD1      ITTKILQQIEEPLALASGALPDWCEQLTSKCPFLIPFETRQLYFTCTAFGASRAIVWLQN   2100
hECTD1       ITTKILQQIEEPLALASGALPDWCEQLTSKCPFLIPFETRQLYFTCTAFGASRAIVWLQN   2100
             ************************************************************

mHECTD1      RREATVERTRTTSSVRRDDPGEFRVGRLKHERVKVPRGESLMEWAENVMQIHADRKSVLE   2160
hECTD1       RREATVERTRTTSSVRRDDPGEFRVGRLKHERVKVPRGESLMEWAENVMQIHADRKSVLE   2160
             ************************************************************
```

```
mHECTD1      VEFLGEEGTGLGPTLEFYALVAAEFQRTDLGTWLCDDNFPDDESRHVDLGGGLKPPGYYV   2220
hHECTD1      VEFLGEEGTGLGPTLEFYALVAAEFQRTDLGAWLCDDNFPDDESRHVDLGGGLKPPGYYV   2220
             ******************************:***************************

mHECTD1      QRSCGLFTAPFPQDSDELERITKLFHFLGIFLAKCIQDNRLVDLPISKPFFKLMCMGDIK   2280
hHECTD1      QRSCGLFTAPFPQDSDELERITKLFHFLGIFLAKCIQDNRLVDLPISKPFFKLMCMGDIK   2280
             ************************************************************

mHECTD1      SNMSKLIYESRGDRDLHCTESQSEASTEEGHDSLSVGSFEEDSKSEFILDPPKPKPPAWF   2340
hHECTD1      SNMSKLIYESRGDRDLHCTESQSEASTEEGHDSLSVGSFEEDSKSEFILDPPKPKPPAWF   2340
             ************************************************************

mHECTD1      NGILTWEDFELVNPHRARFLKEIKDLAIKRRQILGNKSLSEDEKNTKLQELVLRNPSGSG   2400
hHECTD1      NGILTWEDFELVNPHRARFLKEIKDLAIKRRQILSNKGLSEDEKNTKLQELVLKNPSGSG   2400
             **********************************.**.***************:******

mHECTD1      PPLSIEDLGLNFQFCPSSRIYGFTAVDLKPSGEDEMITMDNAEEYVDLMFDFCMHTGIQK   2460
hHECTD1      PPLSIEDLGLNFQFCPSSRIYGFTAVDLKPSGEDEMITMDNAEEYVDLMFDFCMHTGIQK   2460
             ************************************************************

mHECTD1      QMEAFRDGFNKVFPMEKLSSFSHEEVQMILCGNQSPSWAAEDIINYTEPKLGYTRDSPGF   2520
hHECTD1      QMEAFRDGFNKVFPMEKLSSFSHEEVQMILCGNQSPSWAAEDIINYTEPKLGYTRDSPGF   2520
             ************************************************************

mHECTD1      LRFVRVLCGMSSDERKAFLQFTTGCSTLPPGGLANLHPRLTVVRKVDATDASYPSVNTCV   2580
hHECTD1      LRFVRVLCGMSSDERKAFLQFTTGCSTLPPGGLANLHPRLTVVRKVDATDASYPSVNTCV   2580
             ************************************************************

mHECTD1      HYLKLPEYSSEEIMRERLLAATMEKGFHLN        2610
hHECTD1      HYLKLPEYSSEEIMRERLLAATMEKGFHLN        2610
             ****************************
```

Figure A.2. mHectd1 and hHECTD1 amino acid sequence alignment. Sequence alignment to identify the catalytic cysteine in mHectd1. Using the Pairwise Sequence Alignment Tool EMBL (https://www.ebi.ac.uk/Tools/psa/ (accessed 20.01.17)).

MADVDPDTLLEWLQMGQGDERDMQLIALEQLCMLLLMSDNVDRCFETCPPRTFLPALCKIF
LDESAPDNVLEVTARAITYYLDVSAECTRRIVGVDGAIKALCNRLVVVELNNRTSRDLAEQ
CVKVLELICTRESGAVFEAGGLNCVLTFIRDSGHLVHKDTLHSAMAVVSRLCGKMEPQDSS
LEICVESLSSLLKHEDHQVSDGALRCFASLADRFTRRGVDPAPLAKHGLTEELLSRMAAAG
GTVSGPSSACKPGRSTTGAPSTTADSKLSNQVSTIVSLLSTLCRGSPVVTHDLLRSELPDS
IESALQGDERCVLDTMRLVDLLLVLLFEGRKALPKSSAGSTGRIPGLRRLDSSGERSHRQL
IDCIRSKDTDALIDAIDTGAFEVNFMDDVGQTLLNWASAFGTQEMVEFLCERGADVNRGQR
SSSLHYAACFGRPQVAKTLLRHGANPDLRDEDGKTPLDKARERGHSEVVAILQSPGDWMCP
VNKGDDKKKKDTNKDEEECNEPKGDPEMAPIYLKRLLPVFAQTFQQTMLPSIRKASLALIR
KMIHFCSEALLKEVCDSDVGHNLPTILVEITATVLDQEDDDDGHLLALQIIRDLVDKGGDI
FLDQLARLGVISKVSTLAGPSSDDENEEESKPEKEDEPQEDAKELQQGKPYHWRDWSIIRG
RDCLYIWSDAAALELSNGSNGWFRFILDGKLATMYSSGSPEGGSDSSESRSEFLEKLQRAR
GQVKPSTSSQPILSAPGPTKLTVGNWSLTCLKEGEIAIHNSDGQQATILKEDLPGFVFESN
RGTKHSFTAETSLGSEFVTGWTGKRGRKLKSKLEKTKQKVRTMARDLYDDHFKAVESMPRG
VVVTLRNIATQLESSWELHTNRQCIESENTWRDLMKTALENLIVLLKDENTISPYEMCSSG
LVQALLTVLNNSMDLDMKQDCSQLVERINVFKTAFSENEDDESRPAVALIRKLIAVLESIE
RLPLHLYDTPGSTYNLQILTRRLRFRLERAPGETALIDRTGRMLKMEPLATVESLEQYLLK
MVAKQWYDFDRSSFVFVRKLREGQNFIFRHQHDFDENGIIYWIGTNAKTAYEWVNPAAYGL
VVVTSSEGRNLPYGRLEDILSRDNSALNCHSNDDKNAWFAIDLGLWVIPSAYTLRHARGYG
RSALRNWVFQVSKDGQNWTSLYTHVDDCSLNEPGSTATWPLDPPKDEKQGWRHVRIKQMGK
NASGQTHYLSLSGFELYGTVNGVCEDQLGKAAKEAEANLRRQRRLVRSQVLKYMVPGARVI
RGLDWKWRDQDGSPQGEGTVTGELHNGWIDVTWDAGGSNSYRMGAEGKFDLKLAPGYDPDT
VASPKPVSSTVSGTTQSWSSLVKNNCPDKTSAAAGSSSRKGSSSSVCSVASSSDISLGSTK
TERRSEIVMEHSIVSGADVHEPIVVLSSAENVPQTEVGSSSSASTSTLTAETGSENAERKL
GPDSSVRTPGESSAISMGIVSVSSPDVSSVSELTNKEAASQRPLSSSASNRLSVSSLLAAG
APMSSSASVPNLSSRETSSLESFVRRVANIARTNATNNMNLSRSSSDNNTNTLGRNVMSTA
TSPLMGAQSFPNLTTPGTTSTVTMSTSSVTSSSNVATATTVLSVGQSLSNTLTTSLTSTSS
ESDTGQEAEYSLYDFLDSCRASTLLAELDDDEDLPEPDEEDDENEDDNQEDQEYEEVMILR
RPSLQRRAGSRSDVTHHAVTSQLPQVPAGAGSRPIGEQEEEEYETKGGRRRTWDDDYVLKR
QFSALVPAFDPRPGRTNVQQTTDLEIPPPGTPHSELLEEVECTPSPRLALTLKVTGLGTTR
EVELPLTNFRSTIFYYVQKLLQLSCNGNVKSDKLRRIWEPTYTIMYREMKDSDKEKENGKM
GCWSIEHVEQYLGTDELPKNDLITYLQKNADAAFLRHWKLTGTNKSIRKNRNCSQLIAAYK
DFCEHGTKSGLNQGAISTLQSSDILNLTKEQPQAKAGNGQNSCGVEDVLQLLRILYIVASD
PYSRISQEDGDEQPQFTFPPDEFTSKKITTKILQQIEEPLALASGALPDWCEQLTSKCPFL
IPFETRQLYFTCTAFGASRAIVWLQNRREATVERTRTTSSVRRDDPGEFRVGRLKHERVKV
PRGESLMEWAENVMQIHADRKSVLEVEFLGEEGTGLGPTLEFYALVAAEFQRTDLGAWLCD
DNFPDDESRHVDLGGGLKPPGYYVQRSCGLFTAPFPQDSDELERITKLFHFLGIFLAKCIQ
DNRLVDLPISKPFFKLMCMGDIKSNMSKLIYESRGDRDLHCTESQSEASTEEGHDSLSVGS
FEEDSKSEFILDPPKPKPPAWFNGILTWEDFELVNPHRARFLKEIKDLAIKRRQILSNKGL
SEDEKNTKLQELVLKNPSGSGPPLSIEDLGLNFQFCPSSRIYGFTAVDLKPSGEDEMITMD
NAEEYVDLMFDFCMHTGIQKQMEAFRDGFNKVFPMEKLSSFSHEEVQMILCGNQSPSWAAE
DIINYTEPKLGYTRDSPGFLRFVRVLCGMSSDERKAFLQFTTGCSTLPPGGLANLHPRLTV
VRKVDATDASYPSVNTCV

Key:

KEN = KEN box

RxxN = potential D box

RxxN = more likely D box

Figure A.3. Identification of KEN and D box sequences in hHECTD1. KEN and D box sequences within HECTD1 predicted based on the APC/C degron repository (http://slim.ucd.ie/apc/index.php?page=instances&instance_set=dboxes (accessed 25/09/17)). Uniprot ID: Q9ULT8 (HECD1_HUMAN).

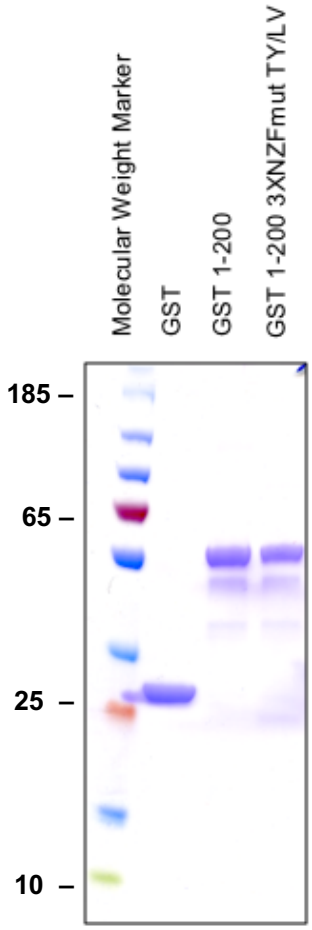

Figure A.4. Coomassie SDS-PAGE for GST, GST-TRABID$_{1-200}$, GST-TRABID$_{1-200}$ 3XNZF (TY/LV). GST fusions of bacterially expressed TRABID$_{1-200}$ and TRABID$_{1-200\ TY/LV}$ were loaded on a on a 4-12% SDS PAGE. GST and GST-fusion proteins were loaded at 5µg each. The gel was then stained in Coomassie Blue reagent, destained and imaged using the GelDoc-It^{TM} Imaging System (UVP). Here, proteins were normalised to 5µg based on the concentration of protein, which was also used for the IP experiments in this thesis.

A

Abcam Ub-1 (anti-Ub)

Exposure 20s ECL prime

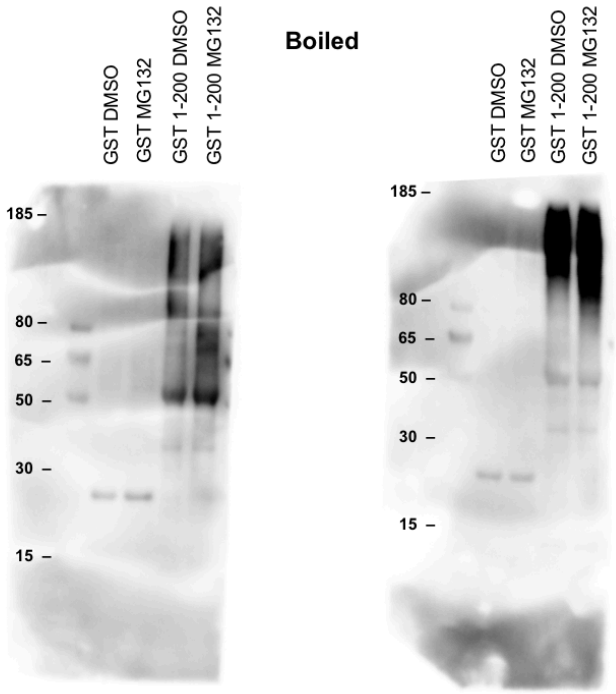

B

Enzo P4D1 (anti-Ub)

Exposure 10s ECL prime

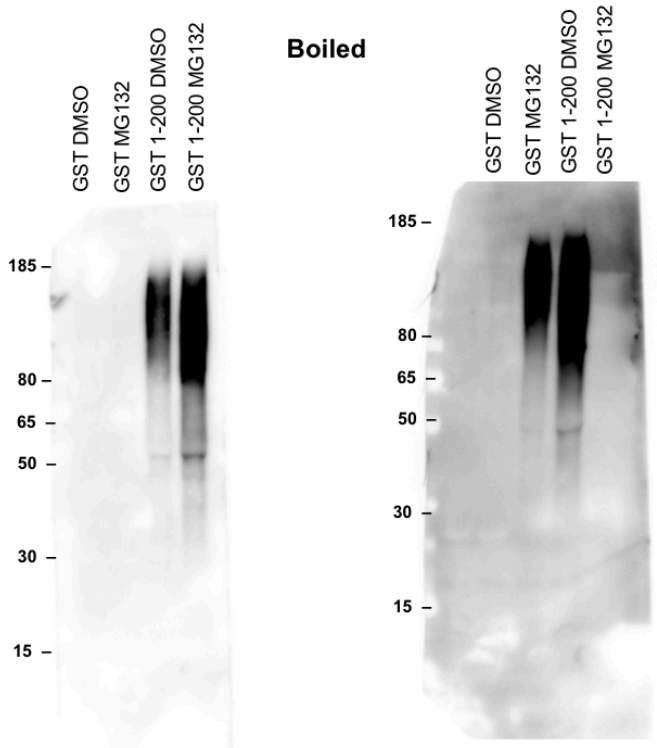

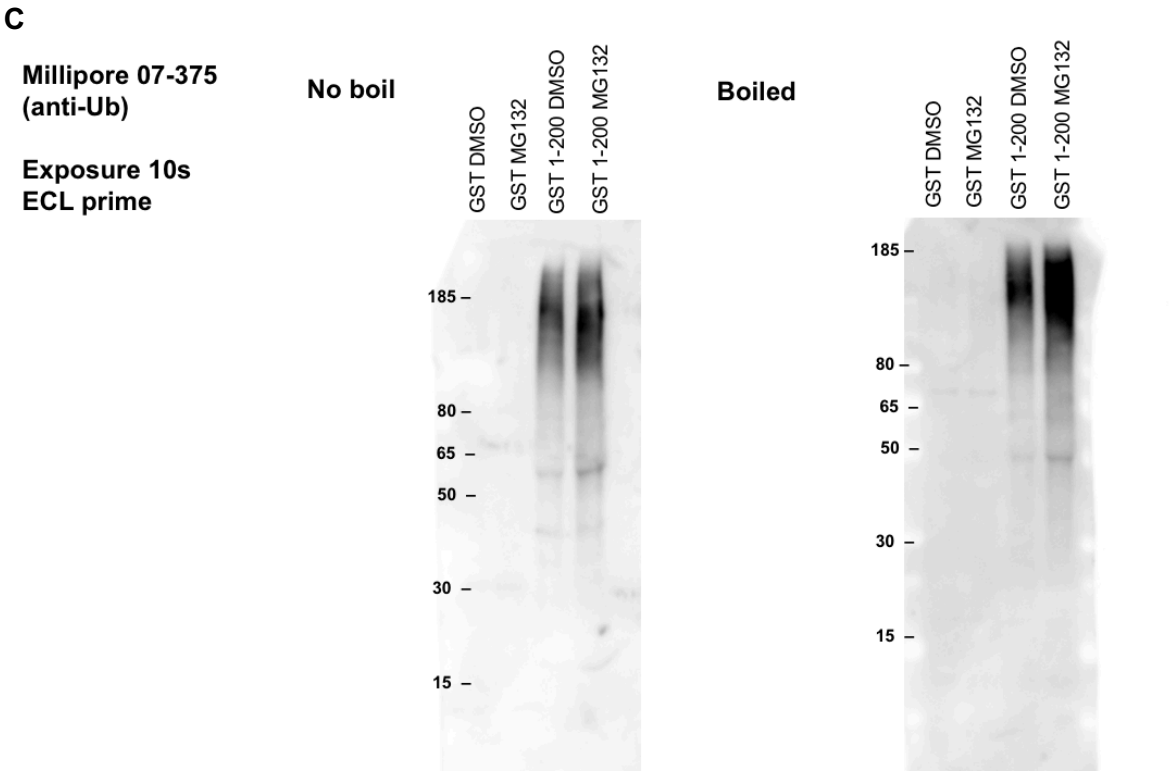

Figure A.5. Anti-Ub antibody optimisation. Optimisation of three different anti-Ub antibodies on non-boiled and boiled PVDF membranes. Antibodies were tested on $TRABID_{1-200}$ pull down assay samples. For the IP GST fusions of bacterially expressed $TRABID_{1-200}$ and $TRABID_{1-200\ TY/LV}$ were used. Western blots of the immunoprecipitation (IP) and Input. Samples were treated with DMSO or 10μM MG132 for 6hrs before lysis. Following western blotting on PVDF, the membrane was blocked in 3%-BSA-PBST and incubated overnight with A) Abcam Ubi-1 anti-Ub antibody (ab7254), B) Enzo P4D1 anti-Ub antibody (BML-PW0930), or C) Millipore anti-Ub antibody (07-375) followed by detection with an appropriate secondary HRP antibody. From this optimisation, Enzo P4D1 anti-Ub was chosen, with membranes that were boiled. All western blots were cropped and displayed with housekeeping gene blots throughout the thesis.

A

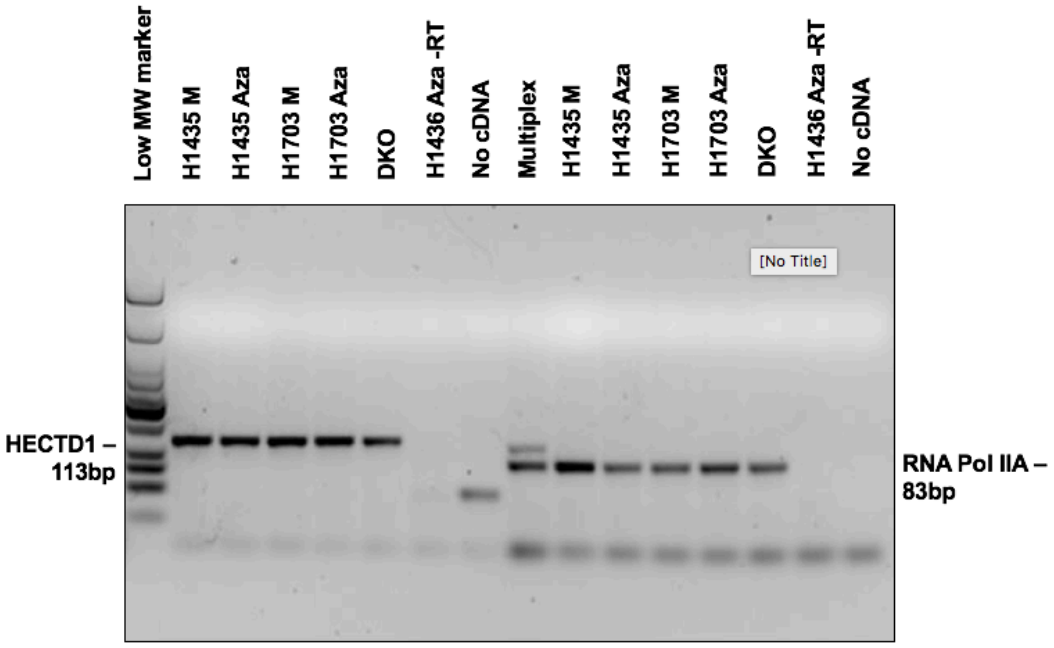
Low MW marker
H1435 M
H1435 Aza
H1703 M
H1703 Aza
DKO
H1436 Aza -RT
No cDNA
Multiplex
H1435 M
H1435 Aza
H1703 M
H1703 Aza
DKO
H1436 Aza -RT
No cDNA
[No Title]
HECTD1 – 113bp
RNA Pol IIA – 83bp

B

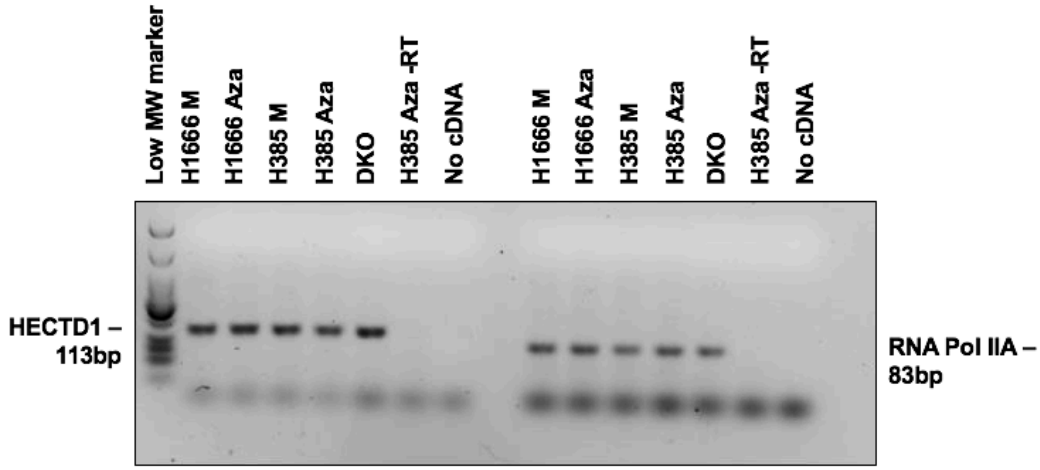
Low MW marker
H1666 M
H1666 Aza
H385 M
H385 Aza
DKO
H385 Aza -RT
No cDNA
H1666 M
H1666 Aza
H385 M
H385 Aza
DKO
H385 Aza -RT
No cDNA
HECTD1 – 113bp
RNA Pol IIA – 83bp

C

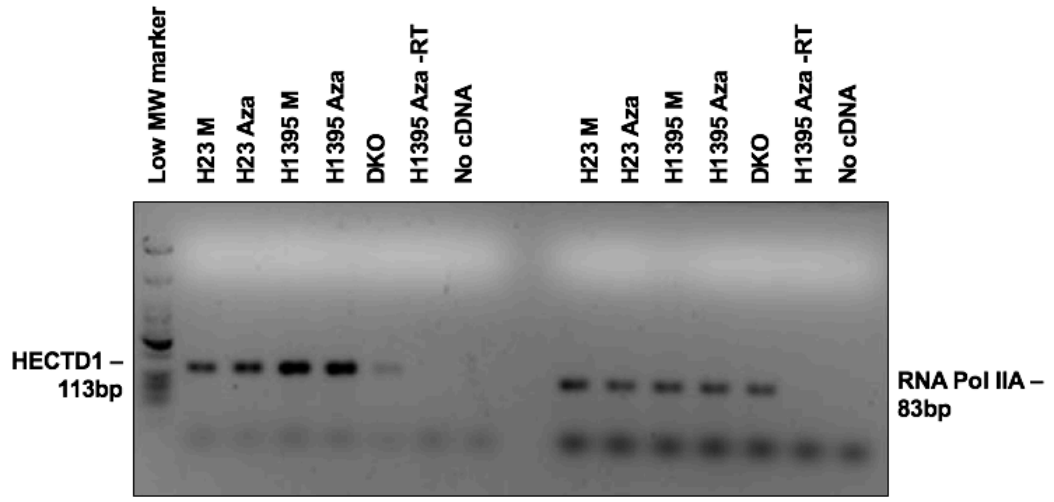

D

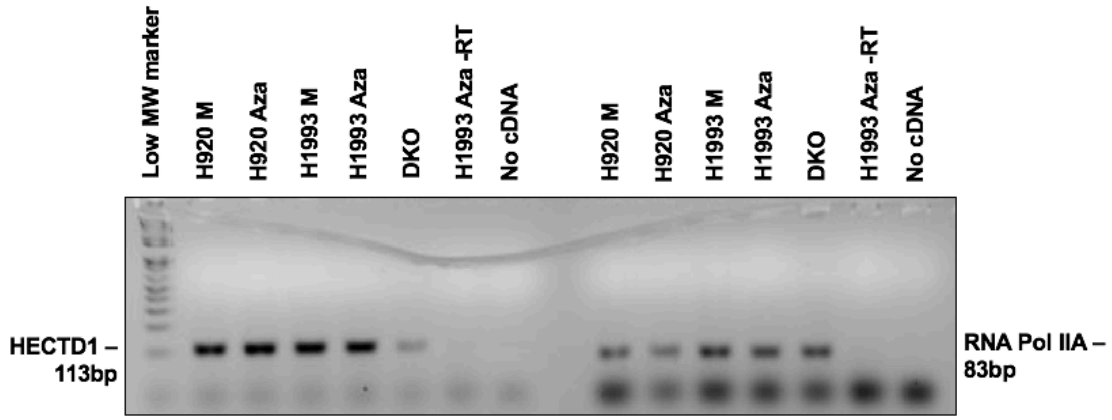

Figure A.6. A panel screen of lung cancer cell lines to assess the presence of *HECTD1* promoter methylation (Full Gels). 3% agarose gel of RT-PCR products, showing *HECTD1* (JL7 + 8) expression in multiple cancer cell lines. A) H1435 and H1703, B) H1666 and H385, C) H23 and H1395, and D) H920 and H1993. Each cell line was treated with DMSO (M = Mock treated) or 5-aza-2'-deoxycytidine (2μM) (A = "Aza" treated). *HECTD1* was compared to *RNA Pol IIA* housekeeping gene. DKO cell line was used as a positive control, -RT and no cDNA were used as a negative control in the reaction. Multiplex sample = *HECTD1* and *RNA Pol II* primers in the same reaction.